INFORMATION TO USERS

The negative microfilm copy of this dissertation was prepared and inspected by the school granting the degree. We are using this film without further inspection or change. If there are any questions about the content, please write directly to the school. The quality of this reproduction is heavily dependent upon the quality of the original material.

The following explanation of techniques is provided to help clarify notations which may appear on this reproduction.

1. Manuscripts may not always be complete. When it is not possible to obtain missing pages, a note appears to indicate this.

2. When copyrighted materials are removed from the manuscript, a note appears to indicate this.

3. Oversize materials (maps, drawings, and charts) are photographed by sectioning the original, beginning at the upper left hand corner and continuing from left to right in equal sections with small overlaps.

4. Most photographs reproduce acceptably on positive microfilm or microfiche but lack clarity on xerographic copies made from the microfilm. For any illustrations that cannot be reproduced satisfactorily by xerography, photographic prints can be purchased at additional cost and tipped into your xerographic copy. Requests can be made to the Dissertations Customer Services Department.

U·M·I Dissertation Information Service

University Microfilms International
A Bell & Howell Information Company
300 N. Zeeb Road, Ann Arbor, Michigan 48106

Order Number 9001202

Averaging of strongly nonlinear oscillators using elliptic functions

Coppola, Vincent Timothy, Ph.D.

Cornell University, 1989

U·M·I
300 N. Zeeb Rd.
Ann Arbor, MI 48106

AVERAGING OF STRONGLY NONLINEAR OSCILLATORS USING ELLIPTIC FUNCTIONS

A Dissertation

Presented to the Faculty of the Graduate School

of Cornell University

in Partial Fulfillment of the Requirements for the Degree of

Doctor of Philosophy

by

Vincent Timothy Coppola

August 1989

Biographical Sketch

Vincent Timothy Coppola was born and raised in northern Virginia, in the suburbs of Washington, D.C. His interest and abilities in mathematics led him to attend George Mason University part-time during his senior year in high school. Vince began his undergraduate engineering studies in 1983 at Virginia Polytechnic Institute and State University, after winning a scholarship in VPI's annual scholarship competition. He completed the requirements for the Bachelor of Science degree in Engineering Science and Mechanics in 1986, graduating near the top of his class. He started graduate school in 1986 at Cornell University in the department of Theoretical and Applied Mechanics. There, he earned the Master of Science degree in 1988 and his doctorate in 1989.

Dedication

To Stacey

my beloved

Acknowledgments

I especially wish to thank Richard Rand for his work with me on this research. Our discussions led to many fruitful investigations.

I wish to thank John Guckenheimer for his suggestion that MACSYMA be used to explore problems which deal with elliptic functions.

I also wish to thank Philip Holmes for suggesting the investigation of the chaotic system of chapter 7.

Table of Contents

Table of Contents (Continued)

Table of Contents (Continued)

List of Tables

List of Figures

List of Figures (Continued)

List of Figures (Continued)

List of Figures (Continued)

0.0 Introduction

In this work, we investigate a class of perturbed strongly nonlinear oscillators using the method of averaging. In particular, we are concerned with the following system:

$$x'' + \alpha(\tau)\, x + \beta(\tau)\, x^3 + \epsilon\, g(x,x',t) = 0 \tag{0.1}$$

where $(')$ denotes $\frac{d}{dt}$, $\tau = \epsilon\, t$, and $\epsilon \ll 1$

In eq.(0.1), both α and β may be postive or negative and may depend on the slow time τ. The perturbation g is assumed to be a polynomial in x and x'. Furthermore, the cubic stiffness β is <u>not</u> assumed to be $O(\epsilon)$. Hence, the solution to the corresponding unperturbed system is not given by trigonometric functions, as it is for the case of a weakly nonlinear oscillator, i.e., $\beta = O(\epsilon)$. In fact, the solution to the unperturbed system is expressed using elliptic functions, which are generalizations of the trignometric functions.

We are interested in approximating solutions to eq.(0.1) for the prediction of its dynamical behavior. The approximation is calculated using the method of averaging, a perturbation method for systems of ordinary differential equations. We have implemented the averaging method in the computer algebra system MACSYMA (see [Ran84]) because calculating the approximation requires a tremendous number of

computations. With the approximation, we investigate many different systems belonging to the class of eq.(0.1).

Readers unfamiliar with elliptic functions and their properties should consult chapter 1 where a summary of these functions, as they pertain to this work, is provided. Chapter 1 serves as a reference guide for the other chapters: complete knowledge of elliptic functions is not necessary to understand the rest of the work. Important notations, however, lie therein.

In chapter 2, we find the solution to the unperturbed system corresponding to eq.(0.1) and apply variation of parameters. This results in a system of differential equations which completely solve eq.(0.1). In chapter 3, we apply the method of averaging to approximate the solution to the variational equations and introduce the MACSYMA program that performs this procedure.

Chapter 4 is concerned with the cubic oscillator, i.e., $\alpha = 0$. In chapter 5, averaging using elliptic functions is compared to averaging using trigonometric functions. We find that the elliptic averaging approximation is more accurate in predicting qualitative behavior even for weakly nonlinear systems where $\beta = O(\epsilon)$. In chapter 6, two more exotic systems are investigated.

Chapters 7 and 8 are concerned with systems whose unperturbed phase portraits contain a separatrix which periodically disappears. The averaging approximation predicts chaos, transient chaos, limit tori, and attractive chaotic orbits to exist in these systems. Chapter 9 is concerned with the failure of the averaging

approximation near a separatrix. In that chapter, another model of separatrix crossing is derived.

Lastly, we investigate the forced Duffing equation in chapter 10.

1.0 Elliptic functions

The properties of elliptic functions, including notation, numerical evaluation, algebraic identities, differentiation, and integration, form the foundation for all the computations in the following chapters. The theory of elliptic integrals (from a theoretical mathematician's viewpoint) has been known for centuries. Early work was done by Euler, Lagrange, and Landen. Legendre then systematically developed elliptic integrals by introducing a reduction to three normal forms. Abel, Jacobi, and Weierstrass each developed elliptic functions by inverting the elliptic integral of the first kind. Although the Weierstrass theory represents the more modern mathematical approach, we find that Jacobian elliptic functions are more convenient for our purposes [Byr54].

The theory of Jacobian elliptic functions is treated in many works. Both Hancock [Han10] and Neville [Nev71] are well-known. While these works contain all the information on elliptic functions that we will need (and more), we choose to rely on Byrd and Friedman's Handbook of Elliptic Integrals for Engineers and Physicists [Byr54] which emphasizes the computational (rather than theoretical) aspects of elliptic functions. Since elliptic functions are not well-known to engineers and scientists, we have provided a summary of them in this chapter.

1.1 Notation, definitions, and properties

Jacobian elliptic functions involve a collection of identities which are similar to those for trigonometric functions but are more complicated algebraically. The use of computer algebra makes manipulation of these identities easier, permitting investigations to proceed on problems which were previously avoided because of the quantities of algebra involved.

Elliptic functions are most easily understood by comparing them with the more familiar trigonometric functions. Corresponding to sin(u) and cos(u) are three fundamental elliptic functions sn(u,k), cn(u,k), and dn(u,k). Each of the elliptic functions depends on the modulus k as well as the argument u. The complementary modulus k' is defined by

$$k' = \sqrt{1 - k^2} \tag{1.1}$$

These functions reduce to sin(u), cos(u), and 1 respectively, when k = 0. The sn and sin functions share common properties as do cn and cos. These are summarized in Table 1.1. The dn function has no trigonometric counterpart. Note that the elliptic functions sn and cn may be thought of as generalizations of sin and cos in which their period depends on the modulus k.

Table 1.1 Properties of Jacobi elliptic functions

	Function f				
Property	sn(u,k)	sin(u)	cn(u,k)	cos(u)	dn(u,k)
Max. value	1	1	1	1	1
Min. value	-1	-1	-1	-1	k'
Period	4 K(k)	2π	4 K(k)	2π	2 K(k)
Odd/Even	Odd	Odd	Even	Even	Even
$\partial f/\partial u$	cn dn	cos	- sn dn	- sin	$-k^2$ sn cn
f | k=0	sin	---	cos	---	1
f | k=1	tanh	---	sech	---	sech

K(k) = complete integral of the first kind

The argument u is identified as the incomplete elliptic integral of the first kind which is usually denoted $F(\theta,k)$ (here θ is a circular angle independent of k). This identification shows that u also depends on k. The value of k normally ranges from 0 to 1. The sn, cn, and dn functions are shown in Fig.1.1 for $k = \sqrt{1/2}$.

From Table 1.1, we see that the period of the elliptic functions is related to the complete elliptic integral of the first kind K(k). Also, the sn function smoothly connects sin with tanh as k ranges from 0 to 1 (similarly, cn connects cos with sech and dn connects 1 with sech over this range of k). This implies that $K(0) = \pi/2$ and

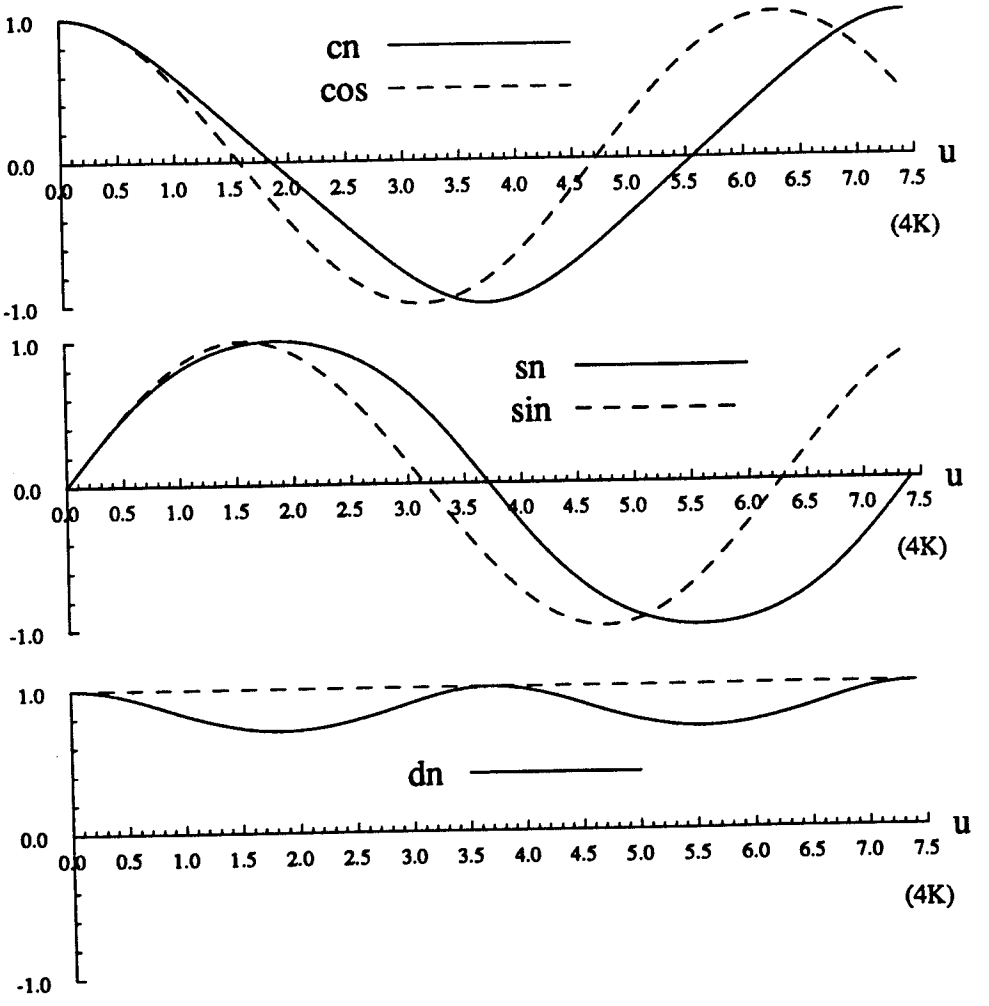

Fig.1.1 Comparison of elliptic functions for $k = \sqrt{1/2}$ with trignometric functions. The period of the elliptic functions is $4\,K(\sqrt{1/2}) \simeq 7.416$.

$K(1) = \infty$. Properties of elliptic integrals of the first and second kinds are given in Table 1.2. (The elliptic integral of the third kind is not needed for our work and is not included in our discussion). Table 1.3 shows some special values of the elliptic integrals. Finally, a graph of the complete elliptic integrals of the first and second kinds is given in Fig.1.2.

The am function defined in Table 1.2 is particularly useful because of the following identities:

(1.2a) $$sn(u,k) = \sin(\theta) \text{ and } cn(u,k) = \cos(\theta)$$
$$\text{where } \theta = am(u,k)$$

(1.2b) $$am(u,0) = u \ , \ am(u,1) = \sin^{-1}(\tanh u)$$

Special values of the am, cn, sn, and dn functions are given in Table 1.4.

The elliptic functions satisfy the following identities which correspond to $\sin^2 + \cos^2 = 1$:

(1.3a) $$sn^2 + cn^2 = 1$$

(1.3b) $$k^2 sn^2 + dn^2 = 1$$

(1.3c) $$1 - k^2 + k^2 cn^2 = dn^2$$

In addition, these functions satisfy an algebraic addition theorem in their arguments just as sin and cos do (i.e., sn(u+v,k) can be

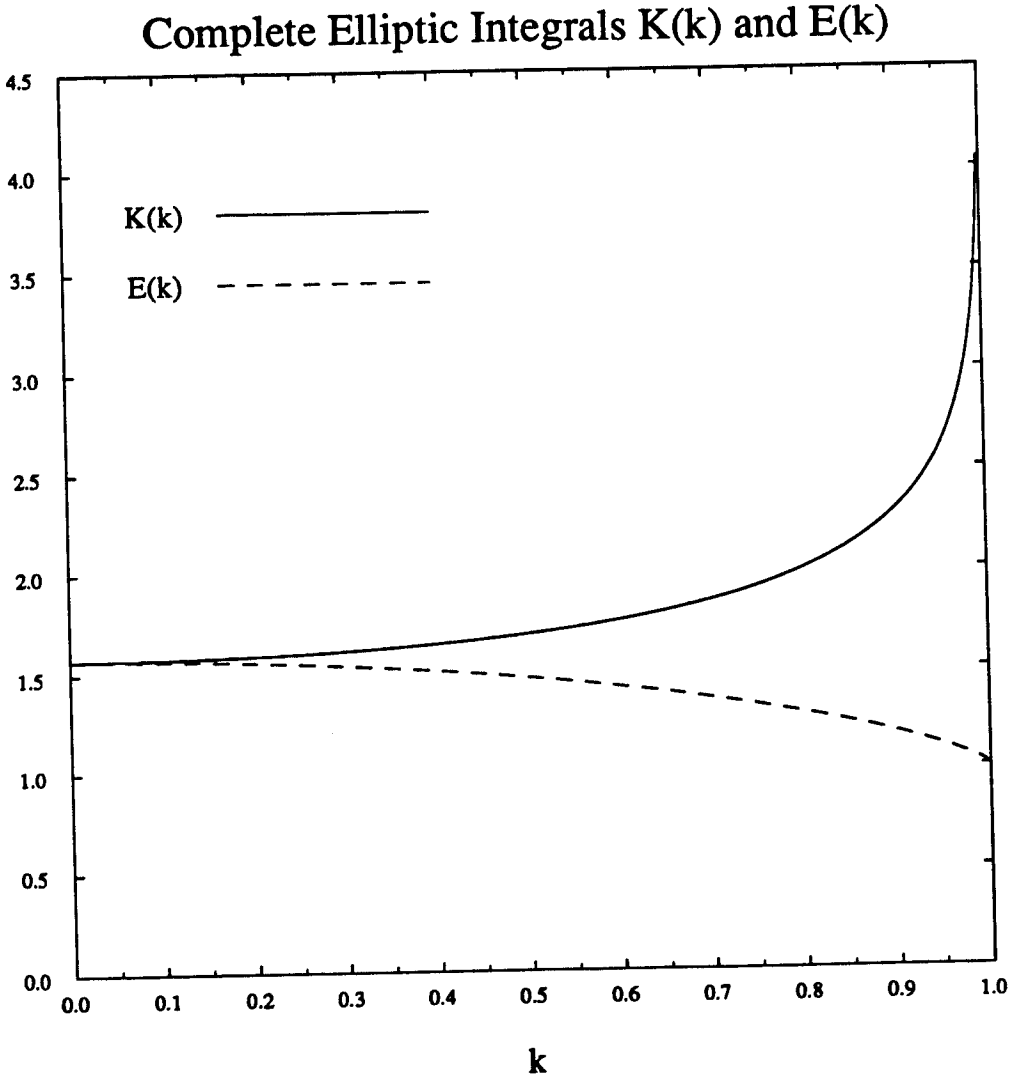

Fig.1.2 Plots of the complete elliptic integrals K(k) and E(k). K(k) becomes infinite at k = 1.

Table 1.2 Elliptic integrals

I. Elliptic integral of the first kind:

(i) Notation

(a) $F(\theta,k) = u$ = incomplete elliptic integral of the first kind

(b) $K = K(k)$ = complete elliptic integral of the first kind

(ii) Mathematical Definition

(a) $$F(\theta,k) = \int_0^{\theta} \frac{d\psi}{\sqrt{1 - k^2 \sin^2(\psi)}}$$

(b) $$K(k) = \int_0^{\pi/2} \frac{d\psi}{\sqrt{1 - k^2 \sin^2(\psi)}}$$

(iii) Description (on $0 \leq k \leq 1$)

(a) F is a monotonically increasing function of θ

(b) K is a montonically increasing function of k

(iv) Properties

(a) $K = F(\frac{\pi}{2},k)$

(b) $F(-\theta,k) = - F(\theta,k)$

(c) $F(m\pi \pm \theta,k) = 2mK \pm F(\theta,k)$

(d) $\theta = F^{-1}(u,k) \equiv am(u,k)$, where am is the amplitude function of u defined as the inverse of $F(\theta,k)$. The am function maps (0,4 K) in u to $(0,2\pi)$ in θ.

Table 1.2 (Continued)

II. Elliptic integral of the second kind:

(i) Notation

(a) $E(\theta,k)$ = incomplete elliptic integral of the second kind

(b) $E = E(k)$ = complete elliptic integral of the second kind

(c) $E(\theta,k) = E(am(u,k),k)$ is also denoted by $E(u,k)$ or simply $E(u)$. When using this notation, it is important to know whether the argument of $E(\cdot,k)$ is an incomplete elliptic integral or not.

(ii) Mathematical Definition

(a) $E(\theta,k) = \int_0^{\theta} \sqrt{1 - k^2\sin^2(\psi)}\, d\psi$

(b) $E(k) = \int_0^{\pi/2} \sqrt{1 - k^2\sin^2(\psi)}\, d\psi$

(iii) Description (on $0 \leq k \leq 1$)

(a) $E(\theta,k)$ is a monotonically increasing function of θ except at $k = 1$ where it is periodic

(b) E is a montonically decreasing function of k

(iv) Properties

(a) $E = E(\theta=\frac{\pi}{2},k)$

(b) $E(-\theta,k) = -E(\theta,k)$

(c) $E(m\pi \pm \theta,k) = 2mE \pm E(\theta,k)$

Table 1.3 Special values of elliptic integrals

Value of k	F(θ,k)	K(k)	E(θ,k)	E(k)
0	θ	$\frac{\pi}{2}$	θ	$\frac{\pi}{2}$
1	$\ln\left[\tan(\theta) + \sec(\theta)\right]$	∞	$\sin(\theta)$	1

The singularity of K is logarithmic: $\lim_{k \to 1} K(k) \to \ln \frac{4}{k'}$.

Table 1.4 Special values of elliptic functions

Value of u	am(u,k)	cn(u,k)	sn(u,k)	dn(u,k)
0	0	1	0	1
K	$\frac{\pi}{2}$	0	1	k'
v + K	$\frac{\pi}{2} + \tan^{-1}\beta$	$-k'\frac{sn(v,k)}{dn(v,k)}$	$\frac{cn(v,k)}{dn(v,k)}$	$k'\frac{1}{dn(v,k)}$
2 K	π	- 1	0	1
v + 2 K	π + am(v,k)	- cn(v,k)	- sn(v,k)	dn(v,k)
3 K	$\frac{3}{2}\pi$	0	- 1	k'
v + 3 K	$\frac{3}{2}\pi + \tan^{-1}\beta$	$k'\frac{sn(v,k)}{dn(v,k)}$	$-\frac{cn(v,k)}{dn(v,k)}$	$k'\frac{1}{dn(v,k)}$
v + 4 K	2π + am(v,k)	cn(v,k)	sn(v,k)	dn(v,k)

where $\beta = k' \frac{sn(v,k)}{cn(v,k)}$, $0 \leq k \leq 1$

expressed in terms of sn, cn, and dn of the arguments u and v at the same modulus k). In fact, this is a most basic property of an elliptic function. (In addition, elliptic functions must be doubly-periodic in the complex plane.)

In addition to the elliptic functions sn, cn, and dn defined before, there are 9 other elliptic functions that one may encounter. These functions are derived from the standard three that we have given. Their properties and algebraic identities are derived using their definitions in terms of sn, cn, and dn. We include them here for completeness, and only use them as a notation convenience:

$$\text{(1.4a)} \qquad \mathrm{ns}(u,k) \equiv \frac{1}{\mathrm{sn}} \quad \mathrm{nc}(u,k) \equiv \frac{1}{\mathrm{cn}} \quad \mathrm{nd}(u,k) \equiv \frac{1}{\mathrm{dn}}$$

$$\text{(1.4b)} \qquad \mathrm{sd}(u,k) \equiv \frac{\mathrm{sn}}{\mathrm{dn}} \quad \mathrm{cd}(u,k) \equiv \frac{\mathrm{cn}}{\mathrm{dn}} \quad \mathrm{cs}(u,k) \equiv \frac{\mathrm{cn}}{\mathrm{sn}}$$

$$\text{(1.4c)} \quad \mathrm{ds}(u,k) \equiv \frac{\mathrm{dn}}{\mathrm{sn}} \quad \mathrm{dc}(u,k) \equiv \frac{\mathrm{dn}}{\mathrm{cn}} \quad \mathrm{tn}(u,k) = \mathrm{sc}(u,k) \equiv \frac{\mathrm{sn}}{\mathrm{cn}}$$

Lastly, a linear combination of E(u) and u is periodic, and called the Jacobi Zeta function $Z(\theta,k)$:

$$\text{(1.5)} \qquad Z(\theta,k) = E(\theta,k) - \frac{E(k)}{K(k)} F(\theta,k)$$

This function is periodic with period 2 K(k) in u and has zero mean. It is often written in abbreviated notation as Z(u) (or Z(u,k)) in

the same manner as E(u). Properties of $Z(\theta,k)$ are given in eqs.(1.6).

(1.6a) $$Z(-\theta,k) = -Z(\theta,k)$$

(1.6b) $$Z(0,k) = Z(\tfrac{\pi}{2},k) = Z(\pi,k) = Z(\theta,0) = 0$$

(1.6c) $$Z(u,1) = \tanh(u)$$

The inverse functions associated with sn, cn, and dn are also defined. They are evaluated as follows:

(1.7a) $$sn^{-1}(y,k) = F(\sin^{-1}y,k) \quad \text{for } 0 \leq y \leq 1$$

(1.7b) $$cn^{-1}(y,k) = F(\sin^{-1}(\sqrt{1 - y^2}),k) \quad \text{for } 0 \leq y \leq 1$$

(1.7c) $$dn^{-1}(y,k) = F(\sin^{-1}(\sqrt{(1 - y^2)/k^2}),k) \quad \text{for } k' \leq y \leq 1$$

1.2 Modulus transformations: Elliptic functions for $-\infty \leq k^2 \leq \infty$

The normal range for the modulus k, as previously mentioned, is the closed interval [0,1]. Hence, the valid range of the square modulus is [0,1] also. However, we can extend the definition of <u>all</u> elliptic functions to the square modulus range of $[-\infty,\infty]$ by employing a <u>modulus transformation</u>. (Similarly, the elliptic functions can be extended from real arguments u to complex arguments through use of an argument transformation.)

For $k^2 \geq 1$, elliptic functions with argument u and modulus k are defined through the reciprocal modulus transformation shown in

Table 1.5, which relates the (u,k) system variables to a new (v,k_1) system.

Table 1.5 Reciprocal modulus transformation

$$k_1 = \frac{1}{k} \ , \ k'^2 = 1 - k^2 \ , \ k_1'^2 = 1 - k_1^2$$

$$cn(u,k) = dn(v,k_1) \ , \ dn(u,k) = cn(v,k_1) \ , \ sn(u,k) = k_1 \, sn(v,k_1)$$

$$u = k_1 v \ , \ K = k_1 K_1 \ , \ E(u) = \frac{1}{k_1}[E(v) - k_1'^2 v] \ , \ E = \frac{1}{k_1}(E_1 - k_1'^2 K_1)$$

$$v = k\,u \ , \ K_1 = k\,K \ , \ E(v) = \frac{1}{k}[E(u) - k'^2 u] \ , \ E_1 = \frac{1}{k}[E - k'^2 K]$$

$$Z(u,k) = \frac{1}{k_1} Z(v,k_1) \ , \ Z(v,k_1) = \frac{1}{k} Z(u,k)$$

$$K \equiv K(k) \ , \ K_1 \equiv K(k_1) \ , \ E \equiv E(k) \ , \ E_1 \equiv E(k_1)$$

$$E(u) \equiv E(am(u,k),k) \ , \ E(v) = E(am(v,k_1),k_1)$$

In Table 1.5 {u, E(u), K, E} are variables that use k while {v, E(v), K_1, E_1} use k_1. Both u and v are incomplete elliptic integrals of the first kind with their completions denoted K and K_1, respectively. Both E(u) and E(v) are incomplete elliptic integrals of the second kind with their completions denoted E and E_1, respectively.

As an example, consider evaluating cn(u,2). Since m = 4, we use Table 1.5 to find that $k_1 = \frac{1}{2}$ and v = 2 u. We then evaluate $dn(2\,u,\frac{1}{2})$ in the normal manner (since its modulus is between 0 and 1). So, $cn(u,2) = dn(2\,u,\frac{1}{2})$.

The definition of elliptic functions can also be extended by allowing the modulus k to be imaginary. This makes $k^2 < 0$. For $k^2 < 0$, elliptic functions are defined through the reciprocal complementary modulus transformation shown in Table 1.6, which relates the (u,k) system to a new (w,k_2) system of variables.

Table 1.6 Reciprocal complementary modulus transformation

$$k_2' = \frac{1}{k'} \quad , \quad k^2 = -\frac{k_2^2}{k_2'^2} \quad , \quad k_2^2 = -\frac{k^2}{k'^2}$$

$$cn(u,k) = cd(w,k_2) \quad , \quad dn(u,k) = nd(w,k_2) \quad , \quad sn(u,k) = k_2' \, sd(w,k_2)$$

$$u = k_2' \, w \quad , \quad K = k_2' \, K_2 \quad , \quad E = \frac{1}{k_2'} \, E_2$$

$$w = k' \, u \quad , \quad K_2 = k' \, K \quad , \quad E_2 = \frac{1}{k'} \, E$$

$$E(u) = \frac{1}{k_2'} \left[E(w) - k_2^2 \, \frac{sd(w,k_2) \, cd(w,k_2)}{nd(w,k_2)} \right]$$

$$E(w) = \frac{1}{k'} \left[E(u) - k^2 \, \frac{sn(u,k) \, cn(u,k)}{dn(u,k)} \right]$$

$$Z(u,k) = \frac{1}{k_2'} \left[Z(w,k_2) - k_2^2 \, \frac{sd(w,k_2) \, cd(w,k_2)}{nd(w,k_2)} \right]$$

$$Z(w,k_2) = \frac{1}{k'} \left[Z(u,k) - k^2 \, \frac{sn(u,k) \, cn(u,k)}{dn(u,k)} \right]$$

$$K \equiv K(k) \quad , \quad K_2 \equiv K(k_2) \quad , \quad E \equiv E(k) \quad , \quad E_2 \equiv E(k_2)$$

$$E(u) \equiv E(am(u,k),k) \quad , \quad E(w) = E(am(w,k_2),k_2)$$

In Table 1.6 {u, E(u), K, E} are variables that use k while {w, E(w), K_2, E_2} use k_2. Both u and w are again incomplete elliptic integrals of the first kind with their completions denoted K and K_2, respectively. Both E(u) and E(w) are incomplete elliptic integrals of the second kind with their completions denoted E and E_2, respectively.

The advantage of defining elliptic functions for all real square modulus values will be demonstrated in solving for the unperturbed solution to eq.(*). It will be shown that the solution can be written in terms of just one function, cn(u,k), where $k^2 \in [-\infty,\infty]$. Thus, instead of representing the solution in differing regions of phase space (defined by either (a) $k^2 < 0$, (b) $0 \leq k^2 \leq 1$, or (c) $k^2 > 1$) by different functions whose modulus lies between 0 and 1 (from Tables 1.5 and 1.6, these are (a) cd(w,k_2), (b) cn(u,k), and (c) dn(v,k_1)), we represent the solution in the one expression cn(u,k). Notation is simplified, the crossing of regions is simplified, and further, we need only to compute the averaged equations once (instead of region by region).

1.3 Differentiation

The derivatives of the elliptic integrals are found by differentiating under the integral sign in their defining equations (see Table 1.2). These are listed in eqs.(1.8). For convenience,

the sn, cn, dn, am, and Zeta functions are written without their explicit argument dependence, i.e. cn = cn(u,k), etc. This notation will be used throughout the dissertation.

(1.8a) $$\frac{dK}{dk} = \frac{(E - k'^2 K)}{k\,k'^2}\,,\quad \frac{dE}{dk} = \frac{1}{k}(E - K)$$

(1.8b) $$\frac{du}{dk} = \frac{E(u) - k'^2 u}{k\,k'^2} - \frac{k}{k'^2}\frac{sn\ cn}{dn}\,,\quad \frac{dE(u)}{dk} = \frac{1}{k}\left[E(u) - u\right]$$

(1.8c) $$\frac{du}{d\theta}(\theta,k) = \frac{1}{\sqrt{1 - k^2 \sin^2\theta}}\,,\quad \frac{dE(\theta,k)}{d\theta} = \sqrt{1 - k^2 \sin^2\theta}$$

(1.8d) $$\frac{dZ}{dk} = \frac{k}{k'^2}\frac{E}{K}\frac{sn\ cn}{dn} - \frac{1}{K}Z\,,\quad \frac{dZ(\theta,k)}{d\theta} = K\,dn - \frac{E}{K}\frac{1}{dn}$$

$$\frac{dZ(u)}{du} = dn^2 - \frac{E}{K}$$

Derivatives of the elliptic functions are calculated using the am function in conjunction with eqs.(1.8). The derivatives of the am function are:

(1.9a) $$\theta = am(u,k) \quad \text{implies} \quad 1 = \frac{\partial am}{\partial u}\frac{du}{d\theta} = \frac{\partial am}{\partial u}\frac{1}{dn}$$

$$\text{Thus:}\quad \frac{\partial am}{\partial u} = dn$$

(1.9b) $$\theta = am(u,k) \quad \text{implies} \quad 0 = \frac{\partial am}{\partial u}\frac{du}{dk} + \frac{\partial am}{\partial k}$$

$$\text{Thus:}\quad \frac{\partial am}{\partial k} = -\,dn\,\frac{du}{dk}$$

Using sn = sin(θ), cn = cos(θ), and eq.(1.2), we find the derivatives of sn, cn and dn:

(1.10a) $$\frac{\partial sn}{\partial u} = cn\ dn \quad \text{and} \quad \frac{\partial sn}{\partial k} = -\ cn\ dn\ \frac{du}{dk}$$

(1.10b) $$\frac{\partial cn}{\partial u} = -\ sn\ dn \quad \text{and} \quad \frac{\partial cn}{\partial k} = sn\ dn\ \frac{du}{dk}$$

(1.10c) $$\frac{\partial dn}{\partial u} = -\ k^2\ sn\ cn \quad \text{and} \quad \frac{\partial dn}{\partial k} = k^2\ sn\ cn\ \frac{du}{dk} - k\ \frac{sn^2}{dn}$$

Using eqs.(1.10) and eqs.(1.3), we find the following helpful formulas:

(1.11a) $$(\frac{\partial sn}{\partial u})^2 = (1 - sn^2)\ (1 - k^2\ sn^2)$$

(1.11b) $$(\frac{\partial cn}{\partial u})^2 = (1 - cn^2)\ (k'^2 + k^2\ cn^2)$$

(1.11c) $$(\frac{\partial dn}{\partial u})^2 = (1 - dn^2)\ (dn^2 - k'^2)$$

(1.12a) $$\frac{\partial^2 sn}{\partial u^2} = sn\ (2\ k^2\ sn^2 - 1 - k^2)$$

(1.12b) $$\frac{\partial^2 cn}{\partial u^2} = cn\ (2\ k^2 - 1 - 2\ k^2\ cn^2)$$

(1.12c) $$\frac{\partial^2 dn}{\partial u^2} = dn\ (1 + k'^2 - dn^2)$$

We now introduce a prime (') to denote a derivative with respect to the argument u for an elliptic function. Hence, we let $cn' \equiv \frac{\partial cn}{\partial u}$ and $cn'' \equiv \frac{\partial^2 cn}{\partial u^2}$, etc. (and similarly for the sn and dn functions). <u>This notation using primes will be used throughout this work</u>.

Finally, we note that differentiating a transformed function (transformed by some modulus transformation) is equivalent to transforming a differentiated function. For example, we consider the reciprocal modulus transformation applied to cn(u,k):

$$\begin{aligned}(1.13)\qquad \frac{\partial}{\partial u}\,\mathrm{cn}(u,k) &= -\,\mathrm{sn}(u,k)\,\mathrm{dn}(u,k)\\ &= -\,k_1\,\mathrm{sn}(v,k_1)\,\mathrm{cn}(v,k_1)\\ &= \frac{1}{k_1}\,\frac{\partial \mathrm{dn}}{\partial v}(v,k_1) = \frac{1}{k_1}\,\frac{\partial \mathrm{dn}}{\partial u}(v,k_1)\,\frac{dv}{du}\\ &= \frac{\partial}{\partial u}\,\mathrm{dn}(v,k_1)\end{aligned}$$

1.4 Integration

Entire volumes have been devoted to integrals that give rise to elliptic integrals. Byrd and Friedman's handbook [Byr54] itself contains thousands of formulas. Using elliptic function substitutions, these integrals can be reduced to integrals of elliptic functions.

However, we will not need a complete library of integrals of elliptic functions for our work. We need only integrals of cn raised to any positive power and integrals arising from integrating those integrals of cn. We note that whereas integrals of trignometric functions of θ can always be expressed as a combination of θ, $\sin\theta$, and $\cos\theta$, integrals of sn, cn, and dn with respect to the argument u involve other functions than u, sn, cn, and dn. This makes repeated integrations (e.g., integrals of the integral of cn^n) much more complicated to compute. Finally, we note that all integrals in this

section are integrals with respect to the argument u and not the modulus k.

We first evaluate the integrals of cn^n. Define $I_n = \int cn^n \, du$. The first two integrals are simple:

$$I_0 = \int cn^0 \, du = \int du = u \tag{1.14a}$$

$$I_1 = \int cn^1 \, du = \int \frac{\cos\theta}{\sqrt{1 - k^2 \sin^2\theta}} \, d\theta = \frac{1}{k} \sin^{-1}(k \, sn(u,k)) = \frac{1}{k} \sin^{-1}(k \, sn) \tag{1.14b}$$

In eq.(1.14b) we have used the substitution $\theta = am(u,k)$ and identity (1.2). Note that (1.14b) is a elementary integral whose result is the elementary function arcsin (not an elliptic function or integral).

The integration of cn^2 proceeds from integrating dn^2. This is shown in (1.15).

$$\int dn^2 \, du = \int \sqrt{1 - k^2 \sin^2\theta} \, d\theta \equiv E(\theta,k) = E(u) \tag{1.15}$$

From (1.3c), we find the integral of cn^2:

$$I_2 = \int cn^2 \, du = \frac{1}{k^2} (E(u) - k'^2 u) \tag{1.16}$$

The integral of cn^3 is found using (1.12b). Integrating both sides of (1.12b) and solving for the integral of cn^3 gives:

$$(1.17) \qquad I_3 = \int cn^3 = \frac{1}{2\,k^3}\left[(2\,k^2 - 1)\,\sin^{-1}(k\,sn) - k\,\frac{\partial cn}{\partial u}\right]$$
$$= \frac{1}{2\,k^3}\left[(2\,k^2 - 1)\,\sin^{-1}(k\,sn) + k\,sn\,dn\right]$$

All the remaining integrals of cn (i.e., I_n for $n>3$) are evaluated recursively. The recursion relation is found by considering a function f where $f(u) = cn^{2n}$. Differentiating twice, we find:

$$(1.18a) \qquad f' = 2n\,cn^{2n-1}cn'$$
$$(1.18b) \qquad f'' = 2n\left[(2n - 1)\,cn^{2n-2}cn'^2 + cn^{2n-1}cn''\right]$$

where we denote $cn' = \frac{\partial cn}{\partial u}$ and $cn'' = \frac{\partial^2 cn}{\partial u^2}$. Using (1.11b) and (1.12b) in (1.18b), we find that:

$$(1.19) \qquad f'' = 2n\left[(2n - 1)\,k'^2 cn^{2n-2} + 2n\,(2\,k^2 - 1)\,cn^{2n} - (2n + 1)\,k^2\,cn^{2n+2}\right]$$

Integrating (1.19) and setting this equal to (1.18a), we find:

$$(1.20) \quad cn^{2n-1}cn' = (2n-1)k'^2\,I_{2n-2} + 2n(2k^2-1)\,I_{2n} - (2n+1)k^2\,I_{2n+2}$$

where the arbitrary constant is found to be zero. Solving for I_{2n+2}, we derive a recursive integration procedure:

$$(1.21)\quad I_{2n+2} = \frac{(2n-1)\,k'^2\,I_{2n-2} + 2n\,(2k^2 - 1)\,I_{2n} - cn^{2n-1}cn'}{(2n+1)\,k^2}$$

We note that integrals for n odd depend on only odd integrals and for n even depend on only even integrals.

The integration of cn^n (eqs.(14,16,17,19)) is easily implemented in MACSYMA. The routine CNINT, listed in Appendix A, integrates cn^n using the integration procedure outlined above. The program uses special symbols for each of the functions encountered in the integration procedure to avoid MACSYMA's confusing the function cn(u,k) with the numerical evaluation of cn(u,k). For example, in the program, the symbol for cn is 'XX' and for cn' is 'YY'.

The cn integration procedure is valid for all values of $k^2 \in [-\infty,\infty]$ (remember that the integral is performed with respect to u and not v or w) but a limiting procedure must be done for $k^2 \in \{-\infty,0,\infty\}$. For these values, it is better to perform the integration in the transformed variables (e.g., for k = 0, use cn = cos).

Moreover, it is easily shown that "transforming the integral is equivalent to integrating the transform." Hence, the procedure above is also the dn integration procedure under the reciprocal

transformation! For example, we compute the integral of dn^3. By Table 1.5, $cn(u,k) = dn(v,k_1)$. So, we have:

$$(1.22) \qquad \int dn^3(v,k_1)\, dv = \int cn^3(u,k)\, k\, du = k\, I_3$$

$$= \frac{1}{2}\frac{1}{k^2}\left[(2k^2 - 1)\sin^{-1}(k\ sn) + k\ sn\ dn\right]$$

$$= \frac{1}{2}k_1^2\left[\frac{1}{k_1^2}(2 - k_1^2)\sin^{-1}(sn(v,k_1) + sn(v,k_1)\ cn(v,k_1)\right]$$

$$= \frac{1}{2}\left[(2 - k_1^2)\ am(v,k_1) + k_1^2\ sn(v,k_1)\ cn(v,k_1)\right]$$

Finally, we note that under the reciprocal complementary modulus transformation (Table 1.6) $cn(u,k) = cd(w,k_2)$. From Table 1.4, we see that $sn(w+K_2,k_2) = cd(w,k_2)$. So, the integration procedure outlined above also works for sn!

As previously mentioned, we will need to be able to integrate some combinations of the functions appearing in the cn integration procedure. For this, it is convenient to express E(u) (using eq.(1.5)) as the linear combination of the periodic function Z(u) and the argument u wherever it appears in I_n (in order to isolate non-periodic terms easily). Then, the functions we must consider are:

$$(1.23) \qquad \text{(i) } cn^n,\ \text{(ii) } Z\ cn^n,\ \text{(iii) } cn^n cn',\ \text{(iv) } Z\ cn^n cn'$$

We have discussed form (i). Form (iii) integrates immediately. Form (iv) is easily integrated using integration by parts in which one part is Z.

Form (ii) is also integrated by integration by parts, taking Z to be one part. However, this requires knowing the integrals of the following functions which have not been computed so far:

(1.24a) (A) Z , (B) $Z\ cn^2$

(1.24b) (C) u , (D) $u\ cn^2$

(1.24c) (E) $\sin^{-1}(k\ sn)$, (F) $\sin^{-1}(k\ sn)\ cn^2$

From advanced theory of elliptic functions (i.e., the theory of Theta functions of Jacobi), one finds the integral of Z:

(1.25) $$\int Z\ du = \ln(\theta(u,k)/\theta(0,k)) \equiv TH(u,k)$$

where $\theta(u,k)$ is a Jacobi Theta function. Such functions arise in formulating numerical approximation procedures. Their theory and use are really unimportant for our purposes. Since the only place where the Theta function arises in this work is in the form TH(u,k), we do not treat $\theta(u,k)$ separately. The properties of THeta functions are unessential for our work but for completeness, we note that $\theta(u,k)$ is a positive, even, 2K periodic function with non-zero mean. Properties of TH(u,k) under the modulus transformations are found using (1.25) since Z is fully known.

The integration of (B) follows from integrating $Z\ dn^2$ and eq.(1.3c):

$$\int Z\ dn^2\ du = \int Z\ (dn^2 - \frac{E}{K})\ du + \frac{E}{K} \int Z\ du \tag{1.26a}$$

$$= \int Z\ dZ + \frac{E}{K}\ TH(u,k)$$

$$= \frac{1}{2} Z^2 + TH(u,k)$$

$$\int Z\ cn^2\ du = \frac{1}{k^2} \frac{Z^2}{2} + \frac{E - k'^2 K}{k^2\ K}\ TH(u,k) \tag{1.26b}$$

Forms (C) and (D) in (1.24) can now be integrated. Form (C) integrates immediately and form (D) follows from integration by parts, from eq.(1.5), and from form (A):

$$\int u\ du = \frac{1}{2} u^2 \tag{1.27a}$$

$$\int u\ cn^2 = \frac{1}{2\ k^2} (\frac{E}{K} - k'^2)\ u^2 + \frac{1}{k^2} (u\ Z - TH(u,k)) \tag{1.27b}$$

This leaves only forms (E) and (F) in (1.24) left to do. Because it is not possible to integrate either of these forms analytically, we define two new functions SO(u,k) and S2(u,k) which are simply:

$$SO(u,k) = \int \sin^{-1}(k\ sn)\ du \tag{1.28a}$$

$$S2(u,k) = \int \sin^{-1}(k\ sn)\ cn^2\ du \tag{1.28b}$$

Properties of S0 and S2 are derived from eqs.(1.28). It is seen that both functions are positive, even, 4K periodic functions with non-zero mean.

We have now derived a procedure for integrating each of function forms (i)-(iv) given in (1.23). A MACSYMA computer routine, GENINT (provided in Appendix B), implements this integration procedure. The utility of the MACSYMA program is apparent: one wishes to perform the highly involved procedure for computing the integrals in an accurate and timely manner.

1.5 Means

As the name 'averaging' (from the title of this work) suggests, we will be highly concerned with finding the means of functions over their natural period in u. For a large class of functions, this is a simple procedure. Since we can integrate functions appearing in eqs.(1.23) explicitly, we need only to evaluate the following expression, where f is an arbitrary periodic elliptic function:

$$(1.29) \quad \text{mean of } f = \frac{1}{4K}\int_0^{4K} f(u,k)\,du = \frac{1}{4K}\left[F(4K,k) - F(0,k)\right]$$

$$\text{where } \int f(u,k)\,du = F(u,k)$$

(Every periodic function with which we deal has 4 K as a fundamental period, i.e., its period is 4 K / n for some integer n.) An analysis

of each term that could ever appear in F(u,k) in eq.(1.29) for any f(u,k) of one of the forms given in (1.23) shows that the mean of f is simply the coefficient of u in F(u,k). However, there now appears a small complication when using a modulus transformation in finding the mean of a function f(u,k).

The complication arises only in the reciprocal modulus transformation, and then only for functions in which $\sin^{-1}(k\ sn)$ appears. Under the reciprocal modulus transformation, $\sin^{-1}(k\ sn) = am(v,k_1)$, which is non-periodic in v. So, when $\sin^{-1}(k\ sn)$ appears in F(u,k) (as it does for $\int cn^{2n+1}$), it contributes to the mean in the (v,k_1) system in addition to the u term. This is demonstrated by simply evaluating the following:

$$\frac{1}{4K_1}\left[am(4K_1,k_1) - am(0,k_1)\right] = \frac{\pi}{2K_1} \tag{1.31}$$

Thus, while $\sin^{-1}(k\ sn)$ has zero mean in the (u,k) and (w,k_2) systems, it is non-periodic in the (v,k_1) system and as such contributes to the mean (by eq.(1.31)). In this special case, the mean of the transform is not equal to the transform of the mean. In all other cases where $\sin^{-1}(k\ sn)$ appears nowhere in F(u,k), the mean of f in the (u,k) system transforms correctly to the mean of f in the (v,k_1) and (w,k_2) systems.

To account for the inability of the transformation to transform this one mean correctly, we introduce the Heaviside step function $H(k^2-1)$ into our calculation of means. $H(k^2-1)$ has value 1 when

$k^2 > 1$ and value 0 otherwise. When $\sin^{-1}(k\ sn)$ appears in F(u,k), we express its contribution to the mean as:

(1.31) contribution of $\sin^{-1}(k\ sn)$ term to mean = $H(k^2-1)\ \frac{\pi}{2K}$

For example, let f = cn(u,k). Then $F(u,k) = \frac{1}{k}\sin^{-1}(k\ sn)$. So, the mean of f is expressed as:

(1.32) $$\text{mean of cn} = \frac{\pi}{2kK}H(k^2-1) = \frac{\pi}{2K_1}H(k^2-1)$$
$$= \begin{bmatrix} 0 & \text{for } k^2 \leq 1 \\ \frac{\pi}{2K_1} & \text{for } k^2 > 1 \end{bmatrix}$$

Since $am(v,k_1)$ is non-periodic, the transformations of the functions SO(u,k), S2(u,k), and Z(u,k) $\sin^{-1}(k\ sn)$ from (u,k) to (v,k_1) will not be periodic. These functions only appear in F(u,k) for f(u,k) of the form Z cn^{2n+1}. Although we cannot explicitly calculate the mean of these three functions in the (v,k_1) system, we have determined that <u>collectively</u> they have zero mean in the manner in which they contribute to any mean of Z cn^{2n+1}. This follows from an analysis of the mean of Z cn^{2n+1} in the transformed variables (v,k_1). By breaking up the integral (in the computation of the mean) into judicious pieces, it can be shown that the mean of Z cn^{2n+1} is zero for all n in the (v,k_1) system.

The elliptic functions that appear in (1.23) are vital for the first order averaging procedure (to be discussed in chapter 3). For

this group of elliptic functions, we can explicitly calculate both the indefinite integral and the mean. Sadly, this will not be true for many of the functions which will be needed to do the second order averaging. We leave the analysis of those functions until chapter 3.

1.6 Numerical evaluation

The numerical evaluation of elliptic integrals and elliptic functions will be of primary importance in applying our method of averaging using elliptic functions to actual systems. Although such functions are not supported in most computer languages, they are easily evaluated using their power series or Fourier series expansions.

Many methods of approximating complete and incomplete elliptic integrals have been developed [Byr54,Abr72]. We list here a few that are easily programmed. First, we give power series expansions for the complete elliptic integrals:

$$(1.33a) \qquad K(k) = \frac{\pi}{2}\,\mathrm{HGF}\left(\tfrac{1}{2},\tfrac{1}{2};1;k^2\right) = \frac{\pi}{2}\sum_{n=0}^{\infty}\left[\frac{(\frac{1}{2})_n}{n!}\right]^2 k^{2n}$$

$$= \frac{\pi}{2}\left[1 + \frac{1}{4}k^2 + \frac{9}{64}k^4 + \frac{25}{256}k^6 + \cdots\right]$$

$$(1.33b)\quad E(k) = \frac{\pi}{2}\,\mathrm{HGF}\left(-\tfrac{1}{2},\tfrac{1}{2};1;k^2\right) = \frac{\pi}{2}\sum_{n=0}^{\infty}\frac{1}{1-2n}\left[\begin{matrix}-\frac{1}{2}\\ n\end{matrix}\right]^2 k^{2n}$$

$$= \frac{\pi}{2}\left[1 - \frac{1}{4}k^2 - \frac{3}{64}k^4 - \frac{5}{256}k^6 - \cdots\right]$$

where $0 \le k^2 \le 1$,

$\mathrm{HGF}(\alpha,\beta;\gamma;\delta)$ is the hypergeometric function,

$$(\alpha)_n = \begin{bmatrix} 1 & \text{for } n = 0 \\ \alpha\,(\alpha+1)\,(\alpha+2)\,(\cdots)\,(\alpha+n-1) & \text{for } n > 0 \end{bmatrix},$$

$$\left[\begin{matrix}\alpha\\ n\end{matrix}\right] = \begin{bmatrix} 1 & \text{for } n = 0 \\ \dfrac{\alpha\,(\alpha-1)\,(\alpha-2)\,(\cdots)\,(\alpha-n+1)}{n!} & \text{for } n > 0 \end{bmatrix}$$

Note that because K and E satisfy a special hypergeometric differential equation [Byr54], they can be expressed by a hypergeometric function.

These formulas arise from a Taylor series about k = 0. They converge well for $k^2 \le \frac{1}{2}$. For k^2 outside this range, it is better to expand K and E about k = 1 (which for K is a singular expansion):

$$(1.34a)\qquad K(k) = \sum_{n=0}^{\infty}\left[\begin{matrix}-\frac{1}{2}\\ n\end{matrix}\right]^2 \left(\ln\frac{4}{k'} - b_n\right) k'^{2n}$$

$$(1.34b)\quad E(k) = 1 + \frac{1}{4}\sum_{n=0}^{\infty}\frac{\left(\frac{1}{2}\right)_n\left(\frac{3}{2}\right)_n}{n!\,(n+1)!}\left(2\ln\frac{4}{k'} - b_{n+1} - b_n\right) k'^{2n+2}$$

where $0 < k'^2 < 1$,

and $b_0 = 0$, $b_n = b_{n-1} + \dfrac{1}{n\,(2n-1)}$

Expansions for incomplete elliptic integrals also converge better when two different power series are used: (1) for $0 \leq k^2 \leq \frac{1}{2}$ and (2) for $\frac{1}{2} < k^2 < 1$. These are given below:

$$F(\theta,k) = \sum_{n=0}^{\infty} \left[\begin{matrix} -\frac{1}{2} \\ n \end{matrix} \right] (-k^2)^n \, t_{2n}(\theta) \tag{1.35a}$$

$$E(\theta,k) = \sum_{n=0}^{\infty} \left[\begin{matrix} \frac{1}{2} \\ n \end{matrix} \right] (-k^2)^n \, t_{2n}(\theta) \tag{1.35b}$$

where $0 \leq k^2 < 1$, $0 \leq \theta < \frac{\pi}{2}$

and $t_0 = \theta$, $t_{2n} = \frac{2n-1}{2n} t_{2n-2} - \frac{1}{2n} \sin^{2n-1}(\theta) \cos(\theta)$

$$F(\theta,k) = \sum_{n=0}^{\infty} \left[\begin{matrix} -\frac{1}{2} \\ n \end{matrix} \right] k'^{2n} \, r_{2n}(\theta) \tag{1.36a}$$

where $0 < k^2 < 1$, $0 \leq k'^2 \tan^2(\theta) < 1$,

and $r_0 = \ln(\sec\theta + \tan\theta)$

$$r_{2n} = \frac{1}{2n} \left[(1 - 2n) \, r_{2n-2} + \tan^{2n-1}(\theta) \sec\theta \right]$$

$$E(\theta,k) = \sum_{n=0}^{\infty} \left[\begin{matrix} \frac{1}{2} \\ n \end{matrix} \right] k'^{2n} \, d_{2n}(\theta) \tag{1.36b}$$

where $0 < k^2 < 1$, $0 \leq k'^2 \tan^2(\theta) < 1$,

and $d_0 = \sin\theta$, $d_{2n} = \frac{1}{2n-2} \left[(1 - 2n) \, d_{2n-2} + \tan^{2n-1}(\theta) \cos(\theta) \right]$

The expansions given above in eqs.(1.33-1.36) are valid on $0 \leq k^2 \leq 1$. Outside this range, the evaluation of these integrals is

computed in the transformed variables (i.e., in the (v,k_1) or (w,k_2) systems).

The elliptic functions (sn, cn, dn, am, and Z) are all approximated by Fourier series. Both sn and Z can be expanded in a Fourier sine series, both cn and dn in a Fourier cosine series. The am function is then found by integrating the Fourier series of dn (see eq.(1.9a)). The Fourier series for Z is developed by first finding the Fourier cosine series for dn^2, and then using (1.8d).

We now show how to compute the Fourier series for cn(u,k). The computations for the other functions follow in a similar manner. The Fourier series for cn can be expressed as:

$$\text{(1.37)} \qquad cn(u,k) = \sum_{n=1}^{\infty} a_n \cos\left(\frac{n \pi u}{2K}\right)$$

$$\text{where } a_n = \frac{1}{2K} \int_{-2K}^{2K} cn(u,k) \cos\left(\frac{n \pi u}{2K}\right) du$$

By breaking the integral for a_n into four equal pieces of length K in u and using Table 1.4, we compute a_n to be:

$$\text{(1.38)} \qquad a_n = \begin{bmatrix} 0 & \text{for n even} \\ \frac{1}{K} \int_{-K}^{K} cn(u,k) \cos\left(\frac{n\pi u}{2K}\right) du & \text{for n odd} \end{bmatrix}$$

The a_n coefficients are computed by integrating eq.(1.38) in the complex plane and using the residue theorem.

As previously noted, elliptic functions are doubly-periodic, having both a real period (like trignometric functions) and imaginary period (like hyperbolic functions). The periods, poles, and residues for sn, cn, and dn are given in Table 1.7.

Table 1.7 Periods, poles and residues of sn, cn, and dn

f(u,k)	Real Period	Complex Period	Pole #1	Residue #1	Pole #2	Residue #2
sn	4K	2iK'	iK'	$\frac{1}{k}$	2K + iK'	$-\frac{1}{k}$
cn	4K	2(K+iK')	iK'	$-\frac{i}{k}$	2K + iK'	$\frac{i}{k}$
dn	2K	4iK'	iK'	- i	3iK'	i

where $i = \sqrt{-1}$ and $K' = K(k')$

We note that every point congruent to pole 1 or 2 modulo the period shown in Table 1.7 is again a pole. Each pole is simple. For our work, Table 1.7 is useful for the derivation of Fourier series expansions. Elsewhere in this work, we will be concerned only with real arguments u.

From Table 1.7, we judiciously choose a rectangular contour in the complex plane that will enclose just one pole at iK'. This is shown in Fig.1.3.

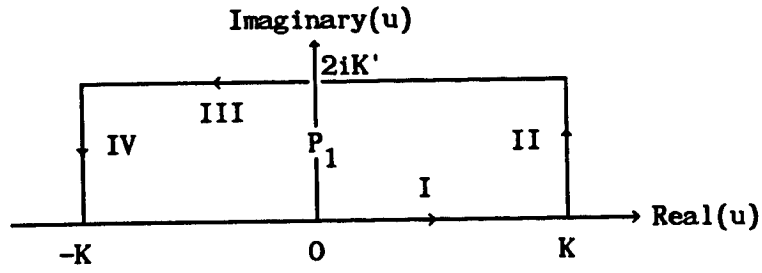

Fig.1.3 Contour for finding a_n in eq.(1.38) showing pole P_1 and integration paths I, II, III, and IV.

The integration path C goes along I, II, III, and IV. We now evaluate the line integral around C of eq.(1.38). The cosine term has value zero on paths II and IV, contributing nothing to the line integral. On IV, cn has the value:

$$(1.38) \qquad cn(u + 2iK', k) = cn(u - 2K, k) = - cn(u, k)$$

so that the integral on IV becomes:

$$(1.39)\ A_{IV} = \frac{1}{K}\int_{K}^{-K} - cn(u,k)\left[\cos\left(\frac{n\pi u}{2K}\right)\cosh\left(\frac{n\pi K'}{K}\right) - i\,\sin\left(\frac{n\pi u}{2K}\right)\sinh\left(\frac{n\pi K'}{K}\right)\right]$$

$$= \frac{1}{K}\cosh\left(\frac{n\pi K'}{K}\right)\int_{-K}^{K} cn(u,k)\,\cos\left(\frac{n\pi u}{2K}\right)\,du$$

$$= \cosh\left(\frac{n\pi K'}{K}\right)\,A_I$$

where A_I equals the integral on path I (which determines a_n). Employing the residue theorem and Table 1.7, we get:

$$(1.40)\quad A_I + A_{IV} = (1 + \cosh(\frac{n\pi K'}{K})\, A_I = 2\cosh^2(\frac{n\pi K'}{2K})\, A_I$$
$$= 2\pi i \frac{1}{K}(-\frac{i}{k})\cos(\frac{n\pi iK'}{2K}) = \frac{2\pi}{kK}\cosh(\frac{n\pi K'}{2K})$$

Solving for A_I, we find:

$$(1.41)\qquad A_I = a_n = \frac{\pi}{kK}\,\mathrm{sech}(\frac{n\pi K'}{2K})\ ,\ n \text{ odd}$$

The Fourier series for sn, cn, dn, Z, and TH(u,k) are given in in eqs.(1.42). In addition, the expansion for the am function is shown.

$$(1.42a)\quad \mathrm{sn}(u,k) = \frac{\pi}{kK}\sum_{n=0}^{\infty}\mathrm{csch}\left[\frac{(2n+1)\pi K'}{2K}\right]\sin\left[\frac{(2n+1)\pi u}{2K}\right]$$

$$(1.42b)\quad \mathrm{cn}(u,k) = \frac{\pi}{kK}\sum_{n=0}^{\infty}\mathrm{sech}\left[\frac{(2n+1)\pi K'}{2K}\right]\cos\left[\frac{(2n+1)\pi u}{2K}\right]$$

$$(1.42c)\quad \mathrm{dn}(u,k) = \frac{\pi}{2K} + \frac{\pi}{K}\sum_{n=1}^{\infty}\mathrm{sech}\left[\frac{n\pi K'}{K}\right]\cos\left[\frac{n\pi u}{K}\right]$$

$$(1.42d)\quad Z(u,k) = \frac{\pi}{K}\sum_{n=1}^{\infty}\mathrm{csch}\left[\frac{n\pi K'}{K}\right]\sin\left[\frac{n\pi u}{K}\right]$$

$$(1.42e)\quad \mathrm{TH}(u,k) = \ln\xi - \frac{1}{2}\ln\frac{2k'K}{\pi} - \sum_{n=1}^{\infty}\frac{1}{n}\mathrm{csch}\left[\frac{n\pi K'}{K}\right]\cos\left[\frac{n\pi u}{K}\right]$$

where ξ = Euler's number $\simeq$ .57721566

$$(1.42f) \qquad \mathrm{am}(u,k) = \frac{\pi u}{2K} + \sum_{n=1}^{\infty} \frac{1}{n} \operatorname{sech}\left[\frac{n\pi K'}{K}\right] \sin\left[\frac{n\pi u}{K}\right]$$

The expansions in (1.42) are valid for $0 < k^2 < 1$. For $k^2 \in \{0,1\}$, consult Table 1.1, Table 1.3, eqs.(1.2), and eqs.(1.6). For other k^2 values, one must compute in the transformed variables (i.e., in the (v,k_1) or (w,k_2) systems) because Fourier series do not transform to Fourier series under modulus transformations. Note also that knowing the expansion for am, one immediately can find sn, cn, and dn from eqs.(1.2) and eqs.(1.3).

The expansions for these elliptic integrals and functions have been programmed both in MACSYMA and Fortran. Program listings in both of these languages are provided in Appendix C.

2.0 Variational equations

Much preliminary work must be done before we may apply the method of averaging. First, we define the unperturbed system corresponding to eq.(0.1) and find its solution explicitly in terms of elliptic functions. The solution will contain two arbitrary constants of integration. Second, we apply variation of parameters to eq.(0.1). This involves looking for a solution to eq.(0.1) in the form generated by the unperturbed solution, but with the constants of integration taken to be unspecified functions of time (i.e., these constant parameters are allowed to vary in time). The result of this procedure will be differential equations (i.e., the variational equations) that the varied parameters must satisfy in order that the assumed solution form hold.

Next, we make a change of variables to a better set that are suitable for averaging. This is an important step, since the method of averaging (in its simplest form) requires that the variational equations be periodic (or be a sum periodic terms, see chapter 10). Finally, we comment on the Hamiltonian nature of the unperturbed problem as it relates to our choice of variables.

2.1 The unperturbed system

We define the unperturbed system corresponding to eq.(0.1) as the system arising from eq.(0.1) in which ϵ g is taken to be zero and τ in $\alpha(\tau)$ and $\beta(\tau)$ is taken as fixed (but τ NOT necessarily zero):

$$x'' + \alpha(\tau)\, x + \beta(\tau)\, x^3 = 0 \tag{2.1}$$

The general solution to eq.(2.1) may be found in many ways, but we pursue an enlightening path. First, we assume a solution form for (2.1) consisting of one elliptic function, cn(u,k). This is motivated by (1.12b). We choose to use cn as it closely resembles the cos solution of the linear oscillator. The solution x and its derivatives are:

$$x = r\, cn(u,k)\ ,\ u = a\, t + u_0 \tag{2.2a}$$

$$x' = r \frac{dcn}{dt} = r \frac{\partial cn}{\partial u} \frac{du}{dt} = r\, a \frac{\partial cn}{\partial u} = r\, a\, cn' \tag{2.2b}$$

$$x'' = r \frac{d^2 cn}{dt^2} = r\, a^2 \frac{\partial^2 cn}{\partial u^2} = r\, a^2\, cn'' \tag{2.2c}$$

where we have used the shorthand notation cn' and cn'' for derivatives with respect to the argument u. In (2.2), r, a, k, and

u_0 are undetermined constants. Substituting (2.2) into eq.(2.1) and using (1.12b), we find:

$$(2.3) \qquad r\left[a^2\,(2k^2 - 1) + \alpha\right] cn + r\left[\beta\, r^2 - 2k^2\, a^2\right] cn^3 = 0$$

This implies two relations among the four undetermined constants, which leaves us with two arbitrary constants (as we expect for the general solution). These relations are:

$$(2.4) \qquad a^2\,(1 - 2k^2) = \alpha \quad \text{and} \quad 2k^2\, a^2 = \beta\, r^2$$

We choose r and u_0, the amplitude and initial phase angle, as our arbitrary constants. Then a^2 and k^2 are found from (2.4):

$$(2.5) \qquad k^2 = \frac{\beta\, r^2}{2\,(\alpha + \beta\, r^2)} \quad \text{and} \quad a^2 = \alpha + \beta\, r^2$$

Eq.(2.1) is now completely solved, since we have defined cn(u,k) for any $k^2 \in [-\infty,\infty]$ by the modulus transformations (see section 1.2).

In (2.5), we take k to be either positive for $k^2 \geq 0$ or purely imaginary in the upper half of the complex plane (i.e., $k = i\,\bar{k}$ where $\bar{k} > 0$) for $k^2 < 0$. Since elliptic integrals and functions depend on k^2 and not k, this choice does not affect the solution. It is convenient, however, because this is assumed in expansions which seem to depend on k rather than k^2.

From (2.5), we see that the value of a may be either real or imaginary. This indicates a critical difference in the types of solutions that (2.2) represents. For imaginary a, solution (2.2) is not an oscillation, because the cn function with imaginary argument is non-periodic. As we are concerned with oscillatory nature of eq.(0.1), we restrict ourselves to real a. (This restriction is mild, as will be seen).

Moreover, the choice of the sign of a in (2.5) is immaterial, since a change in the sign of a is equivalent to a change in the direction of time. Thus, we let $a > 0$. Further, the choice of the sign of r is immaterial <u>if</u> cn takes on both positive and negative values (since a change in the sign of r is then equivalent to a phase change). This is the case except when $k^2 > 1$, since cn(u,k) behaves like dn then. For emphasis of this case, we take r as positive but now include in (2.2) a sign parameter μ (which is either +1 or -1) to indicate the sign of r <u>if it cannot be taken as positive</u>.

Hence, the general solution to eq.(2.1) is written:

(2.6a) $$x = \mu\, r\, cn(u,k)$$

(2.6b) $$x' = \mu\, r\, a\, cn'(u,k)$$

(2.6c) $$a^2 = \alpha + \beta\, r^2 \;,\; u = a\, t + u_0 \;,\; k^2 = \frac{\beta\, r^2}{2\,(\alpha + \beta\, r^2)}$$

(2.6d) $$a \geq 0 \;,\; r \geq 0 \;,\; k^2 \in [-\infty,\infty] \;,\; \mu = \pm 1$$

From (2.5), we see that the value of a may be either real or imaginary. This indicates a critical difference in the types of solutions that (2.2) represents. For imaginary a, solution (2.2) is not an oscillation, because the cn function with imaginary argument is non-periodic. As we are concerned with oscillatory nature of eq.(0.1), we restrict ourselves to real a. (This restriction is mild, as will be seen).

Moreover, the choice of the sign of a in (2.5) is immaterial, since a change in the sign of a is equivalent to a change in the direction of time. Thus, we let $a > 0$. Further, the choice of the sign of r is immaterial <u>if</u> cn takes on both positive and negative values (since a change in the sign of r is then equivalent to a phase change). This is the case except when $k^2 > 1$, since cn(u,k) behaves like dn then. For emphasis of this case, we take r as positive but now include in (2.2) a sign parameter μ (which is either +1 or -1) to indicate the sign of r <u>if it cannot be taken as positive</u>.

Hence, the general solution to eq.(2.1) is written:

(2.6a) $$x = \mu\, r\, cn(u,k)$$

(2.6b) $$x' = \mu\, r\, a\, cn'(u,k)$$

(2.6c) $$a^2 = \alpha + \beta\, r^2 \;,\; u = a\, t + u_0 \;,\; k^2 = \frac{\beta\, r^2}{2\,(\alpha + \beta\, r^2)}$$

(2.6d) $$a \geq 0 \;,\; r \geq 0 \;,\; k^2 \in [-\infty, \infty] \;,\; \mu = \pm 1$$

A closer look at eq.(2.1) shows that it possesses a first integral, the energy h, found by multiplying eq.(2.1) by x' and integrating:

$$h = \frac{1}{2} x'^2 + \frac{1}{2} \alpha x^2 + \frac{1}{4} \beta x^4 \tag{2.7}$$

Eq.(2.7) holds even when τ is allowed to vary. Substituting eqs.(2.6) into (2.7), we find an expression for h in terms of r or k^2:

$$h = \frac{1}{4} r^2 (2\alpha + \beta r^2) = \frac{\alpha^2}{\beta} \frac{k^2 k'^2}{(1 - 2k^2)^2} \tag{2.8}$$

Since h is conserved on the solutions of (2.1), contours of h(x,x') correspond to solutions of (2.1) in (x,x') phase plane. These phase portraits are shown in Fig.2.1 in the α-β parameter plane.

The α-axis and β-axis define 9 regions of the α-β parameter plane. Identification of these regions and a short description of the corrsponding phase portraits that they indicate are given in Table 2.1. Types of equilibria (centers and saddles) and types of separatrices are indicated. (A separatrix is an orbit which is either forward or backward (or both) asymptotic to a saddle.)

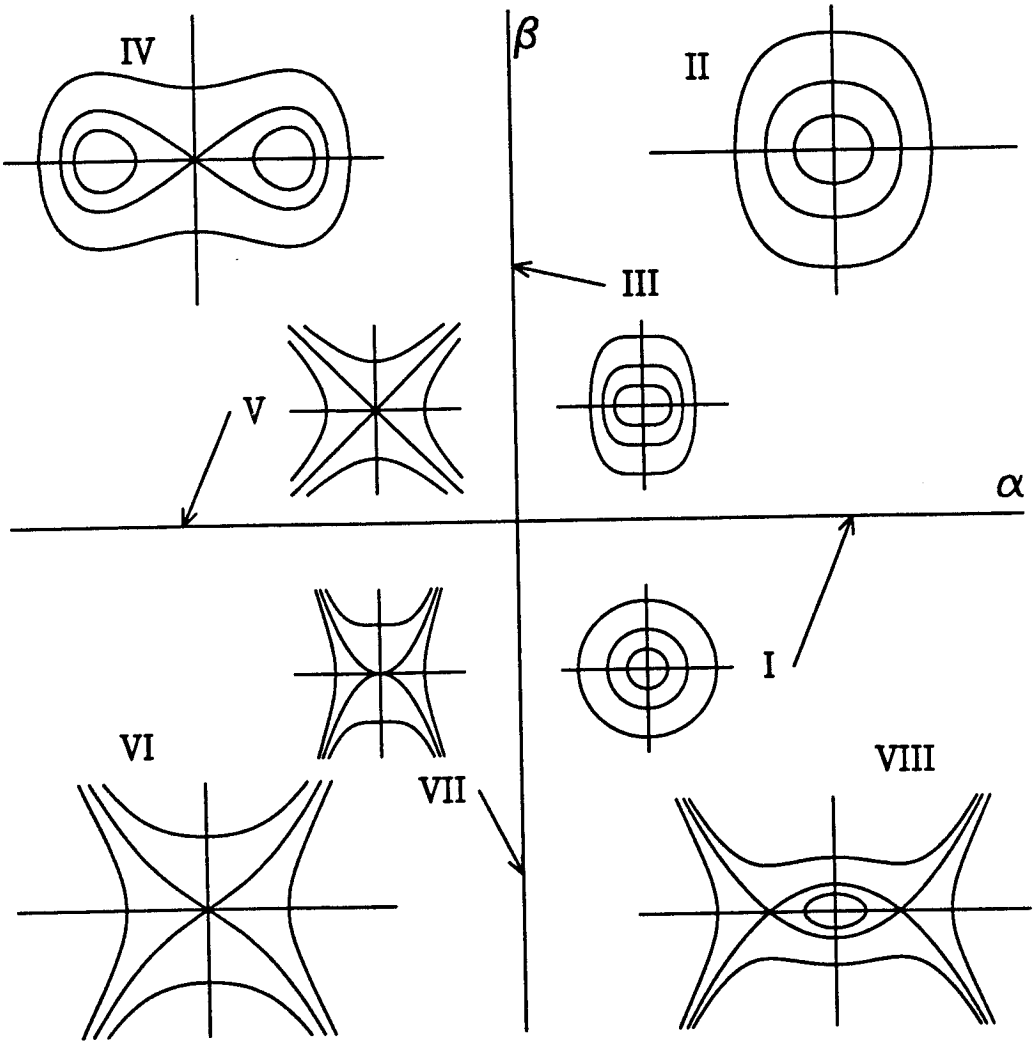

Fig.2.1 Regions I-VIII identified in the α-β parameter plane. For each region, a qualitative picture of a typical x-x' phase portrait is shown. Region 0, the origin, is not shown.

Table 2.1 The α-β Parameter plane

Region	Range of α	Range of β	Description of typical phase portrait
0	0	0	Lines parallel to x-axis, which is a line of equilibria
I	$(0,\infty)$	0	Circles about center at origin; each orbit has same period (linear case).
II	$(0,\infty)$	$(0,\infty)$	Ellipses about center at origin
III	0	$(0,\infty)$	Ellipses about center at origin
IV	$(-\infty,0)$	$(0,\infty)$	Double homoclinic loop separatrix which separates two inside regions of closed orbits from one outside region of closed orbits
V	$(-\infty,0)$	0	Linear separatrix at origin (linear case)
VI	$(-\infty,0)$	$(-\infty,0)$	Separatrix at origin; no closed orbits
VII	0	$(-\infty,0)$	Separatrix tangent to x-axis; no closed orbits
VIII	$(0,\infty)$	$(-\infty,0)$	Separatrix (connecting two saddles) surrounds ellipses about center at origin

We understand Fig.2.1 in terms of the bifurcations in the phase portraits that occur as one traverses the α-β parameter plane counter-clockwise (from I to VIII). By comparing regions VIII with II, we find that two heteroclinic saddles (i.e., saddles which connect to each other) disappear upon crossing region I. Thus, region I (the linear oscillator case) contains a heteroclinic orbit at infinity.

The next bifurcation is a pitchfork occurring in region III, at the origin, where a new center and a saddle are born. As α decreases from 0, the two centers move away from the saddle which stays at the origin. A double homoclinic loop separatrix surrounds the two centers, dividing three regions of closed orbits (i.e., the saddle connects with itself in a figure 8). This separatrix must persist in region V, connecting at infinity.

The last bifurcation, again a pitchfork, occurs in region VII where the bifurcation is of opposite stability than that of region III. In region VII, a new saddle and a center are born and the arms of the separatrix become tangent. As α increases, they pass through each other, connecting between the two saddles, which have moved apart. In this way, the arms of separatrix open a region of closed orbits about the origin.

The equilibria and separatrices of a phase portrait fully determine the global dynamical behavior. Equilibria signal steady-state solutions of eq.(2.1); the separatrices separate

qualitatively different dynamical behavior. We now determine these structures in terms of solution (2.6).

Regions I, II, III each have one center at the origin and no separatrices. The center's location in the (x,x') phase space, energy h, amplitude square r^2, and k^2 value are given in (2.9).

(2.9) Center at (0,0) : $h = r^2 = 0$

Region I and II : $k^2 = 0$, Region III: $k^2 = \frac{1}{2}$

Region IV has two saddles, one center, and a double homoclinic loop separatrix. Its equilibria location, h, r^2, and k^2 values are:

Saddle at (0,0) : $h = r^2 = k^2 = 0$

(2.10) Separatrix : $h = 0$, $r^2 = 2\frac{|\alpha|}{\beta}$, $k^2 = 1$, $\mu = \pm 1$

Centers at $(\pm\sqrt{\frac{|\alpha|}{\beta}}, 0)$: $h = -\frac{\alpha^2}{4\beta}$, $r^2 = \frac{|\alpha|}{\beta}$, $k^2 = \infty$

From (2.10), we see that $h > 0$ corresponds to orbits outside the separatrix, $h = 0$ to the separatrix itself, and $h < 0$ to orbits inside. Note that for $h < 0$, two orbits (a right and left orbit) correspond to one value of h. In that case, one interprets solution (2.6) using the reciprocal modulus transformation (see section 1.2, Table 1.5).

Region VIII contains two saddles, one center, and a heteroclinic separatrix. Its h, r^2, and k^2 values are given by (2.11).

$$\text{Center at } (0,0) : h = r^2 = k^2 = 0$$

(2.11) $$\text{Saddles at } \left(\pm\sqrt{\frac{|\alpha|}{\beta}},0\right) : h = -\frac{\alpha^2}{4\beta},\ r^2 = \frac{\alpha}{|\beta|},\ k^2 = -\infty$$

$$\text{Separatrix} : h = -\frac{\alpha^2}{4\beta},\ r^2 = \frac{\alpha}{|\beta|},\ k^2 = -\infty,\ \mu = \pm 1$$

Solution (2.6) must be interpreted using the reciprocal complementary modulus transformation (see section 1.2, Table 1.6).

Finally, we include a figure to show the relation between k^2 in (2.6) to the phase portraits in Fig.2.1. This is given as Fig.2.2.

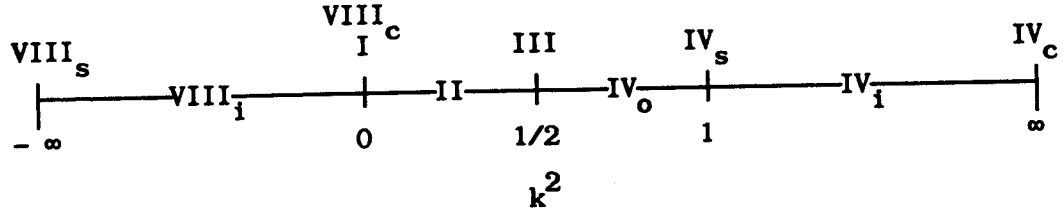

Fig.2.2 Relation between k^2 and regions of Fig.2.1. as k^2 ranges from $-\infty$ to $+\infty$. Subscript s indicates a separatrix; subscript i indicates areas inside separatrices; subscript o indicates areas outside separatrices; and subscript c indicates a center equilibrium.

2.2 Variation of parameters

We are now able to apply variation of parameters to eq.(0.1) using the unperturbed solution (2.6). We look for a solution to

eq.(0.1) in the form of (2.6), where we allow the two undetermined constants r and u_0 to be unspecified functions of time, i.e., $r = r(t)$ and $u_0 = u_0(t)$. Furthermore, we now allow τ to vary ($\tau = \epsilon t$) in both eq.(0.1) and solution form (2.6). Note that the variables a and k appearing in (2.6c) depend on the three time-varying parameters $r(t)$, $\alpha(\tau)$, and $\beta(\tau)$.

Differentiating x in (2.6a) once, we find:

$$(2.12)\quad \frac{dx}{dt} = \mu r' \, cn + \mu r \frac{dcn}{dt}$$
$$= \mu r' \, cn + \mu r \left[\frac{\partial cn}{\partial u} u' + \frac{\partial cn}{\partial k} k'\right]$$
$$= \mu r' \, cn + \mu r \left[cn' \, (a + a' \, t + u_0') - cn' \, \frac{du}{dk} k'\right]$$
$$= \mu r \, a \, cn' + \mu r' \, cn + \mu r \, cn' \left[a' \, t + u_0' - \frac{du}{dk} k'\right]$$

where we have used (1.10b). We now find a' and k':

$$(2.13a)\qquad a' = \epsilon \frac{1}{2a} \left(\frac{d\alpha}{d\tau} + \frac{d\beta}{d\tau} r^2\right) + \beta \frac{r}{a} r'$$

$$(2.13b)\qquad k' = 2 \frac{\alpha}{\beta} \frac{k^3}{r^3} r' + \epsilon \frac{k^3}{\beta^2 r^2} \left(\alpha \frac{d\beta}{d\tau} - \beta \frac{d\alpha}{d\tau}\right)$$

So, (2.12) becomes:

$$(2.14)\quad \frac{dx}{dt} = \mu r \, a \, cn' + \mu r' \left[cn + \beta \frac{r^2}{a} t \, cn' - 2 \frac{\alpha}{\beta} \frac{k^3}{r^2} \frac{du}{dk} cn'\right]$$
$$+ \mu r \, cn' \, u_0' + \frac{\epsilon}{2} \mu \frac{d\alpha}{d\tau} cn' \frac{r}{a} \left[t + \frac{k}{a} \frac{du}{dk}\right]$$
$$+ \frac{\epsilon}{2} \mu \frac{d\beta}{d\tau} cn' \frac{r}{a} \left[r^2 t - \frac{\alpha}{\beta} \frac{k}{a} \frac{du}{dk}\right]$$

Differentiating x' in (2.6b) once, we find:

$$(2.15)\quad \frac{dx'}{dt} = \mu\,(r\,a' + a\,r')\,cn' + \mu\,r\,a\,\frac{dcn'}{dt}$$
$$= \mu\,(r\,a' + a\,r')\,cn'$$
$$+ \mu\,r\,a\left[cn''\,(a + a'\,t + u_0') + \frac{\partial cn'}{\partial k}\,k'\right]$$

We find from identities (1.10) and (1.12) that:

$$(2.16)\qquad \frac{\partial cn'}{\partial k} = -\frac{\partial(sn\ dn)}{\partial k} = cn''\,\frac{du}{dk} + k\,\frac{sn^3}{dn}$$

Thus, (2.15) becomes (after some simplifications):

$$(2.17)\quad \frac{dx'}{dt} = \mu\,r\,a^2\,cn''\,u_0'$$
$$+ \mu\,r'\left[2\,a\,k^2 + a\,cn' + \alpha\,\frac{k^2}{a}\,\frac{sn^3}{dn} + cn''\left[\alpha\,\frac{k}{a}\,\frac{du}{dk} + \beta\,r^2\,t\right]\right]$$
$$+ \frac{\epsilon}{2}\,\mu\,\frac{d\alpha}{d\tau}\,\frac{r}{a}\left[cn' - k^2\,\frac{sn^3}{dn} + a\,cn''\left[t - \frac{k}{a}\,\frac{du}{dk}\right]\right]$$
$$+ \frac{\epsilon}{2}\,\mu\,\frac{d\beta}{d\tau}\,\frac{r}{a}\left[r^2\,cn' + \frac{\alpha}{\beta}\,k^2\,\frac{sn^3}{dn} + cn''\left[r^2\,a\,t + \frac{\alpha}{\beta}\,k\,\frac{du}{dk}\right]\right]$$

We now generate two equations for the two unknowns r' and u_0'. First, set $\frac{dx}{dt}$ in eq.(2.14) equal to x' in (2.6b):

$$(2.18)\quad 0 = \mu\, r' \left[cn + \beta \frac{r^2}{a}\, t\, cn' - 2\, \frac{\alpha}{\beta} \frac{k^3}{r^2} \frac{du}{dk}\, cn'\right] + \mu\, r\, cn'\, u_0' + \frac{\epsilon}{2} \mu \frac{d\alpha}{d\tau}\, cn'\, \frac{r}{a} \left[t + \frac{k}{a} \frac{du}{dk}\right] + \frac{\epsilon}{2} \mu \frac{d\beta}{d\tau}\, cn'\, \frac{r}{a} \left[r^2\, t - \frac{\alpha}{\beta} \frac{k}{a} \frac{du}{dk}\right]$$

Second, substitute (2.17) for x'' in eq.(*):

$$(2.19)\quad 0 = \epsilon\, \mu\, g + \mu\, r\, a\, cn''\, u_0' + \mu\, r' \left[2\, a\, k^2 + a\, cn' + \alpha \frac{k^2}{a} \frac{sn^3}{dn} + cn'' \left[\alpha \frac{k}{a} \frac{du}{dk} + \beta\, r^2\, t\right]\right] + \frac{\epsilon}{2} \mu \frac{d\alpha}{d\tau} \frac{r}{a} \left[cn' - k^2 \frac{sn^3}{dn} + a\, cn'' \left[t - \frac{k}{a} \frac{du}{dk}\right]\right] + \frac{\epsilon}{2} \mu \frac{d\beta}{d\tau} \frac{r}{a} \left[r^2\, cn' + \frac{\alpha}{\beta} k^2 \frac{sn^3}{dn} + cn'' \left[r^2\, a\, t + \frac{\alpha}{\beta} k \frac{du}{dk}\right]\right]$$

Eqs.(2.18) and (2.19) can now be solved for r' and u_0'.

The computations given above and the solutions for r' and u_0' were computed both by hand and by computer algebra (MACSYMA). The derivation, as performed by MACSYMA, is listed in Appendix D. The solutions for r' and u_0' are given in eq.(2.20).

$$(2.20a)\quad r' = -\epsilon \frac{1}{a}\, g\, cn' + \frac{\epsilon}{2} \frac{d\alpha}{d\tau} \frac{r}{a^2} (cn^2 - 1) + \frac{\epsilon}{4} \frac{d\beta}{d\tau} \frac{r^3}{a^2} (cn^4 - 1)$$

$$(2.20b)\quad u_0' = u' - a - a'\, t = u' - a - (u - u_0) \frac{a'}{a}$$

where

$$u' = a + \epsilon \frac{1}{ra} g \left(cn - \frac{\alpha}{a^2} k \frac{du}{dk} cn'\right) \tag{2.20c}$$

$$+ \frac{\epsilon}{2} \frac{d\alpha}{d\tau} \frac{1}{a^2} \left[\frac{cn\ cn'}{dn^2} - \frac{1}{a^2} 2\ k \frac{du}{dk} (\beta\ r^2 - \alpha\ cn^2 + 2\ \alpha)\right]$$

$$+ \frac{\epsilon}{4} \frac{d\beta}{d\tau} \frac{r^2}{a^2} \left[\frac{(cn^2 + 1)\ cn\ cn'}{dn^2} + \frac{1}{a^4} \frac{\alpha}{k} \frac{du}{dk} (\beta\ r^2\ cn^4 + \beta\ r^2 + 2\ \alpha)\right]$$

Close examination of eqs.(2.20) show that the r' equation is periodic in u but the equation for u_0' is (in general) not. The non-periodicity arises from two sources: (1) the $(u - u_0)$ term and (2) the $\frac{du}{dk}$ term in u' (it does not vanish in general). This makes eq.(2.20a) in the correct form for averaging while eqs.(2.20b) and (2.20c) are not.

This result is expected and can be explained in terms of the stability of the unperturbed solution. Although each orbit in phase space in orbitally stable (with the exception of the separatrix in region IV) [Hag82,Min62,Sto50], it is Lyapunov unstable (with exception of region I). This is because the frequency of an orbit depends on its amplitude, so that motions starting close together but on two different orbits eventually become far apart (i.e., out of phase), even though their orbits remain close. This "phase shear" instability is reflected in the equations for u_0. The orbital stability is reflected in the equation for r.

In region I, the linear case, orbits are both orbitally and Lyapunov stable. The equation for u_0' is periodic then and <u>each</u> of eqs.(2.20) can be averaged.

In region III, orbits are only orbitally stable and u_0' is non-periodic; however, u' is periodic. This is a result of using elliptic functions with argument u. The value of k^2 is constant over the entire phase space (being equal to $\frac{1}{2}$) so that the period in u for every orbit is the same (although in time t, the period is orbit dependent). The variable u reflects changes in the time-frequency of different orbits. In this instance, eqs.(2.20a) and (2.20c) can be used for averaging.

In general, then, the equations for u_0 and u in (2.20) are non-periodic and unsuitable for averaging. We would like to define a new angle variable whose variational equation will be periodic. Since this variable must account for period changes in u on different orbits, a natural choice is φ, where φ is defined in (2.21).

$$u = 4\,K\,\varphi \tag{2.21}$$

The variational equation can be found from eqs.(2.20).

$$u' = 4\,\frac{dK}{dk}\,k'\,\varphi + 4\,K\,\varphi' = \frac{u}{K}\,\frac{dK}{dk}\,k' + 4\,K\,\varphi' \tag{2.22a}$$

$$\varphi' = \frac{1}{4K}\left[u' - \frac{u}{K}\,\frac{dK}{dk}\,k'\right] \tag{2.22b}$$

(We note that φ is not independent of k, so that $\frac{du}{dk}$ is defined by (1.8b)). After simplification, we get:

$$(2.23)\quad \varphi' = \frac{a}{4K} + \epsilon g \frac{2\alpha(\alpha+\beta r^2)(cn - Z\,cn') + \alpha\beta r^2 cn^3 + \beta^2 r^4 cn}{4K r (\alpha+\beta r^2)^{3/2}(2\alpha+\beta r^2)}$$

$$+ \epsilon \frac{d\alpha}{d\tau} \frac{\alpha Z cn^2 - (2\alpha+\beta r^2) Z + \alpha\, cn\, cn'}{4K(\alpha+\beta r^2)(2\alpha+\beta r^2)}$$

$$+ \epsilon \frac{d\beta}{d\tau} \frac{\left[\alpha\beta r^2\left[Z\,cn^4 + Z + cn\,cn'(2+cn^2)\right] + 2\alpha^2 Z + \beta^2 r^4 cn\, cn'\right]}{8K\beta(\alpha+\beta r^2)(2\alpha+\beta r^2)}$$

Eq.(2.23) is periodic in the argument u with period 4 K. It is also periodic in φ (via eq.(2.21)) with period 1 independent of orbit.

Thus, we use the independent variables (r,φ) in the averaging scheme, where the variational equations are given by eq.(2.20a) and eq.(2.23). The form of the equations can be written as:

$$(2.24a)\qquad r' = \epsilon F_1(r,\varphi,\tau,t)$$

$$(2.24b)\qquad \varphi' = \Omega(r,\tau) + \epsilon F_2(r,\varphi,\tau,t)$$

In this way, the right hand sides of the variational equations are viewed as functions of (r,φ,t,τ) alone. Eq.(2.6c) defines a and k as functions of r and eq.(2.21) defines u in terms of k and φ.

We observe that the sign parameter μ is not contained in the variational equations. Moreover, μ has not as yet been determined.

This is done now. For system points belonging to any region of Fig.2.1 other than region IV, simply take $\mu \equiv 1$. For system points belonging to region IV, μ is chosen to insure continuity as an orbit crosses the separatrix.

For example, let $\mu = 1$ and let the system point be located within the right separatrix loop. Let t^* be the time just before the point's orbit crosses the separatrix. Inside the separatrix, the cn(u,k) solution in (2.6) acts like a dn(v,k_1) function (see Table 1.5). After crossing, the cn(u,k) function may be either in-phase or out-of-phase with the dn(v,k_1) function at t^*. If it is out-of-phase, then we must take $\mu = -1$ to insure continuity of x and x'. Thus, μ is determined dynamically (i.e., at the time of separatrix crossing) and not beforehand by any equation.

Systems belonging to either regions I or III represent exceptional cases in the α-β parameter plane in which the general variational equations are greatly simplified. This permits investigations to proceed further than in the general case. Perturbations of the linear oscillator (region I) have been studied by many reseachers [Nay73,Nay79,Hag82,Kev81,San85,Sto50]. Computer algebra codes have recently been written to perform the averaging method to any desired order [Ran87]. As this case is exceptional in the α-β plane (Fig.2.1) and well-known, we will not be concerned with it (but note the comparison of the linear case with the nonlinear one in chapter 5).

Little research has been done on the cubic oscillator (region III), perhaps because elliptic functions are not generally well-known to researchers concerned with vibrations. Because of this, we include a specialization and extension of our general theory for this case (see chapter 3).

2.3 Hamiltonian variables

We presented the energy integral associated with eq.(2.1) in (2.7). Eq.(2.7), then, defines a Hamiltonian function of the variables (x,x') for (2.1):

$$H(x,x') = \frac{1}{2} x'^2 + \frac{1}{2} \alpha(\tau)\, x^2 + \frac{1}{4} \beta(\tau)\, x^4 \tag{2.25}$$

The variable τ is <u>not</u> taken as fixed. The action variable J associated with (2.25) is simply the (instantaneous) area enclosed by an orbit, i.e., the area enclosing an orbit for the τ-fixed system of (2.25) [Gol80]. This is easily calculated with solution (2.6) known:

$$J = \oint x'\, dx = \frac{4}{3} a \frac{r^2}{k^2} \left[(2k^2 - 1)\, E(k) + k'^2\, K(k) \right] \tag{2.26}$$

More accurately, J as defined by (2.26) is the instantaneous area associated with an orbit's energy h. Thus, J is <u>twice</u> the area enclosed by an orbit that is located within either the left or right separatrix loop of region IV; otherwise, J simply equals the area.

Eq.(2.26) defines J in terms of r (depending on the parameters α and β). If we express r as a function of h by inverting (2.8), J becomes a function of h. If we can invert this relation between J and h, writing h = h(J), we can express the Hamiltonian function as a function only of the action variable. From there, we can call upon much of Hamiltonian theory. This is the precise procedure followed in the case of the linear oscillator. However, relation (2.26) is not invertible explicitly in r or h (as it is in the linear oscillator). So, the advantages of an action-angle formulation disappear when considering the nonlinear system.

Therefore, we have chosen to use r rather than J in our averaging procedure. The amplitude r functions in a similar manner to J, but is generally not conserved for $\epsilon \neq 0$. Knowing r, we can explicitly calculate the solution (x,x') in (2.6). Furthermore, J is not differentiable for $k^2 = 1$ (the separatrix in region IV), whereas r is (this is important for orbits which cross such a separatrix).

Finally, we note that the angle variable conjugate to J is the variable φ defined in (2.21).

3.0 Averaging

The variational equations derived in chapter 2 generally cannot be solved explicitly. We can, however, compute approximate solutions using an asymptotic approximation method. Many asymptotic methods for the approximation of solutions to differential equations exist [Kev81], including multiple scales [Nay73], the method of Kuzmak-Luke [Kev81], two-variable expansion [Kev81], and the method of averaging [Nay73,Nay79,Kev81,San85,Hag82,Min62,Sto50]. We choose to use the method of averaging since the method lies on a solid mathematical foundation. In addition, the method can be implemented efficiently in the computer algebra system MACSYMA.

Historically, the averaging method goes back to Lagrange, Laplace, and others in the late 18^{th} century. They employed a heuristic argument to average small perturbations on a celestial body over one period in the body's orbit. Poincare [Poi57] then introduced the idea of asymptotic approximations which were valid in the limit that the perturbation vanishes. In the 1930's in the Soviet Union, Krylov and Bogoliubov [Kry37] formalized the method and provided proofs of its validity. This was extended by Bogoliubov and Mitropolsky [Bog61] in the 1960's. In the U.S., Hale [Hal63] and Sethna [Set67] (among others) developed the asymptotic theory of

averaging. A more recent work on the subject is Sanders and Verhulst [San85].

Many authors have applied the method of averaging to nonlinear differential equations: Nayfeh [Nay73], Kevokian and Cole [Kev81], Minorsky [Min62], Stoker [Sto50], Hagedorn [Hag82], Nayfeh and Mook [Nay79], Guckenheimer and Holmes [Guc86], and Mitropolsky [Mit65]. These texts are mainly concerned with perturbations of the linear oscillator (i.e., weakly nonlinear systems). The method of averaging for weakly nonlinear systems has been implemented by Rand and Armbruster [Ran87] in MACSYMA.

Several authors have applied the method to strongly nonlinear systems using elliptic functions. Kuzmak [Kuz59] looks for periodic solutions to eq.(0.1) using a multiple scale method. Bourland and Haberman [Bou88] is a generalization and extension of that work. Davis [Dav62] investigates second order ordinary differential equations. Cap [Cap73] studies the perturbed nonlinear pendulum. Chirikov [Chi79] studies resonance overlap in multiple harmonic excitations of eq.(0.1). Pocobelli [Poc81] studies adiabatic invariance in the the slowly varying nonlinear pendulum equation. Yuste and Bejarano [Yus86] investigate the perturbed cubic oscillator. Garcia-Margallo and Bejarano [Gar] find limit cycles in a generalized van der Pol oscillator using generalized harmonic balance.

Following Nayfeh [Nay73], we apply the method of averaging to the variational equations, using a near-identity transformation to

new variables. The resulting differential equations on the new variables (i.e., the averaged equations) will be shown to be simpler than the variational equations themselves. The solution to these averaged equations will be the approximate solution. We then comment on the validity and accuracy of the averaging method.

An analysis of the computations involved in each step of the procedure will be shown. The results of this analysis take the form of a MACSYMA computer program which implements the averaging procedure for arbitrary $\alpha(\tau)$, $\beta(\tau)$, and $g(x,x',\tau)$ of eq.(0.1) (the case for g depending on time explicitly is discussed separately).

3.1 The averaging procedure

From the beginning, it is necessary to distinguish two different classes of problems: (1) g does not depend on t but may depend on τ and (2) g depends on t explicitly. The procedure for case (2) will be given in chapter 10 where such a perturbation first appears. The procedure for case (1) will be discussed in this chapter.

For convenience, we write the variational equations, eqs.(2.20a) and (2.23) in the compact form of (3.1).

$$r' = \epsilon F_1(r,\varphi,\tau) \tag{3.1a}$$

$$\varphi' = \Omega(r,\tau) + \epsilon F_2(r,\varphi,\tau) \tag{3.1b}$$

$$\tau' = \epsilon \tag{3.1c}$$

In (3.1), we have appended an equation on τ so that eqs.(3.1) are three differential equations in the three variables (r,φ,τ). The next step is to define a near-identity transformation of the form:

$$r = \bar{r} + \delta\, T_1 \tag{3.2a}$$

$$\varphi = \bar{\varphi} + \delta\, T_2 \tag{3.2b}$$

where $\delta << 1$ and T_i depends on some of the variables $(r,\varphi,\bar{r},\bar{\varphi},\tau)$ (this choice will be made shortly). The absolute value of T_i is assumed to be bounded so that as $\delta \to 0$, $(r,\varphi) \to (\bar{r},\bar{\varphi})$. This condition is usually satisfied and can be checked after the choice of T_i is made. Eqs.(3.2) are substituted into (3.1) and expanded in a power series of δ, which determine variational equations for $(\bar{r},\bar{\varphi})$. We shall demonstrate that a proper choice of T_i results in equations for $(\bar{r}',\bar{\varphi}')$ that are independent of $\bar{\varphi}$ (i.e, system (3.1) has been averaged over the angle φ).

While the traditional choice for the T_i is that they depend on the new variables $(\bar{r},\bar{\varphi})$, we choose to use a mixed variable approach in which T_i depends on $(\bar{r},\varphi)$. The reasons behind this choice will be made clearer later. With the choice made, we write the transformation in the form:

$$r = \bar{r} + \delta\, w_1(\bar{r},\varphi,\tau) + \delta^2\, v_1(\bar{r},\varphi,\tau) \tag{3.3a}$$

$$\varphi = \bar{\varphi} + \delta\, w_2(\bar{r},\varphi,\tau) + \delta^2\, v_2(\bar{r},\tau,\tau) \tag{3.3b}$$

We would like the averaged system to be of the form (3.4)

$$\text{(3.4a)} \qquad \bar{r}' = \epsilon\, G_1(\bar{r},\tau) + O(\epsilon\delta)$$

$$\text{(3.4b)} \qquad \bar{\varphi}' = \Omega(\bar{r},\tau) + \epsilon\, G_2(\bar{r},\tau) + O(\epsilon\delta)$$

Using (3.4), the time derivatives of w_i and v_i are computed. For notational convenience, we write $\Omega(\bar{r},\tau)$ as $\bar{\Omega}$, $\partial w_1/\partial \bar{r}$ as w_{1r}, $\partial w_1/\partial\varphi$ as $w_{1\varphi}$, $\partial w_1/\partial\tau$ as $w_{1\tau}$, etc.

$$\begin{aligned}\text{(3.5a)}\ w_1' &= w_{1r}\,\bar{r}' + w_{1\varphi}\,\varphi' + w_{1\tau}\,\tau' \\ &= \epsilon\, G_1\, w_{1r} + w_{1\varphi}\left(\bar{\varphi}' + \epsilon\,\frac{dw_2}{dt}\right) + \epsilon\, w_{1\tau} + O(\epsilon\delta) \\ &= \epsilon\, G_1\, w_{1r} + w_{1\varphi}\left[\bar{\Omega} + \epsilon\, G_2 + \epsilon\,(w_{2r}\,\bar{r}' + w_{2\varphi}\,\varphi' + w_{2\tau}\,\tau')\right] \\ &\quad + w_{1\tau}\,\tau' + O(\epsilon\delta+\epsilon^2) \\ &= \bar{\Omega}\, w_{1\varphi} + \epsilon\,(G_1\, w_{1r} + G_2\, w_{1\varphi} + \bar{\Omega}\, w_{1\varphi}\, w_{2\varphi} + w_{1\tau}) + O(\epsilon\delta+\epsilon^2)\end{aligned}$$

$$\text{(3.5b)}\ w_2' = \bar{\Omega}\, w_{2\varphi} + \epsilon\,(G_1\, w_{2r} + G_2\, w_{2\varphi} + \bar{\Omega}\,(w_{2\varphi})^2 + w_{2\tau}) + O(\epsilon\delta+\epsilon^2)$$

$$\text{(3.5c)}\ v_1' = \bar{\Omega}\, v_{1\varphi} + O(\epsilon)$$

$$\text{(3.5d)}\ v_2' = \bar{\Omega}\, v_{2\varphi} + O(\epsilon)$$

Ω and each F_i are now expanded in a power series in δ:

$$\begin{aligned}\text{(3.6a)}\ F_1(r,\varphi,\tau) &= F_1\Big|_{\delta=0} + \delta\,\frac{dF_1}{d\delta}\Big|_{\delta=0} + O(\delta^2) \\ &= F_1(\bar{r},\varphi,\tau) + \delta\, F_{1r}(\bar{r},\varphi,\tau)\, w_1 + O(\delta^2)\end{aligned}$$

$$\text{(3.6b)}\ F_2(r,\varphi,\tau) = F_2(\bar{r},\varphi,\tau) + \delta\, F_{2r}(\bar{r},\varphi,\tau)\, w_1 + O(\delta^2)$$

$$(3.6c)\quad \Omega(r,\tau) = \Omega(\bar{r},\tau) + \delta\,\Omega_r(\bar{r},\tau)\,w_1 + \tfrac{1}{2}\delta^2\,(\Omega_{rr}(\bar{r},\tau)\,w_1^2 + 2\,\Omega_r(\bar{r},\tau)\,v_1) + O(\delta^3)$$
$$= \bar{\Omega} + \delta\,\bar{\Omega}_r\,w_1 + \delta^2\,\bar{\Omega}_r\,v_1 + \tfrac{1}{2}\delta^2\,\bar{\Omega}_{rr}\,w_1^2 + O(\delta^3)$$

Before finding the equations on $(\bar{r}',\bar{\varphi}')$, we choose to relate δ with ϵ. Since ϵ already appears in (0.1) as an asymptotically small quantity, we set $\delta = \epsilon$ for convenience. Substituting (3.3) into (3.1), using (3.5), and using (3.6) gives the following equations on $(\bar{r}',\bar{\varphi}')$:

$$(3.7a)\quad \bar{r}' = \epsilon\left[F_1(\bar{r},\varphi,\tau) - \bar{\Omega}\,w_{1\varphi}\right] + \epsilon^2\left[H_1(\bar{r},\varphi,\tau) - \bar{\Omega}\,v_{1\varphi}\right] + O(\epsilon^3)$$

$$(3.7b)\quad \bar{\varphi}' = \bar{\Omega} + \epsilon\left[F_2(\bar{r},\varphi,\tau) + \bar{\Omega}_r\,w_1 - \bar{\Omega}\,w_{2\varphi}\right] + \epsilon^2\left[H_2(\bar{r},\varphi,\tau) - \bar{\Omega}\,v_{2\varphi}\right] + O(\epsilon^3)$$

where

$$(3.7c)\quad H_1(\bar{r},\varphi,\tau) = F_{1r}(\bar{r},\varphi,\tau)\,w_1 - G_1\,w_{1r} - w_{1\tau} - w_{1\varphi}\,(G_2 + \bar{\Omega}\,w_{2\varphi})$$

$$(3.7d)\quad H_2(\bar{r},\varphi,\tau) = F_{2r}(\bar{r},\varphi,\tau)\,w_1 - G_1\,w_{2r} - w_{2\tau} - w_{2\varphi}\,(G_2 + \bar{\Omega}\,w_{2\varphi}) + \bar{\Omega}_r\,v_1 + \tfrac{1}{2}\bar{\Omega}_{rr}\,w_1^2$$

We are now ready to choose the generating functions w_i and v_i so that eqs.(3.4) hold. In order for each generating function to be bounded for all time, we require w_i and v_i to be periodic in φ. This condition requires $\partial w_i/\partial\varphi$ and $\partial v_i/\partial\varphi$ to be periodic.

Since each F_i is periodic, F_i can be separated into two pieces: (1) a constant value (the mean value $\bar{F}_i$ of F_i) and (2) an oscillating piece $\tilde{F}_i$ with zero mean:

$$F_i = \bar{F}_i + \tilde{F}_i \tag{3.8}$$

where $\bar{F}_i = \frac{1}{1}\int_0^1 F_i \, d\varphi = \frac{1}{4K}\int_0^{4K} F_i(\bar{r},\bar{u},\tau)\, d\bar{u}$ and $\bar{u} = 4\,K(k(\bar{r}))\,\varphi$

We then choose $G_1 = \bar{F}_1$ and $\bar{\Omega}\, w_{1\varphi} = \tilde{F}_1$, guaranteeing that w_1 is periodic in φ:

$$\bar{\Omega}\, w_{1\varphi} = \tilde{F}_1 = F_1 - \bar{F}_1 \tag{3.9a}$$

$$w_1 = \frac{1}{\bar{\Omega}}\int w_{1\varphi}\, d\varphi = \frac{1}{\bar{a}}\int (F_1(\bar{r},\bar{u},\tau) - \bar{F}_1)\, d\bar{u} + w_{10} \tag{3.9b}$$

(3.9c) where $\bar{a} = a(\bar{r})$, $\bar{k} = k(\bar{r})$, $\bar{K} = K(\bar{k})$, $\bar{\Omega} = \frac{\bar{a}}{4\bar{K}}$, and $\bar{u} = 4\bar{K}\varphi$

It is advantageous to choose the integration constant w_{10} so that w_1 itself has zero mean. We are now able to choose $G_2 = \bar{F}_2$ (since w_1 has been made to have zero mean) and $w_{2\varphi}$ as in (3.10).

$$\bar{\Omega}\, w_{2\varphi} = \tilde{F}_2 + \bar{\Omega}_r\, w_1 = F_2 - \bar{F}_2 + \bar{\Omega}_r\, w_1 \tag{3.10a}$$

$$w_2 = \frac{1}{\bar{a}}\int (F_2(\bar{r},\bar{u},\tau) - \bar{F}_2 + \bar{\Omega}_r\, w_1)\, d\bar{u} + w_{20} \tag{3.10b}$$

We again choose the integration constant w_{20} so that w_2 has zero mean. This completes the first order averaging.

The second order averaging proceeds the same way with v_i determined by:

$$v_i = \frac{1}{\bar{a}} \int (H_i - \bar{H}_i)\, d\bar{u} + v_{i0} \tag{3.11}$$

Each integration constant v_{i0} is chosen so that v_i has zero mean. With w_i and v_i determined, we find the averaged equations from (3.7):

$$\bar{r}' = \epsilon\, \bar{F}_1(\bar{r},\tau) + \epsilon^2\, \bar{H}_1(\bar{r},\tau) + O(\epsilon^3) \tag{3.12a}$$

$$\bar{\varphi}' = \bar{\Omega} + \epsilon\, \bar{F}_2(\bar{r},\tau) + \epsilon^2\, \bar{H}_2(\bar{r},\tau) + O(\epsilon^3) \tag{3.12b}$$

Furthermore, the choice of w_i and v_i insures that the transformation specified by (3.3) remains bounded for all time.

We can now simplify H_i using (3.10):

$$H_1(\bar{r},\varphi,\tau) = F_{1r}(\bar{r},\varphi,\tau)\, w_1 - \bar{F}_1\, w_{1r} - w_{1\tau} - w_{1\varphi}\, (F_2 + \bar{\Omega}_r\, w_1) \tag{3.13a}$$

$$H_2(\bar{r},\varphi,\tau) = F_{2r}(\bar{r},\varphi,\tau)\, w_1 - \bar{F}_1\, w_{2r} - w_{2\tau} - w_{2\varphi}\, (F_2 + \bar{\Omega}_r\, w_1) + \bar{\Omega}_r\, v_1 + \frac{1}{2}\, \bar{\Omega}_{rr}\, w_1^2 \tag{3.13b}$$

In this form, H_1 depends <u>only</u> on F_1, F_2, and w_1 (and not w_2). This allows H_1 and $\bar{H}_1$ to be computed without computing w_2. This was the reason for the mixed variable approach in the transformation. Had we

used $(\bar{r},\bar{\varphi})$ in the generating functions, H_1 would depend on w_2. Of course, to first order, both approaches are exactly the same.

We also point out that it is not necessary to compute v_i in order to produce the second order averaged equations (3.12).

3.2 Validity and Accuracy

The averaging procedure of section 3.1 relies upon an implicit assumption, which we now make explicit. In order that equations for w_i and v_i be solvable, the instantaneous frequency $\bar{\Omega}$ must be non-zero. The frequency $\bar{\Omega}$ can be made zero in two ways: (1) by taking a to be zero and (2) by taking K to be infinite. We consider these two conditions separately.

Taking a to be zero, we find (via eq.(2.6c)) that $k^2 = \pm\infty$. For $k^2 = \infty$, we employ the reciprocal modulus transformation (Table 1.5) to find K and evaluate $\bar{\Omega}$:

(3.14a) $$\text{As } k^2 \to \infty,\ k_1^2 \to 0,\ K = k_1 K_1 \to \frac{2\pi}{k} = \frac{2\pi\sqrt{2}\,a}{\sqrt{\beta}\,r}$$

(3.14b) $$\bar{\Omega} = \frac{a}{4K} \to \frac{\sqrt{\beta}\,r\,a}{8\pi\sqrt{2}\,a} = \frac{\sqrt{\beta}\,r}{8\pi\sqrt{2}}$$

From Fig.2.2, $k^2 = \infty$ indicates a center in the phase portrait for a system of region IV (of Fig.2.1). From (2.10), we find the value of r at the center. Then, (3.14b) can be expressed by:

(3.15) $$\bar{\Omega} = \frac{\sqrt{\beta}}{8\pi\sqrt{2}} \frac{\sqrt{|\alpha|}}{\sqrt{\beta}} = \frac{\sqrt{|\alpha|}}{8\pi\sqrt{2}}$$

From (3.15), $\bar{\Omega} = 0$ for $\alpha = 0$. Hence, for a = 0 and $k^2 = \infty$, $\bar{\Omega}$ is non-zero except in the case that $\alpha = 0$. Interpreting this result in terms of region IV of Fig.2.1, we find the averaging procedure is invalid only in a neighborhood of the origin at the time when $\alpha(\tau)$ passes through $\alpha = 0$ (or is identically zero).

The case for a = 0 and $k^2 = -\infty$ follows in the same manner. In this case $\bar{\Omega}$ is found to be:

(3.16a) $$\text{As } k^2 \to -\infty,\ k_2^2 \to 1$$

(3.16b) $$\bar{\Omega} = \frac{\sqrt{2\alpha + \beta r^2}}{4\sqrt{2}K_2} = \frac{\sqrt{\alpha}}{4\sqrt{2}K_2}$$

In this case, however, $\alpha > 0$ so that the condition a = 0 does not imply that $\bar{\Omega}$ is zero.

The condition for $K = \infty$ is satisfied for two values of k^2, $k^2 = -\infty$ and $k^2 = 1$. The $k^2 = -\infty$ condition was explored in (3.16). Although $\alpha > 0$, $K_2 = \infty$ in (3.16b) so that $\bar{\Omega} = 0$ (we choose to view this arising from $K = \infty$ and not from a = 0). From Fig.2.2, we find that $k^2 = -\infty$ corresponds to the separatrix in a phase portrait of a

system belonging to region VIII (of Fig.2.1). Also from Fig.2.2, $k^2 = 1$ is shown to correspond to the separatrix in a system belonging to region IV (of Fig.2.1). Hence, the averaging procedure is invalid in a neighborhood of a separatrix. We remark that this could have been predicted before, since relation (2.21) cannot define φ from u when $K = \infty$.

These two structures where the averaging procedure fails, the center in region III and the separatrix of regions IV and VIII, share one thing in common: the unperturbed orbits in a neighborhood of these structures have arbitrarily high periods. The averaging method fails to work because the time that an orbit can remain in the neighborhood of one of these structures is unbounded. For a discussion of modelling eq.(0.1) near a separatrix, see chapter 9.

The averaging procedure is valid provided a system point's orbit remains away from separatrices (and the center in region III). This condition can be easily checked for by monitoring $k^2(\bar{r})$ in the solutions to the averaged equations (3.12).

The averaging theorem [San85] guarantees that solutions to the averaged equations (3.12) remain ϵ-close to solutions of the variational equations (3.1) for times of $O(\frac{1}{\epsilon})$ for first order averaging:

(3.17a) $$|\bar{r}(t) - r(t)| < \epsilon \quad \text{for } t = O(\tfrac{1}{\epsilon})$$

(3.17b) $$|\bar{\varphi}(t) - \varphi(t)| < \epsilon \quad \text{for } t = O(\tfrac{1}{\epsilon})$$

For second order averaging, the estimates are:

$$(3.18a) \qquad |\bar{r}(t) + \epsilon\, w_1(\bar{r},\varphi) - r(t)| < \epsilon^2 \quad \text{for } t = O(\tfrac{1}{\epsilon})$$

$$(3.18b) \qquad |\bar{\varphi}(t) + \epsilon\, w_2(\bar{r},\varphi) - \varphi(t)| < \epsilon^2 \quad \text{for } t = O(\tfrac{1}{\epsilon})$$

3.3 Computing the averaged equations

The calculations involved in the averaging procedure presented in section 3.1 warrant close inspection. Contrary to the averaging of the perturbed linear system, computing the functions and means necessary in section 3.1 is not trivial. The reason for the complexity is that integrals of elliptic functions cannot be expressed solely in terms of elliptic functions and the argument u (see section 1.4) whereas integrals of trignometric functions can.

The analysis in this section deals with identifying different function forms that make up the expressions occurring in the averaging procedure. We begin with the perturbation g. Using (2.6), terms of g may be written as:

$$(3.19) \qquad g_{nm}(\tau)\, x^n\, x'^m = g_{nm}(\tau)\, r^{n+m}\, a^m\, cn^n\, cn'^m$$

Using (1.11b), cn'^m can always be written in the form:

$$(3.20) \qquad cn'^m = \Sigma\, cn^{2n} \quad \text{for } m \text{ even}$$
$$= \Sigma\, cn^{2n}\, cn' \quad \text{for } m \text{ odd}$$

So, g can always be written in terms of the cn^n and $cn^n cn'$ function forms.

The function forms that appear in each expression for the first order averaging can be deduced by letting g contain both of its function forms and using eqs.(3.8)-(3.10). These are listed in Table 3.1.

Table 3.1 Function forms for first order averaging

Expression	Function Forms
g	cn^n, $cn^n\ cn'$
F_1	cn^n, $cn^n\ cn'$
F_2	cn^n, $cn^n\ cn'$, $Z\ cn^n$, $Z\ cn^n\ cn'$
$w_{1\varphi}$	cn^n, $cn^n\ cn'$
w_1	cn^n, $cn^n\ cn'$, Z, $\sin^{-1}(k\ sn)$, $H(k^2-1)\ u$
$w_{2\varphi}$	cn^n, $cn^n\ cn'$, $Z\ cn^n$, $Z\ cn^n\ cn'$, $\sin^{-1}(k\ sn)$, $H(k^2-1)\ u$
w_2	cn^n, $cn^n\ cn'$, $Z\ cn^n$, $Z\ cn^n\ cn'$, TH(u,k), Z^2, SO(u,k), S2(u,k), $Z\ \sin^{-1}(k\ sn)$, $\sin^{-1}(k\ sn)$, $H(k^2-1)\ u$, $H(k^2-1)\ u^2$

where Z is the Jacobi Zeta function, TH(u,k) is defined by (1.25), SO(u,k) and S2(u,k) are defined by eqs.(1.28), and $H(k^2-1)$ is the Heaviside step function

As one can clearly see from Table 3.1, new function forms are introduced at each integration. The nonperiodic functions u and u^2 appear in w_i (multiplied by $H(k^2-1)$, see section 1.5) in order to cancel the growth in u of $\sin^{-1}(k\ sn)$ when $k^2 > 1$.

The second order quantities H_i of eqs.(3.13) are made from the first order expressions of Table 3.1. Below, we calculate derivatives of elliptic functions with respect to $\bar{r}$ and φ (see section 1.3). From $u = 4\ K\ \varphi$, we find:

$$\frac{\partial u}{\partial \varphi} = 4\ K \tag{3.21a}$$

$$\frac{\partial u}{\partial r} = 4\ \varphi\ \frac{dK}{dk}\frac{\partial k}{\partial r} = \frac{u}{K}\frac{dK}{dk}\frac{\partial k}{\partial r} = \frac{1}{k\ k'^2}\frac{\partial k}{\partial r}\left(\frac{E}{K} - k'^2\right) u \tag{3.21b}$$

We now can evaluate derivatives of cn, cn', $\sin^{-1}(k\ sn)$, and am(u,k) with respect to φ and $\bar{r}$:

$$\frac{\partial cn}{\partial \varphi} = 4\ K\ cn' \tag{3.22a}$$

$$\frac{\partial cn'}{\partial \varphi} = 4\ K\ cn'' \tag{3.22b}$$

$$\frac{\partial}{\partial \varphi}(\sin^{-1}(k\ sn)) = 4\ k\ K\ cn \tag{3.22c}$$

$$\frac{\partial am}{\partial \varphi} = 4\ K\ dn \tag{3.22d}$$

$$\frac{\partial cn}{\partial r} = \frac{\partial cn}{\partial u}\frac{\partial u}{\partial r} + \frac{\partial cn}{\partial k}\frac{\partial k}{\partial r} \tag{3.23a}$$

$$= -\frac{1}{k\ k'^2}\frac{\partial k}{\partial r}\left[Z\ cn' + k^2\ cn\ (1 - cn^2)\right]$$

$$(3.23b)\quad \frac{\partial cn'}{\partial r} = -\frac{1}{k\,k'^2}\frac{\partial k}{\partial r}\left[Z\,cn'' + k^2\,cn'\,(1 - 2\,cn^2)\right]$$

$$(3.23c)\quad \frac{\partial}{\partial r}(\sin^{-1}(k\,sn)) = \frac{\partial k}{\partial r}\left[\frac{sn}{dn} - \frac{1}{k'^2}\left(Z\,cn - k^2\,\frac{sn\,cn^2}{dn}\right)\right]$$

$$(3.23d)\quad \frac{\partial am}{\partial r} = -\frac{1}{k\,k'^2}\frac{\partial k}{\partial r}\,(Z\,dn - k^2\,sn\,cn)$$

To calculate derivatives of Z, we must remember that Z and Z(u) are just notations for $Z(\theta,k)$ where $\theta = am(u,k)$. Applying the chain rule gives then:

$$(3.24a)\quad \frac{\partial Z}{\partial \varphi} = 4\,K\,dn^2 - 4\,E$$

$$(3.24b)\quad \frac{\partial Z}{\partial r} = \frac{dZ}{d\theta}\frac{\partial \theta}{\partial r} + \frac{dZ}{dk}\frac{\partial k}{\partial r} \quad \text{where } \theta = am(u,k)$$

$$= -\frac{k}{k'^2}\frac{\partial k}{\partial r}\,(Z\,cn^2 + cn\,cn')$$

We note that $\frac{\partial k}{\partial r}$ can found from (2.6).

From eqs.(3.21)-(3.24), it is easy to calculate derivatives with respect to τ, which follows the same pattern as $\bar{r}$. In fact, the derivatives of the functions in eqs.(3.21)-(3.24) can be computed by replacing the $\frac{\partial}{\partial \tau}$ operator by a $\frac{\partial}{\partial r}$ operator:

$$(3.25)\quad \frac{\partial}{\partial \tau} = \left[\frac{\frac{\partial k}{\partial \tau}}{\frac{\partial k}{\partial r}}\right]\frac{\partial}{\partial r}$$

We will now investigate H_1. We see in (3.26) that the $\bar{\Omega}_r\, w_1\, w_{1\varphi}$ term has zero mean.

$$\overline{w_1\, w_{1\varphi}} = \frac{1}{1}\int_0^1 w_1\, w_{1\varphi}\, d\varphi = \frac{1}{2}\, w_1^2\Big|_0^1 = 0 \tag{3.26}$$

Hence, the mean of H_1, $\bar{H}_1$, arises from four terms

$$\bar{H}_1 = \overline{F_{1r}\, w_1} - \bar{F}_1\, \overline{w_{1r}} - \overline{w_{1\tau}} - \overline{F_2\, w_{1\varphi}} \tag{3.27}$$

where overbars over functions denote means over φ.

The comparable calculation for $\bar{H}_2$ is not given because we cannot, in general, compute $\bar{H}_2$ explicitly. This arises from our limited knowledge of the two functions S0(u,k) and S2(u,k) (defined in eqs.(1.28)). Derivatives of these functions with respect to $\bar{r}$ and τ (which appear in the w_{2r} and $w_{2\tau}$ terms in eq.(3.13b)) are difficult to compute. Hence, we will not provide a general procedure for calculating $\bar{H}_2$ (but see the AVERAGE program in section 3.4 concerning special cases and see section 7.1).

A listing of the function forms appearing in H_1 with their means is given in Table 3.2. The means for three of the terms which appear in H_1 are calculated in long involved procedures, denoted A, B, and C. A brief discussion of these procedures is now given.

Table 3.2 Function forms appearing in H_1

Function Form	Mean value
cn^n	$\bar{I}_n$
$cn^n\ cn'$	0
$Z\ cn^n$	0
$Z\ cn^n\ cn'$	$\frac{1}{n+1}\left(\frac{E}{K} - k'^2\right)\bar{I}_{n+1} - \frac{k^2}{n+1}\bar{I}_{n+3}$
$SS\ cn^n$	0 for $k^2 < 1$
$(SS - \frac{\pi u}{2K})\ cn^n$	0 for $k^2 > 1$ [In this case, u appears as $H(k^2-1)\ u$]
$SS\ cn^n\ cn'$	$-\frac{k}{n+1}\bar{I}_{n+2}$ for $k^2 < 1$
$(SS - \frac{\pi u}{2K})\ cn^n\ cn'$	$-\frac{k}{n+1}(\bar{I}_{n+1} + \bar{I}_{n+2})\ H(k^2-1)$ for $k^2 > 1$ [In this case, u appears as $H(k^2-1)\ u$]
$Z^2\ cn^n$	See procedure A
$Z^2\ cn^n\ cn'$	0
$Z\ SS\ cn^n$	See procedure B for $k^2 < 1$
$Z\ (SS - \frac{\pi u}{2K})\ cn^n$	See procedure C for $k^2 > 1$ [In this case, u appears as $H(k^2-1)\ u$]
$Z\ SS\ cn^n\ cn'$	0 for $k^2 < 1$
$Z\ (SS - \frac{\pi u}{2K})\ cn^n cn'$	0 for $k^2 > 1$ [In this case, u appears as $H(k^2-1)\ u$]
$\frac{sn}{dn}$	0
$\frac{sn}{dn}\ cn^2$	0

where $SS = \sin^{-1}(k\ sn)$, $\bar{I}_n$ = mean of $I_n = \int cn^n\ du$

Procedure A computes the mean of $Z^2\ cn^n$. For n odd and $k^2 < 1$, this function has zero mean. For n odd and $k^2 > 1$, no method for finding the mean explicitly could be found. The computer uses a flag (a symbolic mnemonic variable without any numerical value) to indicate this. The flag for the mean of $Z^2\ cn^3$ is 'MEAN_OF_ZSQRCN3'. For n even, one uses integration by parts to determine the mean in terms of the means of Z^2, TH(u,k), $Z^2\ cn^2$, and $\Sigma\ Z\ cn^{2n+1}\ cn'$. An integration by parts of $Z^2\ cn^2$ permits the computation of this mean in terms of Z^2 and TH(u,k).

The mean of TH(u,k) is simply found using (1.42e). The mean of Z^2 is found using Parseval's theorem and (1.42d):

$$\overline{Z^2} = \left(\frac{\pi}{K}\right)^2 \sum_{n=1}^{\infty} \operatorname{csch}^2\left[\frac{n\pi K'}{K}\right] \tag{3.28}$$

The mean of $[\sin^{-1}(k\ sn)]^2$ is found similarly. First, one notes that $\int cn\ du = \frac{1}{k} \sin^{-1}(k\ sn)$. Integrating the Fourier series for cn, eq.(1.42b), and using Parseval's theorem, we find:

$$\overline{[\sin^{-1}(k\ sn)]^2} = \sum_{n=1}^{\infty} \frac{4}{(2n-1)^2} \operatorname{sech}^2\left[\frac{(2n-1)\pi K'}{2K}\right] \tag{3.29}$$

Of course, these formulas are valid only in the (u,k) system. For the means of Z^2, TH(u,k), and $\sin^{-1}(k\ sn)$ in other systems, one must compute in the transformed variables. The computer program does not

compute these last three means explicitly using eqs.(3.27)-(3.29) for that reason: the computer uses flags like 'MEAN_OF_Z^2' to indicate the mean of Z^2. Thankfully, these types of terms have not been encountered often in example problems.

Procedure B computes the mean of $Z \sin^{-1}(k\ sn)\ cn^n$ when $k^2 < 1$. For n even, this has zero mean. For n odd, the function has a non-zero mean that is not explicitly computable. It can be determined in terms of means of known functions plus the mean of $[\sin^{-1}(k\ sn)]^2\ cn^2$, which is not explicitly known.

Procedure C calculates the mean of $Z\ (\sin^{-1}(k\ sn) - \frac{\pi u}{2K})\ cn^n$ for $k^2 > 1$. This follows in the same manner as procedure B. For n even, this function has non-zero mean which is not explicitly computable. The computer uses another flag to indicate this mean. For n odd, the mean is computable just like in procedure B.

From Table 3.2 and procedures A, B, and C, we see that it may not be possible to explicitly calculate $\bar{H}_1$ for $k^2 > 1$. However, for $k^2 < 1$, every function in H_1 has a mean which is explicitly computable except for one function: $[\sin^{-1}(k\ sn)]^2\ cn^2$. Using flags, the computer program indicates which functions cannot be explicitly averaged.

3.4 Vanishing averages

By classifying the kinds of terms found in the perturbation g, it is possible to determine <u>a priori</u> whether $\bar{F}_1$ or $\bar{H}_1$ vanishes

identically. Such information is useful for checking results, for searching for examples which display some desired property, and for reducing computation time.

A classification of perturbation terms which appear in g is given in Table 3.3. In Table 3.4, vanishing of $\bar{F}_1$ and $\bar{H}_1$ is noted for different combination of perturbation types occurring in g. This table is created for α and β not depending on τ.

Table 3.3 Perturbation types

Perturbation Type	g(x,x',τ) term	Function Form
I	$x^{2n}\, x'^{,2m}$	cn^{2p}
II	$x^{2n}\, x'^{,2m+1}$	$cn^{2p}\, cn'$
III	$x^{2n+1}\, x'^{,2m}$	cn^{2p+1}
IV	$x^{2n+1}\, x'^{,2m+1}$	$cn^{2p+1}\, cn'$

From Table 3.4, we see that the only terms in g which contribute a non-zero mean to $\bar{F}_1$ for $k^2 < 1$ are those of type II. Also, $\bar{H}_1 \equiv 0$ for g consisting of terms of only one type. Further, for $k^2 < 1$, only the combinations of (I,IV) and (II,III) contribute non-zero means to $\bar{H}_1$.

If we now allow α and β to depend on τ, we find that this contributes to $\bar{F}_1$ and $\bar{H}_1$ as a type I perturbation term. Table 3.4 can then be consulted.

Table 3.4 Vanishing of $\bar{F}_1$ and $\bar{H}_1$

Perturbation Types in g	$\bar{F}_1 \equiv 0$?	$\bar{H}_1 \equiv 0$?
I	Yes	Yes
II	No	Yes
III	Yes	Yes
IV	Yes for $k^2 < 1$	Yes
I, II	No	Yes for $k^2 < 1$
I, III	Yes	Yes
I, IV	Yes for $k^2 < 1$	No
II, III	No	No
II, IV	No	Yes
III, IV	Yes for $k^2 < 1$	Yes for $k^2 < 1$
I, II, III	No	No
I, II, IV	No	No
I, III, IV	Yes for $k^2 < 1$	No
II, III, IV	No	No
I, II, III, IV	No	No

3.5 The MACSYMA program AVERAGE

We have implemented the averaging procedure described in section 3.1 in the MACSYMA program AVERAGE. The AVERAGE program performs second order averaging of r and first order averaging of φ for the general case of $\alpha \neq 0$ and $\beta \neq 0$. In the special cases where $\alpha = 0$ or $\beta = 0$, the program also computes $\bar{H}_2$, the second order average of φ. The $\beta = 0$ case is the familiar perturbed linear oscillator problem. The $\alpha = 0$ case corresponds to the perturbed cubic oscillator. The computer program listing is provided in Appendix E. A first order averaging version of the program appears in [Cop87b].

A brief description of the program follows. The user first inputs expressions for α, β and g, which may contain symbolic parameters. The computer then asks whether the φ equation is to be averaged. The user specifies this and the averaging order (first or second) to be used. The computer then generates F_1, F_2, and $\bar{\Omega}$ from eqs.(2.20a) and (2.23) (where eqs.(2.6) are substituted for x and x' in g). Using the GENINT integration subroutine (see Appendix B), the program finds $\bar{F}_1$, $\bar{F}_2$, w_1, and w_2 (which completes the first order averaging).

For the second order averaging of r, we proceed in several steps. We found it essential to proceed in steps in order to prevent excessive intermediate expression swell. First, H_1 is computed and

its terms are divided up among the function forms of Table 3.1. The mean of H_1 is then computed form by form. For the special cases, $\bar{H}_2$ is then computed. Once the averaging is completed, the program outputs the averaged system and the first order transformation.

The AVERAGE program consists of 460 lines of code. Typical runs on a Symbolic 3670 computer take from one to six hours. For g consisting of three terms (x', $x\,x'^2$, x'^3) where $\alpha = \beta = 1$, there are 497 second order terms to be averaged.

As examples of the use of AVERAGE, we give three sample runs: one for the general case, and one for each special case.

Sample run of AVERAGE: $\alpha = A(\tau)$, $\beta = 1$, $g = \delta x'$

```
(C1) AVERAGE()$
AVERAGING OF X'' + ALPHA(TAU) X + BETA(TAU) X^3 + EPS G(X,X',TAU) = 0
   WHERE TAU = EPS T AND G IS POLYNOMIAL IN X AND X'
ENTER ALPHA(TAU):
a(tau);
ENTER BETA(TAU):
1;
ENTER G(X,X',TAU) USING Y=X':
del*y;
UNPERTURBED SOLUTION IS: X = RR CN(U,K) AND X' = Y = RR AA CN'(U,K)
WHERE  RR=AMPLITUDE AND U = 4 KC PHI = PHASE.
```

DO PHI EQN (Y/N)?

y;

DO SECOND ORDER IN R (Y/N)?

y;

AVERAGING WILL USE A NEAR-IDENTITY TRANSFORMATION FROM

(RR,PHI) TO (RBAR,PHIBAR) AS FOLLOWS:

RR = RBAR + EPS*W1(RBAR,PHI) + EPS^2*V1(RBAR,PHI)

PHI = PHIBAR + EPS*W2(RBAR,PHI)

DONE WITH FIRST ORDER C EQN

DONE WITH FIRST ORDER PHI EQN

DIVIDING UP H1 (99 TERMS)

THE AVERAGED EQUATIONS ARE

$[RBAR(T)_T = -EPS\,(2\,KC\,A(TAU)\,DEL - 2\,EC\,A(TAU)\,DEL + CBAR^2\,KC\,DEL$

$+ 3\,KC\,A(TAU)_{TAU} - 3\,EC\,A(TAU)_{TAU})/(3\,RBAR\,KC),$

$PHIBAR(T)_T = \frac{SQRT(A(TAU) + RBAR^2)}{4\,KC}$, $KBAR^2 = \frac{RBAR^2}{2\,(A(TAU) + RBAR^2)}$,

KC = KC(KBAR) , EC = EC(KBAR)]

SIMPLIFYING THE TRANSFORMATION

DO YOU WISH TO SEE THE TRANSFORMATION? (Y/N)

n;

[Symbolics 3670 Time = 820 seconds]

In the sample run, RBAR = $\bar{r}$, KBAR = $\bar{k}$, KC = $K(\bar{k})$, EC = $E(\bar{k})$, PHIBAR = $\bar{\varphi}$, and EPS = ϵ. Derivatives are shown as subscripts. The

transformation was not shown because of the long length of the φ transformation. However, the first order r transformation is given below.

$$RR = RBAR + EPS\left(-\frac{4\ ZETA(4\ KC\ PHI)\ SQRT(A(TAU) + RBAR^2)\ DEL}{3\ RBAR}\right.$$

$$+\frac{2\ ZETA(4\ KC\ PHI)\ A(TAU)\ DEL}{RBAR\ SQRT(A(TAU) + RBAR^2)} + \frac{10\ RBAR\ ZETA(4\ KC\ PHI)\ DEL}{3\ SQRT(A(TAU) + RBAR^2)}$$

$$-\frac{RBAR\ CNF(4\ KC\ PHI)\ CNP(4\ KC\ PHI)\ DEL}{3\ SQRT(A(TAU) + RBAR^2)}$$

$$-\frac{2\ RBAR^3\ ZETA(4\ KC\ PHI)\ DEL}{(A(TAU) + RBAR^2)^{3/2}} - \frac{2\ RBAR\ ZETA(4\ KC\ PHI)\ A(TAU)\ DEL}{(A(TAU) + RBAR^2)^{3/2}}$$

$$\left.+\frac{ZETA(4\ KC\ PHI)\ A(TAU)_{TAU}}{RBAR\ SQRT(AT(TAU) + RBAR^2)}\right) + EPS^2\ V1NOTCOMPUTED$$

In the transformation, ZETA = Z, CNF = cn, CNP = cn'.

The next example concerns the special case of the cubic oscillator, i.e., $\alpha \equiv 0$.

Sample run of AVERAGE: $\alpha \equiv 0$, $\beta = 1$, $g = x\cos(\tau)$

```
(C2) AVERAGE()$
AVERAGING OF X'' + ALPHA(TAU) X + BETA(TAU) X^3 + EPS G(X,X',TAU) = 0
   WHERE TAU = EPS T AND G IS POLYNOMIAL IN X AND X'
ENTER ALPHA(TAU):
0;
```

```
ENTER BETA(TAU):
1;
ENTER G(X,X',TAU) USING Y=X':
x*cos(tau);
UNPERTURBED SOLUTION IS: X = RR CN(U,K) AND X' = Y = RR AA CN'(U,K)
WHERE  RR=AMPLITUDE AND U = 4 KC PHI = PHASE.
DO PHI EQN (Y/N)?
y;
DO SECOND ORDER IN R AND PHI (Y/N)?
y;
AVERAGING WILL USE A NEAR-IDENTITY TRANSFORMATION FROM
(RR,PHI) TO (RBAR,PHIBAR) AS FOLLOWS:
     RR  = RBAR   + EPS*W1(RBAR,PHI) + EPS^2*V1(RBAR,PHI)
     PHI = PHIBAR + EPS*W2(RBAR,PHI) + EPS^2*V2(RBAR,PHI)
DONE WITH FIRST ORDER C EQN
DONE WITH FIRST ORDER PHI EQN
DIVIDING UP H1  (6 TERMS)
THE AVERAGED EQUATIONS ARE
```

$$[RBAR(T)_T = 0,\ PHIBAR(T)_T = \frac{RBAR}{4\ KC} - \frac{EPS\ (KC - 2\ EC)\ COS(TAU)}{4\ RBAR\ KC^2}$$

$$- \frac{EPS^2\ (KC^2 - 6\ EC\ KC + 6\ EC^2)\ COS^2(TAU)}{24\ RBAR^3\ KC^3}\ ,$$

$$KBAR^2 = \frac{1}{2}\ ,\ KC = KC\left(\frac{1}{SQRT(2)}\right)\ ,\ EC = EC\left(\frac{1}{SQRT(2)}\right)]$$

```
SIMPLIFYING TRANSFORMATION
DO YOU WISH TO SEE THE TRANSFORMATION? (Y/N)
y;
```

THE TRANSFORMATION IS :

$$[RR = RBAR + EPS(-\frac{CNF^2(4\ KC\ PHI)\ COS(TAU)}{2\ RBAR} + \frac{EC\ COS(TAU)}{RBAR\ KC} - \frac{COS(TAU)}{2\ RBAR})$$

$$+ EPS^2\ V1NOTCOMPUTED,\ PHI = PHIBAR + \frac{3\ EPS\ ZETA(4\ KC\ PHI)\ COS(TAU)}{4\ RBAR^2\ KC}$$

$$+ EPS^2\ V2NOTCOMPUTED]$$

[Symbolics 3670 Time = 120 seconds]

The last example involves the special case of a perturbed linear oscillator, for which $\beta \equiv 0$.

Sample run of AVERAGE: $\alpha = 1$, $\beta \equiv 0$, $g = (1-x^2)\ x'$

```
(C3) AVERAGE()$
AVERAGING OF X'' + ALPHA(TAU) X + BETA(TAU) X^3 + EPS G(X,X',TAU) = 0
   WHERE TAU = EPS T AND G IS POLYNOMIAL IN X AND X'
ENTER ALPHA(TAU):
1;
ENTER BETA(TAU):
0;
ENTER G(X,X',TAU) USING Y=X':
-(1-x^2)*y;
UNPERTURBED SOLUTION IS: X = RR CN(U,K) AND X' = Y = RR AA CN'(U,K)
WHERE  RR=AMPLITUDE AND U = 4 KC PHI = PHASE.
DO PHI EQN (Y/N)?
y;
```

DO SECOND ORDER IN R AND PHI (Y/N)?

y;

AVERAGING WILL USE A NEAR-IDENTITY TRANSFORMATION FROM

(RR,PHI) TO (RBAR,PHIBAR) AS FOLLOWS:

RR = RBAR + EPS*W1(RBAR,PHI) + EPS^2*V1(RBAR,PHI)

PHI = PHIBAR + EPS*W2(RBAR,PHI) + EPS^2*V2(RBAR,PHI)

DONE WITH FIRST ORDER C EQN

DONE WITH FIRST ORDER PHI EQN

DIVIDING UP H1 (16 TERMS)

THE AVERAGED EQUATIONS ARE

$$[RBAR(T)_T = -\frac{RBAR\,(RBAR-2)\,(RBAR+2)\,EPS}{8}\ ,\ PHIBAR(T)_T = \frac{1}{2\,\%PI}$$

$$-\frac{(11\,RBAR^4 - 48\,RBAR^2 + 32)\,EPS^2}{512\,\%PI}\ ,\ KBAR^2 = 0,\ KC = \frac{\%PI}{2}\ ,\ EC = \frac{\%PI}{2}]$$

SIMPLIFYING TRANSFORMATION

DO YOU WISH TO SEE THE TRANSFORMATION? (Y/N)

y;

$$[RR = RBAR + EPS\left(-\frac{RBAR^3\,COS^3(2\,\%PI\,PHI)\,SIN(2\,\%PI\,PHI)}{4}\right.$$

$$+\frac{RBAR^3\,COS(2\,\%PI\,PHI)\,SIN(2\,\%PI\,PHI)}{8}$$

$$\left.+\frac{RBAR\,COS(2\,\%PI\,PHI)\,SIN(2\,\%PI\,PHI)}{2}\right) + EPS^2\ V1NOTCOMPUTED,$$

$$PHI = PHIBAR + EPS\left(\frac{COS^2(2\,\%PI\,PHI)}{4\,\%PI} - \frac{RBAR^2\,COS^4(2\,\%PI\,PHI)}{8\,\%PI}\right)$$

$$+ EPS^2\ V2NOTCOMPUTED]$$

[Symbolic 3670 Time = 75.5 seconds]

In the averaged equations and the transformation, %PI = π.

This last example is the famous van der Pol oscillator which exhibits a stable limit cycle bifurcating from r = 2 in the $\epsilon \to 0$ limit. This follows from the $\bar{r}$ equation where $\bar{r} = 2$ is an equilibrium. The averaged equations presented here agree with those of Rand and Armbruster [Ran87] using their MACSYMA averaging program.

3.6 Application of AVERAGE: A general nonlinear oscillator

Using the AVERAGE program, we may investigate problems of great generality that require an enormous number of calculations. To this end, we find the first order average equation for $\bar{r}$ for the problem described by (3.30).

(3.30a) $\alpha = \alpha(\tau)$ unspecified

(3.30b) $\beta = \beta(\tau)$ unspecified

(3.30c)
$$g(x,x',t) = g_{00}(\tau) + g_{10}(\tau)\, x + g_{01}(\tau)\, x' + g_{20}(\tau)\, x^2 + g_{11}(\tau)\, x\, x' + g_{02}(\tau)\, x'^2 + g_{30}(\tau)\, x^3 + g_{21}(\tau)\, x^2 x' + g_{12}(\tau)\, x\, x'^2 + g_{03}(\tau)\, x'^3$$

In eqs.(3.30), the $g_{ij}(\tau)$ are also unspecified. Using AVERAGE, the $\bar{r}$ equation to first order becomes:

$$
\begin{aligned}
(3.31)\qquad \bar{r}' = {} & \epsilon \frac{d\alpha}{d\tau} \frac{1}{\beta \bar{r}} \left(\frac{E}{K} - 1\right) - \epsilon \frac{d\beta}{d\tau} \frac{1}{6 \beta^2 \bar{r}} \left[\beta \bar{r}^{-2} + 4 \alpha \left(\frac{E}{K} - 1\right)\right] \\
& + \epsilon g_{01}(\tau) \frac{1}{3 \beta \bar{r}} \left[2 \alpha \left(\frac{E}{K} - 1\right) - \beta \bar{r}^{-2}\right] \\
& - \epsilon g_{11}(\tau) \frac{\sqrt{2}\, \pi\, H(\bar{k}^{-2}-1)}{8 K \bar{r}} \left[\frac{\alpha + \beta \bar{r}^{-2}}{\beta}\right]^{3/2} \\
& + \epsilon g_{21}(\tau) \left[\frac{8 \alpha^2}{15 \beta^2 \bar{r}} \left(1 - \frac{E}{K}\right) + \frac{2 \alpha \bar{r}}{15 \beta} \left(5 - 6 \frac{E}{K}\right) + \frac{\bar{r}^{-3}}{5} \left(1 - 2 \frac{E}{K}\right)\right] \\
& + \epsilon g_{03}(\tau) \left[\frac{8 \alpha^3}{35 \beta^2 \bar{r}} \left(\frac{E}{K} - 1\right) + \frac{2}{35} \frac{\alpha^2}{\beta} \bar{r} \left(16 \frac{E}{K} - 15\right) \right. \\
& \qquad \left. + \frac{\alpha \bar{r}^{-3}}{35} \left(16 \frac{E}{K} - 23\right) - \frac{\beta}{7} \bar{r}^{-5}\right]
\end{aligned}
$$

where $E = E(k)$, $K = K(k)$, $k^2 = \dfrac{\beta \bar{r}^{-2}}{2 (\alpha + \beta \bar{r}^{-2})}$,

and $H(k^2-1)$ is the Heaviside step function

The second order contributions to $\bar{r}$ and the first order average of φ are very long, and so will not be listed here.

4.0 Limit cycles in a VDP perturbation of the cubic oscillator

The simplest extension of the theory of the perturbed linear oscillator is the perturbed cubic oscillator. As mentioned in chapter 3, this is just a special case of eq.(0.1) for which $\alpha \equiv 0$. Because the elliptic modulus k does not depend on an orbit and because F_2 is simpler than in the general case, the method of averaging can be readily applied. In fact, the AVERAGE program can proceed to average the φ equation to second order (i.e., it can find $\bar{H}_2$.)

Recently, investigations into the perturbed cubic oscillator have appeared in the literature. Both averaging and generalized harmonic balance are presented by Yuste and Bejarano [Yus86]. They determine a first order approximation to the limit cycle which appears when the cubic oscillator is perturbed by a VDP (i.e., van der Pol) perturbation term. In Garcia-Margallo and Bejarano [Gar87], a second order method using generalized harmonic balance is introduced and applied to the same problem.

We will present the second order averaging approximation for this problem and show that it agrees very well with numerical integration (even for ϵ as large as 1). Then we will comment on the generalized harmonic balance method and show its equivalence to first

order averaging. Finally, we compare our second order results to the Garcia-Margallo and Bejarano results.

4.1 The averaged equations

We consider the cubic oscillator perturbed by a VDP (van der Pol) perturbation term:

$$x'' + x^3 - \epsilon\, x' \,(1 - x^2) = 0 \tag{4.1}$$

Using the AVERAGE program, we compute the averaged system to second order for $(\bar{r},\bar{\varphi})$:

$$\bar{r}' = \epsilon\, \frac{\bar{r}}{15}\left[3\,\bar{r}^2\,(1 - 2\,\frac{E}{K}) + 5\right] + O(\epsilon^3) \tag{4.2a}$$

$$\bar{\varphi}' = \frac{\bar{r}}{4\,K} - \epsilon^2\,\frac{1}{5K}\left[\frac{\bar{r}^3}{5}\,\overline{Z^2} - \frac{\bar{r}^3}{150}\,(12 - 19\,\frac{E}{K}) + \frac{\bar{r}}{126}\,(1 - 84\,\frac{E^2}{K^2}) - \frac{1}{9\,\bar{r}}\,(1 - 2\,\frac{E}{K})\right] + O(\epsilon^3) \tag{4.2b}$$

$$\bar{k}^2 = \frac{1}{2} = k^2 \tag{4.2c}$$

In eqs.(4.2), k does not depend on the amplitude r and always has the same value given in (4.2c). Thus, both K and E have constant values

in eqs.(4.2). The value of $\overline{Z^2}$, the mean of Z^2, is also a constant and is found using 3.28. These values are listed in (4.3).

(4.3a) $$K = 1.85407463...$$

(4.3b) $$E = 1.35064383...$$

(4.3c) $$\overline{Z^2} = 0.02156676...$$

The near-identity transformation is given in (4.4).

(4.4a) $$r = \bar{r} + \epsilon\, w_1(\bar{r},\varphi) + O(\epsilon^2)$$

where $$w_1(\bar{r},\varphi) = -\left[\frac{2}{5}\bar{r}^2\, Z(u) + \frac{1}{5}\bar{r}^2\, cn^3(u,k)\, cn'(u,k) - \frac{1}{3}\, cn(u,k)\, cn'(u,k)\right]$$

(4.4b) $$\varphi = \bar{\varphi} + \epsilon\, w_2(\bar{r},\varphi) + O(\epsilon^2)$$

where $$w_2(\bar{r},\varphi) = \frac{1}{K}\left[\frac{\bar{r}}{10}\, TH(u,k) + \frac{3}{40}\,\bar{r}\, cn^4(u,k) - \frac{1}{6\,\bar{r}}\, cn^2(u,k)\right]$$

(4.4c) $$u = 4\,K\,\varphi$$

In (4.4), Z is defined by (1.5) and TH(u,k) by (1.25). To use the transformation, one solves for φ in terms of $\bar{\varphi}$ in (4.4b) by a recursive substitution:

(4.5) $$\varphi = \bar{\varphi} + \epsilon\, w_2(\bar{r},\, \bar{\varphi} + O(\epsilon)) + O(\epsilon^2)$$
$$= \bar{\varphi} + \epsilon\, w_2(\bar{r},\bar{\varphi}) + O(\epsilon^2)$$

From (4.5), (4.4a) can now be used.

We now look for limit cycles in eq.(4.1). We do this by finding equilibrium points in the $\bar{r}$ equation. Setting the right-hand side of eq.(4.2a) equal to zero, we find an equilibrium at:

$$\bar{r}^{-2} = \bar{r}_*^{-2} = \frac{5}{3\,(2\,\frac{E}{K} - 1)} = 3.6473995... \tag{4.6a}$$

$$\bar{r}_* = 1.9098.... \tag{4.6b}$$

Hence, as ϵ increases from zero, we expect to find a limit cycle of amplitude $\bar{r}_*$ bifurcating from the phase space of closed orbits of the $\epsilon = 0$ system. The shape of the limit cycle is then the orbit corresponding to $r = \bar{r}_*$.

A graph of the limit cycle for $\epsilon = 0.1$ is given in Fig.4.1. The graph for the numerical integration and first order averaging approximation (where only the O(1) transformation is used) are very close.

Two more graphs comparing the numerical integration with the second order averaging (in which the $O(\epsilon)$ transformation is used, i.e., eqs.(4.4) and (4.5)) are shown at higher values of ϵ. Fig.4.2 shows the $\epsilon = 0.5$ case; Fig.4.3 shows the $\epsilon = 1.0$ case. In both these cases, the numerical integration can hardly be distinguished from the numerical integration.

Moreover, the accuracy of the $\epsilon = 1.0$ case is startling since the averaging method itself is based on the assumption that ϵ be small compared to 1. But in this example, the second order averaging

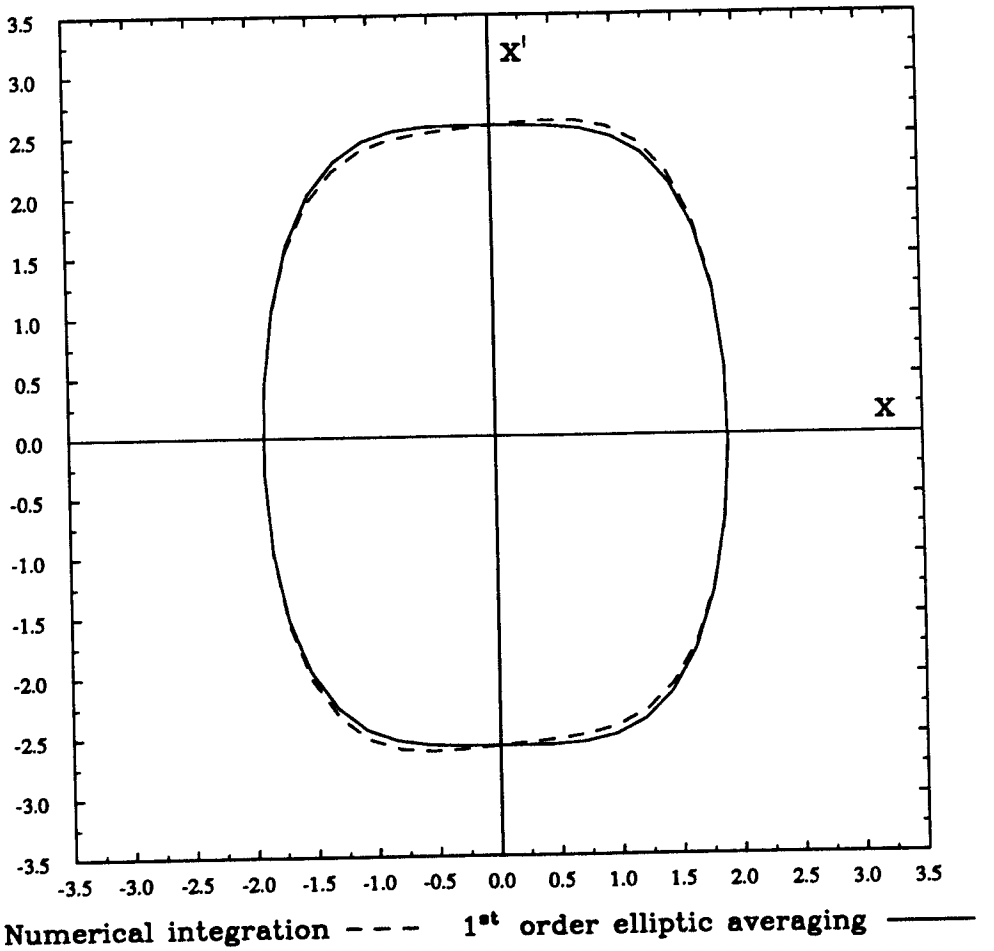

Fig.4.1 Comparison of numerical integration with first order averaging using elliptic functions for the limit cycle in eq.(4.1). $\epsilon = 0.1$.

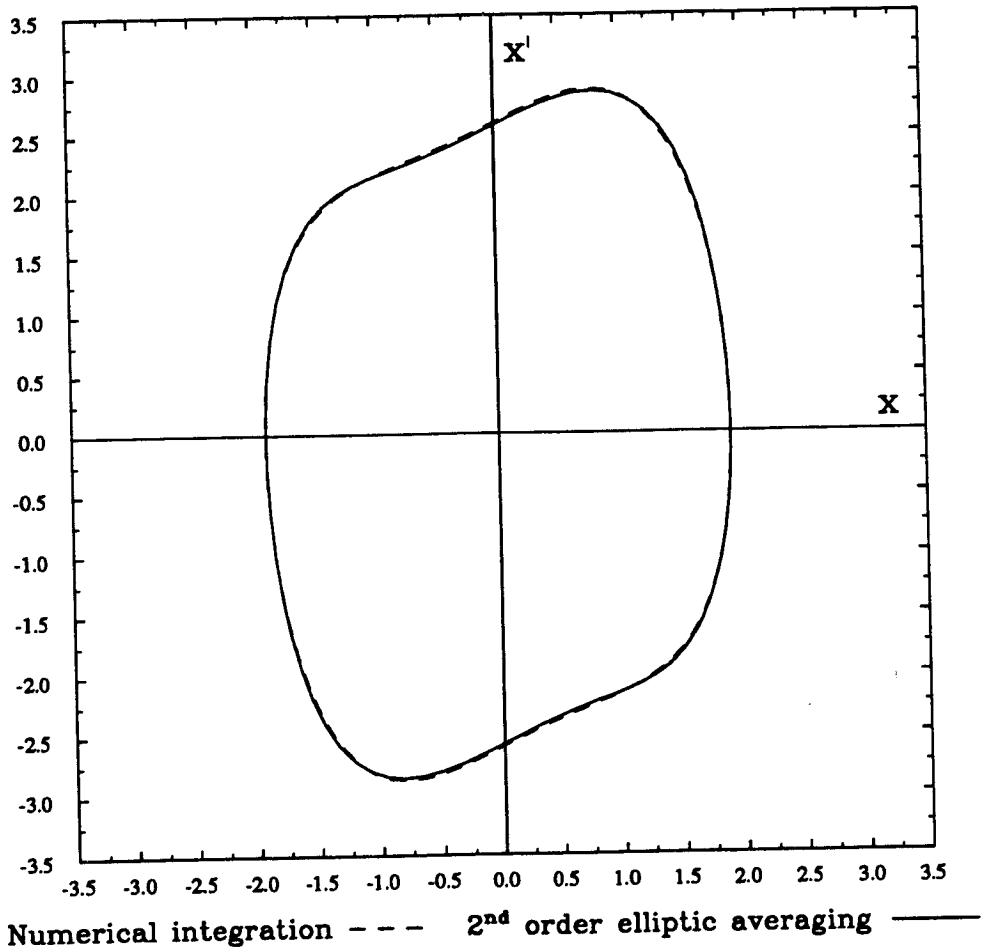

Fig.4.2 Comparison of numerical integration with second order averaging using elliptic functions for the limit cycle in eq.(4.1). $\epsilon = 0.5$.

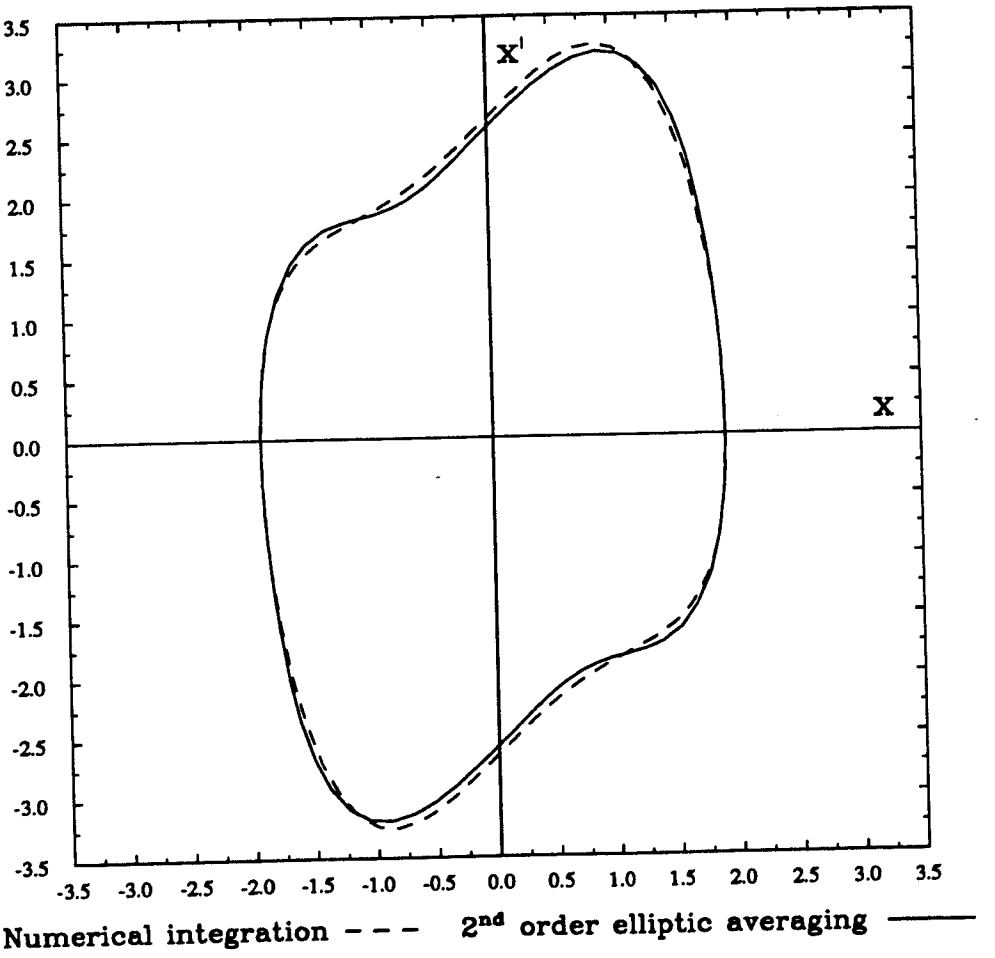

Fig.4.3 Comparison of numerical integration with second order averaging using elliptic functions for the limit cycle in eq.(4.1). $\epsilon = 1.0$.

coupled with the transformation is able to account for the quite deformed shape (as compared to unperturbed system) and the loss of symmetry about the x'-axis. As evidenced by Fig.4.3, the averaging results for even high values of ϵ give close agreement near the limit cycle.

The results from the averaging approximation clearly demonstrate the accuracy of the AVERAGE program and the value that averaging has in treating perturbations of the cubic oscillator.

4.2 Generalized harmonic balance

Recently, there has been much interest in studying eq.(4.1) using a generalized form of harmonic balance. Mickens [Mic84] has given criteria under which the method of harmonic balance seems to work well. In another paper, Mickens proposes a second order method using a generalization of harmonic balance which uses higher harmonics in an assumed solution form [Mic86]. Garcia-Margallo and Bejarano [Gar87] use the generalized harmonic balance method and formulate their own second order method. We will discuss these below.

The method of harmonic balance involves assuming a solution of the following form:

$$x = r\cos(\omega t) \tag{4.7}$$

without regard to the unperturbed system solution form. This is done merely as a computational convenience. Such an approximation for x is certainly valid in a neighborhood about a center in the unperturbed system's phase portrait. How large the neighborhood is for a nonlinear system is unknown, but it is assumed large enough that the results are meaningful.

One then substitutes the solution form into a nonlinear differential equation (for us, eq.(4.1)) and sets the coefficients of the lowest order harmonic equal to zero. For conservative systems, this procedure results in an expression relating the frequency ω with the amplitude r. For non-conservative systems containing a limit cycle, the procedure results in equations for r and ω that must be satisfied on the limit cycle.

Higher order methods involve assuming a solution form containing higher harmonics and setting coefficients of these harmonics equal to zero after substitution in the differential equation. Of course, while the procedure is computationally efficient there is no guarantee of its accuracy nor a priori knowledge that its approximation will be close to limit cycles in the original equation. In Mickens [JSV111], which is concerned with the cubic oscillator, this method of higher harmonics is extended somewhat by assuming a solution form consisting of a rational fraction of Fourier series.

The generalized method of harmonic balance again involves a solution form involving cosine, but its argument is taken to the amplitude function am(u,k):

(4.8) $$x = r\cos(\theta) \text{ where } \theta = am(u,k)$$
$$u = \omega t,\ k^2 = \frac{1}{2}$$

The value of ω is to be found in the procedure to follow. From (1.2a), we see that this method really involves the elliptic function solution of the unperturbed system (i.e., cn(u,k) where $k^2 = \frac{1}{2}$) which is written in a different notation (but is in every way equivalent). Substitution of (4.8) into (4.1) gives:

(4.9) $$[\tfrac{3}{4} r\,(r^2 - \omega^2)]\cos(\theta) + \epsilon L(r,\omega)\sin(\theta)$$
$$+ \text{higher order harmonics} = 0$$

From the O(1) coefficient of the cos(θ) term of (4.9), we find $\omega = r$ (the correct value) for the unperturbed system. By setting L = 0 and using $\omega = r$, we find the same limit cycle amplitude predicted by the first order average result (4.6).

The reason that this method gives the same result is that the method involves the same calculation. From the averaging method , we find setting $\bar{F}_1 = 0$ involves:

(4.10a) $$r' = \epsilon f(r)\, g(x,x')\, cn'$$

$$\bar{r}' = \epsilon f(r) \frac{1}{4K} \int_0^{4K} g \, cn' \, du = \bar{F}_1 \tag{4.10b}$$

$$\bar{F}_1 = 0 \rightarrow \int_0^{4K} g \, cn' \, du = 0 \tag{4.10c}$$

Since g is odd in x' (and it must be for the harmonic balance method to work [Mic84]), it can be expanded in a Fourier series in the angle θ:

$$g(x,x') = \sum_{n=1}^{\infty} g_n \sin(n\theta) \tag{4.11a}$$

$$g_n = \frac{1}{\pi} \int_0^{2\pi} g \sin(n\theta) \, d\theta \tag{4.11b}$$

The lowest order harmonic is then easily evaluated:

$$g_1 = \frac{1}{\pi} \int_0^{4K} g \, sn(u,k) \, dn(u,k) \, du \tag{4.12}$$

$$= -\frac{1}{\pi} \int_0^{4K} g \, cn' \, du$$

Setting the lowest order harmonic equal to zero then gives (4.10c). The two methods agree because the unperturbed system is odd in x and g is odd in x'.

Garcia-Margallo and Bejarano's second order method [Gar87] is simply a projection method akin to modal analysis. One looks for a solution to (4.1) in the form:

$$x = r_1\, cn(u,k) + r_2\, pq(u,k) \tag{4.13}$$

where pq(u,k) is some other elliptic function which oscillates (the choice is not essential). One substitutes (4.13) into (4.1), expands each function occurring in the resulting expression by its Fourier series in θ, and collects terms of the lowest harmonic. Using the first order value for r_1 given by taking $r_2 = 0$ (see (4.6)), one then sets the coefficients for the lowest order harmonics equal to zero assuming $r_2 = O(\epsilon)$. The value of r_2 can then be found.

In their work, Garcia-Margallo and Bejarano tried sn(u,k) and sd(u,k) for pq(u,k) in (4.13) and compared their approximation with numerical integration at $\epsilon = 1.0$. They found that using either function destroyed the symmetry of the first order approximation (which is apparent in the numerical integration) and gave limit cycles with deformed shapes similar to the exact one. Using sd(u,k) did not change the limit cycle radius along the line $x' = 0$ but using sn(u,k) did. They decided that sd(u,k) was better than sn(u,k) for that reason. They conjectured that this might be a result of sd(u,k) being a solution to the unpertubed system of eq.(4.1) (sd(u,k) is the K-shift of cn(u,k) like sin(θ) is the $\frac{\pi}{2}$-shift of cos(θ)). Still, their choice for pq(u,k) is ad hoc with no known way of guaranteeing

a "better" solution than the first approximation. The second order average solution, Fig.4.3, is much more accurate than their second order approximations (see [Gar87]).

In summary, the generalized method of harmonic balance works well (for the specific types of problems where it works at all) in determining a first order approximation to limit cycle radius. Its success is its relative computational ease; its failure is its poor description of the oscillation unless ϵ is small. Moreover, its extension into a second order approximation does not work as well as the averaging approach.

Because we will be concerned with systems where the generalized method of harmonic balance will not work (e.g., near separatrices, away from centers, vibrations for which the first harmonic is not dominant, etc.), we choose to rely on the averaging method in all our investiagtions of strongly nonlinear systems. Besides, with the MACSYMA program AVERAGE, computationally intensive calculations are not performed by the user anyway.

5.0 Comparing elliptic with trigonometric averaging

In this chapter, we explore the relationship between averaging using elliptic functions and averaging using trigonometric functions. We investigate systems for which the perturbation g depends on three parameters and gives rise to limit cycles. We then investigate the bifurcation of limit cycles as the parameters in g are varied. We show that both the choice of the averaging method (elliptic or trigonometric) and the choice of the averaging order affect the qualitative prediction of the number of limit cycles in the system. Moreover, higher order methods are not necessarily better predictors.

First, we shall provide the first and second order averaging approximations using elliptic functions and trigonometric functions for the perturbation g. The perturbation g is a generalized van der Pol perturbation depending on the parameters δ, ρ, and η. Second, the bifurcation diagram showing the number of limit cycles in the system for $\eta = 0$ is presented. Then, the more interesting bifurcation diagram of $\eta \neq 0$ is investigated. Finally, two concrete examples are explored which show the the failure of the trigonometric approach and the success of the elliptic approach.

We note that the analysis of some parts of this chapter have been published separately (see [Cop89a] and [Cop89c]).

5.1 Averaging approximations

Throughout this chapter we will use the expression 'first order trig averaging' to mean first order averaging using trigonometric functions. Similar expressions for second order and averaging using elliptic functions will be used. If the order (first or second) is not specified then both orders are implied. We now present the averaging approximations for elliptic and trig averaging, both first and second order.

We shall be concerned with the system described by (5.1).

$$\alpha > 0 \ , \ \beta > 0 \ , \ g = \delta x' + \rho x^2 x' + \eta x'^3 \tag{5.1}$$

For elliptic averaging, the cubic term βx^3 is accounted for in the the unperturbed solution. For trig averaging, β is considered as an $O(\epsilon)$ term so that βx^3 belongs to the perturbation g. It is this difference that can make for different qualitataive predictions of limit cycles. We note that a limit cycle is predicted in the system described by (5.1) for values $\bar{r}$ that make $\bar{r}' = 0$.

We will discuss elliptic averaging first. Using (3.31), we find the first order averaged equation for $\bar{r}$ to be:

$$(5.2)\qquad \bar{r}' = \epsilon\,\delta\,\frac{1}{3\,\beta\,\bar{r}}\left[2\,\alpha\,(\frac{E}{K}-1) - \beta\,\bar{r}^{-2}\right]$$

$$+\,\epsilon\,\rho\left[\frac{8\,\alpha^2}{15\,\beta^2\,\bar{r}}\,(1-\frac{E}{K}) + \frac{2\,\alpha\,\bar{r}}{15\,\beta}\,(5-6\,\frac{E}{K}) + \frac{\bar{r}^{-3}}{5}\,(1-2\,\frac{E}{K})\right]$$

$$+\,\epsilon\,\eta\left[\frac{8\,\alpha^3}{35\,\beta^2\,\bar{r}}\,(\frac{E}{K}-1) + \frac{2}{35}\,\frac{\alpha^2}{\beta}\,\bar{r}\,(16\,\frac{E}{K}-15)\right.$$

$$\left. +\,\frac{\alpha\,\bar{r}^{-3}}{35}\,(16\,\frac{E}{K}-23) - \frac{\beta}{7}\,\bar{r}^{-5}\right]$$

where $E = E(k)$, $K = K(k)$, $k^2 = \dfrac{\beta\,\bar{r}^{-2}}{2\,(\alpha+\beta\,\bar{r}^{-2})}$

Since the terms in g are all of perturbation type II (see Table 3.3), Table 3.4 shows that the second order mean $\bar{H}_1$ is identically zero. Therefore, the prediction of limit cycles for first order and second order elliptic averaging is the same.

In the analysis of bifurcations of limit cycles in (5.2) it is easier to work with the following form of $\bar{r}'$:

$$(5.3)\qquad \bar{r}' = -\,\epsilon\,\bar{r}\left[\delta\,V_1 + \rho\,\bar{r}^{-2}\,V_2 + \eta\,\bar{r}^{-2}\,(\alpha+\beta\,\bar{r}^{-2})\,V_3\right]$$

where

$$V_1 = \frac{1}{3k^2}\left[(2k^2-1)\,\frac{E}{K} + k'^2\right]$$

$$V_2 = \frac{1}{15k^4}\left[(k^2 - 2)\,k'^2 + 2\,\frac{E}{K}\,(k^4 - k^2 + 1)\right]$$

$$V_3 = \frac{1}{35k^4}\left[8k^6 - 13k^4 + 3k^2 + 2 - 2\,\frac{E}{K}\,(8k^6 - 12k^4 + 2k^2 + 1)\right]$$

$$\text{and } E = E(k)\ ,\ K = K(k)\ ,\ k^2 = \frac{\beta\,\bar{r}^{-2}}{2\,(\alpha + \beta\,\bar{r}^{-2})}$$

In (5.3), V_i depend only on k^2 and are always positive for α and β satisfying (5.1). We also note that V_1, V_2, and V_3 are the means of cn'^2, $cn^2\,cn'^2$, and cn'^4 respectively. This form of $\bar{r}$ can be found from (5.2) by using the relation:

$$\bar{r}^{-2} = \frac{\alpha}{\beta}\,\frac{2k^2}{1 - 2k^2} \tag{5.4}$$

Before we apply trig averaging, we introduce a new parameter $\hat{\beta}$ defined in (5.5).

$$\beta = \epsilon\,\hat{\beta} \tag{5.5}$$

Using (5.5), the term $\beta\,x^3$ can now be considered as part of the perturbation g. Note that we are ultimately interested in problems for fixed α and β where ϵg is considered as small but finite. Hence, we intend that (5.5) hold <u>to fix β for any ϵ</u>. This means that smaller and smaller values of ϵ require larger and larger values of $\hat{\beta}$ so that (5.5) holds for some constant β. Since the rescaling of β

depends on ϵ, the normal interpretation of the validity of the averaging method as $\epsilon \to 0$ must be altered slightly.

Using AVERAGE, we compute the second order averaged equation for $\bar{r}$ to be:

$$(5.6) \qquad \bar{r}' = -\epsilon \bar{r} \left[\frac{\delta}{2} + \frac{\rho}{8}\bar{r}^{-2} + \frac{3}{8}\alpha\eta\,\bar{r}^{-2}\right] + \epsilon^2 \hat{\beta} \frac{1}{32\alpha}\bar{r}^{-5}(\rho - 3\alpha\eta)$$

The first order trig average for $\bar{r}$ is given by (5.6) ignoring the ϵ^2 term. The second order trig average for $\bar{r}$ includes the ϵ^2 term. Furthermore, (5.5) can be used to give:

$$(5.7) \qquad \bar{r}' = -\epsilon \bar{r} \left[\frac{\delta}{2} + \frac{\rho}{8}\bar{r}^{-2} + \frac{3}{8}\alpha\eta\,\bar{r}^{-2} + \frac{\beta}{32\alpha}\bar{r}^{-4}(\rho - 3\alpha\eta)\right]$$

which is valid to $O(\epsilon^3)$.

The limit cycle conditions for first and second order trig averaging and for elliptic averaging are now written concisely below:

(5.8a) 1^{st} Trig $\qquad 4\delta + (\rho + 3\alpha\eta)\bar{r}^{-2} = 0$

$$\text{or} \quad \bar{r}^{-2} = -\frac{4\delta}{\rho + 3\alpha\eta}$$

(5.8b) 2^{nd} Trig $\qquad \beta(3\alpha\eta - \rho)\bar{r}^{-4} + 4\alpha(3\alpha\eta + \rho)\bar{r}^{-2} + 16\alpha\delta = 0$

$$\text{or} \quad \bar{r}^{-2} = \frac{2\alpha(\rho + 3\alpha\eta) \pm 2\sqrt{\alpha^2(\rho + 3\alpha\eta)^2 + 4\alpha\beta\delta(\rho - 3\alpha\eta)}}{\beta(\rho - 3\alpha\eta)}$$

(5.8c) Elliptic $$\delta V_1 + \rho \bar{r}^{-2} V_2 + \eta \bar{r}^{-2} (\alpha + \beta \bar{r}^{-2}) V_3 = 0$$

Note that V_i in eq.(5.8c) depend on $k(\bar{r})$ so that eq.(5.8c) cannot be solved explicitly for $\bar{r}$. However, (5.8c) is easily solved numerically. Also, (5.8a) agrees with previous work [Ran87].

5.2 The bifurcation set for $\eta = 0$

We consider the bifurcation set of the number of limit cycles predicted by each of the averaging methods when $\eta = 0$. First, we define a new parameter μ_0:

(5.9) $$\mu_0 = -\frac{\delta}{\rho}$$

Then, we express the limit cycle condition of eqs.(5.8) in terms of μ_0:

(5.10a) 1^{st} Trig $$\mu_0 = \frac{1}{4} \bar{r}^{-2}$$

(5.10b) 2^{nd} Trig $$\mu_0 = \frac{\bar{r}^{-2}}{16\alpha} (4\alpha - \beta \bar{r}^{-2}) = \frac{1}{4} \bar{r}^{-2} - \frac{\beta}{16\alpha} \bar{r}^{-4}$$

(5.10c) Elliptic $$\mu_0 = \bar{r}^{-2} \frac{V_2}{V_1}$$

A graph of μ_0 vs. $\bar{r}$ given by eqs.(5.10) is shown in Fig.5.1. The first order trig and the elliptic predictions are qualitatively the same. Each predicts one limit cycle for each positive value of μ_0.

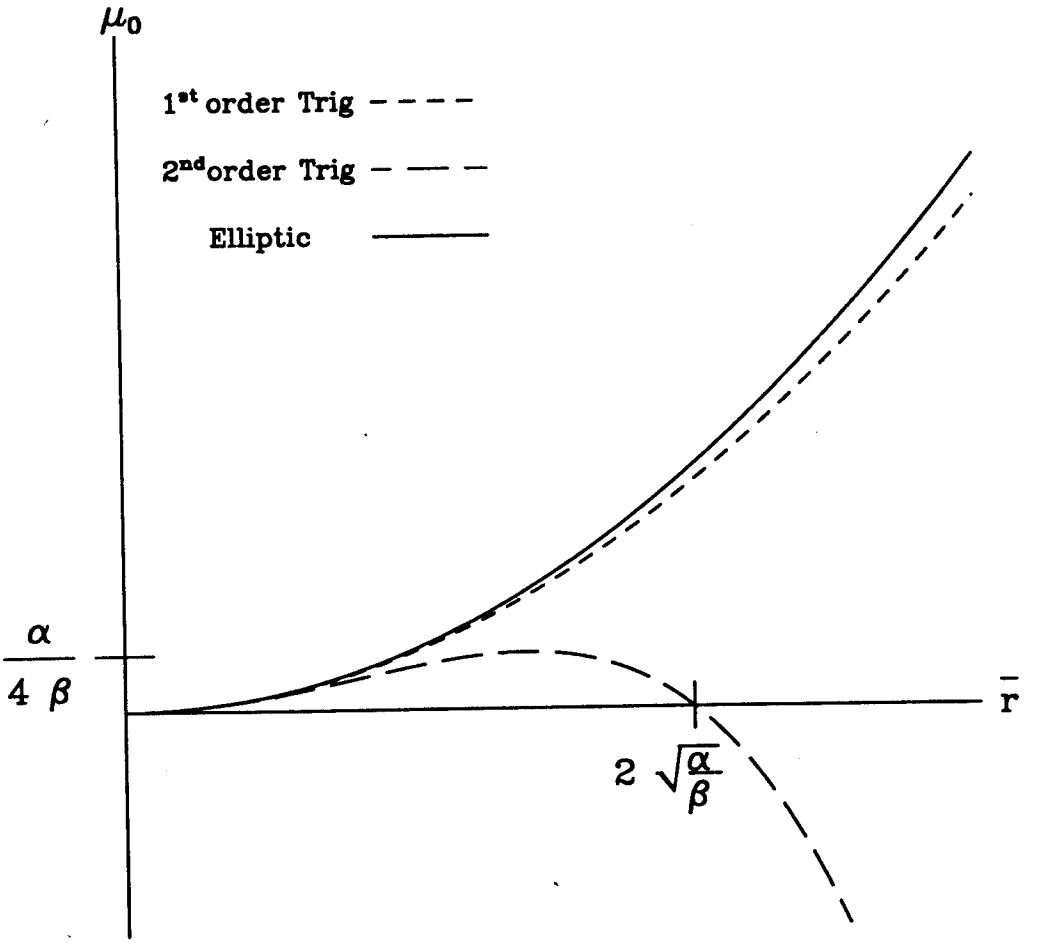

Fig.5.1 The limit cycle condition for $\eta = 0$, as determined by elliptic averaging and trig averaging (first and second order) given by eqs.(5.10). The second order trig averaging can give qualitatively incorrect results.

which increases from zero amplitude at $\mu_0 = 0$. Viewed this way, the limit cycle is a result of a Hopf bifurcation at $\bar{r} = 0$ at the μ_0-bifurcation value of zero.

The second order trig averaging predicts two limit cycles for $0 < \mu_0 < \frac{\alpha}{4\beta}$ (since one value of μ_0 intersects the bifurcation curve at two $\bar{r}$ values), one for $\mu_0 < 0$, and none for $\mu_0 > \frac{\alpha}{4\beta}$. While the second order trig curve lies close to the first order trig curve for smaller $\bar{r}$, it begins to flatten out and turn downward crossing the $\mu_0 = 0$ line again at $\bar{r}^2 = \frac{4\alpha}{\beta}$. Limit cycles with amplitudes greater than $\bar{r}^2 = \frac{4\alpha}{\beta}$ are predicted when μ_0 is negative.

Simple energy arguments show that the second order trig predictions are totally inaccurate for $\bar{r}$ values away from the first order trig curve. The first order trig and elliptic curves are qualitatively correct. In concrete examples where μ_0 is numerically specified, however, we find the elliptic averaging prediction of limit cycle amplitude and shape to be more accurate.

We wish to make clear that the averaging theorem has not failed even though the second order approach was not an improvement over the first order approach. This is because of our treatment of β as $\epsilon \hat{\beta}$. If we examine where the second order curve first becomes inaccurate, we see that this scales as $\frac{1}{\beta}$. So, had we <u>not</u> fixed β at some finite constant but had instead treated the x^3 term as asymptotically small, the second order approach would be qualitatively inaccurate only in predicting very large limit cycles, where $x = O(\frac{1}{\epsilon})$ and not $x = O(1)$.

5.3 The bifurcation set for $\eta \neq 0$

We now consider the bifurcation set of the number of limit cycles predicted by each of the averaging methods when $\eta \neq 0$. First, we define two new parameters μ_1 and μ_2:

$$\mu_1 = \frac{\rho}{\eta} \tag{5.11a}$$

$$\mu_2 = -\frac{\delta}{\eta} \tag{5.11b}$$

Using (5.11), we express the limit cycle condition given by eqs.(5.8) as a family of straight lines of constant limit cycle amplitude $\bar{r}$ in the (μ_1,μ_2) parameter plane:

$$1^{st}\ \text{Trig} \qquad \mu_2 = \frac{1}{4}\bar{r}^{-2}(\mu_1 + 3) \tag{5.12a}$$

$$2^{nd}\ \text{Trig} \qquad \mu_2 = \frac{\bar{r}^{-2}}{16\alpha}\left[(4\alpha - \beta\bar{r}^{-2})\,\mu_1 + 3\alpha\,(4\alpha + \beta\bar{r}^{-2})\right] \tag{5.12b}$$

$$\text{Elliptic} \qquad \mu_2 = \frac{\bar{r}^{-2}}{V_1}\left[V_2\,\mu_1 + (\alpha + \beta\bar{r}^{-2})\,V_3\right] \tag{5.12c}$$

In eqs.(5.12), the slopes and intercepts of the family of lines are parameterized by α, β, and $\bar{r}$. We will now discuss each of eqs.(5.12) separately and thereby generate the bifurcation diagram for each averaging method.

We begin with first order trig averaging. From (5.12a), the slope of each line and its μ_2-intercept increases with $\bar{r}$. The μ_1-intercept for every line is the point $(\mu_1,\mu_2) = (-3\alpha,0) \equiv P$. A

graph of (5.12a) is shown in Fig.5.2. The regions I_u and I_l each contain one limit cycle; regions O_u and O_l contain none. The u and l subscripts denote upper and lower, respectively.

The μ_2-axis is a Hopf bifurcation line where a limit cycle is born at with zero amplitude. The line $\mu_1 = -3\alpha$ is a bifurcation line where a limit cycle of infinite amplitude is predicted. Point P is a highly singular point: points nearby are very sensitive to small changes in μ_1 and μ_2.

The second order trig bifurcation diagram is much more complicated. This is shown in Fig.5.3. There are six distinct regions of the (μ_1,μ_2) plane: two regions where there are two limit cycles (denoted II_u and II_l), two regions with one limit cycle (i.e., I_u and I_l) and two regions with no limit cycles (i.e., O_u and O_l). The μ_1-axis is again a Hopf bifurcation line. The line $\mu_1 = 3\alpha$ is bifurcation line where a limit cycle of infinite amplitude is predicted. In addition, there are two fold bifurcation lines where two limit cycles of finite amplitude coalesce.

The fold bifurcation curve can be found analytically. The envelope of the family of lines of (5.12b) is found by simultaneously solving eq.(5.12b) and the following:

$$\text{(5.13a)} \qquad \frac{\partial}{\partial \bar{r}^{-2}} \left[\frac{\bar{r}^{-2}}{16\alpha} \left[(4\alpha - \beta\bar{r}^{-2})\,\mu_1 + 3\alpha\,(4\alpha + \beta\bar{r}^{-2}) \right] \right] = 0$$

$$(2\alpha - \beta\bar{r}^{-2})\,\mu_1 + 3\alpha\,(2\alpha + \beta\bar{r}^{-2}) = 0$$

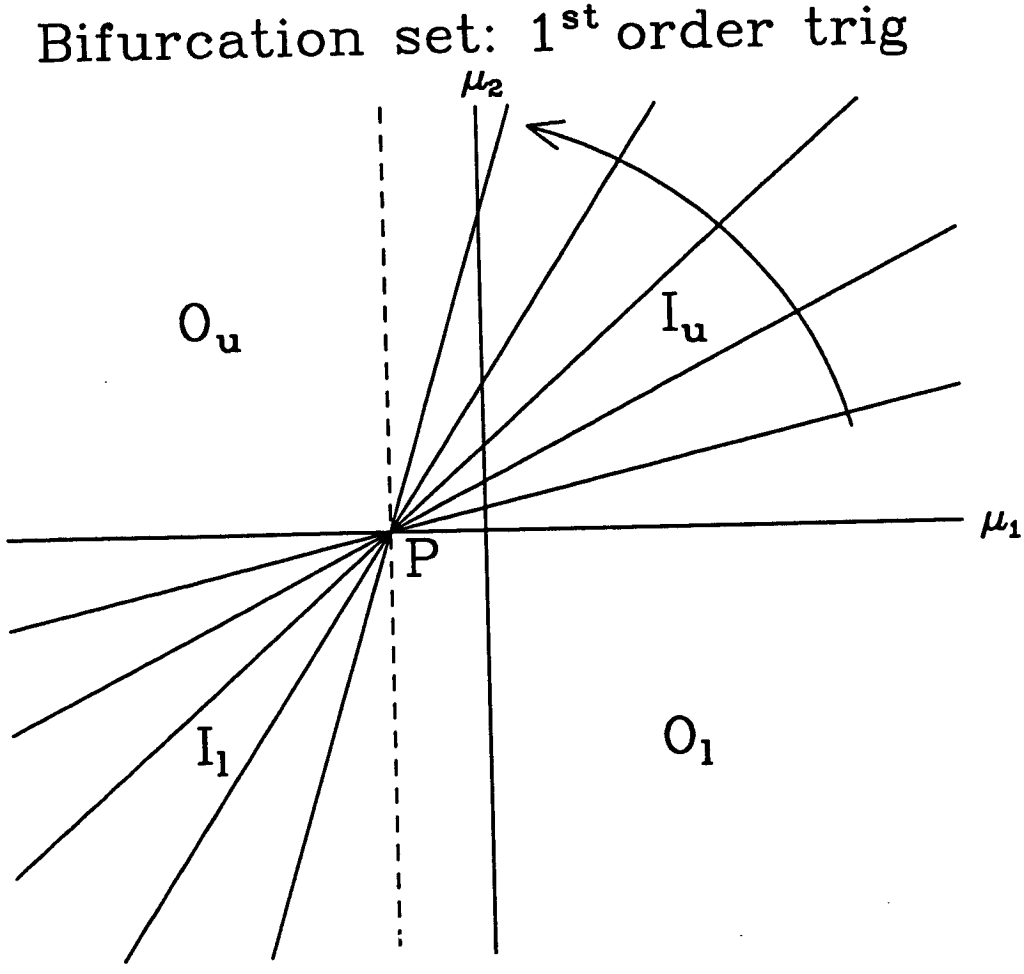

Fig.5.2 Bifurcation set for $\eta \neq 0$, as determined by first order trig averaging (eq.(5.12a)). Along each straight line there exists a limit cycle of fixed amplitude. In regions I_u and I_l there is 1 limit cycle; in O_u and O_l there are none. The μ_1-axis is a Hopf bifurcation curve. The dashed line corresponds to a limit cycle of infinite amplitude. The arrow show the direction of increasing limit cycle amplitude.

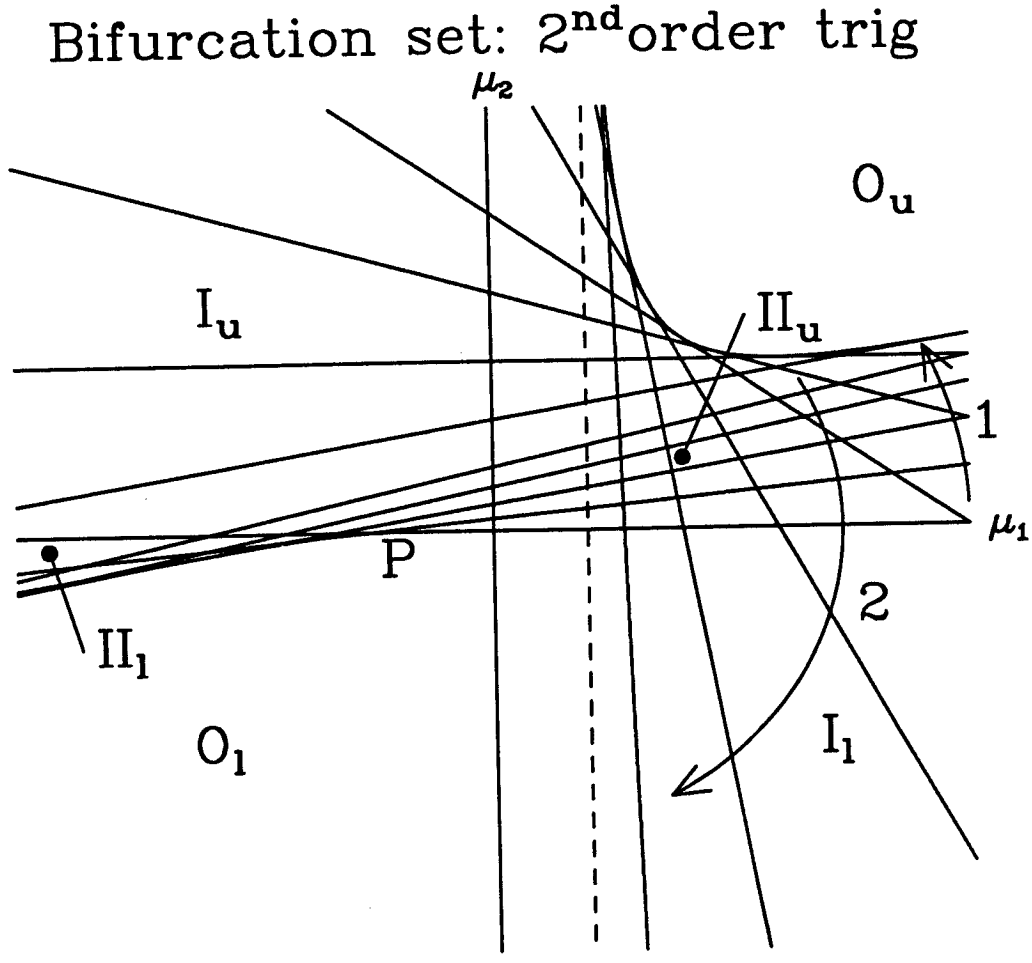

Fig.5.3 Bifurcation set for $\eta \neq 0$, as determined by second order trig averaging (eq.(5.12b)). Along each straight line there exists a limit cycle of fixed amplitude. In regions II_u and II_l there are 2 limit cycles; in I_u and I_l there is 1; in O_u and O_l there are none. The μ_1-axis is a Hopf bifurcation curve. Along the curves separating O_u from II_u and O_l from II_l 2 limit cycles coalesce in a fold bifurcation. The dashed line corresponds to a limit cycle of infinite amplitude. Limit cycle amplitude first increases in the direction of arrow 1, then in the direction of arrow 2.

(5.13b) $$\mu_1 = -3\alpha \frac{(2\alpha + \beta\bar{r}^{-2})}{(2\alpha - \beta\bar{r}^{-2})}$$

A brief analysis of (5.13b) shows which values of $\bar{r}^{-2}$ generate the two bifurcation curves in Fig.5.3:

(5.14a) $$0 \leq \bar{r}^{-2} < 2\frac{\alpha}{\beta} : \quad \mu_1 < 0 \quad \text{on the fold}$$

(5.14b) $$\bar{r}^{-2} = 2\frac{\alpha}{\beta} : \quad \mu_1 = \pm\infty \quad \text{on the fold}$$

(5.14c) $$2\frac{\alpha}{\beta} < \bar{r}^{-2} : \quad \mu_1 > 0 \quad \text{on the fold}$$

From (5.14), we see that the lines in Fig.5.3 sweep along in the direction shown by the arrow marked 1 for $\bar{r}^{-2}$ of (5.14a). On this range, the lines "roll" along the left fold, which begins at the point P given above. The lines then sweep out in the direction shown by the arrow marked 2 for $\bar{r}^{-2}$ of (5.14c). On this range, the lines "roll" along the right fold.

The equation of the fold is found from (5.13b) and (5.12b) (and (5.14)):

(5.15) $$\mu_2 = \frac{\alpha}{4\beta}\frac{(\mu_1 + 3\alpha)^2}{(\mu_1 - 3\alpha)} \quad , \quad |\mu_1| \geq 3\alpha$$

The line horizontally tangent to the right fold occurs for $\bar{r}^{-2} = 4\frac{\alpha}{\beta}$. This tangency occurs at the point given by:

$$(\mu_1,\mu_2) = (9\alpha, 6\frac{\alpha^2}{\beta}) \tag{5.16}$$

The bifurcation diagram for elliptic averaging is shown in Fig.5.4. It contains a region of two limit cycles (II_1), a region of one limit cycle (I_u) and a region of no limit cycles (0_1). The μ_1-axis is a Hopf bifurcation line. The diagram contains a fold bifurcation on which the lines of eq.(5.12c) "roll" for $\bar{r}$ increasing. The fold again begins at the point P given above. The equation for the fold can be derived in the same manner as was done for the second order trig diagram but we do not present it because of its long length.

Looking at the three bifurcation diagrams, we see that the three methods give very different qualitative results. A comparison diagram showing the important structures from Fig.5.2-5.4 is shown in Fig.5.5. It identifies 11 different regions marked a, b, ... , k. A comparison of the predictions made by each method in each of these regions is given in Table 5.1.

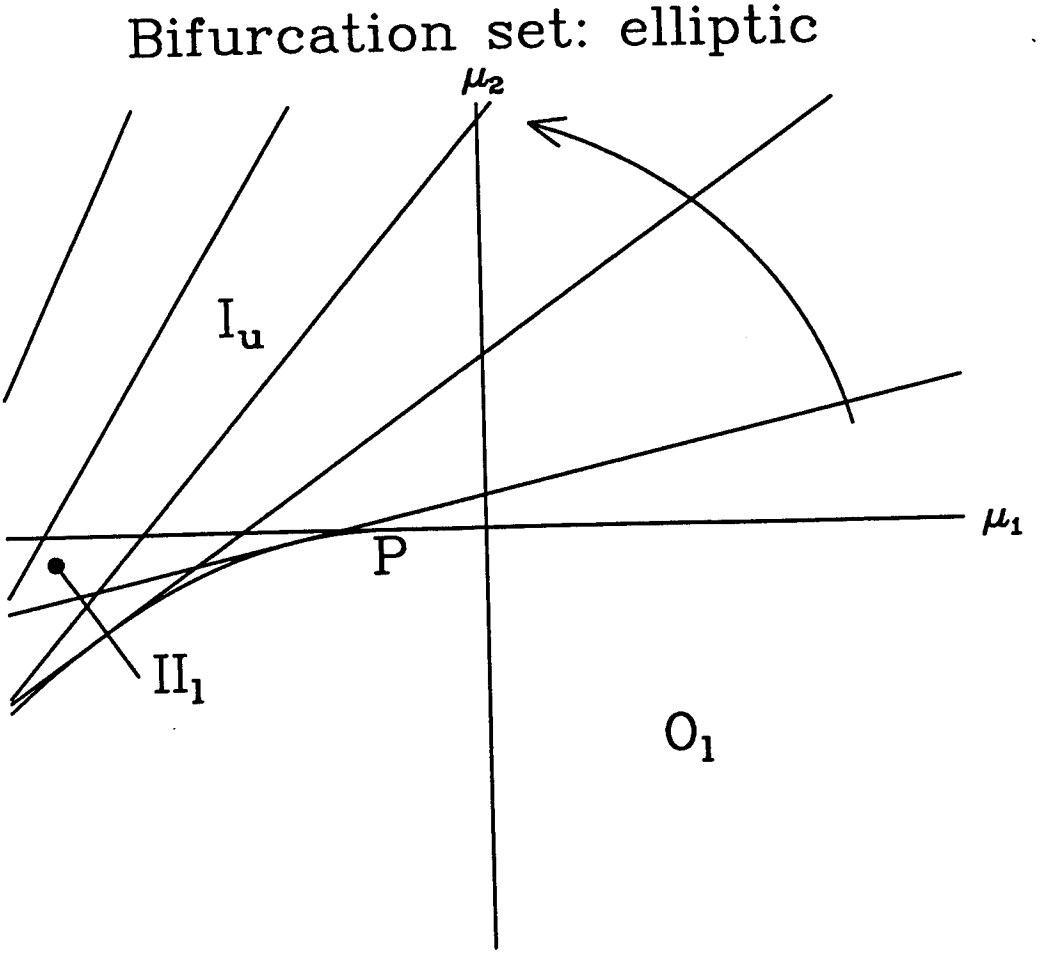

Fig.5.4 Bifurcation set for $\eta \neq 0$, as determined by elliptic averaging (eq.(5.12c)). Along each straight line there exists a limit cycle of fixed amplitude. In region II_1 there are 2 limit cycles; in I_u there is 1; in O_1 there are none. The μ_1-axis is a Hopf bifurcation curve. Along the curves separating O_1 from II_1 2 limit cycles coalesce in a fold bifurcation. The arrow shows the direction of increasing limit cycle amplitude.

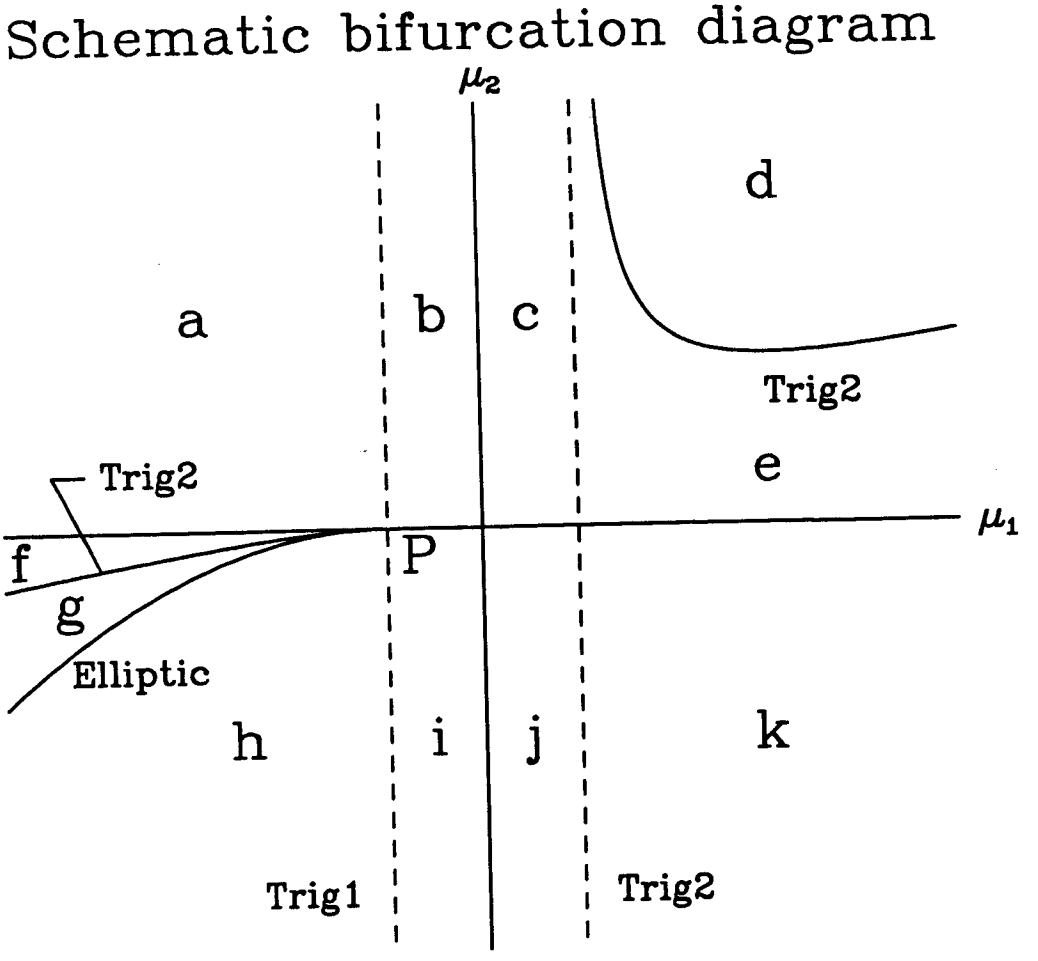

Fig.5.5 Schematic bifurcation diagram for $\eta \neq 0$, which shows the bifurcation curves of Fig.s 5.2 (denoted Trig1), 5.3 (denoted Trig2), and 5.4 (denoted Elliptic). The number of limit cycles predicted by the three methods for each region (a-k) is given in Table 5.1.

Table 5.1 Comparison of limit cycle predictions

	Number of limit cycles predicted by		
Region	Elliptic	1^{st} Trig	2^{nd} Trig
a	1	0	1
b	1	1	1
c	1	1	1
d	1	1	0
e	1	1	2
f	2	1	2
g	2	1	0
h	0	1	0
i	0	0	0
j	0	0	0
k	0	0	1

In 7 of the 11 regions (a,d,e,f,g,h,k), the predictions made by the three methods differ. We have found (using numerical integration) that the prediction made by elliptic averaging has always been correct. We believe that the elliptic averaging has been more successful than the trig averaging for two reasons: (1) it uses all of the integrable terms in the unperturbed solution and (2) the frequency-amplitude dependence is already built into the cn function solution.

Therefore, the qualitative prediction that a limit cycle exists in a system is dependent on the method and order of the averaging. Moreover, Table 5.1 clearly demonstrates that the second order trig method does not guarantee better results than the first order.

5.4 Examples

We will now show two examples showing the success of the elliptic averaging when trig averaging fails. The first example is given in (5.17).

$$x'' + x + .1\,x^3 - .05\,x' - .31\,x^2 x' + .1\,x'^3 = 0 \tag{5.17}$$

For convenience, we choose $\epsilon = 0.1$. This makes $\alpha = 1$, $\beta = 0.1$, $\hat{\beta} = 1$, $\delta = -0.5$, $\rho = -3.1$, and $\eta = 1$. Then from eqs.(5.11), $\mu_1 = -3.1$ and $\mu_2 = 0.5$. These parameter values locate system (5.17) in region a of Fig.5.5 near P.

From Table 5.1, we see that first order trig averaging predicts no limit cycle, second order trig averaging predicts (using eq.(5.8b)) a limit cycle at $\bar{r} = 1.9910$, and elliptic averaging (using eq.(5.8c)) predicts a limit cycle at $\bar{r} = 1.9861$.

Fig.5.6 and Fig.5.7 show a comparison of second order trig averaging and elliptic averaging with numerical integration of (5.17). For elliptic averaging, Fig.5.7a shows the first order approximation; Fig.5.7b shows the second order approximation. (The

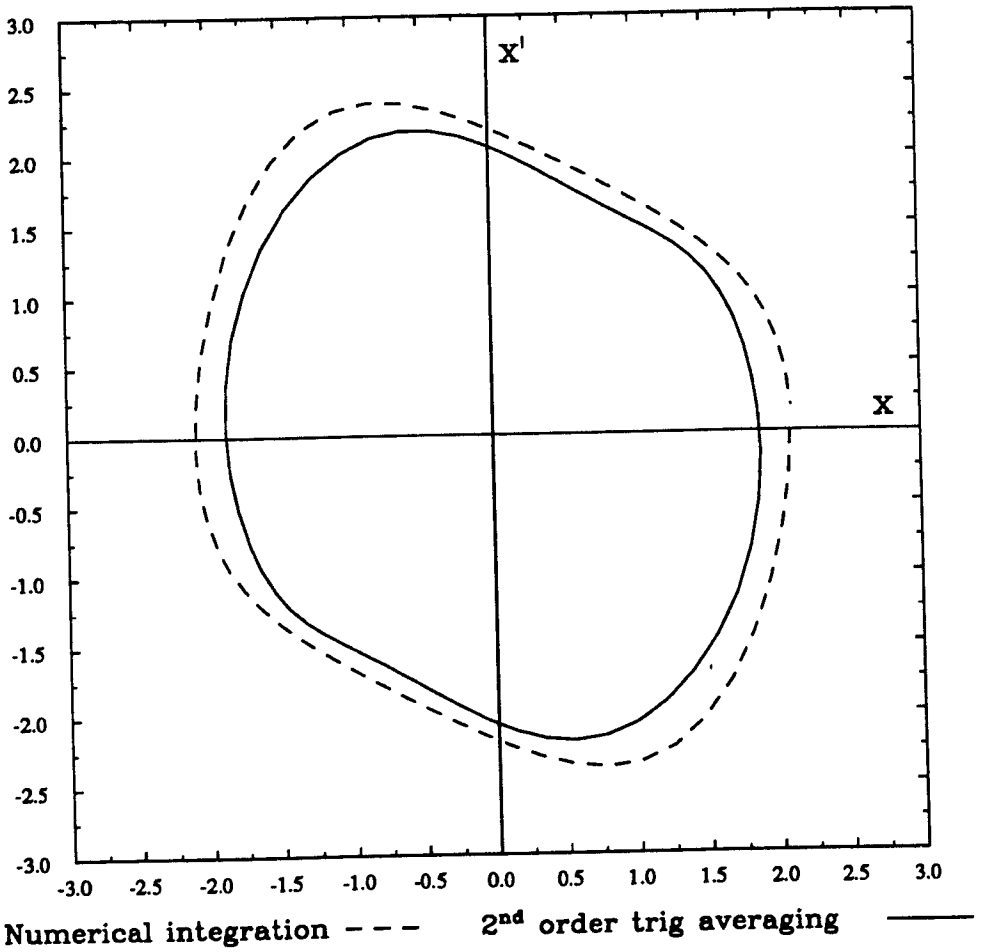

Fig.5.6 Comparison of numerical integration with second order trig averaging for the limit cycle in eq.(5.17).

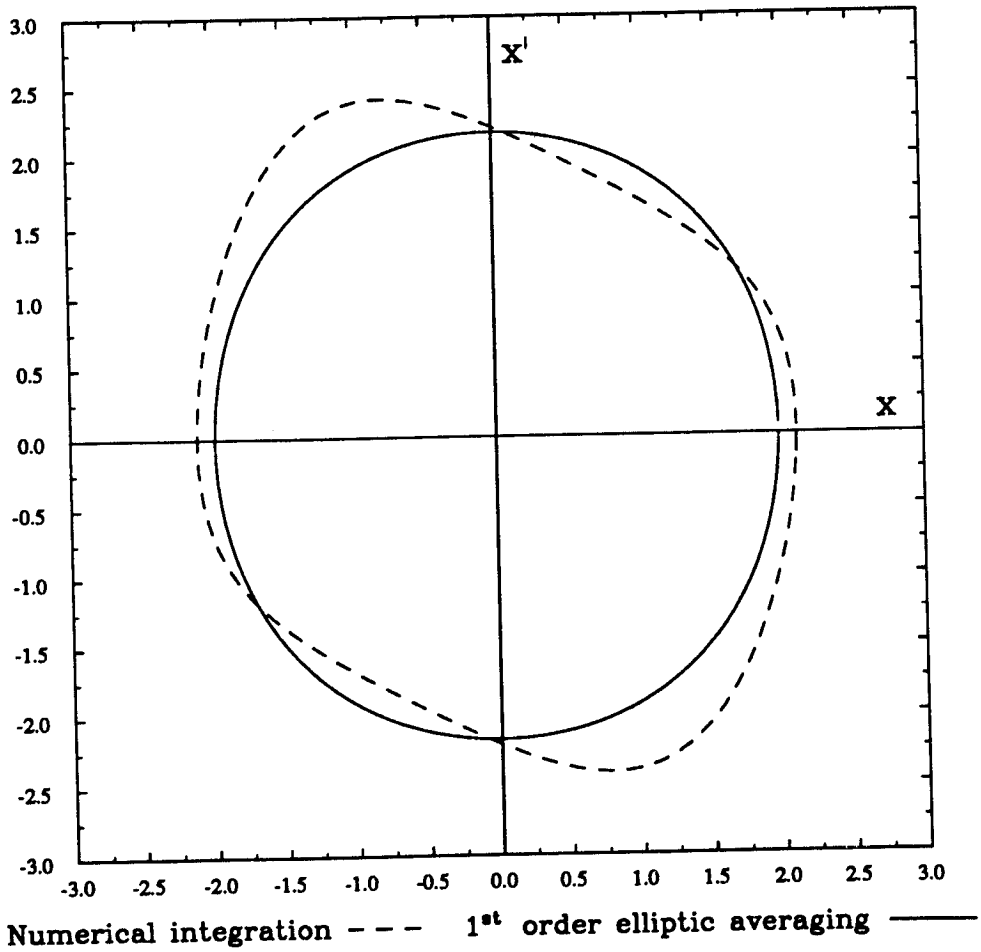

Fig.5.7a Comparison of numerical integration with first order elliptic averaging for the limit cycle in eq.(5.17).

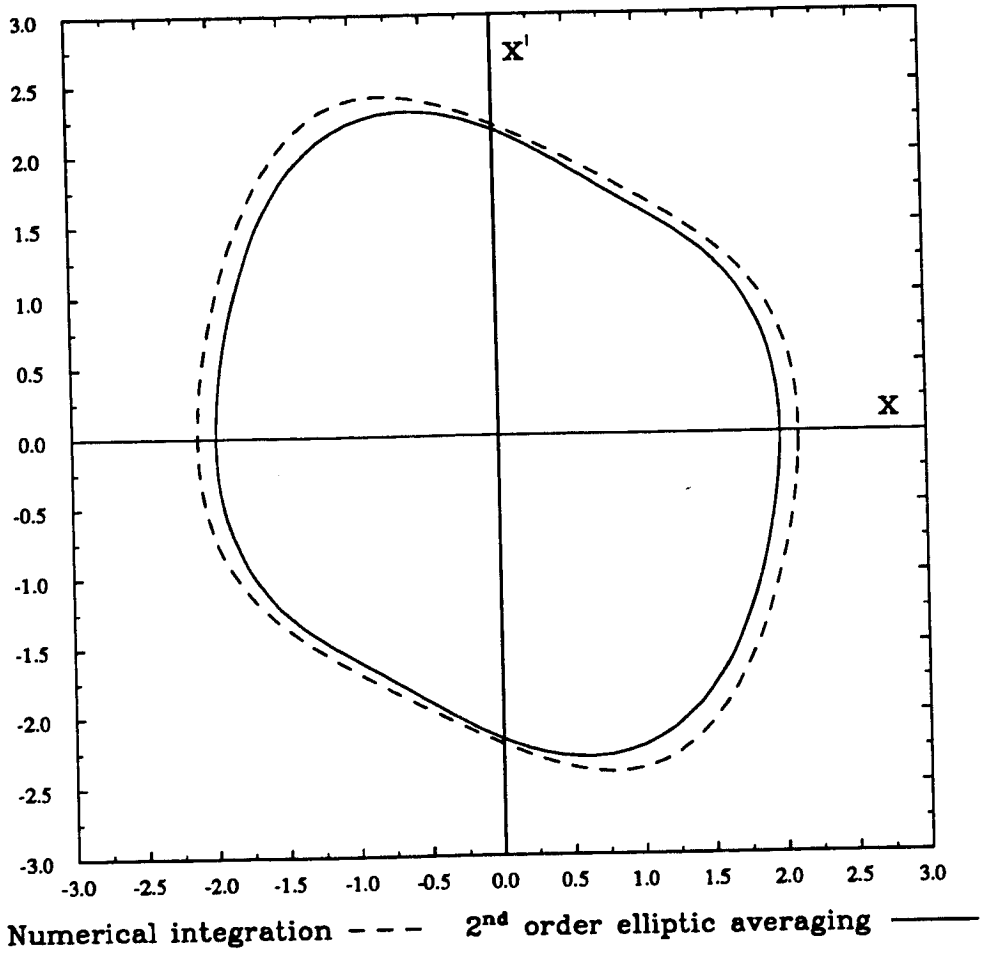

Fig.5.7b Comparison of numerical integration with second order elliptic averaging for the limit cycle in eq.(5.17).

$O(\epsilon)$ transformation has been used in the two second order approximations.)

The best approximation is seen to be the second order elliptic approximation, but the second order trig approximation is also good. The first order elliptic approximation, though not very good, is still much better than the first order trig averaging which did not even predict a limit cycle.

The second example shows that second order trig averaging does not necessarily give better results than first order trig averaging. The second example concerns the system described by (5.18).

$$(5.18) \qquad x'' + x + x^3 + 0.035\,x' - 0.6\,x^2\,x' + .1\,x'^3 = 0$$

Again, we choose $\epsilon = 0.1$ for convenience. This makes $\alpha = 1$, $\beta = 1$, $\hat{\beta} = 10$, $\delta = 0.35$, $\rho = -6$, and $\eta = 1$. Using eqs.(5.11), we find $\mu_1 = 6$ and $\mu_2 = -0.35$. This locates system (5.18) in region g of Fig.5.5.

Second order averaging predicts no limit cycles. First order averaging predicts one limit cycle at $\bar{r} = 0.68$. Elliptic averaging predicts two limit cycles, one at $\bar{r} = 1.12675$ (which is stable, i.e., attractive) and one at $\bar{r} = 0.83984$ (which is unstable, i.e., repelling). Fig.5.8 shows a comparison between first order elliptic averaging and numerical integration. The elliptic averaging approximation to the two limit cycles is excellent. At second order, the elliptic approximation coincides with the numerical integration.

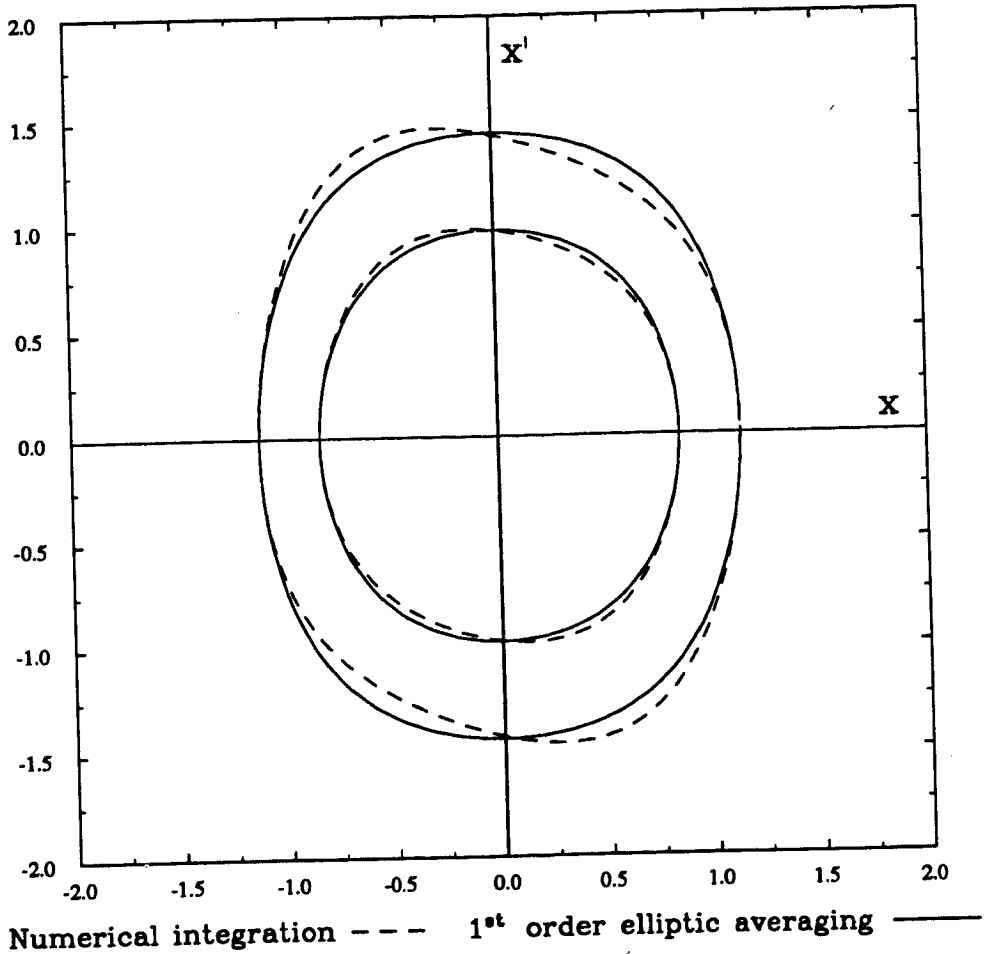

Fig.5.8 Comparison of numerical integration with first order elliptic averaging for the limit cycle in eq.(5.18).

These two examples show the superiority of elliptic averaging over trig averaging for eq.(0.1).

6.0 Limit cycles in the general case

The examples that have been presented so far in chapters 4 and 5 have had two properties in common: (1) each example has had a zero second order mean (using elliptic functions) and (2) the unperturbed system for each example has had just one center at the origin. In this chapter, we present examples with different properties.

First, we shall investigate a system which has an identically zero first order mean. Second order averaging is then required for predicting the correct qualitative behavior of the system. Then we consider an example from region IV of Fig.2.1 which has a double homoclinic loop separatrix in its unperturbed system.

For each of these examples, we will compute the averaged system using the AVERAGE computer program. Then we will look for limit cycles by examining the $\bar{r}'$ equation. Finally, we provide a comaparison of the averaged system's limit cycle(s) with numerical integration.

6.1 A second order averaging example

Although first order averaging determines system behavior in many systems, there are instances in which second order averaging must be used. These cases occur when the first order mean of the r

equation is identically zero. Then, the $O(\epsilon^2)$ truncated term from first order avergaing dominates the system behavior.

We will consider such a system, which was chosen by consulting Table 3.4. For convenience, we choose:

(6.1) $$\alpha = 1 \quad \text{and} \quad \beta = 1$$

in eq.(0.1) which makes the system lie in region II of the α-β plane (Fig.2.1). The perturbation is chosen to contain perturbation types I and IV (see Table 3.3):

(6.2) $$g = g_1 x^2 + g_2 x x' + g_3 x^4$$

The difference between this example and those from chapters 4 and 5, then, is that the first order mean is identically zero but the second order mean is not.

Using AVERAGE, the averaged equations for r and φ become:

(6.3a) $$\bar{r}' = \epsilon^2 g_2 \left[g_1 G_1(\bar{r}) + g_3 G_3(\bar{r}) \right] + O(\epsilon^3)$$

where

$$G_1 = \frac{50\,\bar{r}^{-6} + 299\,\bar{r}^{-4} + 436\,\bar{r}^{-2} + 52}{450\,\bar{r}^{-3}\,(1 + \bar{r}^{-2})} - \frac{E}{K}\,\frac{199\,\bar{r}^{-4} + 498\,\bar{r}^{-2} + 152}{225\,\bar{r}^{-3}\,(2 + \bar{r}^{-2})}$$

$$+ \frac{4}{9}\left(\frac{E}{K}\right)^2 \frac{(1 + \bar{r}^{-2})}{\bar{r}^{-3}\,(2 + \bar{r}^{-2})}$$

and

$$G_3 = -\frac{882\,\bar{r}^{-8} + 4470\,\bar{r}^{-6} + 8665\,\bar{r}^{-4} + 7050\,\bar{r}^{-2} + 608}{7350\,\bar{r}^{-3}\,(1+\bar{r}^{-2})}$$

$$+\frac{E}{K}\frac{882\,\bar{r}^{-8} + 3969\,\bar{r}^{-6} + 8104\,\bar{r}^{-4} + 8956\,\bar{r}^{-2} + 2176}{3675\,\bar{r}^{-3}\,(2+\bar{r}^{-2})}$$

$$-\left(\frac{E}{K}\right)^2\frac{(1+\bar{r}^{-2})\,(9\,\bar{r}^{-4} + 18\,\bar{r}^{-2} + 32)}{75\,\bar{r}^{-3}\,(2+\bar{r}^{-2})}$$

(6.3b) $$\bar{\varphi}' = \frac{\bar{a}}{4K} + O(\epsilon^2)$$

(6.3c) $$r = \bar{r} + \epsilon\, w_1(\bar{r},\varphi) + O(\epsilon^2)$$

where

$$w_1(\bar{r},\varphi) = -g_1\frac{\bar{r}^{-2}}{3a^2}\,cn^3 - g_3\frac{\bar{r}^{-4}}{5a^2}\,cn^5 - g_2\frac{1}{4a}\,(1+\bar{r}^{-2}\,cn^2)\,cn'$$

$$-g_2\frac{\sqrt{2}}{4\bar{r}}\,(1+\bar{r}^{-2})\,\sin^{-1}(\bar{k}\,sn)$$

(6.3d) $$E = E(k)\ ,\ K = K(k)\ ,\ k^2 = \frac{\bar{r}^{-2}}{2\,(1+\bar{r}^{-2})}$$

$$cn = cn(u,k)\ ,\ sn = sn(u,k)\ ,\ cn' = \frac{\partial cn}{\partial u}$$

$$u = 4\,K\,\varphi\ ,\ \varphi = \bar{\varphi} + O(\epsilon)\ ,$$

Limits cycles are predicted for values of $\bar{r}$ which make $\bar{r}' = 0$.

The limit cycle condition can be written:

(6.4) $$\frac{g_3}{g_1} = -\frac{G_1(\bar{r})}{G_3(\bar{r})} \quad \text{and} \quad g_2 \neq 0$$

Fig.6.1 shows a graph of $G_1(\bar{r})/G_3(\bar{r})$ vs. $\bar{r}$. From the graph and (6.4), it is seen that at most one limit cycle exists for fixed values of g_1 and g_3.

We now compare the averaging approximation to numerical integration. We choose parameter values for g_i that will result in a limit cycle, using Fig.6.1:

$$g_1 = 1 \ , \ g_2 = 1 \ , \ g_3 = -\frac{1}{2} \tag{6.5}$$

We numerically solve (6.4) using (6.5) and predict a limit cycle amplitude of $\bar{r} = 2.05$. A comparison of the averaging approximation with numerical integration of the original equation (i.e., eq.(0.1) subject to (6.1), (6.2), and (6.5)) is shown in Fig.6.2 for $\epsilon = .1$. The averaging approximation and the numerical integration agree very well. Since the limit cycle is shown to exist at $O(\epsilon^2)$ rather than $O(\epsilon)$, the attraction toward the limit cycle is slow.

This example shows the necessity of using a second order averaging method. The first order averaged equation for r predicts the perturbed system to be filled with closed orbits. It misses the limit cycle entirely. This error in the qualitative dynamics is corrected by going to $O(\epsilon^2)$.

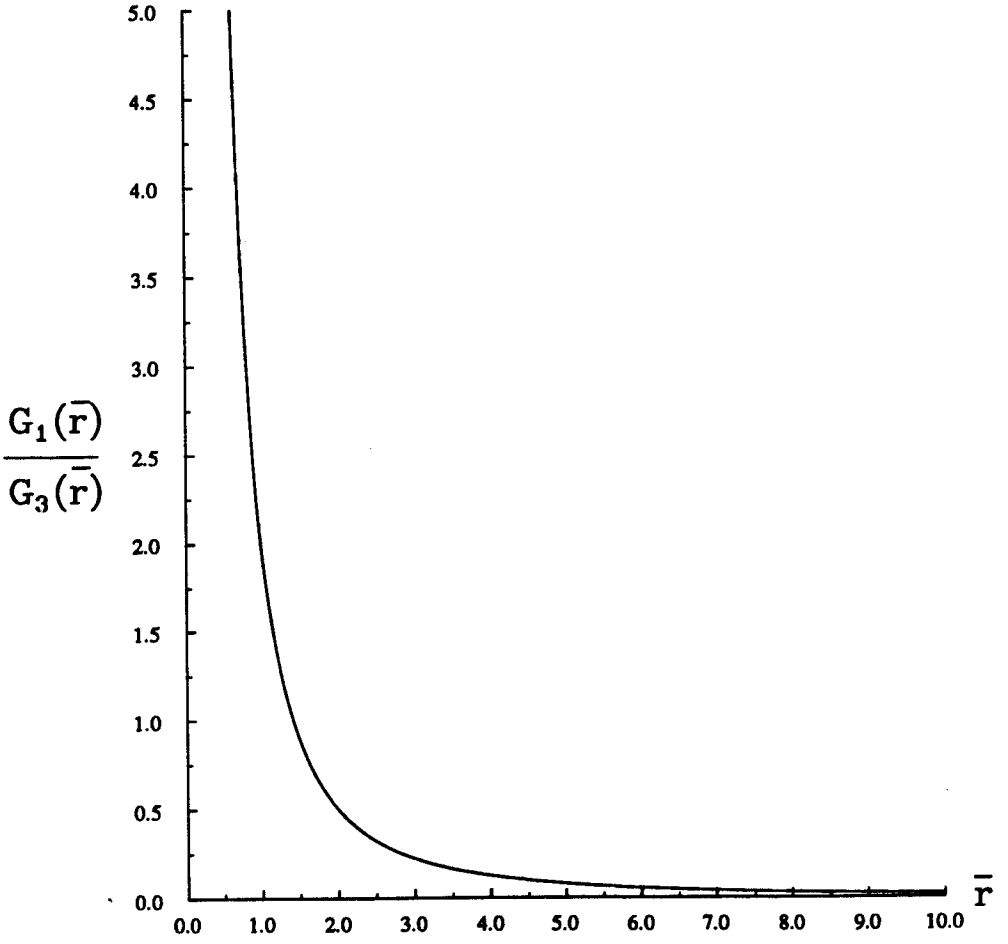

Fig.6.1 The limit cycle condition (6.4) for the system defined by eq.(0.1), (6.1), and (6.2). The functions $G_1(\bar{r})$ and $G_3(\bar{r})$ are defined in (6.3a). For given parameter ratio $-g_3/g_1$, a limit cycle of amplitude $\bar{r}$ is predicted to exist when $-g_3/g_1 = G_1(\bar{r})/G_3(\bar{r})$. For g_3/g_1 negative, exactly 1 limit cycle is predicted; for g_3/g_1 negative, no limit cycles are predicted.

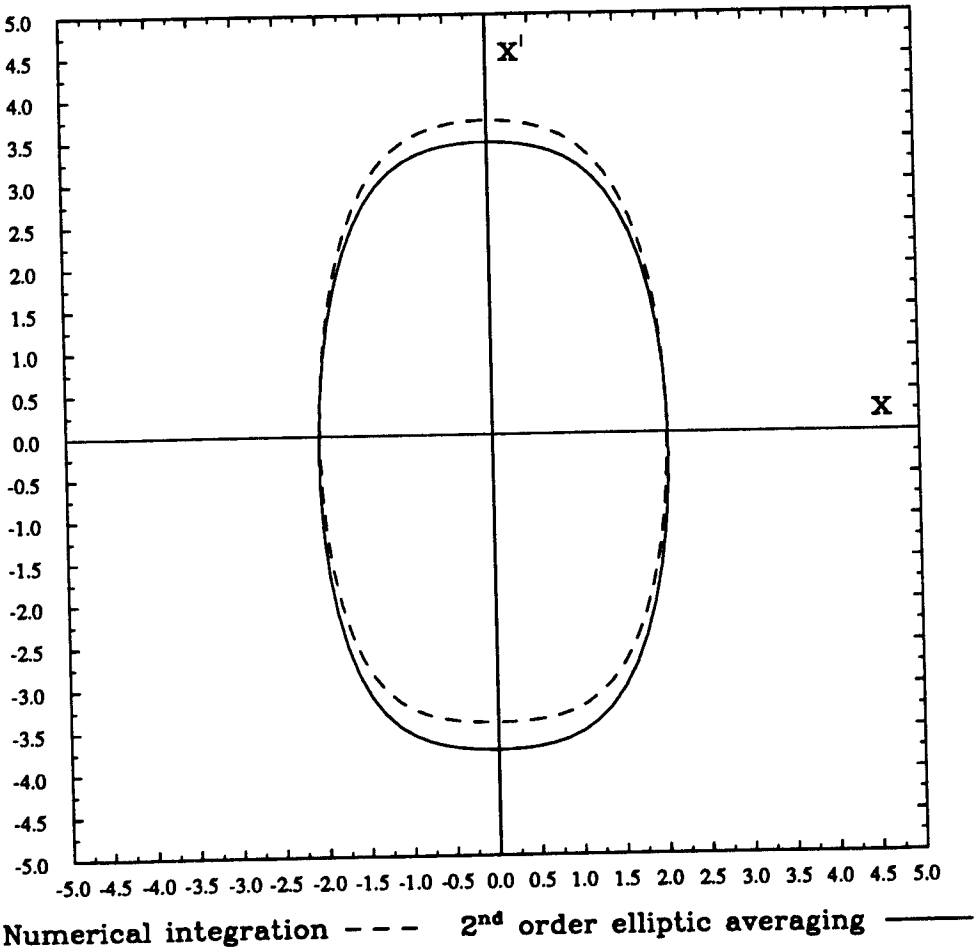

Fig.6.2 Comparison of numerical integration with second order elliptic averaging for the limit cycle of the system described by eq.(0.1), (6.1), (6.2), (6.5), and $\epsilon = 0.1$. No limit cycle is predicted at first order.

6.2 An example from region IV

In all of the previous examples, the unperturbed systems belong to regions I, II, or III of the α-β plane (Fig.2.1). Each of these systems is dynamically similar, containing just one center at the origin. No modulus transformations were needed to extend the normal definitions of any of the elliptic functions.

We now consider a system from region IV which is not dynamically similar. It contains a double homoclinic loop separatrix which divides the unperturbed phase space into three distinct regions (see Fig.2.1 and Table 2.1). Inside the separatrix, we must use the reciprocal modulus transformation (see section 1.2) to extend the normal definitions of the elliptic functions. This example will provide a check of our work and show that the modulus transformation saves us work.

For convenience, we choose the system parameters α and β to be constant. Consulting Table 3.4, we choose a van der Pol type perturbation for g so that the first order mean is not identically zero. The values for α, β, and g of eq.(0.1) are given in (6.6).

$$\alpha = -1 \ , \ \beta = 1 \ , \ g = \delta x' + \rho x^2 x' \tag{6.6}$$

From (2.10), the unperturbed separatrix lies at $r = \sqrt{2}$ and $r \geq 1$ except at the saddle. Using AVERAGE (or (3.31)), the averaged system becomes:

$$(6.7a)\quad \bar{r}' = -\epsilon \frac{\delta}{3\bar{r}}\left[\bar{r}^{-2} + 2\left(\frac{E}{K} - 1\right)\right] - \epsilon \frac{\rho}{15\bar{r}}\left[3\bar{r}^{-4}\left(2\frac{E}{K} - 1\right) + 2\bar{r}^{-2}\left(5 - 6\frac{E}{K}\right) + 8\left(\frac{E}{K} - 1\right)\right] + O(\epsilon^2)$$

$$= -\epsilon\left[\delta D(\bar{r}) + \rho R(\bar{r})\right] + O(\epsilon^2)$$

$$(6.7b)\quad \bar{\varphi}' = \frac{a}{4K} + O(\epsilon^2)$$

$$(6.7c)\quad E = E(k)\ ,\quad K = K(k)\ ,\quad k^2 = \frac{\bar{r}^{-2}}{2\left(\bar{r}^{-2} - 1\right)}\ ,\quad a^2 = \bar{r}^{-2} - 1$$

Note that (6.7) is valid inside and outside the separatrix. The reciprocal modulus transformation defines K and E inside the separatrix where $k^2 > 1$.

A limit cycle is predicted to exist at values of $\bar{r}$ where $\bar{r}' = 0$. From (6.7a), this limit cycle condition can be expressed by:

$$(6.8)\quad \frac{\delta}{\rho} = -\frac{R(\bar{r})}{D(\bar{r})}$$

A plot of $R(\bar{r})/D(\bar{r})$ vs. $\bar{r}$ is shown in Fig.6.3. As $\bar{r}$ increases from 1 (the lowest value permissble for a in eq.(6.7c) to be real), the curve descends from a value of 1.0 to a minmium value of approximately 0.75, and then grows without bound. In so doing, the curve passes through the value of $\bar{r} = \sqrt{2}$ at $R(\bar{r})/D(\bar{r}) = 0.8.$, which

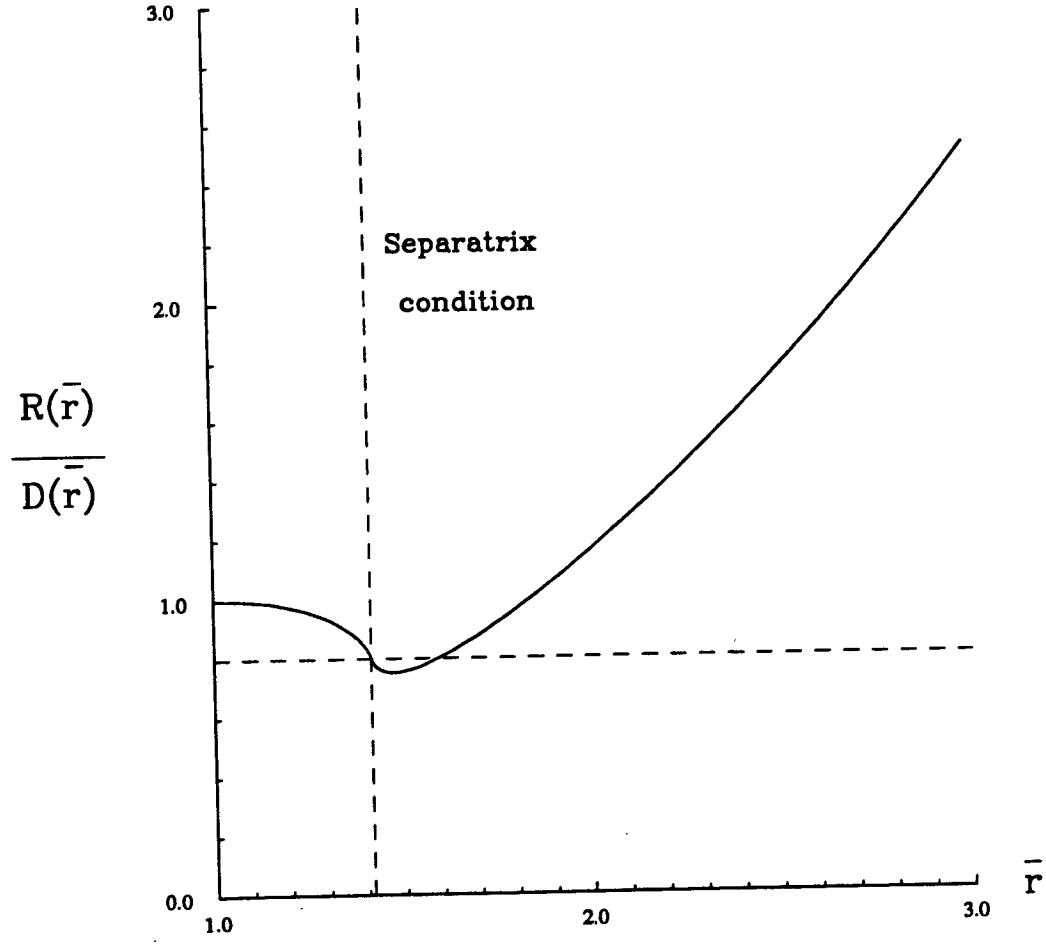

Fig.6.3 The limit cycle condition (6.8) for the system defined by eq.(0.1) and (6.6). The functions $R(\bar{r})$ and $D(\bar{r})$ are defined in (6.7a). For given parameter ratio $-\delta/\rho$, a limit cycle of amplitude $\bar{r}$ is predicted to exist when $-\delta/\rho = R(\bar{r})/D(\bar{r})$. The separatrix condition $\bar{r} = \sqrt{2}$ is shown dashed; it intersects the bifurcation curve at R/D = 0.8 which is also shown dashed. The number and location of limit cycles determined by the bifurcation curve is discussed in the text.

is the value of $\bar{r}$ corresponding to the separatrix. Thus, a double homoclinic loop separatrix is predicted to exist under the perturbation when $-\delta/\rho = 0.8$. In addition, a limit cycle located outdside this septatrix is predicted at this ratio of $-\delta/\rho$.

Given a fixed ratio $-\delta/\rho$, the number of limit cycles predicted to exist is equal to the number of values $\bar{r}$ satisfying eq.(6.8). These can be found from the graph by projecting a horizontal line from the vertical axis of Fig.6.3 at the value $-\delta/\rho$ and counting intersections with the curve. In addition, the separatrix condition $\bar{r} = \sqrt{2}$ (shown as a dashed line on Fig.6.3) separates the regions outside the separatrix and inside the separatrix. Since $\bar{r}$ does not distinguish between the right and left separatrix loops, a value of $\bar{r} < \sqrt{2}$ on the bifurcation curve corresponds to <u>two</u> limit cycles, one within each loop.

Thus, we can interpret Fig.6.3 as follows:

1: For $-\delta/\rho < \sim 0.75$, no limit cycles are predicted.

2: For $\sim 0.75 < -\delta/\rho < 0.8$, 2 limit cycles are predicted to exist outside the separatrix.

3: For $-\delta/\rho = 0.8$, the double homoclinic loop separatrix is predicted to exist in addition to a limit cycle located outside it.

4: For $0.8 < -\delta/\rho < 1.0$, 3 limit cycles are predicted, 1 outside the separatrix and 2 inside it (1 inside each loop)

5: For $1.0 < -\delta/\rho$, 1 limit cycle is predicted which is located outside the separatrix.

The study of the bifurcations in this system (i.e., eq.(0.1) with the conditions (6.6)) was first studied by Takens [Tak74]. The work was then completed by Carr [Car81] and others. A summary appears in Guckenheimer and Holmes [Guc86].

Now, we compare the averaging predictions with numerical integration. We take the parameter values:

$$\delta = 1 \quad \text{and} \quad \rho = -1.1 \tag{6.9}$$

so that $-\delta/\rho \simeq 0.91$. From Fig.6.3, we find that there are two solutions, r_1 and r_2, to eq.(6.8). Numerically solving (6.8) for r_1 and r_2 we find:

$$\bar{r} = r_1 = 1.33 \tag{6.10a}$$

$$\bar{r} = r_2 = 1.74 \tag{6.10b}$$

The amplitude r_1 lies inside the separatrix and corresponds to <u>two</u> limit cycles. The amplitude r_2 lies outside the separatrix. The choice of the signs of δ and ρ make r_1 limit cycles stable and the r_2 limit cycle unstable.

Fig.6.4 shows a graph of the limit cycles for the system given by (6.6) subject to the parameter values (6.9) for $\epsilon = 0.1$. The

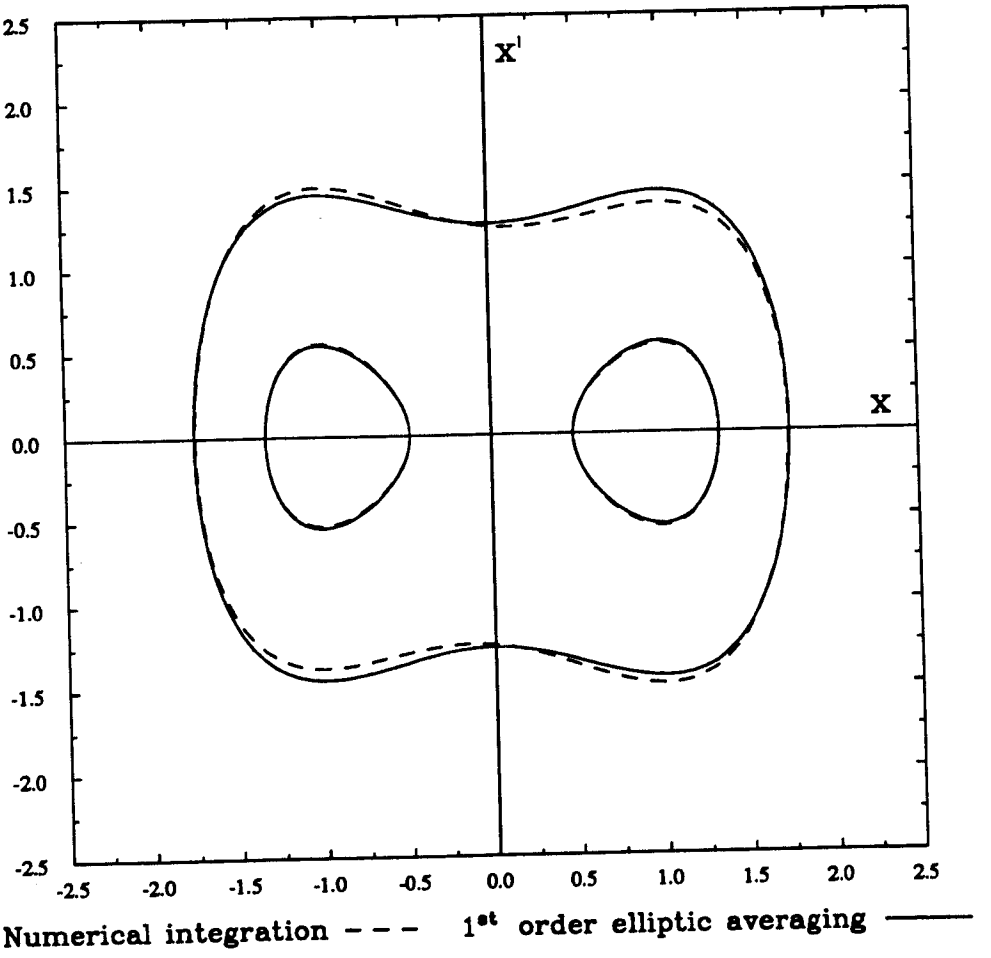

Fig.6.4 Comparison of numerical integration with first order elliptic averaging for the limit cycle of the system described by eq.(0.1), (6.6), (6.9), and $\epsilon = 0.1$. The interior limit cycles are stable; the outside one is unstable.

graphs of the first order averaging approximation and the numerical integration are very close.

For higher ϵ, one can use second order averaging to approximate the limit cycles. This proceeds easily since by Table 3.4, the second order mean of r (i.e., $\bar{H}_1$) is identically zero. It is then valid to use the transformation to $O(\epsilon)$ in the approximation of r. The transformation, found using AVERAGE, is given in (6.11).

(6.11a) $$r = \bar{r} + \epsilon\, w_1(\bar{r},\varphi) + O(\epsilon^2)$$

where

(6.11b) $$w_1(\bar{r},\varphi) = -\frac{\delta}{3\bar{r}a}\left[2Z + \bar{r}^{-2}cn\ cn'\right] + \frac{\rho}{15\bar{r}a}\left[-2Z\,(3\bar{r}^{-4} - 6\bar{r}^{-2} + 4) + \bar{r}^{-2}(2 - 3\bar{r}^{-2}cn^2)cn\ cn'\right]$$

where Z, cn, and cn' depend on (u,k), $u = 4K\varphi$, and both a^2 and k^2 are defined in (6.7c)

In using (6.11), we use the $O(1)$ φ-transformation, i.e., $\varphi = \bar{\varphi}$.

Fig.6.5 shows a graph comparing this second order approximation with numerical integration for the same problem with $\epsilon = 1.0$. At this high value of ϵ, the outside limit cycle is highly deformed from its elliptical unperturbed orbit. Even so, the averaging approximation is very good.

We point out that it is not possible to rescale the nonlinear term β to $O(\epsilon)$ and perturb using the linear equation since the linear equation does not possess oscillatory solutions. (Its solutions are

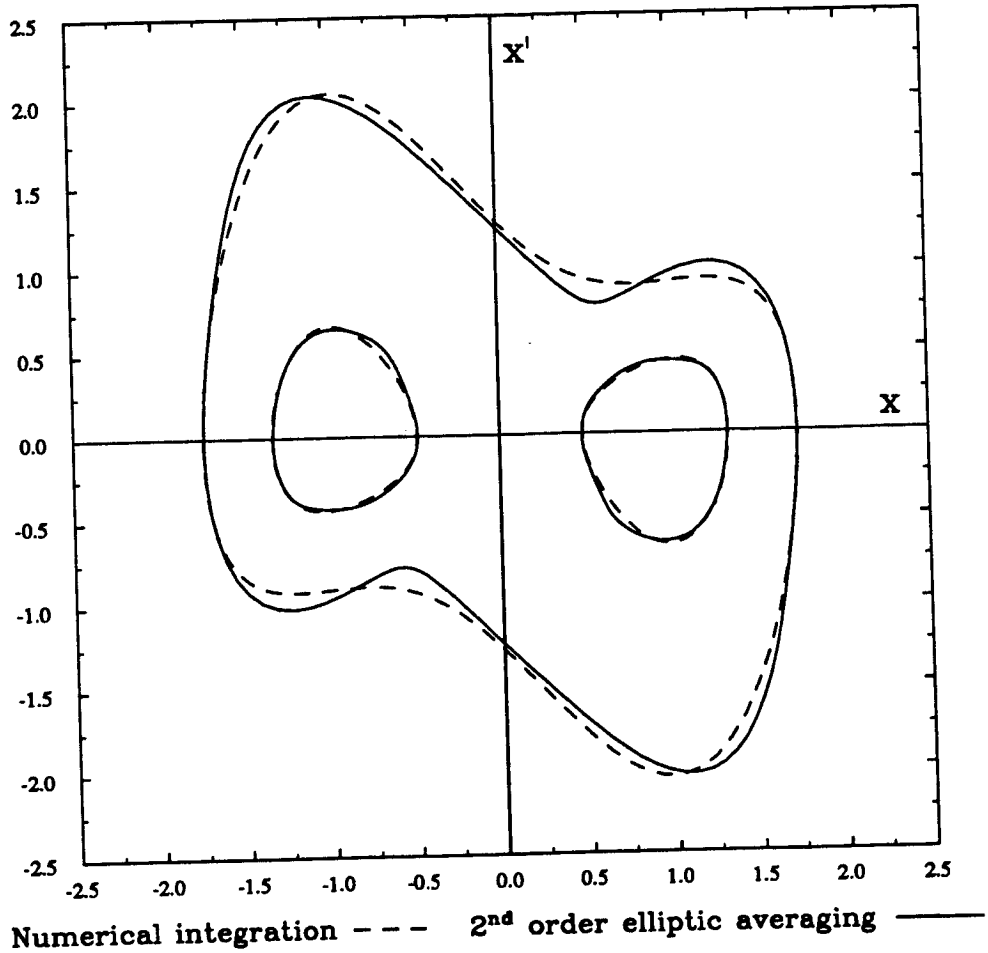

Fig.6.5 Comparison of numerical integration with first order elliptic averaging for the limit cycle of the system described by eq.(0.1), (6.6), (6.9), and $\epsilon = 1.0$. The agreement of the averaging approximation with numerical integration for this high value of ϵ is still quite good. The interior limit cycles are stable; the outside one is unstable.

expressed by sinh and cosh). By translating to the center in the unperturbed orbit, one could perturb using the linear system, but this will only give good results for limit cycles close to the centers. The outside limit cycle can be found by treating α as $O(\epsilon)$ and rescaling, but this involves perturbations of the cubic oscillator (chapter 4) and <u>not</u> a linear one. Still, for larger ϵ, the more general approach (which is just as simple to apply because of the computer program AVERAGE) gives better results.

7.0 Chaos in a system with a periodically disappearing separatrix

We now explore a slowly varying Hamiltonian system whose unperturbed system contains a double homoclinic loop separatrix. The size of separatrix changes periodically with slow time τ ($=\epsilon t$) and disappears completely from the unperturbed phase portrait for half of the cycle. When the separatrix is present, it distinguishes between three qualitatively different dynamical behaviors: (1) motions that pass through the right separatrix loop; (2) motions that pass through the left separatrix loop; and (3) motions that pass through neither loop.

We are interested in the motions which pass through a separatrix loop during a periodic cycle in τ. After each cycle, we associate a symbol L (=left) or R (=right) which indicates which side the motion finds itself. Each orbit of the system in time then corresponds to a symbol sequence of L's and R's. The chaos in the system is related to the unpredictability of the symbol sequence for a given initial condition, when the initial condition is known only within some small tolerance.

We begin with a preliminary discussion of the system, including a short investigation by numerical integration. We also relate the system to the familiar rotating plane pendulum. The averaging model is then derived, analyzed, and shown to exhibit chaos in the form we

have discussed. Next, we compare the averaging model with numerical integration. This leads us to introduce an improved model that compensates for some of the averaging model's shortcomings. A careful proof of the chaos, along with the explicit symbolic dynamics, is presented last.

7.1 Preliminary discussion

This chapter concerns the dynamics of a slowly varying Hamiltonian system for which the unperturbed phase portrait changes qualitatively with time. In particular, we shall be concerned with the system in (7.1), suggested by Philip Holmes of Cornell.

$$x'' - \cos(\tau)\, x + x^3 = 0 \ , \ \tau = \epsilon t \ , \ \epsilon \ll 1 \tag{7.1}$$

In the notation of eq.(0.1), we find:

$$\alpha = -\cos(\tau) \ , \ \beta = 1 \ , \ g = 0 \tag{7.2}$$

The unperturbed system corresponding to eq.(7.1) is the system for which τ is fixed.

From (7.2), we see that eq.(7.1) belongs to regions II, III, and IV of Fig.2.1, depending on the value of τ. As τ varies, the unperturbed phase portrait changes from one in which a separatrix exists (region IV) to one without a separatrix (regions II and III).

and then back again periodically (since α is periodic). Since the unperturbed solution is known for any fixed τ (see section 2.1), eq.(7.1) is viewed as a system of slowly varying phase portraits. Thus, we shall interpret solutions of eq.(7.1) in terms of the underlying "instantaneous phase portrait", i.e., the phase portrait of the unperturbed system at time τ.

Since α is periodic, we see that the phase space for eq.(7.1) is $\mathbb{R}^2 \times S^1$, i.e., a plane crossed with a circle. As previously stated, we choose to interpret eq.(7.1) in terms of the τ-fixed cross-sections, i.e., by projecting onto $\mathbb{R}^2$. Hence, we will be concerned with the (x,x') phase portrait projection (at a "snapshot" in τ) in understanding the dynamics of the system.

We wish to make clear, however, that the instantaneous phase portraits are not really part of the dynamics; they only aid in its analysis. Therefore, when we speak of a separatrix, it is clear that we mean the separatrix in the instantaneous phase portrait and not in the system itself. Likewise, the fixed point centers inside each separatrix loop are not fixed points of eq.(7.1). Eq.(7.1) admits only one fixed point, the origin, whose instantaneous linear stability in (x,x') changes with τ.

Before we present the averaging analysis, it is wise to investigate eq.(7.1) using numerical integration to get a sense of its dynamical behavior. In Fig.7.1a and Fig.7.1b, we show projections of two orbits of eq.(7.1) onto (x,x'), for different

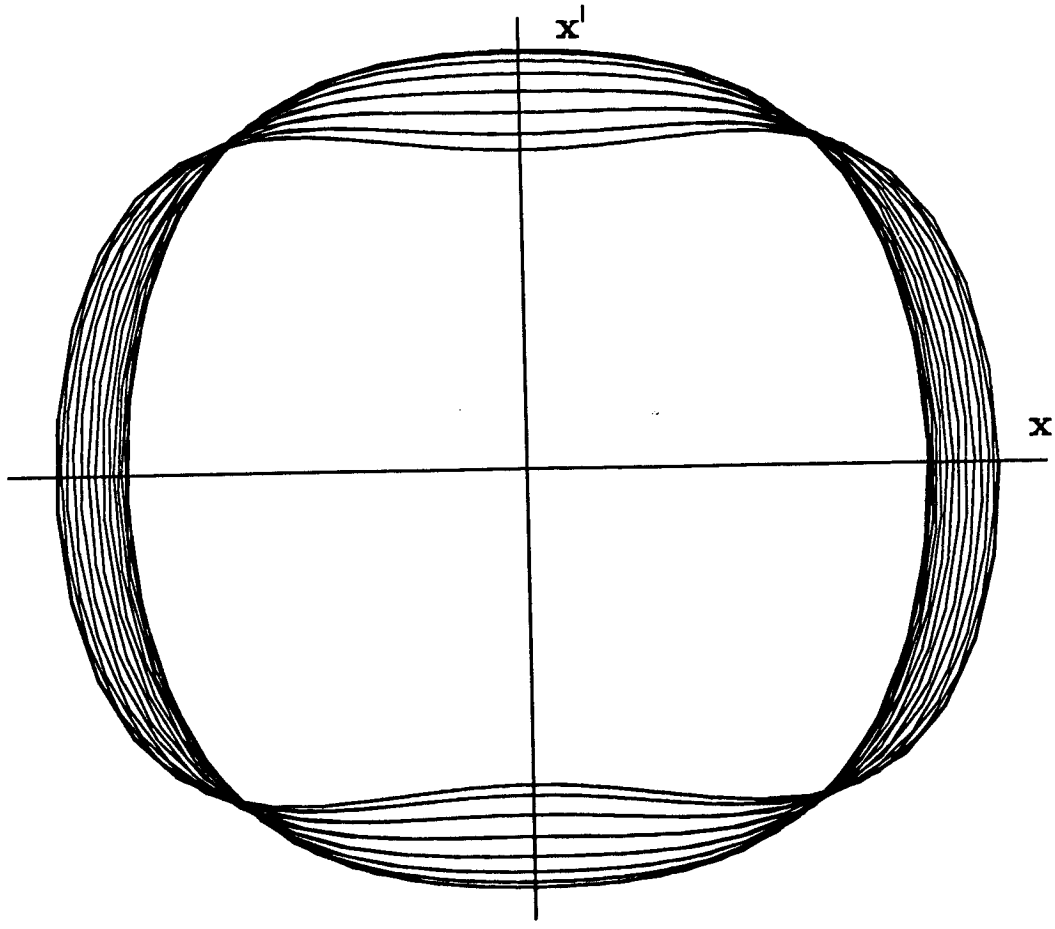

Fig.7.1a Projection of an orbit of eq.(7.1), computed using numerical integration, onto (x,x'). $\epsilon = 0.1$. The motion is simply an oscillation about the origin with slightly varying amplitude.

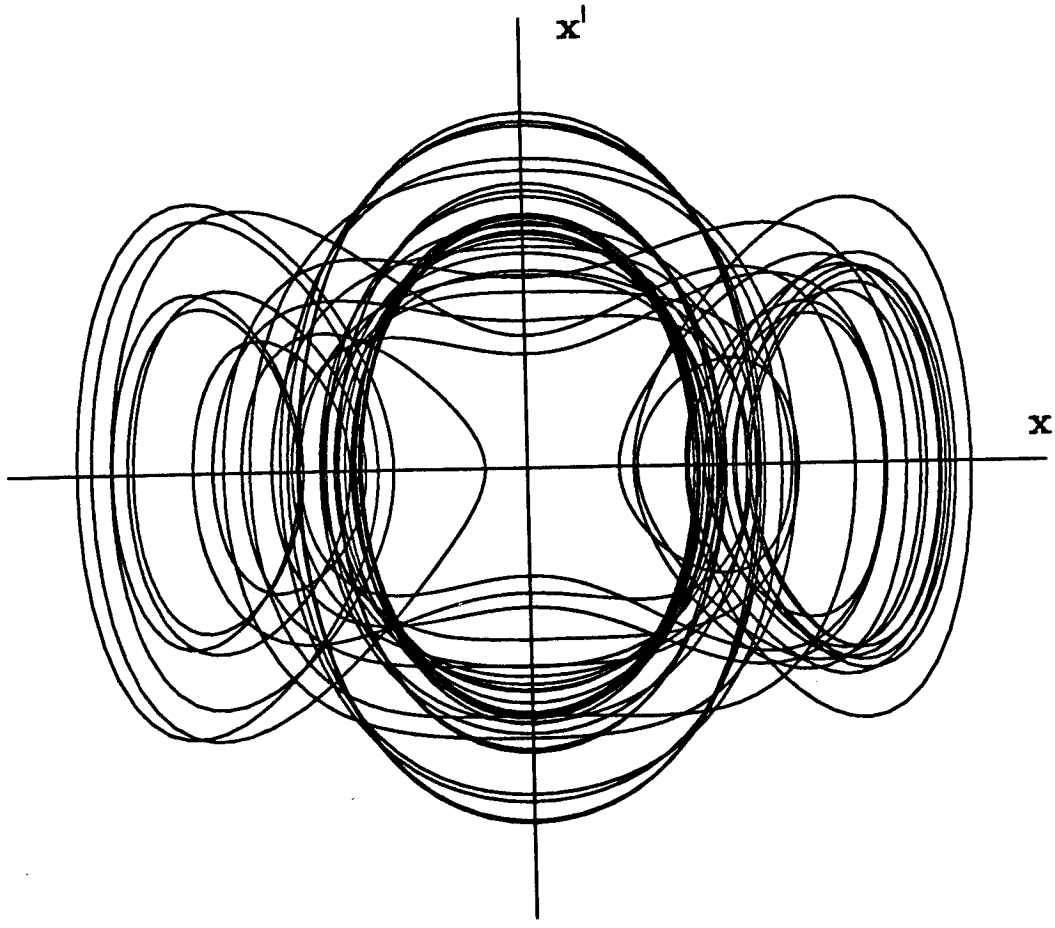

Fig.7.1b Projection of an orbit of eq.(7.1), computed using numerical integration, onto (x,x'). $\epsilon = 0.1$. The motion shows oscillation to the left of the origin, about the origin, and to the right of the origin.

initial conditions. The first figure shows regular motion with slightly varying amplitude. The second figure shows very complicated motion with three distinctive features: (1) oscillatory motion about the origin; (2) oscillatory motion to the right of the origin; and (3) oscillatory motion to the left of the origin.

The left and right oscillatory nature of an orbit is easier to see in a plot of x vs.t. This is shown in Figs.7.2a-d for four different initial conditions, each of which lies on the same initial energy curve. Oscillations to the left of the origin occur for $x < 0$; those to the right for $x > 0$. The symbol sequence for each orbit is easily found by examining the pattern of oscillation shown in its x vs.t plot. This is indicated on the figures. The figures clearly show the three distinctive oscillatory features mentioned above.

Moreover, Figs.7.2a-d motivate the search for chaos. After each birth of the separatrix, some trajectories will oscillate within the left loop while others oscillate within the right loop. Each orbit must make a choice of either left or right. The averaging model will show that the sequence of L's and R's exhibit sensitive dependence on initial conditions, i.e. chaos.

Finally, as a physical example of the chaotic dynamics which occur in eq.(7.1), we consider the familiar rotating-plane pendulum [Gre65] shown in Fig.7.3. A plane pendulum is forced to rotate about

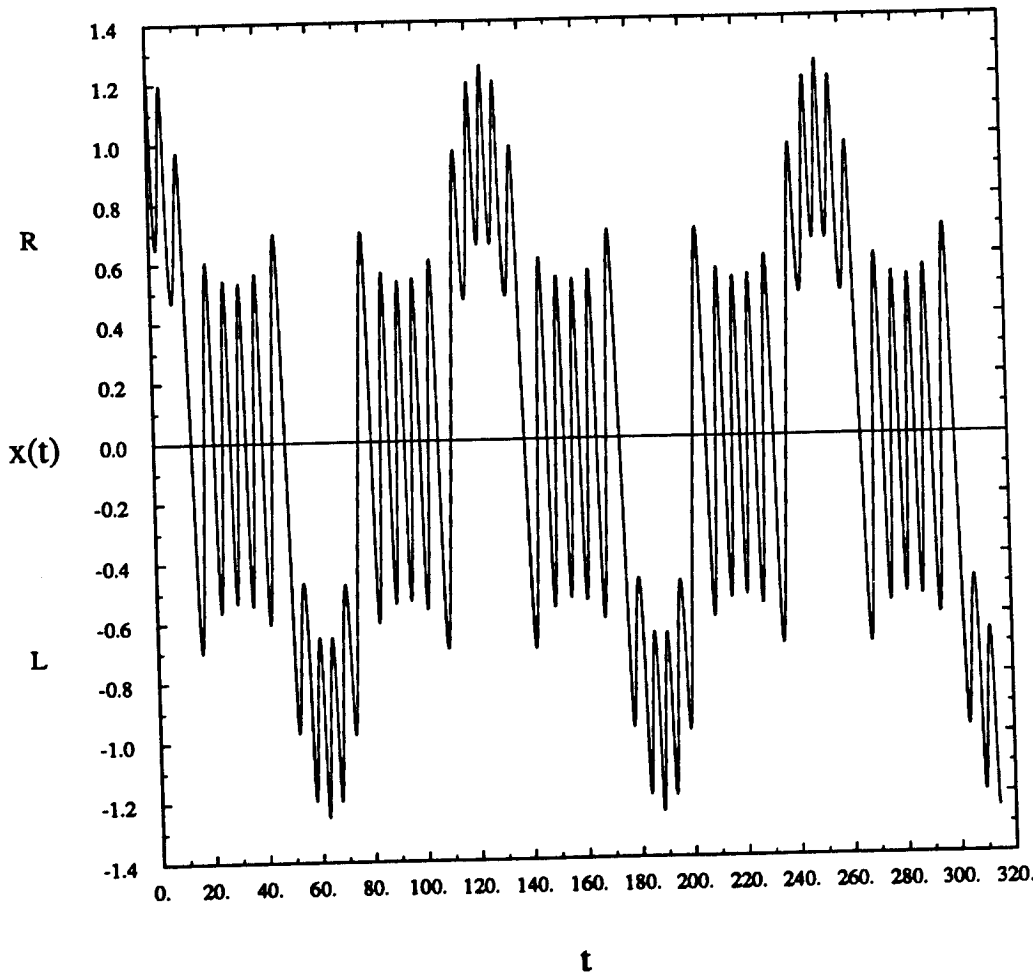

Fig.7.2a Plot of x vs. t for an orbit of eq.(7.1), computed using numerical integration, with x(0) = 1.25, y(0) = 0.0, and ϵ = 0.1. Oscillations on the right occur for x > 0, on the left for x < 0. The motion's symbol sequence is RLRLRL.

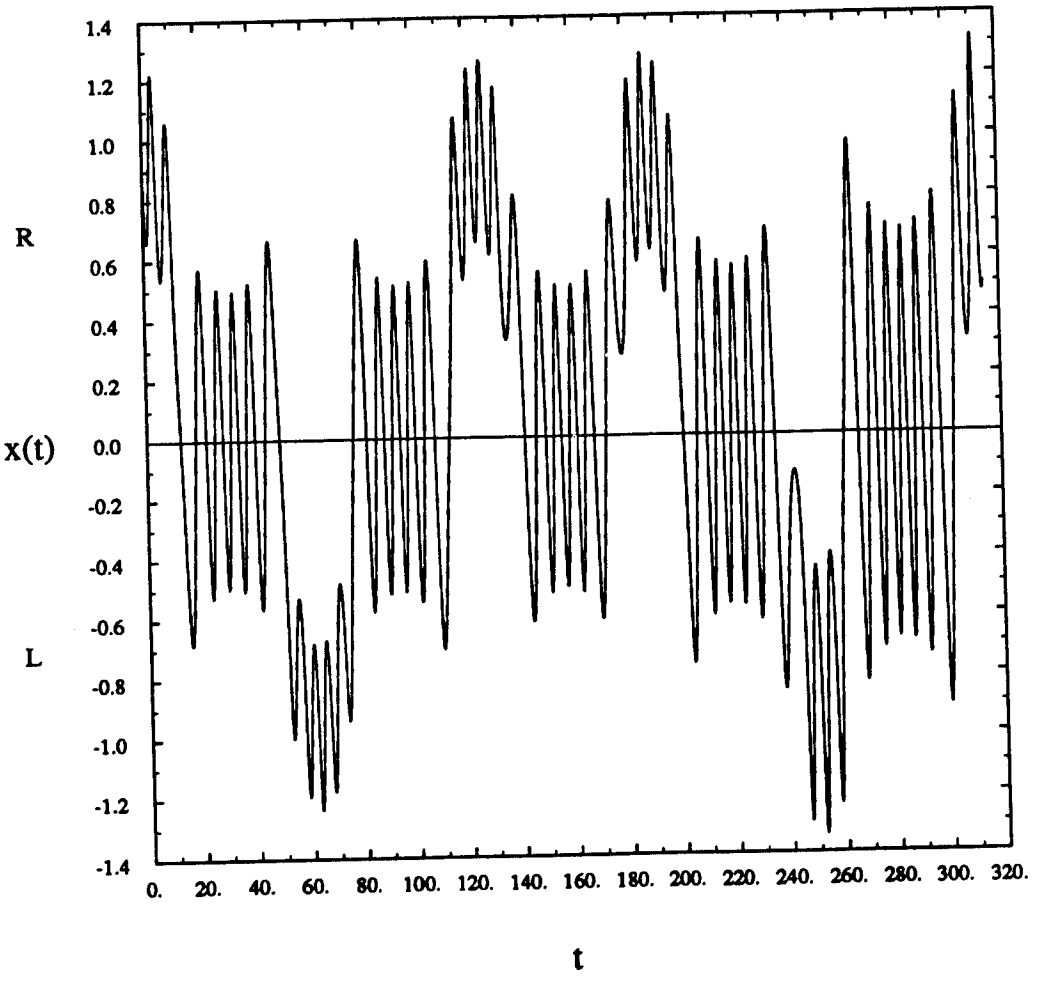

Fig.7.2b Plot of x vs. t for an orbit of eq.(7.1), computed using numerical integration, with x(0) = 0.909, y(0) = −0.378, and ϵ = 0.1. Oscillations on the right occur for x > 0, on the left for x < 0. The motion's symbol sequence is RLRRLR.

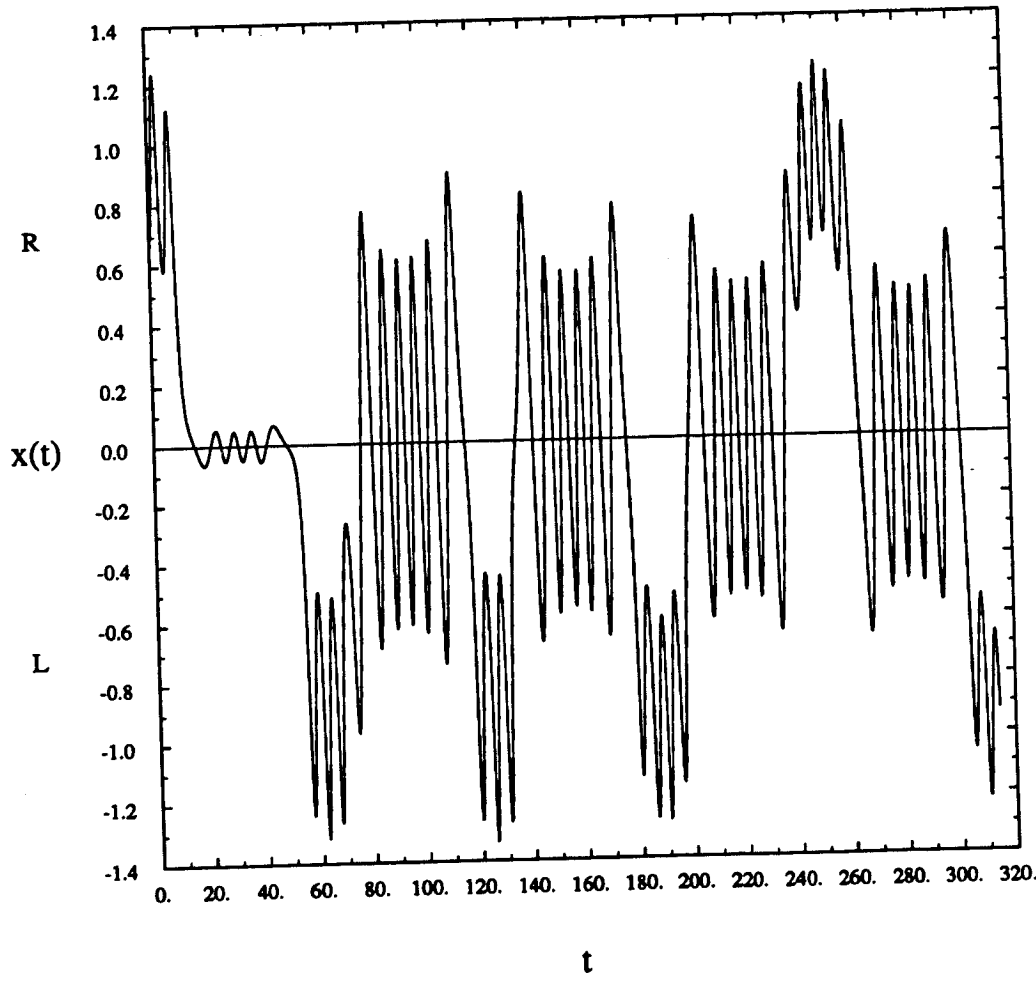

Fig.7.2c Plot of x vs. t for an orbit of eq.(7.1), computed using numerical integration, with x(0) = 0.661, y(0) = 0.0, and ϵ = 0.1. Oscillations on the right occur for x > 0, on the left for x < 0. The motion's symbol sequence is RLLLRL.

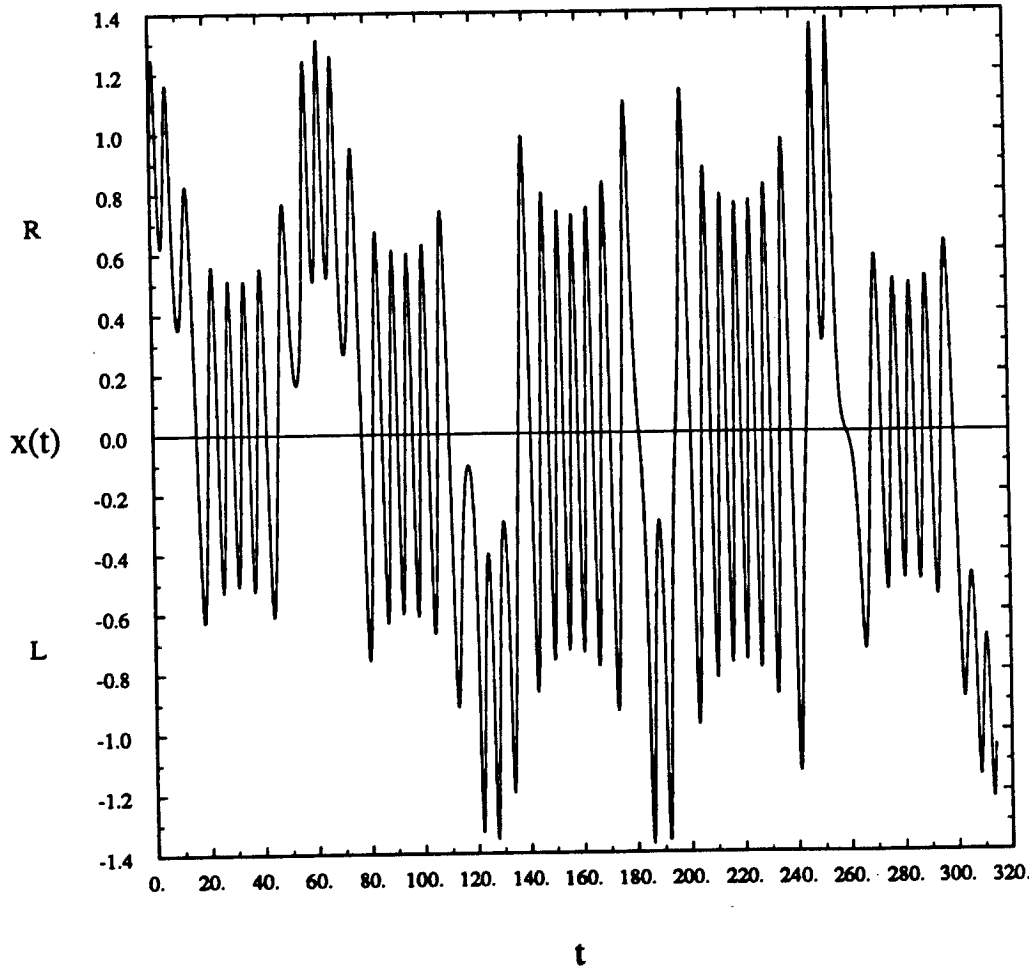

Fig.7.2d Plot of x vs. t for an orbit of eq.(7.1), computed using numerical integration, with x(0) = 0.909, y(0) = 0.378, and ϵ = 0.1. Oscillations on the right occur for x > 0, on the left for x < 0. The motion's symbol sequence is RRLLRL.

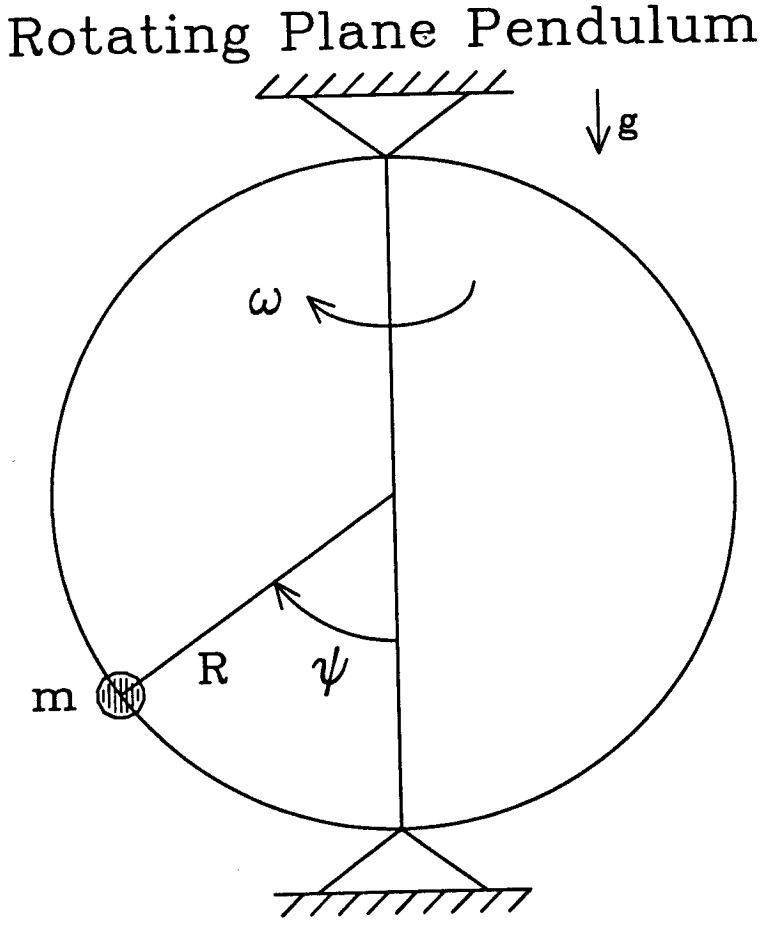

Fig.7.3 The rotating plane pendulum. The mass m slides (without friction) along a circular hoop of radius R making an angle of ψ with respect to the vertical. The hoop rotates about a vertical axis with angular velocity ω.

a vertical axis with angular velocity $\omega(t)$. The Lagrangian function for such a system is:

$$(7.3) \qquad L = \frac{m}{2}\left[R\,\psi'^2 + R^2\,\omega(t)^2\,\sin^2\psi\right] + m\,g\,R\cos\psi = 0$$

where m is the mass of the pendulum, R is the hoop's radius, g is the acceleration of gravity, and ψ measures angular displacement. The corresponding equation of motion is

$$(7.4) \qquad \psi'' + \left[\frac{g}{R} - \omega(t)^2\cos\psi\right]\sin\psi = 0$$

As is well known [Gre65,Arn84], this system, for fixed ω, possesses 1 or 3 equilibria depending respectively on whether ω^2 is smaller or larger than g/R. In order to see the relation between eq.(7.4) and eq.(7.1), we use the following scalings:

$$(7.5) \qquad \omega^2 = \frac{g}{R} + \epsilon\cos(\epsilon^{3/2}t), \quad \psi = \epsilon^{1/2}\,x, \quad t = \epsilon^{-1/2}\eta$$

Substituting eqs.(7.5) into eq.(7.4) and expanding for small ϵ, we obtain

$$(7.6) \qquad \frac{d^2x}{d\eta^2} - x\cos(\epsilon\eta) + \frac{g}{2R}\,x^3 + O(\epsilon) = 0$$

Note that (7.6) is of the form (7.1) for g/R = 2.

7.2 The averaging model

We will now derive the averaging model for eq.(7.1). Using (2.20a) and (2.23), the variational equations become:

$$r' = -\epsilon \frac{k^2}{r} \sin(\tau) \, (1 - cn^2) \tag{7.7a}$$

$$\varphi' = \frac{a}{4K} + \epsilon \left[\upsilon_0 \, Z + \upsilon_1 \, (Z \, cn^2 + cn \, cn') \right] \tag{7.7b}$$

where

$$\upsilon_0 = -\frac{\sin(\tau)}{4 \, K \, a^2} \quad \text{and} \quad \upsilon_1 = \upsilon_0 \frac{\cos(\tau)}{\rho - 2 \cos(\tau)}$$

and

$$a^2 = r^2 - \cos(\tau) \, , \; k^2 = \frac{r^2}{2a^2}$$

Using AVERAGE, we find the averaged equations to be:

$$\bar{r}' = -\frac{\epsilon}{\bar{r}} \sin(\tau) \left[1 - \frac{E}{K} \right] + O(\epsilon^3) \tag{7.8a}$$

$$\bar{\varphi}' = \frac{a}{4K} + \epsilon^2 \bar{H}_2 + O(\epsilon^3) \tag{7.8b}$$

where $\bar{H}_2$ cannot be computed at the present time (This will be done shortly). In eqs.(7.8), the auxiliary variables a, k, K, and E are defined in terms of $\bar{r}$:

$$a^2 = \bar{r}^{-2} - \cos(\tau) \tag{7.9a}$$

$$k^2 = \frac{\bar{r}^{-2}}{2 \, (\bar{r}^{-2} - 1)} \tag{7.9b}$$

(7.9c) $E = E(k)$, $K = K(k)$ with k found from (7.9b)

In addition, we define the variable ρ as follows:

(7.9d) $$\rho = \bar{r}^{-2}$$

since $\bar{r}$ is frequently encountered as the expression $\bar{r}^{-2}$. Using (7.9d), a^2 and k^2 in (7.9a) and (7.9b) can be expressed using ρ. Henceforth, the variables a, k, ρ, E, and K shall be defined using (7.9).

The generating functions w_i are found to be:

(7.10a) $$w_1(\bar{r},\varphi) = \frac{1}{ar} \sin(\tau)\ Z$$

(7.10b) $$w_2(\bar{r},\varphi) = \frac{a}{\rho} v_1\ Z^2 + \frac{1}{2a} v_1\ cn^2 + v_3\ TH(u,k)$$

where

$$v_3 = v_0 \frac{a}{\rho} \frac{1}{\rho - 2\cos(\tau)} \left[2\rho - \left[1 - \frac{E}{K}\right] \cos(\tau)\right].$$

Z is the Jacobi Zeta function defined in (1.5)

and TH(u,k) is defined by (1.25)

In (7.10b), we have chosen the constant of integration w_{20} to be zero, which allows the mean of w_2 to be non-zero.

Because the functions w_1 and w_2 are sufficiently simple, the second order average for φ (i.e., $\bar{H}_2$) can be computed without too much extra effort. For this computation, it is easier to take $w_{20} = 0$. Using the results from section 3.3, we can compute all

terms of H_2 in (3.13b) except for v_1, w_{2r}, and $w_{2\tau}$. Since we take v_1 to have zero mean, it does not contribute to $\bar{H}_2$ and can be ignored. The other two terms cannot be computed yet because of the TH(u,k) function in w_2.

To compute $\frac{\partial TH}{\partial r}$, we differentiate (1.25). It is important to remember that r and φ are <u>independent</u> variables, unlike r and u. We find the derivative to be:

$$(7.11)\quad \frac{\partial TH}{\partial r} = \frac{\partial}{\partial r}\left[\int Z\,du\right] = \frac{\partial}{\partial r}\left[4K\int Z\,d\varphi\right]$$

$$= 4\frac{dK}{dk}\frac{\partial k}{\partial r}\int Z\,d\varphi + 4K\int \frac{\partial Z}{\partial r}\,d\varphi$$

$$= \frac{1}{K}\frac{dK}{dk}\frac{\partial k}{\partial r}\int Z\,du + \int \frac{\partial Z}{\partial r}\,du$$

$$= -\frac{\partial k}{\partial r}\frac{1}{2kk'^2}\left[Z^2 + k^2\,cn^2\right]$$

The value for $\frac{\partial TH}{\partial \tau}$ can be found from (7.11) and (3.25).

Now that we are able to compute each term in H_2 (except for v_1), we can find all the functions appearing in the computation of $\bar{H}_2$. These are listed in Table 7.1.

Table 7.1 Functions appearing in the computation of $\bar{H}_2$

cn^2, cn^4, cn^6, cn cn', cn^3 cn', Z cn cn', Z cn^3 cn', TH

Z^2, $Z^2\,cn^2$, $Z^2\,cn^4$, Z^3 cn cn'

The mean of every function in Table 7.1 can be computed as in section 3.3, except for Z^3 cn cn'. This mean is easily found using integration by parts:

$$(7.12) \qquad \overline{Z^3 \text{ cn cn}'} = -\frac{3}{2} k^2 \overline{Z^2 \text{ cn}^4} - \frac{3}{2}\left[k'^2 - \frac{E}{K}\right] \overline{Z^2 \text{ cn}^2}$$

Using a MACSYMA program very similar to AVERAGE, we compute the value of $\bar{H}_2$ to be:

$$(7.13) \qquad \bar{H}_2 = \xi_0 + \xi_1 \overline{Z^2} + \xi_2 \overline{TH}$$

where

$$\xi_0 = -\frac{\cos}{24K\rho^2 a^5} \frac{1}{(\rho-2\cos)^2} \left[-24a^4 \cos \sin^2(\frac{E}{K})^3 \right.$$

$$- 2a^2 \sin^2(\frac{E}{K})^2 \left[40\cos^2 - 48\rho\cos + 15\rho^2\right]$$

$$+2\frac{E}{K}\left[-3\rho^4\cos + (15-3\cos^2)\rho^3 - 15\cos^3\rho^2 + 2\cos^2(38-35\cos^2)\rho - 36\cos^3\sin^2\right]$$

$$\left. + 3\rho^4\cos - (4+11\cos^2)\rho^3 + 6\cos(3+\cos)\rho^2 - 4\cos^2(7-4\cos^2)\rho + 16\cos^3\sin^2\right]$$

$$\xi_1 = -\frac{1}{4K\rho^2 a^3} \frac{1}{(\rho-2\cos)^2} \left[-2a^2\cos^2\sin^2(\frac{E}{K})^2 - 2\cos^2(6-5\cos^2)\rho + 4\cos^3\sin^2\right.$$

$$\left. - \cos \sin^2(\frac{E}{K})(\rho-2\cos)(5\rho-3\cos) + (\cos^2-2)\rho^3 + 3\cos(3-2\cos^2)\rho^2\right]$$

$$\xi_2 = -\frac{1}{2K\rho^2 a^3} \frac{1}{(\rho-2\cos)^2} \left[2\cos(1-\frac{E}{K}) - \rho\right] \left[4a^2\cos \sin^2(\frac{E}{K})^2 + \rho^3\cos\right.$$

$$\left. + \rho^2(2-5\cos^2) + 2\cos(3\cos^2-1)\rho + 4\sin^2(\frac{E}{K})(\cos^2+\rho\cos-\rho^2)\right]$$

In (7.13), cos = cos(τ) and sin = sin(τ) in ξ_1. We see from the enormous length of the expressions in (7.13) that $\bar{H}_2$ is not useful from a practical standpoint (since computing $\bar{H}_2$ at each step of a numerical integration of $(\bar{r}', \bar{\varphi}')$ involves so many computations that it dominates the procedure).

We will discuss the first order averaging model. For convenience, we will take (ρ, φ) rather than $(\bar{r}, \varphi)$ as independent variables (where $\rho = \bar{r}^2$). The first order averaging model is then:

(7.14a)
$$\rho' = -2\epsilon \sin(\tau)\left[1 - \frac{E}{K}\right]$$

or
$$\frac{d\rho}{d\tau} = -2 \sin(\tau)\left[1 - \frac{E}{K}\right]$$

(7.14b)
$$\varphi' = \frac{a}{4K}$$

where a, k, E, and K are defined by (7.9) in terms of ρ using (7.9d). The expression for the energy h will be important in the analysis of eqs.(7.14). From (2.7) and (2.8), the energy h is found to be:

(7.15a)
$$\frac{1}{2}x'^2 - \frac{1}{2}\cos(\tau)\, x^2 + \frac{1}{4}x^4 = h$$

(7.15b)
$$h = \frac{1}{4}\rho\,(\rho - 2\cos(\tau))$$

We note that it is also possible to consider $m = k^2$ as an independent variable instead of $\bar{r}$ or ρ. The resulting averaged equation on m is separable, but not integrable in closed form:

$$\frac{dm}{d\tau} = (1-2m)\left[m - (2m-1)\left[1 - \frac{E}{K}\right]\right] \tan(\tau) \tag{7.16}$$

Since the amplitude-like variable ρ is easier to interpret physically, we prefer to use eqs.(7.14).

Eq.(7.14a) is defined on the half-cylinder $\mathcal{H} = \{(\rho,\tau) \in \mathbb{R}^+ \times S\}$. Since both E and K depend on the modulus k, we see that the slope field of (7.14a) is an odd function of τ on $\mathcal{H}$. Thus the transformation $\tau \to -\tau$ leaves (7.14a) invariant, and all orbits are symmetric about the line $\tau = 0$. Since (7.14a) has no singularities, there can be no equilibria in the flow on $\mathcal{H}$. Moreover no orbits can escape to infinity since for large ρ, $k \sim 1/\sqrt{2}$, $E \sim 1.350644\ldots$, $K \sim 1.854075\ldots$, so that (7.14a) gives $\frac{d\rho}{d\tau} \sim -0.543053\ldots \sin\tau$ and $\rho \sim 0.543053\ldots \cos\tau + \rho_0$, which is a closed orbit. The possibility of limit cycles in the flow on $\mathcal{H}$ is precluded by the Hamiltonian nature of the unperturbed problem. Thus all orbits are closed and we may conclude that for arbitrary initial conditions, $\rho(\tau)$ is an even 2π-periodic function.

This result is illustrated in Fig.7.4a, which shows the results of numerical integration of eq.(7.14a) for an initial condition starting within the separatrix. The points A, A', B, B', and C in Fig.7.4a lie on the same $\rho(\tau)$ orbit. As ρ changes, a given motion

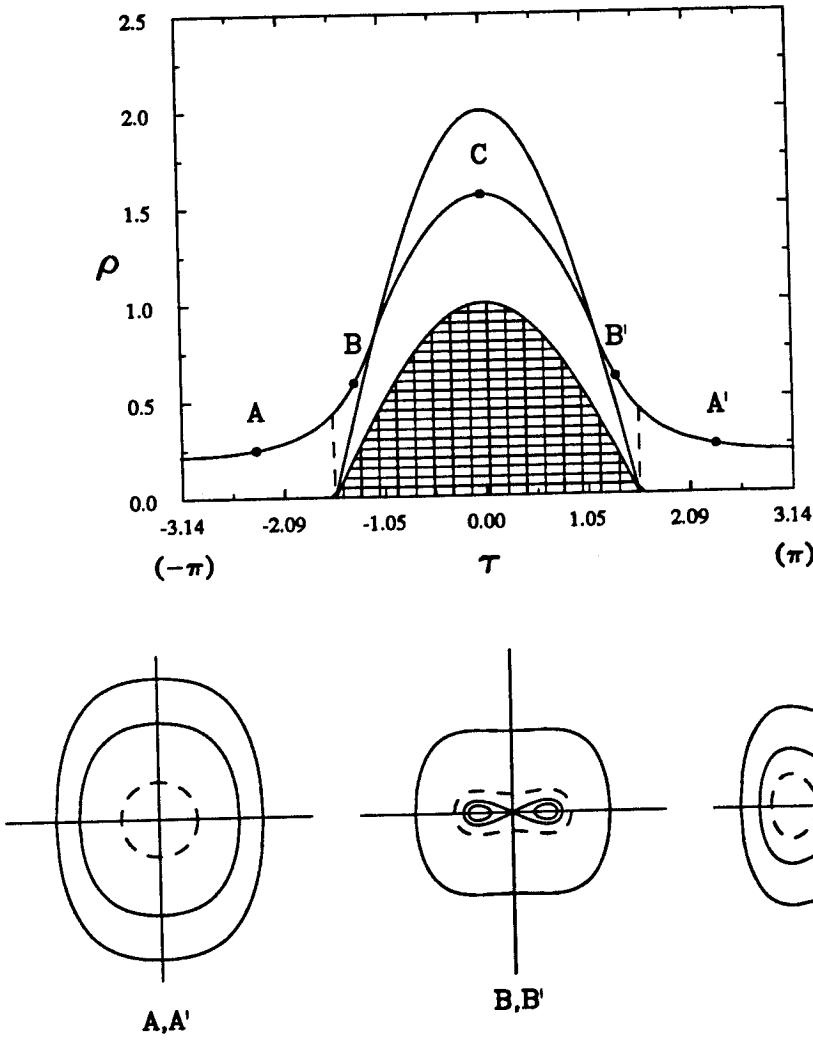

Fig.7.4a Numerical integration of eq.(7.14a) (shown solid in the (ρ,τ) phase space) for an initial condition given inside the separatrix. The separatrix condition, (7.17b) is shown dashed. The gridded region is not meaningful for the model and should be ignored. The instantaneous phase portraits for the points A, A', B, B', and C are also shown. The orbits corresponding to these points are shown dashed in the phase portraits.

moves (slowly, since τ is slow time) from one instantaneous energy curve (given by (7.15a)) to another. Using (2.10), we find the instantaneous energy value h and the instantaneous position of the separatrix:

(7.17a) $$h = 0$$

(7.17b) $$\text{separatrix:} \quad \rho = 2 \cos \tau > 0$$

The separatrix condition, eq.(7.17b), is shown as a dashed curve on the (ρ,τ) phase space in Fig.7.4a. Note that the region of $\mathcal{H}$ lying between $\rho = 0$ (the origin) and $\rho = \cos \tau$ (the instantaneous centers lying inside the homoclinic loops), shown gridded in Fig.7.4a, is unreachable from any physically meaningful initial conditions and should be ignored (the instantaneous frequency a is imaginary in this region).

The instantaneous phase portraits at the times τ corresponding to the points A, A', B, B', and C appear below the (ρ,τ) graph in Fig.7.4a. The energy curves corresponding to the points A, A', B, B', and C are shown dashed in the phase portraits. From Fig.7.4a, we see that the area enclosed by the dashed energy curves remains constant for this $\rho(\tau)$ orbit. Thus, this verifies that the adiabatic invariant J remains constant on an orbit (see section 2.3).

In Fig.7.4b, we show the numerical integration of eq.(7.14a) for 5 initial conditions: 2 starting outside the separatrix, 2 starting inside the separatrix, and 1 starting on the separatrix. The

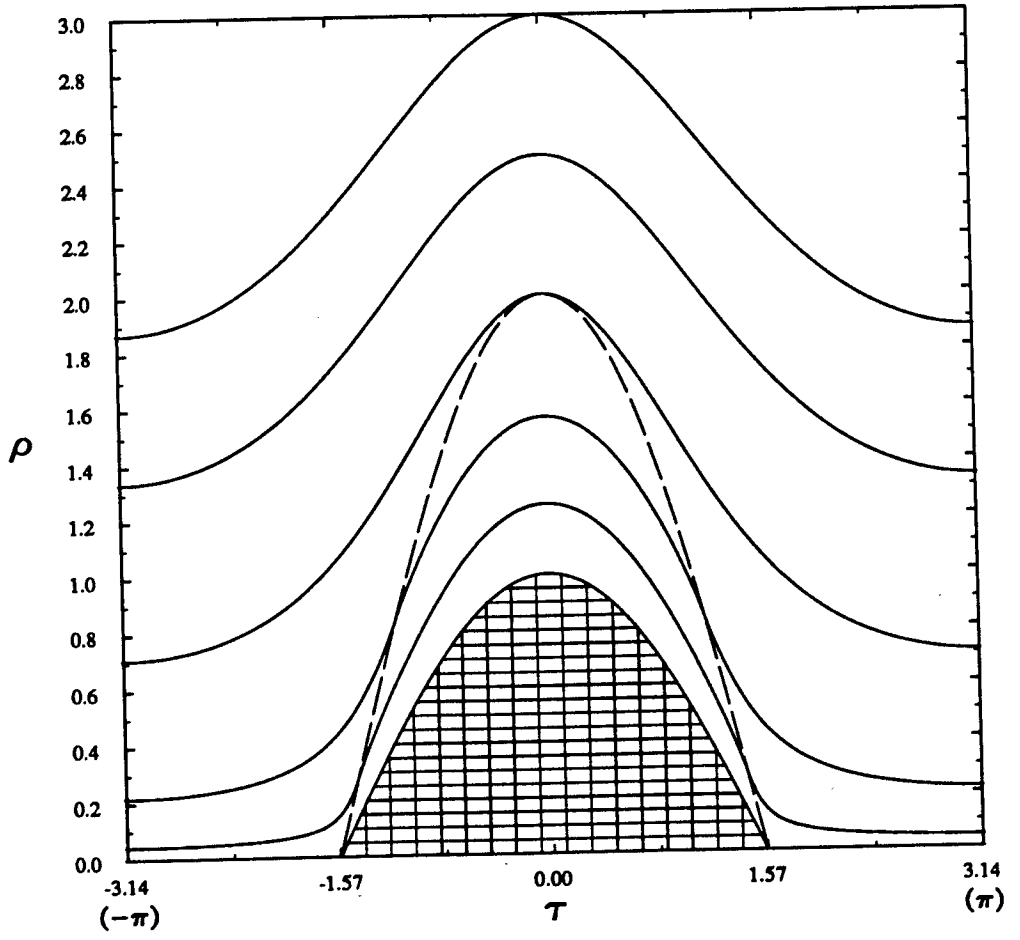

Fig.7.4b Numerical integration of eq.(7.14a) (shown solid in the (ρ,τ) phase space) for 5 initial conditions. The separatrix condition, (7.17b) is shown dashed. Some orbits cross the separatrix condition curve (corresponding to crossing into or out of the separatrix) while others do not. We denote by τ_s the time τ at which at orbit starting at $\tau = 0$ first crosses the separatrix condition curve (for orbits which do cross). The gridded region is not meaningful for the model and should be ignored.

separatrix condition (eq.(7.17b)) is again shown dashed on the (ρ,τ) phase space. The gridded region is unreachable from any physically meaningful initial condition and should be ignored. This figure verifies that all orbits on (ρ,τ) are closed. As expected, we see that some motions always remain outside the separatrix ($h > 0$), while others cross through it, moving between inside the separatrix ($h < 0$) and outside the separatrix. (For a discussion of interpreting the averaging model near the separatrix, consult the end of section 9.1.)

Next let us consider eq.(7.14b) on $\frac{d\varphi}{dt}$. From the fact that $\rho(\tau)$ is an even 2π-periodic function, it follows that so are $r(\tau)$, $a(\tau)$ and $k(\tau)$. This makes $\frac{d\varphi}{dt}$ an even 2π-periodic function of τ with a nonzero mean. Hence $\varphi(\tau)$ can be written as:

$$\varphi(\tau) = \varphi_{av}\,\tau + \varphi_{per}(\tau) + \varphi_0 \tag{7.18}$$

where $\varphi_{per}(\tau)$ is an odd 2π-periodic function. Both φ_{av} and $\varphi_{per}(\tau)$ depend on ρ_0, the initial value of ρ, but are independent of φ_0.

In order to better understand the dynamics of the averaged system, we consider a Poincare map P. We choose the surface of section Σ as a cross section of the phase space:

$$\Sigma\colon \{(x,x',\tau)\,|\,\tau = 0 \pmod{2\pi}\} \tag{7.19}$$

where the values of x and x' are given by eqs.(2.6). Alternately we may view P as mapping $(\rho,\varphi)_{\tau=0}$ to $(\rho,\varphi)_{\tau=2\pi}$, which results in (from the fact that $\rho(\tau)$ is 2π-periodic and from eq.(7.18)):

$$P: (\rho_0,\varphi_0) \rightarrow (\rho_0, 2\pi\ \varphi_{av}+\varphi_0) \tag{7.20}$$

Since ρ is unchanged in (7.20), we see that instantaneous energy curves at $\tau = 0$ remain invariant under the Poincare map P. For those curves which lie outside the separatrix at $\tau = 0$ (corresponding to $h > 0$ in eq.(7.15b)), eq.(7.20) shows that P simply represents a rotation resulting from a change of $2\pi\ \varphi_{av}$ in φ .

However, the situation for those instantaneous energy curves which lie inside of the double loop separatrix at $\tau = 0$ is more interesting. For given ρ_0 (and hence given $h < 0$ in eq.(7.15b)), there are two such disconnected closed curves (L = left, R = right), each lying within its own homoclinic loop. The Poincare map P maps the set of points {L,R} onto itself.

Let τ_s be the slow time between $\tau = 0$ and the crossing of the separatrix, cf.Fig.7.4b. From Fig.7.4b, $\tau_s < \pi/2$. Since τ_s is determined by eq.(7.14a) on ρ without use of eq.(7.14b) on φ, it is clear that τ_s depends on ρ_0 but not on φ_0, i.e., all points on a given instantaneous energy curve reach the separatrix at the same

instant. Then the motion generating P may be decomposed into three stages:

1: $0 < \tau < \tau_s$, during which time a motion remains inside its original homoclinic loop

2: $\tau_s < \tau < 2\pi - \tau_s$, during which time the motion lies outside of the separatrix

and 3: $2\pi - \tau_s < \tau < 2\pi$, during which time the motion lies inside one of the homoclinic loops, but possibly not the loop within which the motion started.

Let us consider the changes occurring during each of these stages. We will follow a typical set of points, call them C, which are located on instantaneous energy curves L and R at $\tau = 0$. At the end of stage 1 the points C have moved to new instantaneous energy curves lying just inside of the left and right homoclinic loops respectively. During stage 1, the separatrix loops have themselves changed shape, becoming smaller with increasing τ. See Figs.7.5a-b. We denote by φ_s the change in φ accompanying this motion, and find from (7.18),

(7.21) $\Delta\varphi$ for stage 1: $\varphi_s = \varphi_{av}\,\tau_s + \varphi_{per}(\tau_s)$

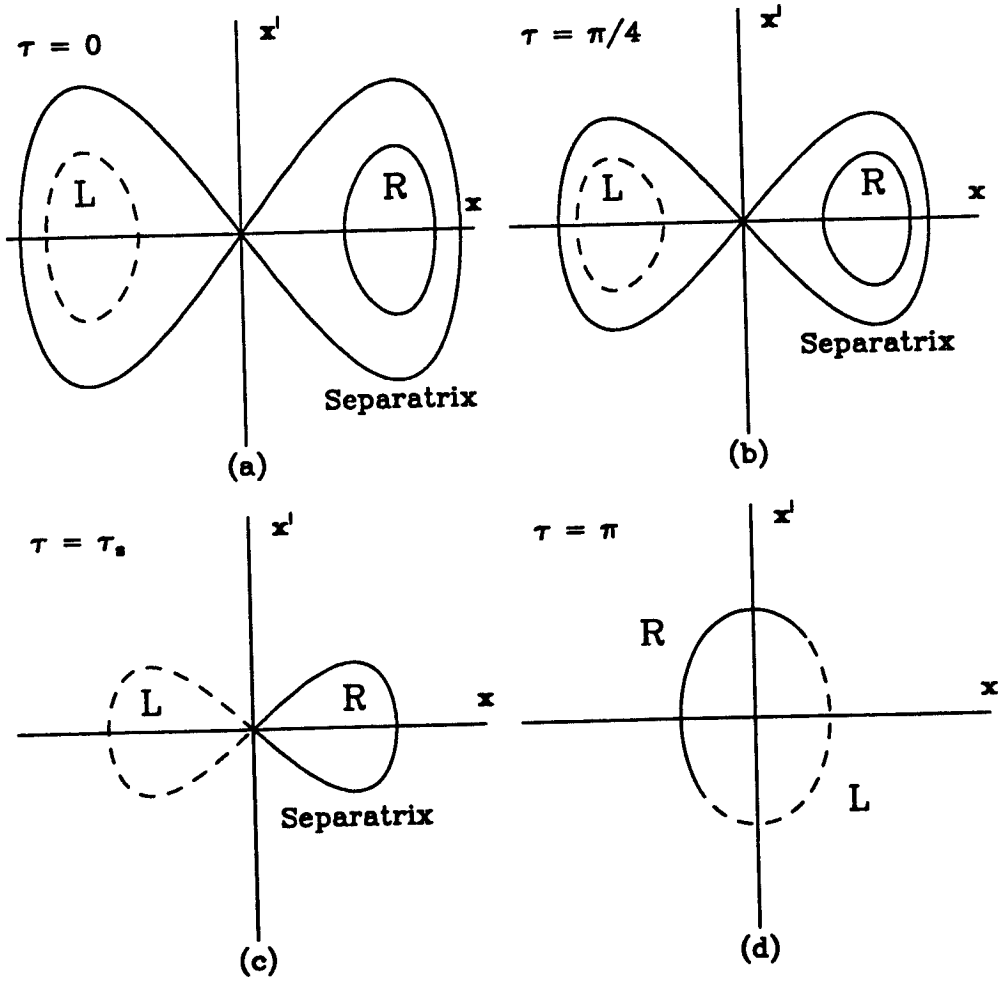

Fig.7.5 Schematic of the averaging model flow. The six pictures (a-f) show the motion of the two initial curves L and R displayed in (a) through one 2π perioid in τ. The motion can be divided into three stages, see the text. The Poincare map is shown in (f).

Fig.7.5 (Continued)

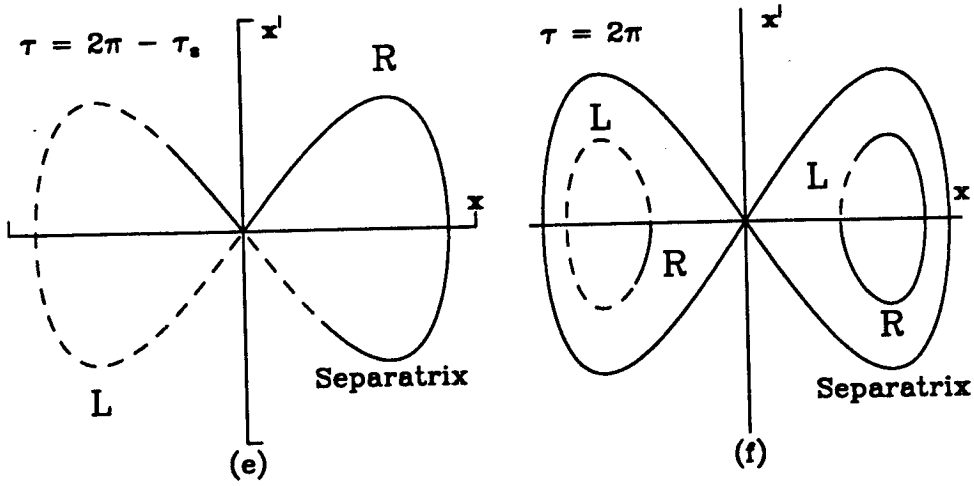

Fig.7.5 Schematic of the averaging model flow (continued).

During stage 2, all of the points in C find themselves on the same instantaneous energy curve, located outside of the separatrix, see Figs.7.5c-e. Stage 2 lasts more than half of the forcing period, during which time the separatrix shrinks to a point, disappears, and then reappears and grows to the same size it was at the beginning of stage 2. The change in φ during stage 2 is, from (7.18),

(7.22) $\Delta\varphi$ for stage 2: $\varphi(2\pi-\tau_s)-\varphi(\tau_s) = (2\pi-2\tau_s)\varphi_{av}-2\varphi_{per}(\tau_s)$

$$= 2\pi\ \varphi_{av} - 2\ \varphi_s$$

where we have used the fact that $\varphi_{per}(\tau)$ is an odd 2π-periodic function. At the beginning of stage 3, the set C is once again located on two disconnected instantaneous energy curves which are just inside of the two separatrix loops. By symmetry, the change in φ accompanying stage 3 is the same as that for stage 1:

(7.23) $\Delta\varphi$ for stage 3: $\varphi_s = \varphi_{av}\ \tau_s + \varphi_{per}(\tau_s)$

At the end of stage 3, the set C has returned to its original position, see Fig.7.5f. However, because of the phase flow φ during stage 2, some points which were originally on curve L are now on curve R and vice versa.

The effect of the Poincare map P on the set C = {L,R} may thus be described as a rotation of magnitude (from (7.21)-(7.23)):

$$\Delta\varphi = 2\pi\,\varphi_{av} \tag{7.24}$$

combined with an interchange of two intervals between L and R. The magnitude of the interchanged intervals is, from (7.22):

$$\text{magnitude of interchanged interval} = 2\pi\,\varphi_{av} - 2\,\varphi_s \tag{7.25}$$

The endpoints of the interchanged intervals separate initial conditions which end up on opposite sides of the homoclinic loops after one forcing period.

The Poincare map P may be characterized by a one dimensional discontinuous function $F(\psi)$ which maps the set C onto itself. ($F(\psi)$ is an example of an interval exchange map [Kea75].) The angle ψ parameterizes C on the range $[-1,1)$. It is found from φ by first parameterizing L and R in φ on the range $[-\frac{1}{4},\frac{1}{4})$ and then using (7.26):

$$\text{On L:}\quad \psi = 2\,\varphi - \frac{1}{2} \tag{7.26a}$$

$$\text{On R:}\quad \psi = 2\,\varphi + \frac{1}{2} \tag{7.26b}$$

The graph of the function $F(\psi)$ lies in the square region $[-1,1) \times [-1,1)$ and is displayed in Fig.7.6a.

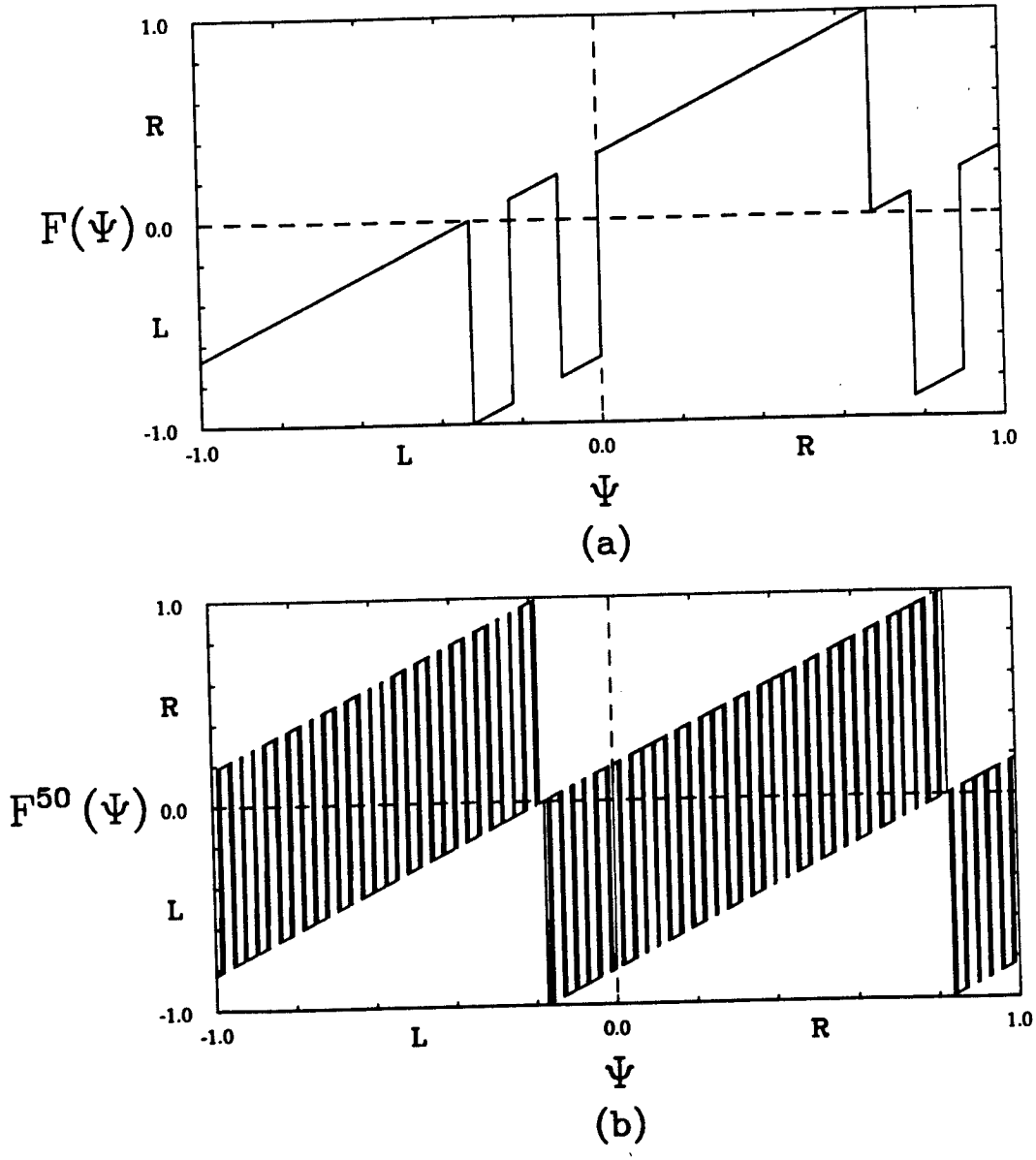

Fig.7.6 The Poincare map is displayed as the map F(ψ) in (a). Each point on C (where C = L U R) corresponds to a unique ψ value which gets mapped under F to another point of C. F is composed of an exchange of an interval between R and L and a translation in ψ. The 50th iterate of F, showing many exchanged intervals, is shown in (b).

As we vary the particular instantaneous energy curve C on which P so acts, the magnitude of the rotation, $2\pi\ \varphi_{av}$, varies continuously. In general this magnitude will be incommensurate with the circumference of the instantaneous energy curve C, which is 1 when measured in ψ, and so we are generically dealing with an irrational flow on S^1 [Arn84]. If the mapping P is iterated, the set of endpoints Ψ will continue to grow, and in the limit as $\tau \to \infty$, this set will be dense in C. Thus the sequences of L's and R's corresponding to a particular point on C will be different from those of other neighboring points on C. This implies sensitive dependence on initial conditions, a criterion often used to describe chaos [Dev87]. In terms of the Poincare map function $F(\psi)$ shown in Fig.7.6a, high iterates of $F(\psi)$ will contain many points of discontinuity, see Fig.7.6b.

For a set of instantaneous energy curves of measure zero, however, the rotation magnitude will be commensurate with the circumference of the instantaneous energy curve C and the action of P will be that of a rational flow on S^1. In this nongeneric case no chaos will result, as the model predicts periodic orbits.

In section 7.4, we present a full discussion and proof of the chaos in the averaging model.

7.3 Accuracy of the averaging model and an improved model

The analysis of chaos presented briefly in section 7.2 is approximate. In order to test the validity of the approximation, we compare the predictions of the averaged equations with the results of numerical integration of eq.(7.1).

In order to generate a numerical version of the Poincare map P, cf.eqs.(7.19),(7.20), we choose an initial condition (x(0),x'(0)) and integrate eq.(7.1) from t = 0 to t = 2π. For a comparison with the averaging results, we choose a number of initial conditions all lying on the same instantaneous energy curve C corresponding to a given value of the energy h. These initial conditions are shown in Fig.7.5a. Four snapshots in time of the flow of C during the period 2π in τ are shown in Figs.7.7a-d and Figs.7.8a-d for $\epsilon = 0.1$. Figs.7.7a-d were computed using the averaging model; Figs.7.8a-d were computed using numerical integration of eq.(7.1). The Poincare map P is shown as plate (d) in the figures.

Many of the points of P lie in a neighborhood of the right (= R) or left (= L) instantaneous energy curves corresponding to the energy h, as predicted by the averaging analysis. However, some points lie on "threads" which reach from one side of Fig.7.5a to the other, winding around R and L, and lying close to the "instantaneous unstable manifold" associated with the instantaneous separatrix of the unperturbed system. (For a discussion of separatrices, see section 7.1 and section 9.1.) The threads represent a continuous

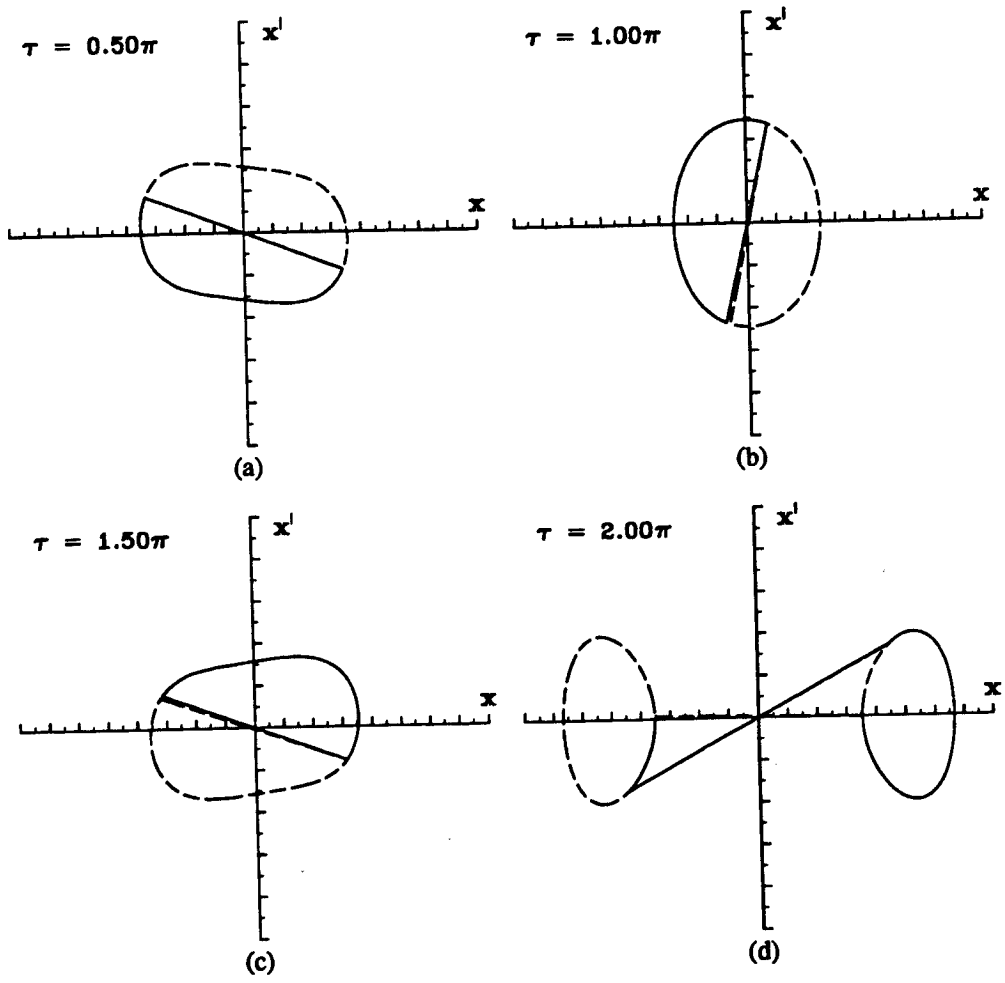

Fig.7.7 Snapshots of the flow of C: averaging model. Plates (a-d) show 4 pictures of the flow of the initial set C (given in Fig.7.5a) at equally spaced quarter-periods. Plate (d) is the Poincare map. The lines which separate R from L are <u>not</u> part of the model; they merely make evident the discontuity in the initial curves R and L, pictured in Fig.7.5a.

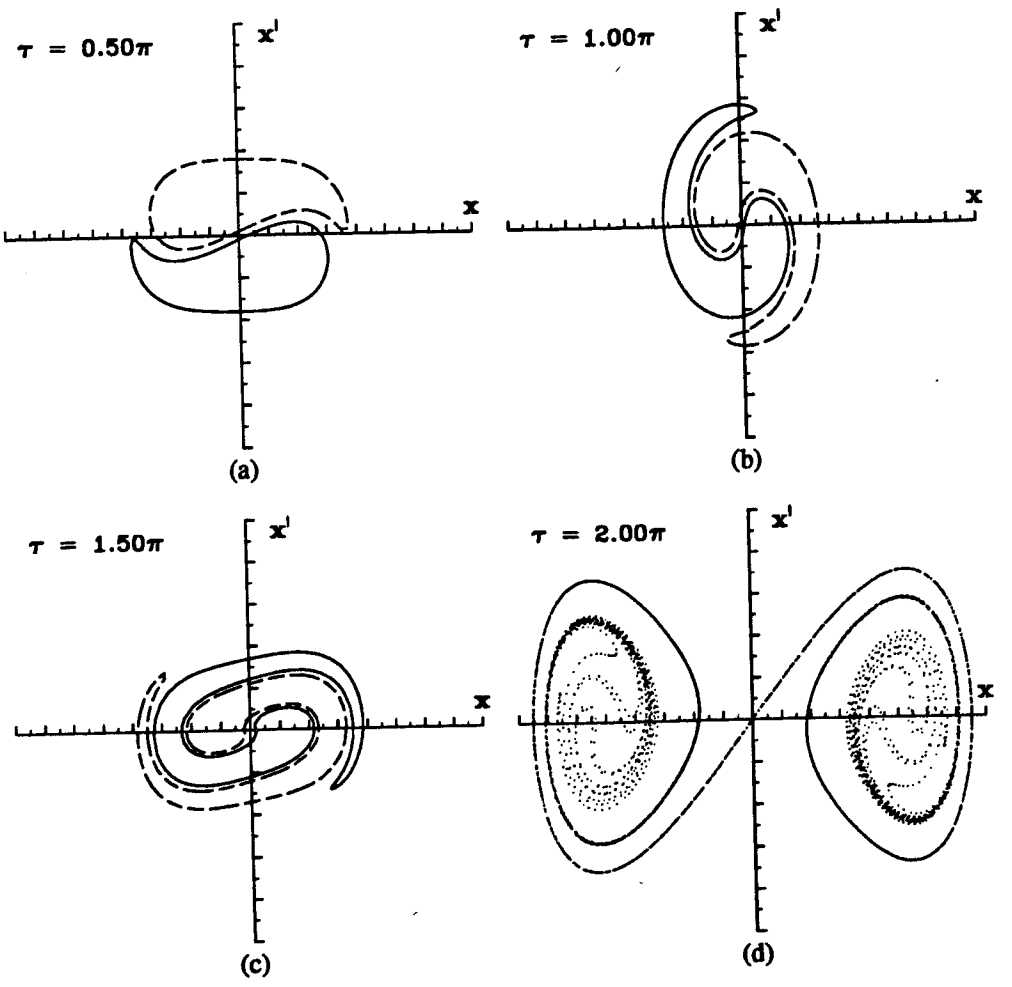

Fig.7.8 Snapshots of the flow of C: numerical integration of eq.(7.1). Plates (a-d) show 4 pictures of the flow of the initial set C (given in Fig.7.5a) at equally spaced quarter-periods. Plate (d) is the Poincare map. While many points of (d) lie near the initial set C, some points lie on "threads" which wind around R, L, and the unstable manifold of the instantaneous separatrix.

version of the jump which was predicted at the ends of the interchanged intervals, cf.Fig.7.7d. However, the nature of the intervals which are interchanged is much more complicated in the numerical integration results than in the averaging results. Instead of just a single interval being interchanged, as in Fig.7.7d, we find that many intervals are interchanged.

Although the Poincare maps shown in Fig.7.7d and Fig.7.8d differ significantly, it turns out that the averaging method has worked quite well except for the threads. A more careful analysis of the numerical integration that created Fig.7.8d shows that while the threads make up a large portion of the picture, they arise from very tiny intervals of the original initial energy curve C (some intervals as small as 10^{-10} in length). So, while the averaging method works well on large intervals of C, there exist extremely small intervals where it fails completely.

Thus, while the averaging results offer a simplified explanation of the chaos in eq.(7.1), in qualitative agreement with the kind of unpredictable behavior seen numerically, cf.Fig.7.2a-d, they do not appear to be asymptotically valid, i.e., the difference between the behavior of the averaged system and the original system does not approach zero as $\epsilon \to 0$. The following discussion is aimed at trying to explain this.

Comparing Figs.7.7d and 7.8d, we see that the adiabatic invariance of the instantaneous energy curves in the Poincare map P predicted by the averaging analysis is verified to a limited extent

(i.e., the presence of the threads represents a localized failure of this invariance). However the manner in which each set of instantaneous energy curves is mapped onto itself is poorly described by the averaged eqs. (i.e., many intervals are interchanged, rather than just a single interval). This suggests that while eq.(7.14a) on ρ' seems to be in limited agreement with the behavior of eq.(7.1), eq.(7.14b) on φ' does not.

A closer inspection of the averaging scheme reveals two technical problems which arise on the separatrix (i.e., $k^2 = 1$):

(i) φ in eq.(2.21) is undefined at $k^2 = 1$ (because $K = \infty$) so that eqs.(7.7b) and (7.14b) are meaningless, and

(ii) eq.(7.14a) is not differentiable (nor Lipschitz), so that solutions to eq.(7.14a) are not unique.

These problems are discussed in section 3.2 and chapter 9. A brief summary of chapter 9, as it pertains to eqs.(7.14) follows.

The separatrix is a singular region at which the transformation to (ρ,φ) coordinates is ill-defined. Once a motion reaches the instantaneous separatrix, its future motion is not uniquely specified, i.e., the location of where and when it gets off the separatrix is unknown. In our analysis we have tacitly assumed that such a motion gets off the separatrix at the same point at which it gets on, i.e., crossing is instantaneous. We believe that the differences between the averaged solution and the results of numerical integration of eq.(7.1) are due to this assumption.

We view the region near the separatrix as a boundary layer. We take this approach in creating an improved model of eq.(7.1), i.e., we will augment the averaging model with a boundary layer model applicable in a neighborhood of the instantaneous separatrix.

A full discussion of the separatrix crossing model is presented in chapter 9. Section 9.1 provides a background to the general model derived in section 9.2. In section 9.3, the general theory is applied to this specific system, eq.(7.1), which is summarized below.

In the following discussion, $m = k^2$. Since $m = 1$ corresponds to the separatrix at any time τ, we take (m,u) as variables within the separatrix boundary layer. The boundary layer then corresponds to values of m near unity. Taking $m = 1 + \epsilon\,\sigma$, the model of separatrix crossing away from the saddle at the origin is given by (see chapter 9) (cf.eqs.(9.25)):

$$u = \sqrt{\cos(\tau)}\,(t - t_*) + u_* \tag{7.27a}$$

$$\sigma = -\frac{\tan(\tau)}{\sqrt{\cos(\tau)}}\left[\tanh(u) - \tanh(u_*)\right] + \sigma_* \tag{7.27b}$$

where (σ_*, u_*, t_*) are the initial values of (σ,u,t) when the motion first reaches the boundary layer. The values (σ_*, u_*, t_*) will be obtained by patching the averaging model to eqs.(7.27) at the boundary layer.

Although eqs.(7.27) offer an approximation for the separatrix crossing away from the saddle, they are not valid near the saddle (see the derivation in sections 9.2 and 9.3). Another model is

introduced for motions which cross the instantaneous separatrix near the saddle. Letting $\delta << 1$, the near-saddle separatrix crossing model is given by (cf.eqs.(9.20), (9.21), (9.27)):

$$x = \delta \hat{x} \quad \text{and} \quad x' = \epsilon \delta \hat{x}_\tau \tag{7.28}$$

$$\hat{x} = \hat{x}(\tau_*) \cosh(\ell(\tau)/\epsilon) + \epsilon \frac{\hat{x}_\tau(\tau_*)}{\sqrt{\cos(\tau_*)}} \sinh(\ell(\tau)/\epsilon) \tag{7.29}$$

$$\ell(\tau) = 2\sqrt{2} \left[E(z) - E(z_*) + \frac{1}{2}(z_* - z) \right] \tag{7.30}$$

$$\text{where } z = sn^{-1}(\sqrt{2}\, \upsilon\, |\sin \tfrac{\tau}{2}|)\ ,\ \upsilon = \text{sign}(\sin \tau),\ \hat{k}^2 = \frac{1}{2}$$

In (7.30), the elliptic functions have the modulus $\hat{k}^2 = \frac{1}{2}$. The value of τ_* corresponds to the value of τ at which a motion enters this boundary layer. The value of z_* is found from (7.30) at $\tau = \tau_*$. The separatrix crossing model then consists of two parts:

(i) away from the origin eqs.(7.27) are used, and

(ii) near the origin, eqs.(7.28)-(7.30) are used.

The model is an analytic approximation for the flow near the instantaneous separatrix of eq.(7.1), depending on σ_*, u_*, and t_*.

The improved model combines the averaged eqs.(7.14) with this separatrix crossing model. Although it would be desirable to asymptotically match the two boundary layer approximations with the averaged equations, this is not possible due to the unavailability of a closed form solution to the averaged equations. Instead, we numerically patched the averaged equations to the separatrix crossing model, as follows. As an orbit is numerically computed, the computer

checks which equations are currently valid, converts to the proper variables, and uses the proper model equations.

We can understand the improved model in terms of Fig.7.4b. An orbit starting at $\tau = 0$ travels along the averaged orbit $\rho(\tau)$ until it reaches a neighborhood of the separatrix. Depending on the orbit's phase φ at entry, the orbit may cross through the separatrix boundary layer quickly or slowly. Upon exit, the orbit begins to travel along (possibly) a different averaged $\rho(\tau)$ curve until the boundary layer is encountered again. Thus the separatrix crossing approximation determines how long a motion stays in the neighborhood of the instantaneous separatrix, and which new averaged curve $\rho(\tau)$ a motion lies on after leaving the separatrix neighborhood. In other words, the separatrix crossing model determines the change in the adiabatic invariant J (see section 9.1).

We generated a Poincare map using the improved model for $\epsilon = 0.1$. We show four snapshots of the flow of the initial set C in Figs.7.9a-d. The qualitative agreement between this model and eq.(7.1) is excellent. The improved model correctly predicts the threads which appear in Fig.7.8d and does not produce the discontinutites which the averaging model did (Fig.7.7d). This shows that the separatrix crossing model is vital to understanding the complicated dynamics of the system.

Finally, we prepared three computer movies (one for the averaging model, one for numerical integration, and one for the improved model) which show snapshots of the flow of C at each second

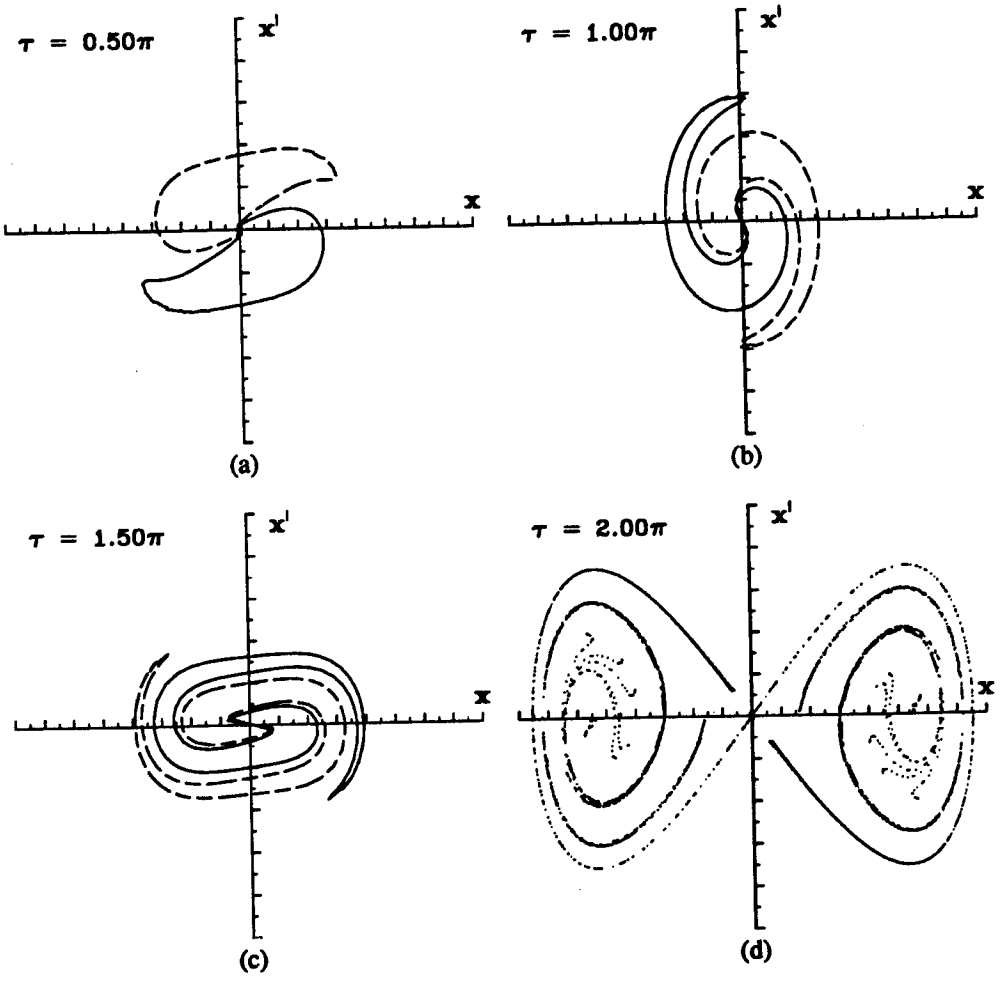

Fig.7.9 Snapshots of the flow of C: improved model. Plates (a-d) show 4 pictures of the flow of the initial set C (given in Fig.7.5a) at equally spaced quarter-periods. Plate (d) is the Poincare map. Each plate compares very well with numerical integration, Fig.7.8.

of time for the period of 2π in τ ($\epsilon = 0.1$). Using the movies, we see how the Poincare map P is created. We see the discontinuities that the averaging model predicts, the long threads of the numerical integration, and the improved model's excellent qualitative agreement with eq.(7.1).

7.4 Proof of chaos in the averaging model

This section is concerned with a proof of chaos in the averaging model, based on the one dimensional map $F(\psi)$ which was introduced in section 7.2. Although the proof is not especially difficult, it is rather technical, involved, and tedious. The proof relies on introducing a symbol dynamics of L's and R's on the averaging model, as discussed in section 7.2. In fact, the proof merely makes explicit that discussion.

Because this section involves a proof, the details of each step are considered to be of primary importance, not the overall discussion (which has already been presented in section 7.2). An outline of the proof follows. We first make a few necessary definitions. Then we identify the interval E_g on the right side which is interchanged (i.e., switch sides from right to left) during stage 2 (cf. (7.22)). Next we find the pre-image E_{fg} of this interval with respect to stage 1 (cf. (7.21)). We then define the symbolic coding map $\tilde{F}$ and the symbolic coding intervals E_{fg}^{-j}. The symbol sequence coding procedure of L's and R's for any ψ (or φ) is

then made explicit. An analysis of the set of E_{fg}^{-j} shows that the system has sensitive dependence on initial conditions almost everywhere within the initial condition space enclosed by the separatrix.

1. Definition of mod I

Let I = [a,b) be a non-empty half-open interval of $\mathbb{R}$. Define $v = \hat{v}$ mod I if $v \in I$ and $\hat{v} - v = n\,(b - a)$ for some integer n.

2. Interval definitions

We parameterize C in ψ using (7.26) where $\varphi \in [-\frac{1}{4},\frac{1}{4})$ on each curve L and R:

$$\psi \in [-1,1)$$

Define:

$$I_L = [-1,0) \qquad I_R = [0,1)$$

$$I_U = I_L \cup I_R = [-1,1)$$

On the left side of x = 0, $\psi \in I_L$; on the right $\psi \in I_R$. In this way, ψ combines the information of the angle φ with the sign parameter μ, providing a canonical representation of each point on any given energy curve. Also define the symbol I_ψ:

$$I_\psi = \begin{bmatrix} I_L & \text{if } \psi \in I_L \\ I_R & \text{if } \psi \in I_R \end{bmatrix}$$

3. The Poincare map

From (7.21)-(7.23) and (7.26), we define the relative difference in angular position $\Delta\psi$ between the initial and final ψ values of

motion during stages 1, 2, and 3 as follows:

$$\Delta\psi \text{ for stage 1 and stage 3} = 2\,\varphi_s \bmod I_R \equiv \upsilon$$

$$\Delta\psi \text{ for stage 2: } = 4\,(\pi\,\varphi_{av} - \varphi_s) \bmod I_U \equiv \tau$$

The value for $\Delta\psi$ ignores the number of full cycles (i.e., complete oscillations) during any particular stage. Define the $\Delta\psi$ maps f and g as follows:

$$f(\psi) = \psi + \upsilon \bmod I_\psi$$

$$g(\psi) = \psi + \tau \bmod I_U$$

Then the Poincare map $F(\psi)$, which is the relative difference in angular position for one complete period of τ, is simply:

$$F(\psi) = f \circ g \circ f(\psi)$$

$F(\psi)$ is pictured in Fig.7.6a. A large iterate of F is shown in Fig.7.6b. As Fig.7.6b clearly shows, the j^{th} iterate of F, F^j, is a very complicated function with many discontinuities and interchanged intervals.

4. The antisymmetric bar operator

Define the antisymmetric bar operator as follows. Let $\psi \in I_U$. Define:

$$\bar{\psi} = \begin{bmatrix} \psi + 1 & \text{if } \psi \in I_L \\ \psi - 1 & \text{if } \psi \in I_R \end{bmatrix}$$

$\bar{\psi}$ is the antisymmetric image of ψ with respect to the origin in the (x,x') plane. It is easily seen that:

$$\overline{(\bar{\psi})} = \psi$$

$$\overline{\psi \bmod I_L} = \psi \bmod I_R + 1 = \psi \bmod I_R$$

$$\overline{\psi \bmod I_R} = \psi \bmod I_R - 1 = \psi \bmod I_L$$

Lemma: $f(\bar{\psi}) = \overline{f(\psi)}$

Let $\psi \in I_R$. Then $f(\psi) = \psi + \upsilon \bmod I_R$, $f(\bar{\psi}) = \bar{\psi} + \upsilon \bmod I_L$ and $\bar{\psi} = \psi - 1$. Then $f(\bar{\psi}) = \psi - 1 + \upsilon \bmod I_L = \psi + \upsilon \bmod I_L = \psi + \upsilon \bmod I_R - 1 = f(\psi) - 1 = \overline{f(\psi)}$. Let $\psi \in I_L$. Then $\bar{\psi} \in I_R$ so that $f(\bar{\psi}) = \overline{f(\bar{\psi})} \rightarrow f(\psi) = \overline{f(\bar{\psi})} \rightarrow \overline{f(\psi)} = f(\bar{\psi})$.

Lemma: $g(\bar{\psi}) = \overline{g(\psi)}$

Let $\psi \in I_R$. Then $\psi + \tau \in [-1,2)$. Then $g(\psi)$ is given by:

$$g(\psi) = \begin{bmatrix} \psi + \tau & \text{if } \psi + \tau \in [-1,1) \\ \psi + \tau - 2 & \text{if } \psi + \tau \in [1,2) \end{bmatrix}$$

Now $g(\bar{\psi}) = \bar{\psi} + \tau \bmod I_U = \psi - 1 + \tau \bmod I_U$

$$= \begin{bmatrix} \psi + \tau + 1 & \text{if } \psi + \tau \in [-1,0) \\ \psi + \tau - 1 & \text{if } \psi + \tau \in [0,2) \end{bmatrix}$$

$$= \overline{g(\psi)}$$

Let $\psi \in I_L$. Then $\bar{\psi} \in I_R \rightarrow g(\psi) = g(\bar{\psi}) = \overline{g(\bar{\psi})} \rightarrow \overline{g(\psi)} = g(\bar{\psi})$

Lemma: $F(\bar{\psi}) = \overline{F(\psi)}$

$$F(\bar{\psi}) = f \circ g \circ f(\bar{\psi}) = f \circ g(\overline{f(\psi)}) = f(\overline{g \circ f(\psi)}) = \overline{f \circ g \circ f(\psi)} = \overline{F(\psi)}$$

5. Intervals interchanged during stage 2

Note that f preserves right and left while g does not. Because g is antisymmetric (see 4. above), the interval E_g of I_R that maps to I_L has an antisymmetric image $\bar{E}_g$ of I_L which maps to I_R. E_g is found to be:

For $\gamma = -1$: $E_g = [0,1) = I_R$

For $\gamma \in (-1,0)$: $E_g = [0,-\gamma)$

For $\gamma = 0$: $E_g = [0,0)$ (the empty interval)

For $\gamma \in (0,1)$: $E_g = [1-\gamma,1)$

Note the special cases for $\gamma = -1$ in which every point of I_R changes sides and $\gamma = 0$ in which no point changes sides.

6. Pre-images of E_g

The pre-image of E_g with respect to the map f is important beacuse it is the interval in I_R which changes sides under the map F. We denote the pre-image of E_g by E_{fg}. Then $f(E_{fg}) = E_g$. E_{fg} is found to be:

For $\gamma = -1$: $E_{fg} = [0,1) = I_R$

For $\gamma \in (-1,0)$:

For $\upsilon \in [0,-\gamma]$: $E_{fg} = [0,-\upsilon-\gamma) \cup [1-\upsilon,1)$

For $\upsilon \in (-\gamma,1)$: $E_{fg} = [1-\upsilon,1-\gamma-\upsilon)$

For $\gamma = 0$: $E_{fg} = [0,0)$

For $\gamma \in (0,1)$:

For $\upsilon \in [0,1-\gamma]$: $E_{fg} = [1-\gamma-\upsilon,1-\upsilon)$

For $\upsilon \in (1-\gamma,1)$: $E_{fg} = [0,1-\upsilon) \cup [2-\gamma-\upsilon,1)$

Then $E_{fg} \in I_R$ but $F(E_{fg}) \in I_L$. Similarly, $\bar{E}_{fg} \in I_L$ but $F(\bar{E}_{fg}) \in I_R$.

7. Define the symbolic coding map $\tilde{F}$

We create a map $\tilde{F}$ similar to F that is used to code the symbol sequence of L's and R's for any initial condition. Define:

$$\tilde{F}(\psi) = F(\psi) \bmod I_R$$

Then $\tilde{F}$ makes no distiction between left or right as F does. It is easily shown that:

$$\tilde{F}(\psi) = \begin{bmatrix} F(\psi) & \text{for } F(\psi) \in I_R \\ \overline{F(\psi)} & \text{for } F(\psi) \in I_L \end{bmatrix}$$

From above, we deduce that $\tilde{F}(\psi) = \tilde{F}(\bar{\psi})$. Furthermore, $\tilde{F}$ can be expressed as a much simpler function than F, i.e.,

$$\tilde{F}(\psi) = \psi + 2\upsilon + \tau \bmod I_R$$

8. Exceptional cases: $\tau = -1$ and $\tau = 0$

For $\tau = -1$, the entire left and right sides are interchanged in the Poincare map. Therefore, every initial condition on the left has the same symbol sequence, namely L.RLRLRLRL••• where the first digit indicates the initial side L. Similarly, every initial condition from the right side has for its symbol sequence R.LRLRLRLR•••.

For $\tau = 0$, no intervals are ever interchanged so that every initial condition from the left has L.LLLLLLLL••• for its symbol sequence and every initial condition from the right has R.RRRRRRRR••• for its symbol sequence.

We define a regular value of τ to be one for which τ is not 0 or -1, i.e., not an integer. These cases allow for much more interesting symbol sequences.

9. Symbol coding intervals in the regular case

Using 6. above, we find that the interval E_{fg} has one of the two following forms for some values $\psi_E^{\pm}$ depending on υ and τ:

$$\text{(i) } E_{fg} = [\psi_E^-, \psi_E^+) \quad \text{or} \quad \text{(ii) } E_{fg} = [0, \psi_E^+) \cup [\psi_E^-, 1)$$

Define $\psi_j^{\pm}$ by:

$$\psi_j^+ = \tilde{F}^{-j}(\psi_E^+) \quad \text{and} \quad \psi_j^- = \tilde{F}^{-j}(\psi_E^-)$$

Then $\tilde{F}^j(\psi_j^{\pm}) = \psi_E^{\pm}$, i.e., $\psi_j^{\pm}$ are the pre-images of $\psi_E^{\pm}$ with respect to $\tilde{F}^j$. Define the symbol coding intervals E_{fg}^{-j} as follows:

$$E_{fg}^{-j} = \begin{bmatrix} [\psi_j^-, \psi_j^+) & \text{for } \psi_j^+ > \psi_j^- \\ [0, \psi_j^+) \cup [\psi_j^-, 1) & \text{for } \psi_j^+ < \psi_j^- \end{bmatrix}$$

Then $\tilde{F}^j(E_{fg}^{-j}) = E_{fg}$. From that and 7., $F^j(E_{fg}^{-j})$ is either E_{fg} or $\bar{E}_{fg}$.

Lemma: For $\psi \in E_{fg}^{-j}$ or $\overline{E_{fg}^{-j}}$, $F^j(\psi)$ and $F^{j+1}(\psi)$ are on different sides.

Suppose $F^j(E_{fg}^{-j}) = E_{fg} \in I_R$. Then $F^{j+1}(E_{fg}^{-j}) = F(E_{fg}) \in I_L$ by definition of E_{fg}. Also, $F^j(\overline{E_{fg}^{-j}}) = \overline{F^j(E_{fg}^{-j})} = \bar{E}_{fg}$ and $F^{j+1}(\overline{E_{fg}^{-j}}) = \overline{F^{j+1}(E_{fg}^{-j})} = \overline{F(E_{fg})} \in I_R$. Therefore, the lemma holds. The supposition that $F^j(E_{fg}^{-j}) = \bar{E}_{fg}$ follows similarly.

10. Symbol coding procedure

For $\psi \in I_U$, define its symbol sequence as $d(\psi) = d_0 . d_1 d_2 d_3 d_4 \cdots$ where d_0 represents the side that the initial condition is located and d_j represents the side which the orbit is located at $\tau = 2\pi j$, i.e., after j iterates of the Poincare map. Each digit d_j is coded by:

$$d_j(\psi) = \begin{bmatrix} L & \text{if } F^j(\psi) \in I_L \\ R & \text{if } F^j(\psi) \in I_R \end{bmatrix}$$

Since F^j is much more difficult to work with than $\tilde{F}^j$, an alternate (but equivalent) method based on $\tilde{F}$ and E_{fg}^{-j} is used. First, define the two successor functions S and $\bar{S}$:

S = Use same digit as the previous one (i.e., use R for d_j if $d_{j-1} = R$)

$\bar{S}$ = Use opposite digit as the rpevious one (i.e., use R for d_j if $d_{j-1} = L$)

Now define $\psi_R = \psi \bmod I_R$. Then $d(\psi)$ is characterized by:

$$d_0 = \begin{bmatrix} L & \text{if } \psi \in I_L \\ R & \text{if } \psi \in I_R \end{bmatrix}$$

$$d_{j+1} = \begin{bmatrix} S & \text{if } \psi_R \notin E_{fg}^{-j} \\ \bar{S} & \text{if } \psi_R \in E_{fg}^{-j} \end{bmatrix}$$

Once $d(\psi)$ is known in terms of d_0 and a sequence of S and $\bar{S}$, the L-R symbol sequence for $d(\psi)$ is easily found using the definitions of the successor functions S and $\bar{S}$ above.

We now explain the coding procedure. For $\psi_R \in E_{fg}^{-j}$, either $\psi \in E_{fg}^{-j}$ or $\bar{\psi} \in E_{fg}^{-j}$. Then by 9. above, $F^j(\psi)$ and $F^{j+1}(\psi)$ are on

different sides. Therefore, the $(j+1)^{th}$ digit is opposite to the j^{th} digit (i.e., $\bar{S}$ is the appropriate coding). For $\psi_R \notin E_{fg}^{-j}$, neither ψ nor $\bar{\psi}$ belongs to E_{fg}^{-j}. Therefore, $F^j(\psi)$ and $F^{j+1}(\psi)$ must be on the same side (i.e., S is the appropriate coding).

11. Properties of $\psi_j^{\pm}$

Let $\Psi = \{ \psi_j^{\pm} \} = \{ \psi_j^+, \psi_j^- : j = 0,1,2,3,\cdots \}$. Also, let $\Lambda = I_R - \Psi$.

Suppose $\psi_j^+ = \psi_{j+q}^+ \ \forall j$ for some integer $q > 0$. Since $\tilde{F}$ is simply a translation map, $\psi_j^- = \psi_{j+q}^-$ also occurs. By definition then,

$$\tilde{F}^q(\psi_E^+) = \psi_E^+ + q\ (2\upsilon + \tau) \bmod I_R = \psi_E^+$$

Thus, $q\ (2\upsilon + \tau) = p$ for some integer p. Hence, $(2\upsilon + \tau)$ must be rational, having the value $\frac{p}{q}$. Furthermore, the implication follows in reverse so that:

$$\psi_j^{\pm} = \psi_{j+q}^{\pm} \quad \text{iff} \quad (2\upsilon + \tau) = \frac{p}{q} \quad \text{iff} \quad E_{fg}^{-j} = E_{fg}^{-(j+q)}$$

This implies that $d_{j+1} = d_{j+q+1} \ \forall j$ so that all sequences $d(\psi)$ are periodic with period q. Moreover, the cardinality of Ψ (denoted $|\Psi|$) is at most 2q, i.e. finite. Thus, Λ contains open intervals of I_R in which every ψ has the same symbol sequence $d(\psi)$.

Suppose $\forall q > 0$, $\psi_j^{\pm} \neq \psi_{j+q}^{\pm} \ \forall j$. Then $(2\upsilon + \tau)$ is irrational and $|\Psi| = \infty$. Detailed information about sequences is not known. However, Ψ is dense in I_R because $\tilde{F}$ is an irrational translation map on the rational circle [0,1). This implies that given two points ψ_0 and ψ_1 of I_R no matter how close, there exists a ψ_j^+ between them. Thus, $d(\psi_0)$ and $d(\psi_1)$ can only agree for the first j digits because

they must disagree at the $(j+1)^{th}$ digit. By definition, then, I_R has sensitive dependence on initial conditions.

The discussion of the sequences generated by I_L follows analogously. The characterization of I_R above holds equally well for I_L.

12. Chaos in the system

We have shown that the initial set C either: (i) generates only periodic symbol sequences; or (ii) has sensitive dependence on initial conditions. The characterization of C depends only on the values υ and τ, which depend on ρ and ϵ. For fixed ϵ, both υ and τ are continuous 1-1 functions of ρ. Therefore, the quantity $(2\upsilon + \tau)$ changes continuously with ρ.

Since the initial set C also changes continuously with ρ, we see that $(2\upsilon + \tau)$ changes continuously with the initial set C. Now the the number of initial sets C within the initial separatrix for which $(2\upsilon + \tau)$ is rational has Lebesgue measure zero. Therefore, $(2\upsilon + \tau)$ is irrational almost everywhere within the initial separatrix.

Consequently, the interior of the initial separatrix has sensitive dependence on initial conditions almost everywhere. Thus, the system is chaotic [Dev87].

8.0 Perturbations of the disappearing separatrix system

The disappearing separatrix system of chapter 7 serves as the foundation for investigations into more complicated related systems. In chapter 7, we found that the qualitative dynamical behavior of the system is predicted by analyzing the system on the (ρ,τ) phase space, where ρ is the square amplitude and τ is slow time (see sections 7.2 and 7.3). Using the flow on the (ρ,τ) phase space, computed using the averaged equations, we showed that the system exhibits chaotic behavior.

In this chapter, we investigate a related system constructed by adding a constant linear stiffness γ and a van der Pol type perturbation g to the system of chapter 7. This system is investigated by analyzing its (ρ,τ) phase flow, computed using the averaged equations. We show that for various ranges of parameters, this system exhibits transient chaos and "limit tori", and that the averaging model predicts attracting chaotic orbits.

We begin by using the MACSYMA program AVERAGE to obtain the averaged system. Then we discuss the effect of γ and g by analyzing the (ρ,τ) flow. Finally, we investigate the averaged system for the existence of limit cycles on the (ρ,τ) phase space. Such limit cycles are interpreted as "limit tori" and attracting chaotic orbits in the original (x,x',τ) phase space.

8.1 The averaged system

This chapter is concerned with a perturbed slowly varying Hamiltonian system which is similar to the disappearing separatrix system of eq.(7.1). In particular, we shall be concerned with the system in:

$$(8.1) \qquad x'' + \left[\gamma - \cos(\tau)\right] x + x^3 + \epsilon \left[\delta x' + \eta x^2 x'\right] = 0$$

In the notation of eq.(0.1), we find:

$$(8.2) \qquad \alpha = \gamma - \cos(\tau) \ , \ \beta = 1 \ , \ g = \delta x' + \eta x^2 x'$$

where γ, δ, and η are constant parameters. System (7.1) is recoverable from (8.1) by taking $\gamma = \delta = \eta = 0$. The phase space for eq.(8.1) is $(x,x',\tau) \in \mathbb{R}^2 \times S^1$, a plane crossed with a circle. As in chapter 7, we shall interpret solutions to eq.(8.1) in terms of the instantaneous phase portrait of the unperturbed system at time τ (see section 7.1), i.e. we shall project onto $\mathbb{R}^2$. The unperturbed system corresponding to eq.(8.1) is the system in which $g = 0$ and τ is fixed.

The averaged system is computed using the AVERAGE program (see section 3.5). Just as in chapter 7, we take (ρ,φ) as independent variables, where $\rho = \bar{r}^2$, rather than $(\bar{r},\varphi)$, since the averaged

equations depend on $\bar{r}$, only in the form $\bar{r}^{-2}$. The averaged system for (ρ,φ) is then found to be:

(8.3a) $$\frac{d\rho}{d\tau} = F(\rho,\tau) + \delta\, f_1(\rho,\tau) + \eta\, f_2(\rho,\tau)$$

where

$$F(\rho,\tau) = -\,2\,\sin(\tau)\left[1 - \frac{E}{K}\right]$$

$$f_1(\rho,\tau) = -\,\frac{2}{3}\left[\rho + 2\left[\gamma - \cos(\tau)\right]\left[1 - \frac{E}{K}\right]\right]$$

$$f_2(\rho,\tau) = \frac{2}{15}\left[8\left[\gamma - \cos(\tau)\right]^2\left[1 - \frac{E}{K}\right] + 2\,\rho\left[\gamma - \cos(\tau)\right]\left[5 - 6\,\frac{E}{K}\right] + 3\,\rho^2\left[1 - 2\,\frac{E}{K}\right]\right]$$

(8.3b) $$\varphi' = \frac{a}{4K}$$

In eqs.(8.3), ρ, k^2, and a^2 are defined as follows:

(8.4a) $$\rho = \bar{r}^{-2}$$

(8.4b) $$a^2 = \rho + \gamma - \cos(\tau)$$

(8.4c) $$k^2 = \frac{\rho}{2\,a^2} = \frac{\rho}{2\,(\rho + \gamma - \cos(\tau))}$$

Since the right-hand side of eq.(8.3a) is periodic in τ with period 2π, the phase space (ρ,τ) for (8.3a) lies on the cylinder $\mathcal{C} = \mathbb{R}\times S^1$.

The position of the instantaneous separatrix as a function of the time τ is important to know for describing the qualitative behavior of orbits in (x,x',τ). Points in (ρ,τ) which correspond to

the separatrix (i.e., which make $k^2 = 1$ in (8.4c)) lie on the curve $\rho_s(\tau)$ given by:

$$\rho_s(\tau) = 2\left[\cos(\tau) - \tau\right] \quad , \quad \tau < \cos(\tau) \tag{8.5}$$

The curve $\rho_s(\tau)$ is denoted the separatrix curve.

Recalling section 2.1, the assumed solution form given in eqs.(2.6) (i.e., $x = \mu\, r\, cn(u,k)$, where $u = a\, t + u_0$) is oscillatory only when the instantaneous frequency a is real. Thus, requiring a to be real in (8.4b) gives the restriction:

$$\rho \geq \cos(\tau) - \tau \tag{8.6}$$

Since the unperturbed phase portraits for eq.(8.1) belong to regions II, III, and IV of Fig.2.1 (because $\beta = 1$), the restriction given by (8.6) is met for any point of the (x,x',τ) phase space. Hence, those points of the (ρ,τ) cylinder not meeting condition (8.6) do not correspond to any point (x,x',τ) of the phase space: they are not physically meaningful for the model and should be ignored.

We note that eq.(8.1) has a trivial solution $x \equiv 0$, which is of the solution form $x = r\, cn(u,k)$ for $r \equiv 0$. Hence, $\rho = r^{-2} \equiv 0$ is a solution to (8.3a) when k^2 in (8.4c) is interpreted as also being identically zero. Because this solution is fully known and not interesting, we will ignore the existence of the trivial solution throughout this chapter.

The restriction given by (8.6) determines a boundary of the orbits of the (ρ,τ) phase space on the cylinder. We call this boundary the <u>ρ-boundary curve</u> and denoted it $\rho_b(\tau)$:

$$\rho_b(\tau) = \max(\cos(\tau) - \gamma, 0) \tag{8.7}$$

All orbits on $\mathcal{C}$ (except the trivial one) lie above the ρ-boundary curve (i.e., $\rho \geq \rho_b$).

We first discuss the effect of the linear stiffness γ, i.e. we take $\delta = \eta = 0$ in what follows. First, for $\gamma \geq 1$, condition (8.6) is satisfied $\forall\rho$ and no separatrix exists (from (8.5)). The system never possesses an instantaneous separatrix at any time τ, and the instantaneous (x,x') phase space always contains just one fixed point at the origin.

For $\gamma < 1$, an instantaneous separatrix exists for some interval in τ (since $\gamma < \cos(\tau)$ for some τ in (8.5)). Moreover, the ρ-boundary curve encloses a physically unmeaningful region of the cylinder $\mathcal{C}$. For $|\gamma| \leq 1$, the separatrix and ρ-boundary curves intersect $\rho = 0$ at the value of τ given by:

$$\tau = \cos^{-1}(\gamma) \quad , \quad |\gamma| \leq 1 \tag{8.8}$$

For $\gamma < -1$, the separatrix and ρ-boundary curves exist $\forall\tau$ and do not intersect $\rho = 0$. The separatrix curve is twice the height in ρ of the ρ-boundary curve at each value of τ (cf. eqs.(8.5) and (8.7)).

The maximum height of the separatrix occurs at $\tau = 0$ at which time $\rho_s = 2\ (1 - \tau)$.

The three intervals of τ which are qualitatively different are then:

(8.9a) Case (i): $\tau \geq 1$

(8.9b) Case (ii): $-1 < \tau < 1$

(8.9c) Case (iii): $\tau \leq -1$

For case (i), no separatrix exists. For case (ii), the separatrix exists for part of the period 2π in τ. For case (iii), the separatrix exists for the whole period.

A picture of the vectorfield given by eq.(8.3a) for $\delta = \eta = 0$ and the trivial equation:

$$\frac{d\tau}{d\tau} = 1 \tag{8.10}$$

on the (ρ,τ) phase space is shown in Figs.8.1a-c. Plates (a-c) correspond to the cases (i), (ii), and (iii), respectively. (Fig.8.1b is simply a different representation of Fig.7.4b.) The flow in each figure is conservative and the (ρ,τ) phase space is filled with close orbits. This can be seen by tracing along an orbit from $\tau = -\pi$ to $\tau = \pi$ following the direction of the vectorfield. The separatrix curve $\rho_s(\tau)$ and the ρ-boundary curve $\rho_b(\tau)$ are shown as solid lines in each figure.

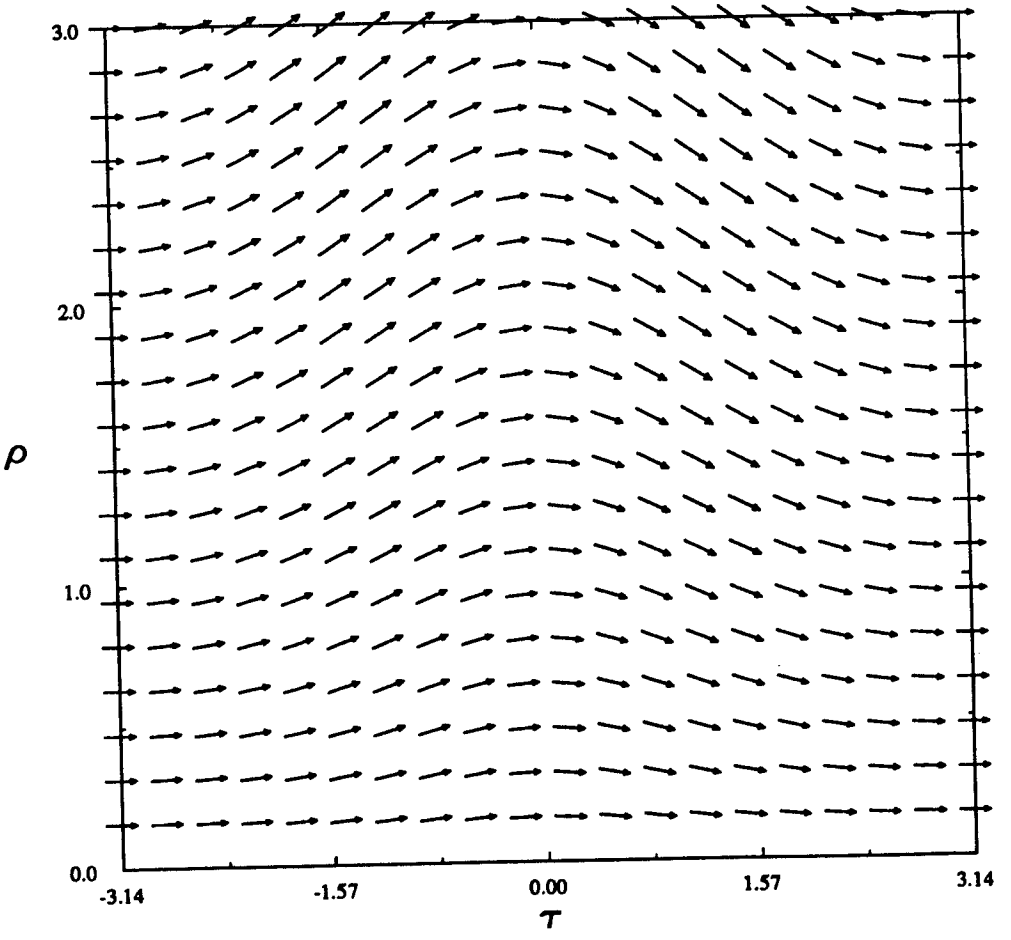

Fig.8.1a Effect of γ in eq.(8.1). Plot of the (ρ,τ) vectorfield given by (8.3a) and (8.10) for $\gamma = 1.5$, $\delta = \eta = 0$. The phase space is filled with closed orbits.

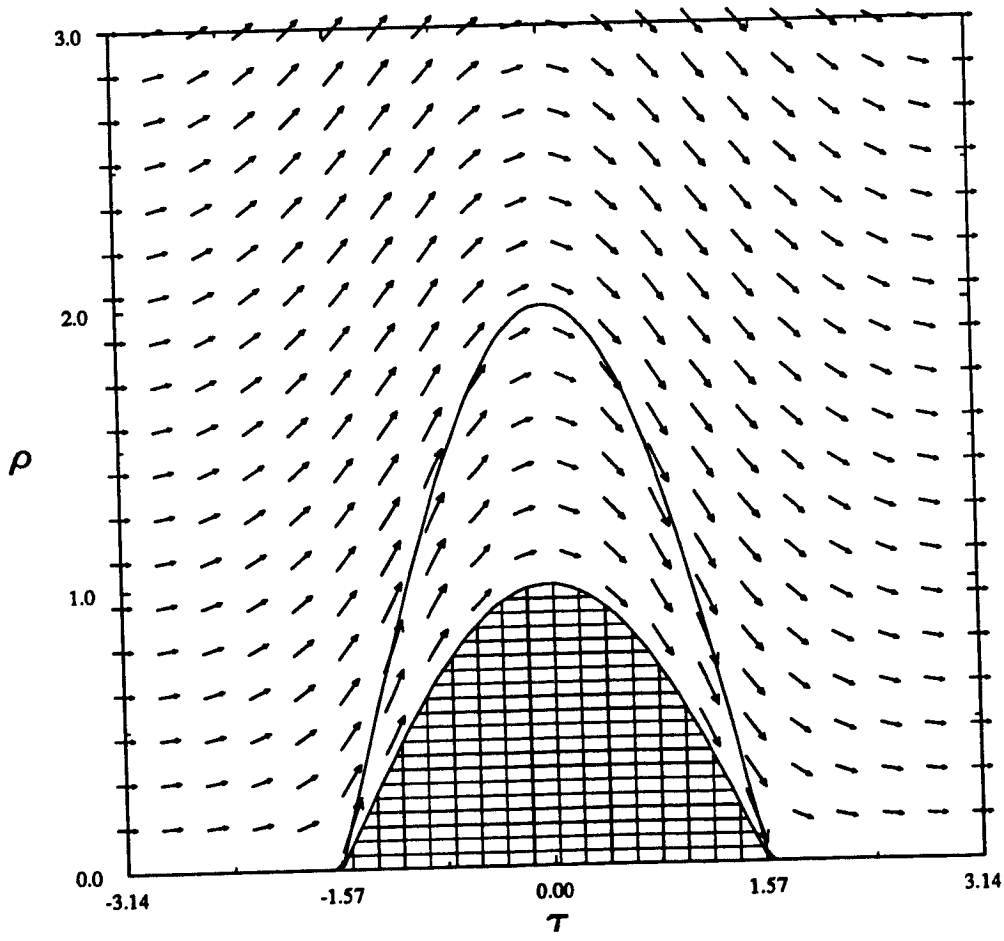

Fig.8.1b Effect of τ in eq.(8.1). Plot of the (ρ,τ) vectorfield given by (8.3a) and (8.10) for $\tau = 0$, $\delta = \eta = 0$. The separatrix curve is shown using a solid line. The ρ-boundary curve, also shown using a solid line, encloses the unmeaningful region (shown gridded). The phase space is filled with closed orbits. Some pass through the separatrix curve, while others do not.

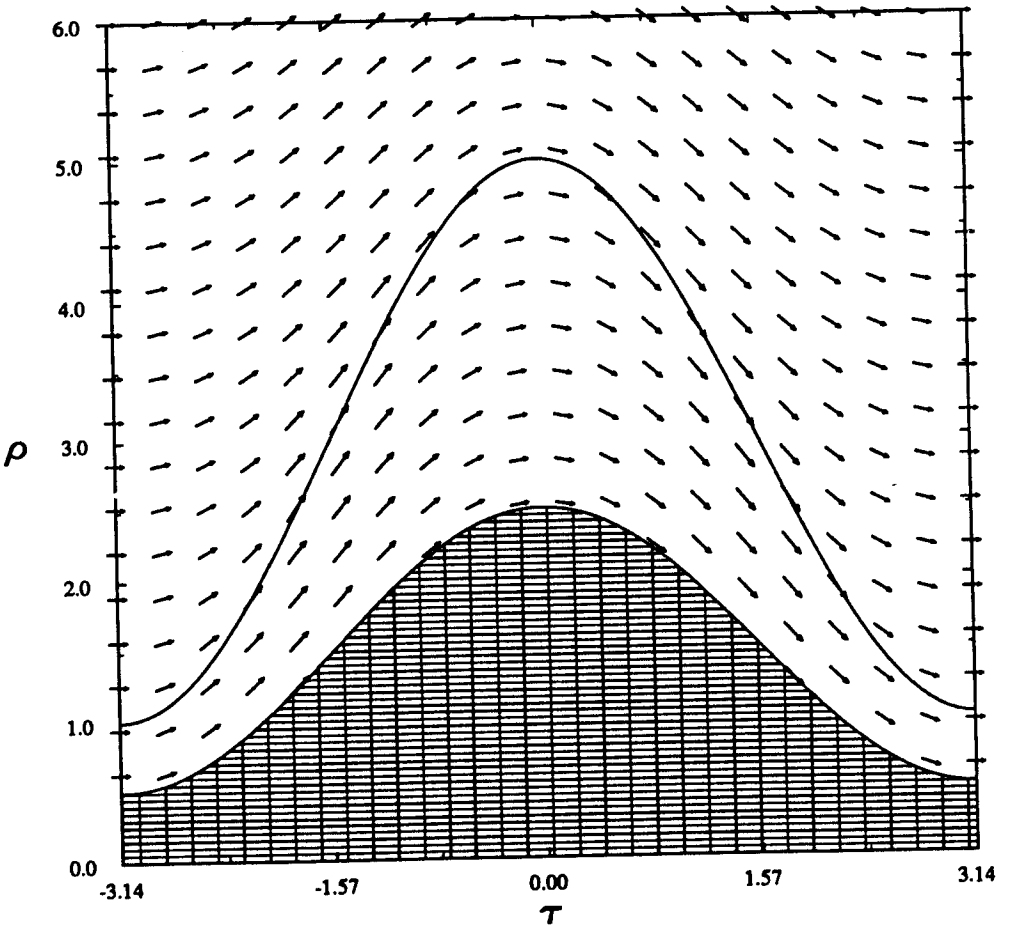

Fig.8.1c Effect of τ in eq.(8.1). Plot of the (ρ,τ) vectorfield given by (8.3a) and (8.10) for $\tau = -1.5$, $\delta = \eta = 0$. The separatrix curve is shown using a solid line. The ρ-boundary curve, also shown using a solid line, encloses the unmeaningful region (shown gridded). The phase space is filled with closed orbits. Some pass through the separatrix curve, while others do not.

In Fig.8.1a, the phase space consists of the entire cylinder $\mathcal{C}$. The ρ-boundary curve is simply the line $\rho = 0$. The separatrix curve does not exist.

In Fig.8.1b, some orbits cross from outside the separatrix to the inside and back again, while others remain outside the separatrix $\forall\tau$.

There are three distinct regions in Fig.8.1c: (1) a region where orbits remain outside the separatrix $\forall\tau$; (2) a region where orbits cross from outside to inside and back again; and (3) a region where orbits remain inside the separatrix $\forall\tau$. Orbits which remain inside the separatrix $\forall\tau$ can never change sides (right or left); the averaging model works well for these orbits (except for those too near the separatrix at $\tau = \pm\pi$). The orbits which remain within the separatrix $\forall\tau$ are simply modulated oscillations with non-zero mean (i.e., they oscillate about the instantaneous fixed point within the separatrix loop).

We now discuss the effect of the damping term $\delta x'$, i.e., we take $\eta = 0$. In Figs.8.2a-c, a picture of the vectorfield is shown for fixed δ at the same τ values of Figs.8.1a-c. In Fig.8.2a, the entire vectorfield has a negative slope, indicating ρ decreasing everywhere in (ρ,τ), i.e., a damped oscillation in (x,x',t).

In Fig.8.2b, much of the vectorfield has a negative slope; however, near the separatrix for $\tau < 0$ the vectorfield has positive slope. Investigating f_1 in eq.(8.3a), we see that $f_1(\rho,\tau) = 0$ on the separatrix since $E/K \to 0$ as $k \to 1$. So, the only contribution to $\frac{d\rho}{d\tau}$

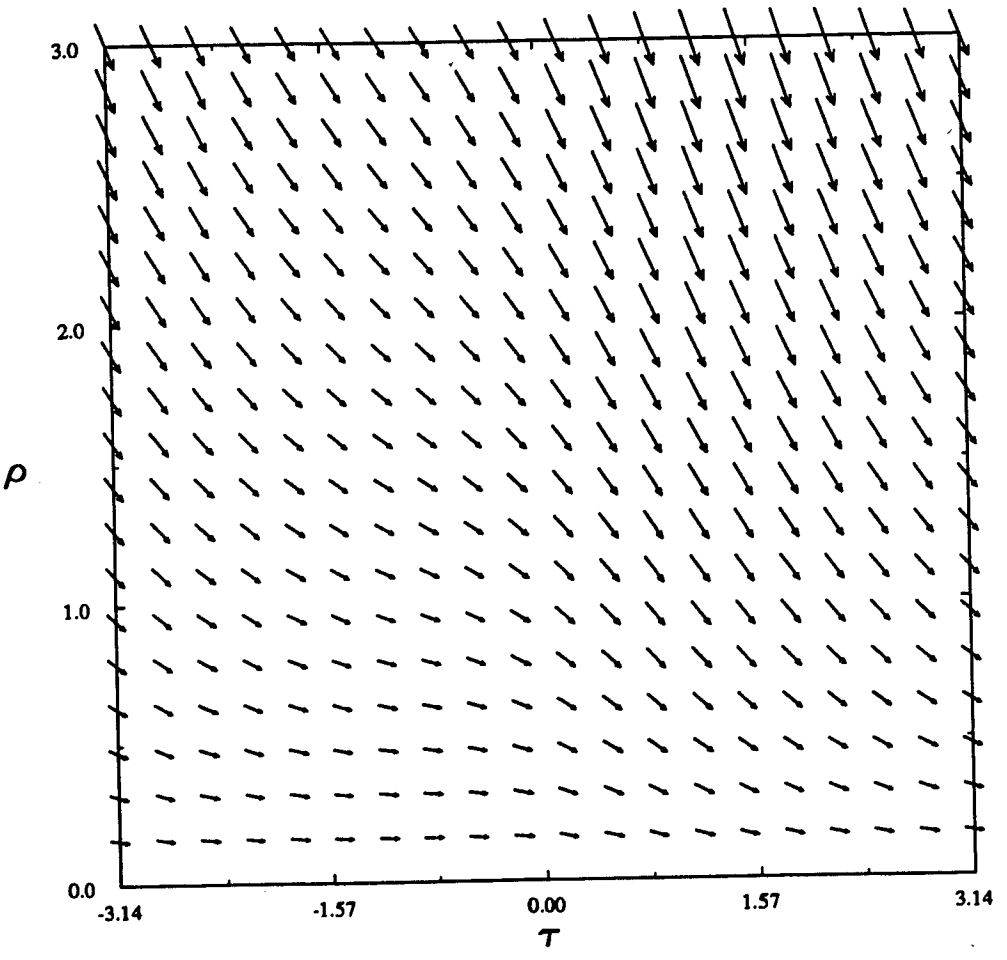

Fig.8.2a Effect of δ in eq.(8.1). Plot of the (ρ,τ) vectorfield given by (8.3a) and (8.10) for $\tau = 1.5$, $\delta = 0.5$, $\eta = 0$. All orbits damp toward $\rho = 0$.

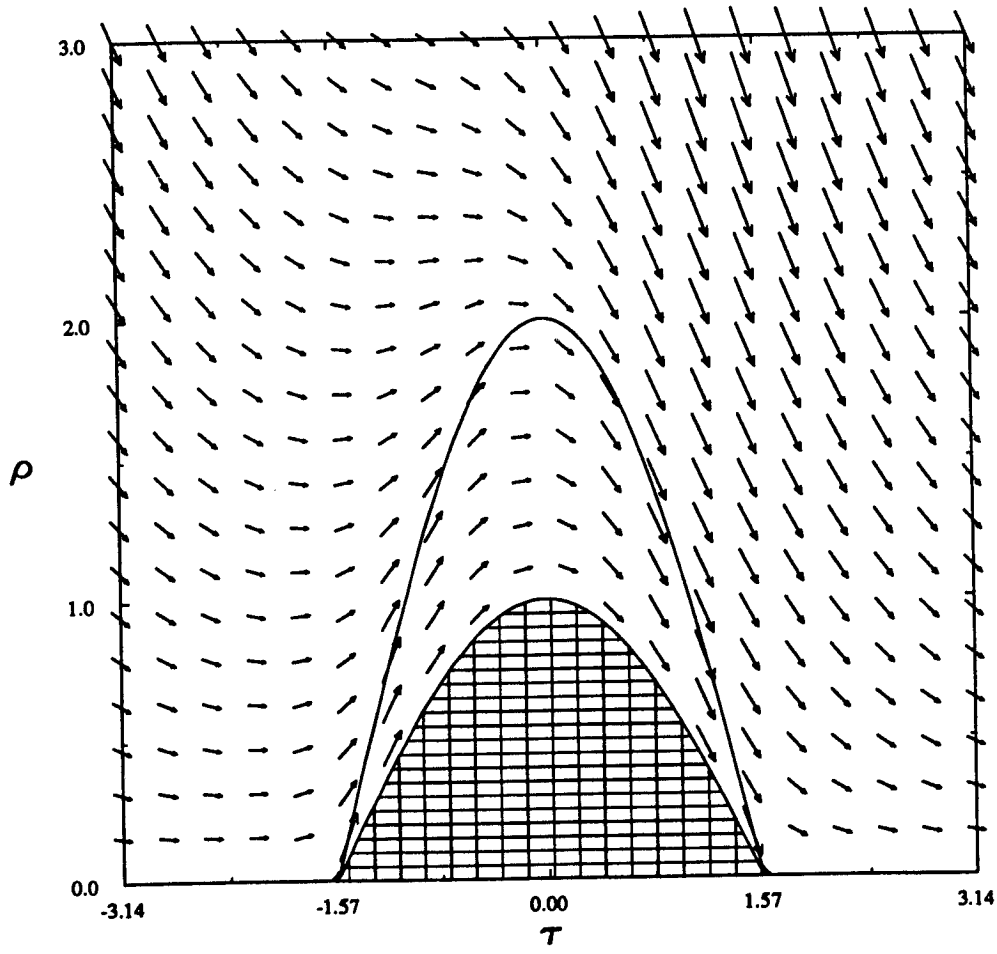

Fig.8.2b Effect of δ in eq.(8.1). Plot of the (ρ,τ) vectorfield given by (8.3a) and (8.10) for $\gamma = 0$, $\delta = 0.5$ $\eta = 0$. The separatrix curve is shown using a solid line. The ρ-boundary curve, also shown using a solid line, encloses the unmeaningful region (shown gridded). While each orbit damps overall during each period, some which pass near the left of the separatrix curve increase in ρ for a short time in τ.

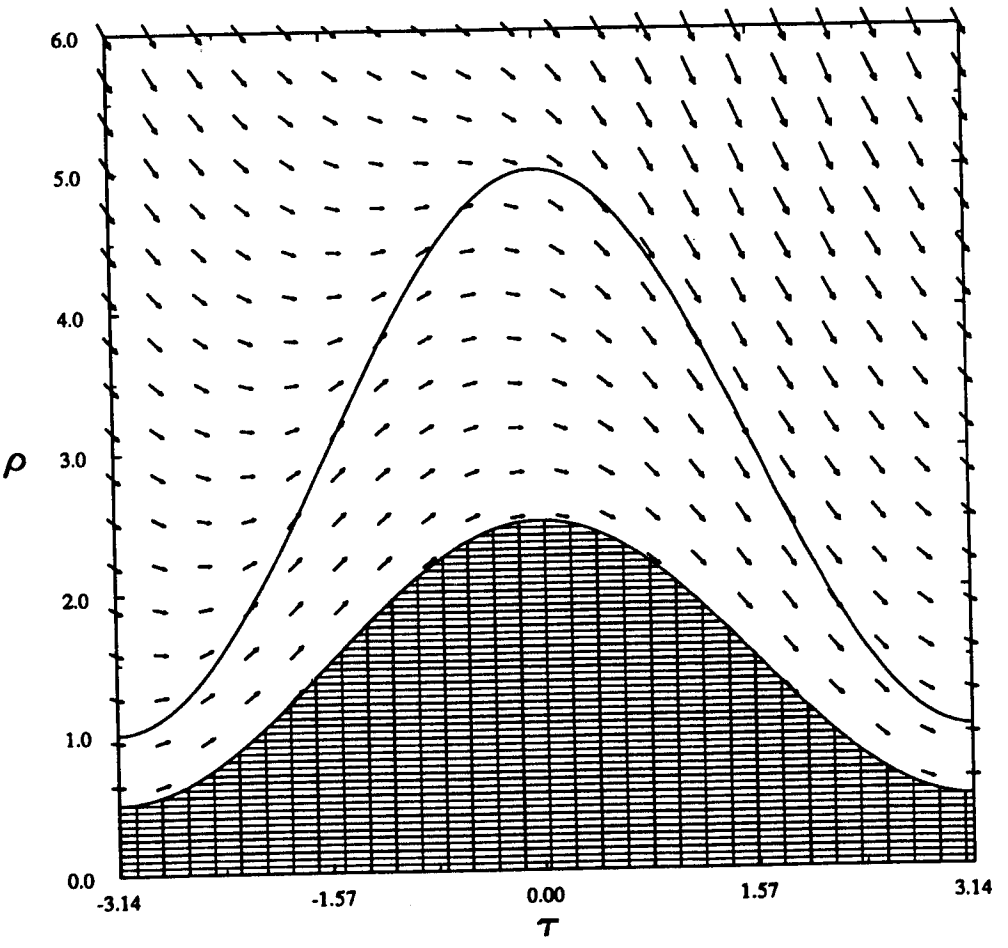

Fig.8.2c Effect of δ in eq.(8.1). Plot of the (ρ,τ) vectorfield given by (8.3a) and (8.10) for $\gamma = -1.5$, $\delta = 0.5$, $\eta = 0$. The separatrix curve is shown using a solid line. The ρ-boundary curve, also shown using a solid line, encloses the unmeaningful region (shown gridded). While each orbit damps overall during each period, some which pass near the left of the separatrix curve increase in ρ for a short time in τ.

comes from the $F(\rho,\tau)$ term, which has positive slope on the separatrix. Hence, no matter the value of δ, the vectorfield slope near the separatrix is positive for $\tau < 0$.

From this, we conclude that while ρ decreases overall during one period in τ, there exists a region of the (ρ,τ) phase space for which ρ must increase. That is, for some interval of slow time τ (which may be a very long time in t when ϵ is very small), the amplitude of the oscillation increases even under damping.

For this damped case, the averaging model predicts that all orbits in (ρ,τ) eventually decay in ρ, becoming asymptotic to $\rho_b(\tau)$, the ρ-boundary curve. If we consider separatrix crossing effects as was done in section 7.3, we must suppose that some orbits will cross the separatrix more slowly than the averaging method assumes. These orbits will increase greatly in ρ (compared to the averaging model prediction) by remaining close to the unstable manifold of the saddle as the separatrix grows. Once the orbit has crossed the separatrix, ρ again decreases. This dynamical behavior has been verified in numerical simulations of eq.(8.1). In fact, since an orbit must cross inside the separatrix and then out again during each period in τ, the system is still conjectured to be chaotic in the same manner as (7.1).

Fig.8.2c is similar to Fig.8.2b in that for $\tau < 0$ near the separatrix, the vectorfield slope is positive irrespective of $\delta > 0$. The dynamical behavior, however, is different since the ρ-boundary curve exists $\forall\tau$. Points on $\rho_b(\tau)$ with $\rho > 0$ correspond to the

instantaneous fixed points within the instantaneous separatrix (cf. eq.(2.10), eq.(8.7)). Since $\rho_b(\tau)$ exists $\forall\tau$, these instantaneous fixed points exist $\forall\tau$. Therefore, the attraction of an orbit toward $\rho_b(\tau)$ indicates attraction to one of the instantaneous fixed points.

The approach to the ρ-boundary curve for most points, however, must pass through the separatrix curve first. Depending on the strength of the damping δ, an orbit may change sides from R to L many times before approaching a particular instantaneous fixed point. The averaging model, then, predicts *transient chaos*, at least for very small but positive δ. If we again consider separatrix crossing effects, the prediction of *transient chaos* for some orbits still holds.

Lastly, we discuss the effect of η, i.e., we take $\delta = 0$. A picture of the vectorfield in (ρ,τ) is shown in Figs.8.3a-c for the same values of γ as in Figs.8.1a-c. It can again be verified that $f_2(\rho,\tau) = 0$ (with f_2 defined by (8.3a)) on the separatrix, so that there exists regions in (ρ,τ) where ρ is increasing although $\eta\, x^2\, x'$ is a (nonlinear) damping term. The type of dynamical behavior follows very closely the case for $\delta > 0$ and will not be repeated. We do note, however, that the vectorfields for $\delta > 0$ and for $\eta > 0$ are not identical so that the possibility of limit cycles in (ρ,τ) for particular values of δ and η exist. This is explored in the next section.

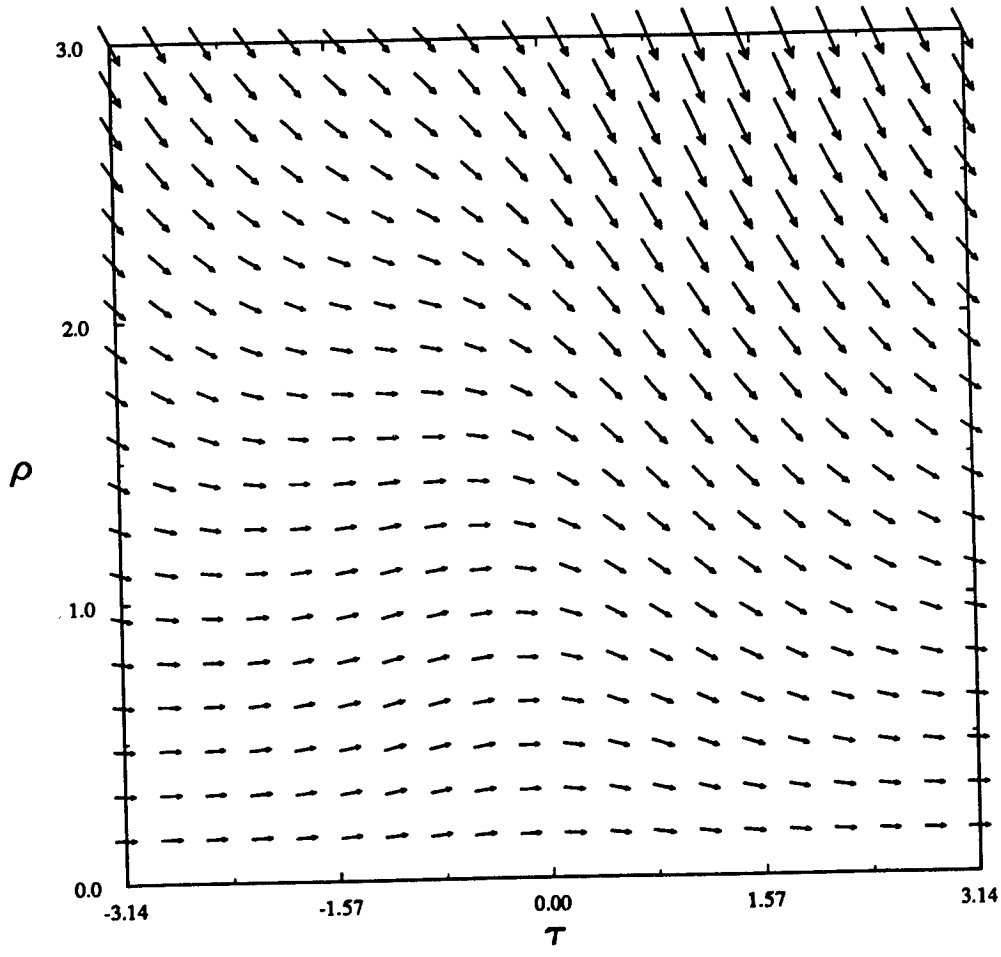

Fig.8.3a Effect of η in eq.(8.1). Plot of the (ρ,τ) vectorfield given by (8.3a) and (8.10) for $\tau = 1.5$, $\delta = 0$, $\eta = 0.5$. All orbits damp toward $\rho = 0$.

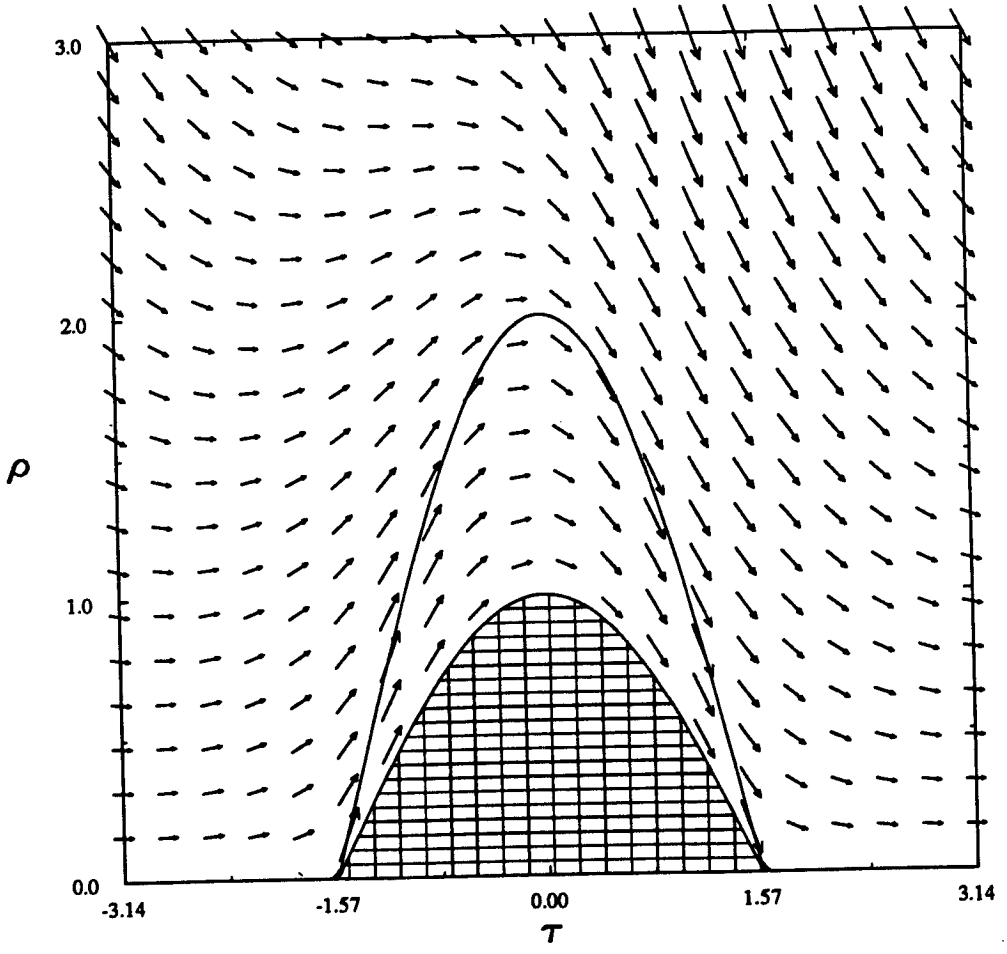

Fig.8.3b Effect of η in eq.(8.1). Plot of the (ρ,τ) vectorfield given by (8.3a) and (8.10) for $\tau = 0$, $\delta = 0$ $\eta = 0.5$. The separatrix curve is shown using a solid line. The ρ-boundary curve, also shown using a solid line, encloses the unmeaningful region (shown gridded). While each orbit damps overall during each period, some which pass near the left of the separatrix curve increase in ρ for a short time in τ.

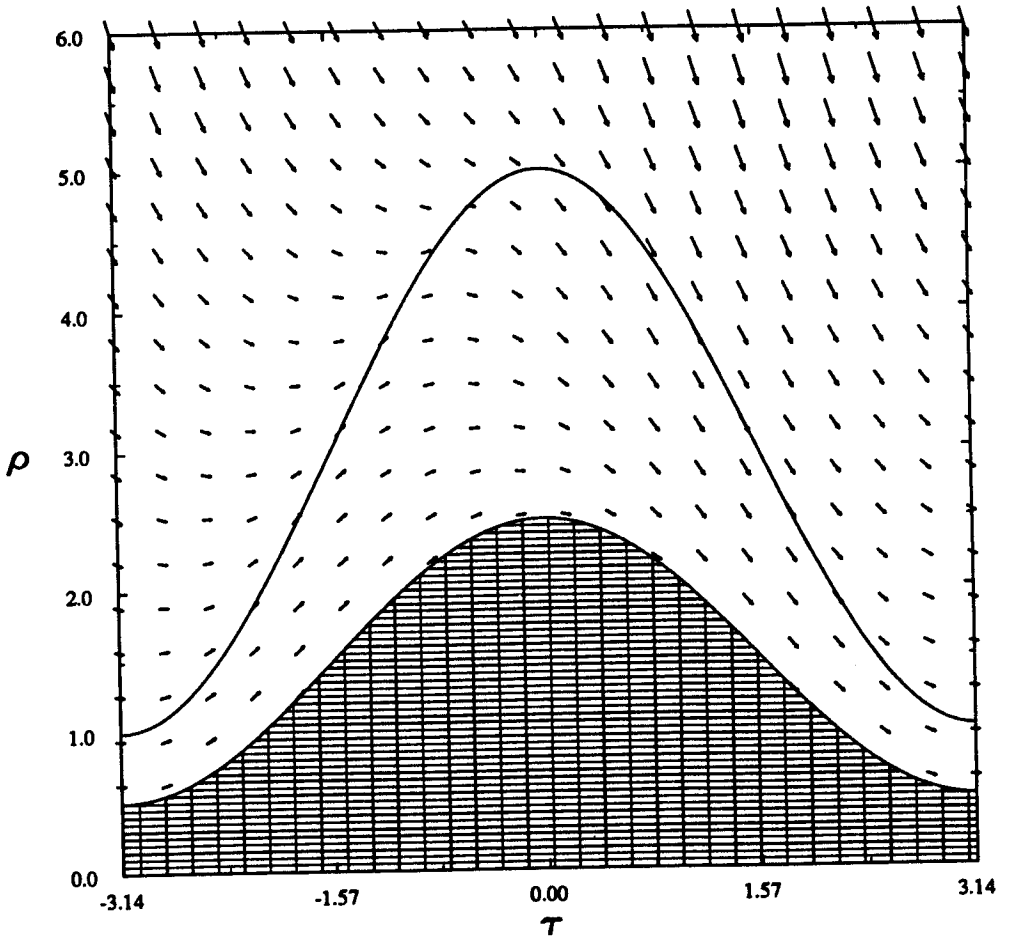

Fig.8.3c Effect of η in eq.(8.1). Plot of the (ρ,τ) vectorfield given by (8.3a) and (8.10) for $\gamma = -1.5$, $\delta = 0$, $\eta = 0.5$. The separatrix curve is shown using a solid line. The ρ-boundary curve, also shown using a solid line, encloses the unmeaningful region (shown gridded). While each orbit damps overall during each period, some which pass near the left of the separatrix curve increase in ρ for a short time in τ.

8.2 Limit Cycles on (ρ,τ)

We now explore conditions for the existence of limit cycles on the (ρ,τ) phase space and its implications for the (x,x',τ) phase space. In searching for limit cycles on the (ρ,τ) cylinder, we cannot simply require $\rho' = 0$ (as is done in chapters 4, 5, and 6 for $\bar{r}'$) because ρ = constant is <u>not</u> a solution to the unperturbed system ($\bar{r}$ = constant is a solution to the unperturbed systems of chapters 4, 5, and 6). Therefore, we will derive a condition for the bifurcation of a limit cycle from the periodic orbits on (ρ,τ) based on the Fredholm alternative [Gre78]. (For the systems of chapters 4, 5, and 6, this gives the requirement that $\bar{r}' = 0$.)

For $g = 0$, the (ρ,τ) phase space is filled with closed orbits, i.e., ρ is 2π periodic in τ. The solution of (8.3a) for $\delta = \eta = 0$ is denoted $\rho^*(\tau;\rho_0)$, where $\rho^*(0;\rho_0) = \rho_0$. For $g \neq 0$, the closed orbits (in general) break apart. However, some closed orbit may give rise to a limit cycle because the vectorfield in the ρ direction due to δ and η cancel on the average.

The derivation of the limit cycle bifurcation condition follows. First, we must scale the perturbation terms δ and η in a new asymptotic variable ϵ_1 (i.e., $\epsilon_1 << 1$):

(8.11a) $$\delta = \epsilon_1 \hat{\delta}$$

(8.11b) $$\eta = \epsilon_1 \hat{\eta}$$

Now, we re-write eq.(8.3a) in short-hand notation:

$$\frac{d\rho}{d\tau} = F(\rho,\tau) + \epsilon_1 f(\rho,\tau) \ , \ \epsilon_1 << 1 \tag{8.12}$$

$$\text{where } f(\rho,\tau) = \hat{\delta}\, f_1(\rho,\tau) + \hat{\eta}\, f_2(\rho,\tau)$$

and $F(\rho,\tau)$, $f_1(\rho,\tau)$, and $f_2(\rho,\tau)$ are defined in (8.3a)

The solution to the $\epsilon_1 = 0$ system of (8.12) is $\rho^*(t;\rho_0)$. We look for a solution to the $\epsilon_1 \neq 0$ system in the form:

$$\rho = \rho^* + \epsilon_1 q + O(\epsilon_1^2) \tag{8.13}$$

Substituting (8.13) into (8.12) and expanding the result in a Taylor series in ϵ_1 gives:

$$\frac{d\rho^*}{d\tau} + \epsilon_1 \frac{dq}{d\tau} = F(\rho^*,\tau) + \epsilon_1 \left.\frac{\partial F}{\partial \rho}\right|_{\rho=\rho^*} q + \epsilon_1 f(\rho^*,\tau) + O(\epsilon_1^2) \tag{8.14}$$

Solving (8.14) for $\frac{dq}{d\tau}$ (noting that ρ^* solves the $\epsilon_1 = 0$ system) gives:

$$\frac{dq}{d\tau} = A(\tau;\rho_0)\, q + f(\rho^*,\tau) \tag{8.15}$$

$$\text{where } A(\tau;\rho_0) = \left.\frac{\partial F}{\partial \rho}\right|_{\rho=\rho^*}$$

Eq.(8.15) is a linear first order equation for q.

We now introduce a linear operator structure for (8.15). Define the inner product (u,v) by the integral over 2π in τ and the linear operator L via eq.(8.15):

$$(u,v) = \int_0^{2\pi} u\, v\, d\tau \tag{8.16a}$$

$$L = \frac{d}{d\tau} - A(\tau;\rho_0) \tag{8.16b}$$

Then eq.(8.15) can be written in operator notation:

$$Lq = f(\rho^*,\tau) \tag{8.17}$$

A bifurcation from a closed orbit ρ^* (indexed by ρ_0) to a limit cycle occurs if q is 2π periodic in τ so that ρ in (8.13) is periodic to $O(\epsilon_1^2)$. We now suppose q is 2π periodic in τ. Then the adjoint operator L^* is found to be:

$$L^* = -\frac{d}{d\tau} - A(\tau;\rho_0) \tag{8.18}$$

The Fredholm alternative [Gre78] states that for solutions to (8.17) to exist (for q a 2π periodic function of τ), (z,f) must be zero for

all z that make $L^*z = 0$. Since $L^*z = 0$ is a first order linear equation, we can easily solve it. The solution is given by:

$$z(\tau) = c_1 \exp\left(-\int_0^{\tau} A(s;\rho_0)\, ds\right) \tag{8.19}$$

Therefore, the bifurcation condition $(z,f) = 0$ is written as:

$$\int_0^{2\pi} \exp\left(-\int_0^{\tau} A(s;\rho_0)\, ds\right) f(\rho^*,\tau)\, d\tau = 0 \tag{8.20}$$

For ease of notation, define the function $I(\rho_0)$ as follows:

$$I(\rho_0) = \int_0^{2\pi} \exp\left(-\int_0^{\tau} A(s;\rho_0)\, ds\right) f(\rho^*,\tau)\, d\tau \tag{8.21}$$

Then the bifurcation condition, eq.(8.20), is expressed by $I(\rho_0) = 0$. The closed orbit $\rho^*(\tau;\rho_0)$ that makes $I(\rho_0) = 0$ gives rise to a limit cycle.

We now find conditions on the parameters δ and η for the existence of a limit cycle. We first define the functions $\hat{f}_1(\rho_0)$ as follows:

$$\hat{f}_1(\rho_0) = \int_0^{2\pi} \exp\left(-\int_0^{\tau} A(s;\rho_0)\, ds\right) f_1(\rho^*,\tau)\, d\tau \tag{8.22a}$$

$$\text{(8.22b)} \qquad \hat{f}_2(\rho_0) = \int_0^{2\pi} \exp\left(-\int_0^{\tau} A(s;\rho_0)\, ds\right) f_2(\rho^*,\tau)\, d\tau$$

Then the bifurcation condition, eq.(8.20), is expressed by:

$$\text{(8.23)} \qquad \hat{\delta}\, \hat{f}_1(\rho_0) + \hat{\eta}\, \hat{f}_2(\rho_0) = 0$$

Solving (8.23) for the ratio of $\hat{\delta}/\hat{\eta}$, we find:

$$\text{(8.24)} \qquad \frac{\hat{\delta}}{\hat{\eta}} = -\frac{\hat{f}_2(\rho_0)}{\hat{f}_1(\rho_0)}$$

We define υ to be the ratio $\hat{\delta}/\hat{\eta}$. Eq.(8.24) is then written:

$$\text{(8.25)} \qquad \upsilon = -\hat{f}(\rho_0)$$

$$\text{where } \hat{f}(\rho_0) \equiv \frac{\hat{f}_2(\rho_0)}{\hat{f}_1(\rho_0)}$$

A value of ρ_0 satisfying eq.(8.25) for a fixed parameter ratio $\upsilon = \hat{\delta}/\hat{\eta} = \delta/\eta$, corresponds to a limit cycle bifurcating from the orbit $\rho^*(\tau;\rho_0)$ at $\epsilon_1 = 0$.

As an example of the limit cycle condition given by eq.(8.25), we consider eq.(8.1) for $\tau = 0$. From (8.6), we see that $\rho_0 \geq 1$. On the separatrix, $\rho_0 = 2$ (from (8.5)). A graph of $\hat{f}(\rho_0)$ vs. ρ_0 is

shown in Fig.8.4. The graph starts with value $\hat{f}(1) \simeq 0.3$ and increases montonically as ρ_0 increases, becoming nearly a straight line for large ρ_0. On the range $1 \lesssim \rho_0 \lesssim 2$, the curve is nearly horizontal. For $-\upsilon > \hat{f}(1)$, one limit cycle is predicted (since a horizontal line through $-\upsilon$ intersects the $\hat{f}(\rho_0)$ curve at one point). For $-\upsilon < \hat{f}(1)$, no limit cycles are predicted.

Now we interpret limit cycles in the (ρ,τ) phase space in terms of the system phase space (x,x',τ). Consider an orbit of the averaging model which lies on a limit cycle in (ρ,τ) located wholely outside or inside the separatrix. Since ρ is periodic in τ, $\bar{r}$, $a(\bar{r})$, and $k^2(\bar{r})$ must also be periodic in τ. Therefore, the averaging approximation for x and x' (given by eqs.(2.6) and (2.21)) lies on a torus with angles τ and φ. If the period of motion in φ over the time $\tau = 2\pi$ is commensurate with 2π, the motion is periodic; otherwise, it is quasiperiodic. This is an example of a "limit-torus", a generalization of a limit cycle in 2 degree of freedom systems. The "limit-torus" is predicted to occur in the original system, eq.(8.1).

Limit cycles on the (ρ,τ) phase space can also give rise to transient chaos. Suppose a stable limit cycle is contained wholely within the separatrix. Then motions starting outside the separatrix which are attracted to the limit cycle pass through the separatrix curve on its way toward the limit cycle. If the attraction is weak, an orbit may cross the separatrix curve many times before reaching

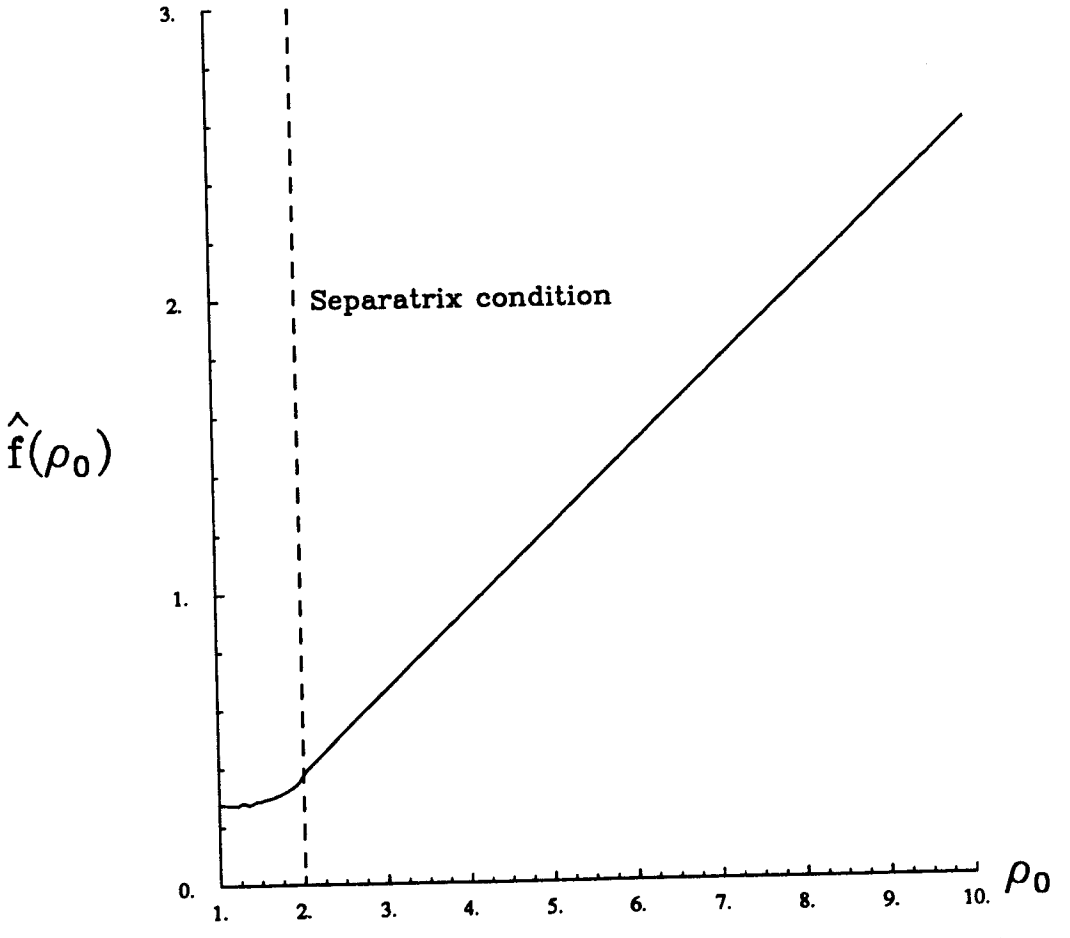

Fig.8.4 Example of the limit cycle condition for $\tau = 0$, given by (8.25). A limit cycle is predicted for the parameter ratio $\upsilon = \delta/\eta$ bifurcating from the closed orbit $\rho^*(\tau;\rho_0)$ for ρ_0 values satisfying $-\upsilon = \hat{f}(\rho_0)$.

the limit cycle, changing from right side to left side after each 2π period in τ in an unpredictable fashion.

Now consider an orbit of the averaging model which lies on a limit cycle on (ρ,τ) which passes through the separatrix. The x and x' motion cannot lie on a torus because the sign parameter μ in eqs.(2.6) is not periodic in τ (in general). If μ were periodic in τ, then every initial condition on an instantaneous energy curve would switch sides in the same manner, regardless of φ, which does not occur in general. The averaging model predicts that the initial conditions lying on the instantaneous energy curve C (= L U R) corresponding to the ρ_0 value of the limit cycle have sensitive dependence on initial conditions (in general). This follows from the arguments presented in chapter 7. Orbits generated by these initial conditions are chaotic. Since the limit cycle in the (ρ,τ) phase space is attractive, orbits initially near C are attracted toward the orbits of C. Hence, the (x,x',τ) phase space is predicted to contain attractive chaotic orbits.

We found in chapter 7 that the averaging model is an excellent predictor of the qualitative behavior of a system away from separatrices. Therefore, the averaging model prediction for limit cycles which pass through the separatrix must be treated with some skepticism. In using deriving the bifurcation condition, we assumed that the orbits $\rho^*(\tau)$ were periodic. This is not truly the case when we consider the effects of separatrix crossing, at least for most

initial conditions. Hence, we cannot conclude that limit cycles exist on (ρ,τ) which pass through the separatrix. Numerical integrations, however, suggest that the system is chaotic.

9.0 Separatrix crossing

We briefly discussed the problems with the averaging method near a separatrix in sections 3.2 and 7.3. We extend our discussion in this chapter. As noted in section 3.2, the averaging method becomes invalid in a neighborhood of a separatrix because the leading order instantaneous frequency (i.e., $\frac{a}{4K}$) becomes zero. The period then becomes arbitrarily high independent of ϵ. The averaging approximation, however, is only valid for times of $O(\frac{1}{\epsilon})$, which is less than the period of the unperturbed periodic orbits near the separatrix. Therefore, the notion that a perturbed orbit remains close to the unperturbed orbit over one periodic cycle breaks down.

In order to remedy this problem with the averaging approximation, we introduce a new model of separatrix crossing. This model will replace the averaging approximation in a neighborhood of a separatrix. In this way, the neighborhood of a separatrix is viewed as a boundary layer (abbreviated b.l.) in the phase space.

We begin with a general discussion of separatrix crossing problems. Then we present the separatrix crossing model as a combination of two different models: one which is valid away from the separatrix's saddle, the other valid near it. Finally, we apply the general theory to the disappearing separatrix system of chapter 7.

9.1 Discussion

Before we can investigate separatrix crossing, we must first understand some properties of separatrices themselves. A separatrix is a special orbit of a dynamical system which is asymptotic to a saddle as $t \to \pm \infty$. Points of a separatrix that are forward asymptotic (i.e., as $t \to + \infty$) belong to the stable manifold of the saddle; points that are backward asymptotic (i.e., $t \to - \infty$) belong to the unstable manifold. It is possible for a point to be both forward and backward asymptotic to a saddle. In region IV of Fig.2.1, the separatrix consists of two homoclinic loops (i.e., the stable and unstable manifolds of one saddle coincide); in region VIII of Fig.2.1, the separatrix consists of two heteroclinic connections (i.e., one saddle's unstable manifold coincides with the other's stable manifold).

In the unperturbed systems corresponding to eq.(0.1) which contain closed orbits (see Fig.2.1), the separatrix is either homoclinic or heteroclinic. In the perturbed systems corresponding to eq.(0.1), however, this is (usually) not true. While the stable and unstable manifolds of a saddle persist under perturbations, the saddle-saddle connections generically break.

In both the unperturbed and perturbed systems, the separatrix separates qualitatively distinct regions of phase space. In the unperturbed system, the regions consist of closed orbits. In the

perturbed system, the regions consist of the global basins of fixed points and the point at infinity. (The global basin of a sink is the set of points in initial condition space which is attracted (forward asymptotic) to the sink. A similar definition holds for sources and the point at infinity.)

Since the separatrix is an orbit and each orbit is unique (from the uniqueness theorem for differential equations), no orbits can cross a separatrix (which is why it forms a boundary). The term "separatrix crossing" cannot, therefore, refer to a crossing of the actual separatrix of a system. What it does refer to is an orbit of the perturbed system crossing the unperturbed system's separatrix. This can occur because the unperturbed system's separatrix is not an orbit of the perturbed system.

The unperturbed system's separatrix is important to the approximation, however, because the approximation is based on the dynamics of the unperturbed system. Its variables (e.g., the averaged variables $(\bar{r},\bar{\varphi})$) must be interpreted in terms of the unperturbed system. For example, the value $k(\bar{r}) = 1$ corresponds to a separatrix in the perturbed (averaged) system just as $k(r) = 1$ indicates a separatrix in the unperturbed system. Thus, the problems in the averaging procedure noted in section 3.2 arise in a neighborhood of the unperturbed system's separatrix.

For the rest of this chapter, we shall use the term "separatrix" to mean the separatrix in the unperturbed system, not in the actual (perturbed) system.

The concept of separatrix crossing in a perturbed system is not new. In fact, this has been explored for many years in slowly varying Hamiltonian systems from fields such as particle physics, celestial mechanics, etc. Henrard [Hen82] has studied capture into resonance for the slowly varying pendulum equation. Cary, Escande, and Tennyson [Car86] have investigated adiabatic invariant changes for general slowly varying Hamiltonian systems. Henrard [Hen] has written a treatise of the adiabatic invariant in classical mechanics.

These works have dealt with perturbed systems which are Hamiltonian. Their goal is the accurate prediction of changes in the adiabatic invariant J (see section 2.3) after a separatrix crossing. They are able to show that the change in J is sensistive to the angle φ at entry into the boundary layer. Moreover, J changes by $O(\epsilon)$ for most φ values but changes by O(1) for others. They also show that the probability of capture into a loop is the same for the left and right loops of the separatrix of region IV (of Fig.2.1) since the loops are symmetric with equal area. (More generally, they show that the probability of capture is proportional to the area of the loop.) While these results are interesting and do relate to eq.(0.1) through our variable r, the approach that is used to find the change in J is not suited for modelling the flow of a particular orbit.

Since the problem with averaging near a separatrix involves the O(1) instantaneous frequency becoming zero, it is also possible to view separatrix crossing as a resonance problem. In this way, the separatrix b.l. is simply a resonance b.l. Resonance b.l.s are

discussed in the texts by Kevorkian and Cole [Kev81] and Sanders and Verhulst [San85]. In the boundary layer, the perturbed system is expanded in a Taylor series using an appropriate normal variable. The solution to the truncated b.l. equations can then be matched to the solution outside the b.l. It is this approach which is used in modelling separatrix crossing in section 9.2.

Finally, we wish to note how the averaging procedure fails on a separatrix. It is not necessary that the generating functions in the transformation become unbounded. For example, in the disappearing separatrix example of chapter 7, the generating function $w_1(\bar{r},\varphi)$ remains bounded at $k = 1$. The averaged equations, however, do not satisfy the uniqueness condition for differential equations (i.e., they are not Lipschitz on the separatrix). Hence, solutions to the averaged equations are no longer unique: once on the separatrix, a solution may remain there indefinitely.

From a practical standpoint, the lack of uniqueness of the averaged equations on the separatrix is not a problem, at least to numerical simulations of the averaged equations. Because K approaches infinity very slowly (see Table 1.3), the computer does not compute very high values for K (the true high value of K being the source of the averaging problem). It is easily shown that for $k = 1 - 10^{-100}$, the value of K is approximately 116.17 which is not very high compared to the highest number that the computer can use. Since most computers do not have the precision of 100 floating point

decimal places anyway, the value of K at the separatrix is calculated to be on the order of 10.

Therefore, the instantaneous frequency $\frac{a}{4K}$ is never computed to be very close to zero, which results in solutions being uniquely prescribed. These solutions correspond to the separatrix crossing condition that all orbits cross the separatrix instantaneously, i.e., they lie on the separatrix for only one instant of time. Furthermore, this poor numerical approximation of K near the separatrix permits φ to be defined by eq.(2.21) everywhere in the phase space. Thus, the averaging model is well-defined numerically, even close to the separatrix.

9.2 Separatrix crossing model

In this section, we derive a separatrix crossing model from eq.(0.1) which is valid in a boundary layer about the separatrix. It is preferable to consider the two different separatrices separately. Thus, we will model the separatrix in region IV (of Fig.2.1). For region VIII (of Fig.2.1), one would use the transformed system variables (w,k_2) to model the separatrix crossing. This case follows analogously.

Since $k^2 = 1$ corresponds to the separatrix for any r and τ, we take (k^2,u) as variables in the boundary layer. For convenience, define m by:

$$m = k^2 \tag{9.1}$$

The variable m measures distances normal to the separatrix; the variable u measures distances along the separatrix, see Fig.9.1. The separatrix boundary layer, then, is defined to be a small neighborhood about $m = 1$.

The variational equation for u is given by (2.20c); the variational equation for m is found from eqs.(2.20a), (2.6c), and (9.1). The equations are expressed in the compact notation of (9.2):

$$m' = \epsilon F_1(m,u,\tau) \tag{9.2a}$$

$$u' = a(m,\tau) + \epsilon F_2(m,u,\tau) \tag{9.2b}$$

where

$$a(m,\tau) = \left[\frac{\alpha}{1-2m} \right]^{1/2}$$

$$F_1(m,u,\tau) = - g (1-2m)^2 \frac{\sqrt{2m\beta}}{\alpha} cn'$$
$$+ m (1-2m) \frac{1}{\alpha} \frac{d\alpha}{d\tau} \left[(2m-1) sn^2 - 1 \right]$$
$$+ m (1-2m) \frac{1}{\beta} \frac{d\beta}{d\tau} \left[m (cn^4 - 1) + 1 \right]$$

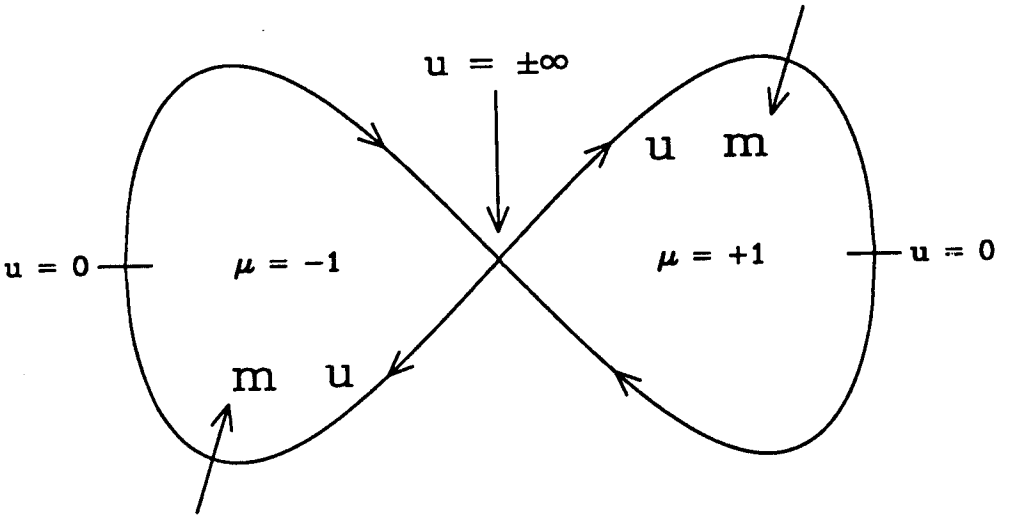

Fig.9.1 The boundary layer variables (m,u). The variable m measures normal to the separatrix; the variable u measures along the separatrix. m = 1 on the separatrix, and m > 1 on the inside. The saddle is indicated by u = ± ∞, with u = 0 being the furthest from the saddle.

$$F_2(m,u,\tau) = g\,(1-2m)\,\frac{1}{\alpha}\,\frac{\sqrt{\beta}}{\sqrt{2m}}\left[cn - 2m\,(1-2m)\,cn'\,\frac{du}{dm}\right]$$
$$+ \frac{1}{2}\,\frac{1}{\alpha}\,\frac{d\alpha}{d\tau}\,(1-2m)\left[\frac{cn\,cn'}{dn^2} - 4\,m\,\frac{du}{dm}\left[1 + (1-2m)\,sn^2\right]\right]$$
$$+ \frac{1}{2}\,\frac{1}{\beta}\,\frac{d\beta}{d\tau}\,m\left[\frac{(cn^2+1)\,cn\,cn'}{dn^2} + 4\,(1-2m)\,\frac{du}{dm}\left[m\,(cn^4 - 1) + 1\right]\right]$$

Now consider an $O(\delta)$ neighborhood of $m = 1$, where $\delta \ll 1$, and introduce the boundary layer variable σ:

$$m = 1 + \delta\,\sigma \tag{9.3}$$

We now substitute (9.3) into eqs.(9.2) and expand in a Taylor series about $m = 1$, i.e., $\delta = 0$:

$$\delta\,\sigma' = \epsilon\left[F_1(1,u,\tau) + \delta\,\sigma\,\left.\frac{\partial F_1}{\partial m}\right|_{m=1} + \frac{1}{2}\,\delta^2\,\sigma^2\,\left.\frac{\partial^2 F_1}{\partial m^2}\right|_{m=1} + \cdots\right] \tag{9.4a}$$

$$u' = a(1,\tau) + \delta\,\sigma\,\left.\frac{\partial a}{\partial m}\right|_{m=1} + \frac{1}{2}\,\delta^2\,\sigma^2\,\left.\frac{\partial^2 a}{\partial m^2}\right|_{m=1} + \cdots$$
$$+ \epsilon\left[F_2(1,u,\tau) + \delta\,\sigma\,\left.\frac{\partial F_2}{\partial m}\right|_{m=1} + \frac{1}{2}\,\delta^2\,\sigma^2\,\left.\frac{\partial^2 F_2}{\partial m^2}\right|_{m=1} + \cdots\right] \tag{9.4b}$$

Here δ is a free parameter and can be chosen in any way we wish. Since the problem also involves ϵ, we choose $\delta = \epsilon$ for convenience in what follows. Eqs.(9.4) become:

$$\sigma' = F_1(1,u,\tau) + \epsilon\,\sigma\,\left.\frac{\partial F_1}{\partial m}\right|_{m=1} + \frac{1}{2}\,\epsilon^2\,\sigma^2\,\left.\frac{\partial^2 F_1}{\partial m^2}\right|_{m=1} + \cdots \tag{9.5a}$$

$$(9.5b)\quad u' = a(1,\tau) + \epsilon \left[\sigma \left.\frac{\partial a}{\partial m}\right|_{m=1} + F_2(1,u,\tau)\right] + \epsilon^2 \left[\frac{1}{2}\sigma^2 \left.\frac{\partial^2 a}{\partial m^2}\right|_{m=1} + \sigma \left.\frac{\partial F_2}{\partial m}\right|_{m=1}\right] + \cdots$$

In eqs.(9.5), one must remember than u depends on k and therefore on m. Hence, the derivatives of u with respect to m are computed to be:

$$(9.6a)\quad \frac{du}{dm} = \frac{du}{dk}\frac{dk}{dm} = \frac{1}{2k}\frac{du}{dk} = \frac{1}{2\sqrt{m}}\frac{du}{dk}$$

$$(9.6b)\quad \frac{d^2u}{dm^2} = \frac{1}{4m}\frac{d^2u}{dk^2} - \frac{1}{4m\sqrt{m}}\frac{du}{dk}$$

$$(9.6c)\quad \frac{d^iu}{dm^i} = \sum_{n=1}^{i} b_n(m)\frac{d^nu}{dk^n}$$

where $b_n(m)$ depends only on m. We have noted that $\frac{du}{dk}$ is nonperiodic; $\frac{d^nu}{dm^n}$ is similarly nonperiodic.

Furthermore, $\frac{d^nu}{dm^n}$ is unbounded at m = 1. This can be seen by evaluating $\frac{d^nu}{dm^n}$ by differentiating under the integral sign in the defining equation for u:

$$(9.7)\quad u = F(\theta,m) = \int_0^{\theta} \frac{d\psi}{\sqrt{1 - m\sin^2(\psi)}}$$

Then setting m = 1 results in the formula:

$$(9.8)\quad \frac{d^i u}{dm^i} = \frac{(2i)!}{4^i\, i!} \int_0^u \sinh^{2i}(u)\, du$$

$$= d_0\, u + \sum_{n=1}^{i} d_n \sinh^{2n-1}(u) \cosh(u)$$

where d_n are simply numbers

Formula (9.8) shows $\frac{d^i u}{dm^i}$ as exponentially unbounded for large u. Knowing this result, we see that eqs.(9.5) can be an asymptotic series in ϵ only for:

$$(9.9)\qquad |u| \leq u_{max} < \infty$$

so that the $\frac{d^i u}{dm^i}$ terms arising in the series are always bounded. The condition that u satisfy (9.9) restricts the validity of eqs.(9.5) to a region in the separatrix boundary layer away from the saddle point (where $u \to \pm \infty$).

Under the restriction of (9.9), it is valid to truncate eqs.(9.5):

$$(9.10a)\qquad \sigma' = F_1(1,u,\tau)$$

$$(9.10b)\qquad u' = a(1,\tau)$$

In eqs.(9.10), we have assumed $a(1,\tau) = O(1)$. If this is not the case, then the u equation must be truncated after the $O(\epsilon)$ term. We do not discuss this case.

The solution of (9.10b) is easily found using the two-variable expansion method or the method of multiple scales. We look for a solution in the form $u = u(t,\tau)$ where $\tau = \epsilon t$. The solution for u is found by:

$$u' = \frac{du}{dt} = \frac{\partial u}{\partial t} + \epsilon \frac{\partial u}{\partial \tau} = a(1,\tau) + O(\epsilon) \tag{9.11a}$$

$$\frac{\partial u}{\partial t} = a(1,\tau) \tag{9.11b}$$

$$u = a(1,\tau)\ (t-t_*) + u_* \tag{9.11c}$$

where t_* and u_* are constants. With the solution for u known, eq.(9.10a) can be solved by quadrature:

$$\sigma = \int_{t_*}^{t} F_1(1, a(1,\tau)\ (t-t_*) + u_*, \tau)\ dt + \sigma_* \tag{9.12}$$

The values of x and x' are easily determined from σ and u. First, note that:

$$k^2 = m = 1 + \epsilon\ \sigma \tag{9.13}$$

Using (2.6c), we find the amplitude r in terms of k^2:

$$r^2 = \frac{\alpha}{\beta} \frac{2k^2}{1 - 2k^2} \tag{9.14}$$

Expressions for x and x' may then be found using eqs.(2.6):

$$x = \mu\, r\, cn(u,k) \tag{9.15a}$$

$$x' = \mu\, r\, a\, cn'(u,k) \tag{9.15b}$$

$$\text{where } a^2 = \alpha + \beta\, r^2 \text{ and } \mu = \pm 1$$

The choice for the sign parameter μ is determined upon entry into the boundary layer. For entries from the right side (i.e., $x > 0$), $\mu = +1$; from the left side (i.e., $x < 0$), $\mu = -1$.

The inverse transformation, from (x,x') to (σ,u), is found by first solving for σ in (9.13) and then for u in (9.15a). In solving for σ, it is assumed that the value of k^2 for (x,x',t) is known (e.g., from the averaging model). The value of u is chosen to be its *principal value*, i.e. u lies within the range given below:

$$-K(k) \leq u < K(k) \tag{9.16}$$

Using (9.16), each point (σ,u,t,μ) corresponds to exactly one point (x,x',t).

We now explicitly characterize the boundary layer. A system point (x,x',t) lies in the boundary layer if, when expressed as (σ,u,t,μ), its σ value satisfies:

$$|\sigma| < \sigma_{bl} \tag{9.17}$$

where σ_{bl} is the half-width of the b.l. The value of σ_{bl} is rather arbitrary, cf. eq.(9.13) where $\epsilon\,\sigma_{bl}$ measures the half-thickness of the b.l. in terms of the quantity m. For a given ϵ, the value of σ_{bl} is chosen to be small enough so that the Taylor series approximations for (σ',u') in the b.l., eqs.(9.5), remain valid. In addition, the value of σ_{bl} must be large enough so that the numerical integration of the averaging model does not step over the b.l without passing through it. The point at which an orbit enters the b.l. determines the values of (σ_*,u_*,t_*,μ). The separatrix crossing model then determines $u(t;t_*,u_*)$ and $\sigma(t;\sigma_*,t_*,u_*)$ using (9.11c) and (9.12).

There are two different ways an orbit can leave the b.l. The most common is that σ no longer satisfies (9.17). The other way arises from insuring that (σ,u,t,μ) corresponds to exactly one (x,x',t) point. This is guaranteed when u satisfies (9.16). But the solution for u given by (9.11c) may not satisfy (9.16) at some time $t_1 > t_*$. This corresponds geometrically to a motion which either (a) passes across the x-axis close to the saddle inside the separatrix, or (b) passes across the y-axis close to the saddle outside the separatrix. If this does occur, then we treat the system point at

$t = t_1$ as a *new entry into the b.l.* (although the point may always satisfy (9.17)). The values $(\sigma_*, u_*, t_*, \mu)$ are re-computed at $t = t_1$ and the solutions (9.11c) and (9.12) are used again.

If we did not treat u in this way, we could not uniquely specify σ'. The expression for σ' is a non-periodic function of u because it is computed from a Taylor series of $F_1(m,u,\tau)$ (cf. eq.(9.2a)) about $m = 1$, the separatrix. On the separatrix, the elliptic functions appearing in F_1 are non-periodic (or, equivalently, they have infinite period). Thus, allowing two different u values, u_1 and u_2, to specify the same point in phase space would give two <u>different</u> values for σ'.

The separatrix crossing model based on eqs.(9.10) is valid only under the restriction of (9.9) (insuring that the series in eqs.(9.5) are asymtptotic in ϵ). Therefore, we cannot use these equations when $|u|$ is arbitrarily large, i.e., in a neighborhood of the saddle point itself. Near the saddle, another model must be used that is not dependent on the Taylor series expansions in eqs.(9.5). For this model, we use eq.(0.1) directly. First, scale x by $x(t) = \delta\, \hat{x}(\tau)$ where $\delta << 1$ and $\tau = \epsilon t$. Then eq.(0.1) becomes:

$$\epsilon^2\, \hat{x}_{\tau\tau} + \alpha\, \hat{x} + \delta^2\, \hat{x}^3 + \epsilon\, g(\delta\, \hat{x},\ \epsilon\, \delta\, \hat{x}', \tau) = 0 \qquad (9.18)$$

We assume that $\hat{x}_{\tau\tau}$ is $O(1/\epsilon^2)$. Then to first order, eq.(9.18) becomes:

$$\epsilon^2 \hat{x}_{\tau\tau} + \alpha x = 0 \tag{9.19}$$

We then can apply the WKB method [Ben78,Sim86] to (9.19) to find $\hat{x}$ to leading order:

$$\hat{x} = \hat{x}(\tau_*) \cosh\left(\frac{\ell(\tau)}{\epsilon}\right) + \epsilon \frac{\hat{x}_\tau(\tau_*)}{\sqrt{-\alpha(\tau_*)}} \sinh\left(\frac{\ell(\tau)}{\epsilon}\right) \tag{9.20}$$

$$\text{where } \ell(\tau) = \int_{\tau_*}^{\tau} \sqrt{-\alpha(\tau)}\, d\tau$$

(valid for τ such that $\alpha(\tau) < 0$)

In (9.20), τ_* is a constant at which time $\hat{x}$ and $\hat{x}_\tau$ are known (usually taken to be at the entry point of the saddle neighborhood boundary layer). The solution in (9.20) is well-defined since the system lies in region IV (of Fig.2.1) where $\alpha < 0$. The values of x and x' are given in (9.21):

$$x = \delta \hat{x} \quad \text{and} \quad x' = \epsilon \delta \hat{x}_\tau \tag{9.21}$$

Thus, the separatrix crossing model consists of two parts: (1) away from the saddle point, where (9.11c) and (9.12) are used; and (2) near the saddle, where eqs.(9.20) and (9.21) are used. The time

taken to cross through the separatrix boundary layer is dependent on the angle u_* at entry into the b.l. This property is in contrast to the averaging model of chapter 7 in which it was assumed that motions instantaneously crossed the separatrix.

The separatrix crossing model is an analytic approximation for the flow near the separatrix, which depends on the three parameters σ_*, u_*, and t_*. It is characterized by its action on an orbit as it crosses through the b.l. Viewed in this way, the model is a 2-dimensional map from (u_*, t_*) at $\sigma = \sigma_{bl}$ (i.e., at entry) to (u_{out}, t_{out}) at $\sigma = -\sigma_{bl}$ (i.e., at exit). Simply put, *the model determines the time and change in phase within the b.l. for a system point.*

9.3 Application to the periodically disappearing separatrix system

As an example of the separatrix crossing model, we apply the method outlined in section 9.2 to the disappearing separatrix system of chapter 7 ($\alpha = -\cos(\tau)$, $\beta = 1$, $g = 0$). We find F_i and a in (9.2) to be:

$$(9.22a)\quad F_1(m,u,\tau) = m\,(1-2m)\,\tan\tau\left[2\,(1-m) + (2m-1)\,cn^2\right]$$

$$(9.22b)\quad F_2(m,u,\tau) = \frac{1}{2}\,(1-2m)\,\tan\tau\left[\frac{sn\,cn}{dn} + 4\,m\,\frac{du}{dm}\,(2\,dn^2 - cn^2)\right]$$

$$(9.22c)\quad a = \left[\frac{\cos\tau}{2m-1}\right]^{1/2}$$

From (9.22), we then calculate the terms appearing in eqs.(9.5):

(9.23a) $F_1(1,u,\tau) = -\tan\tau\,\mathrm{sech}^2$

(9.23b) $\left.\frac{\partial F_1}{\partial m}\right|_{m=1} = \frac{1}{2}\tan\tau\left[3 + \mathrm{sech}^2\,(u\tanh - 9)\right]$

(9.23c) $\left.\frac{\partial^2 F_1}{\partial m^2}\right|_{m=1} = \frac{1}{16}\tan\tau\left[-64 + 187\tanh^2 + 67\,u\,\mathrm{sech}^2\tanh + 2u^2\mathrm{sech}^2(1 - 3\tanh^2) - 2\sinh^2\tanh^2\right]$

(9.23d) $a(1,\tau) = \sqrt{\cos\tau}$

(9.23e) $\left.\frac{\partial a}{\partial m}\right|_{m=1} = -\sqrt{\cos\tau}$

(9.23f) $\left.\frac{\partial^2 a}{\partial m^2}\right|_{m=1} = \frac{3}{2}\sqrt{\cos\tau}$

(9.23g) $F_2(1,u,\tau) = -\frac{1}{2}\tan\tau\left[2\tanh - u\,\mathrm{sech}^2\right]$

(9.23h) $\left.\frac{\partial F_2}{\partial m}\right|_{m=1} = \frac{1}{16}\tan\tau\left[-32\tanh + 13u + 3\sinh\cosh - 21u\tanh^2 - 4u^2\mathrm{sech}^2\tanh - \tanh\sinh^2\right]$

where the argument for all hyperbolic functions is u

We see that the expressions in (9.23c) and (9.23h) are exponentially unbounded in u. Eqs.(9.9) become:

(9.24a) $\sigma' = -\tan\tau\,\mathrm{sech}^2(u)$

(9.24b) $u' = \sqrt{\cos\tau}$

The solutions to eqs.(9.24) are then:

$$\sigma = -\frac{\tan\tau}{\sqrt{\cos\tau}}\left[\tanh(u) - \tanh(u_*)\right] + \sigma_* \tag{9.25a}$$

$$u = \sqrt{\cos\tau}\,(t - t_*) + u_* \tag{9.25b}$$

It is also possible to explicitly find $\ell(\tau)$ in eq.(9.20) for the near-saddle separatrix crossing model. Using the substitution:

$$\tau = 2\sin^{-1}(\hat{k}\,\mathrm{sn}(z,\hat{k})) \tag{9.26a}$$

$$\hat{k}^2 = \frac{1}{2} \tag{9.26b}$$

$\ell(\tau)$ is found using elliptic functions! The solution is expressed as:

$$\ell(\tau) = 2\sqrt{2}\left[E(z) - E(z_*) + \frac{1}{2}(z_* - z)\right] \tag{9.27a}$$

$$z = \mathrm{sn}^{-1}(\sqrt{2}\,\upsilon\,|\sin\tfrac{\tau}{2}|) \tag{9.27b}$$

$$\text{where } \upsilon = \mathrm{sign}(\sin\tau)$$

in which z is the incomplete elliptic integral of the first kind and the modulus is given by (9.26b).

Recall that the crossing dynamics depend on σ_*, u_* and t_*, the b.l. entry values of σ, phase and time. For the purposes of numerical computation, we will now fix σ_* and t_* and compute the time taken to cross through the boundary layer for a set of points on the boundary layer edge (which are specified by u_*). We choose $\epsilon = 0.1$

for convenience. We found that for this ϵ, $\sigma_{bl} = 0.4$ works well numerically. Initially, all points are located on the same instantaneous energy curve (determined by $\sigma_* = \sigma_{bl}$) located inside the right separatrix loop.

We expect that some orbits will be carried near the instantaneous unstable manifold of the separatrix and quickly moved away from the saddle and through the b.l. We also expect that some orbits will be carried near the instantaneous stable manifold of the separatrix. These orbits will approach the saddle very closely, remaining there until the separatrix shrinks by them. For these orbits, the time taken to cross through the b.l. will be much longer.

A graph of the crossing time, computed without the near-saddle approximation, vs. the initial angle u_* for $t_* = 5.0$ is given in Fig.9.2. In Fig.9.3, the near-saddle b.l. approximation has been included in computing the crossing time for the same initial data. The near-saddle b.l. width associated with eqs.(9.21) was taken to be $0.05\sqrt{\cos(\tau)}$, which changes with the size of the separatrix. This was done so that the near-saddle b.l. model applies only near the saddle point for any size separatrix.

Both figures bear out our expectations. We see that including the near-saddle approximation does not affect the graph much, although the crossing times for u_* which took a long time to cross without the near-saddle model have been elongated slightly. This shows that the near-saddle approximation is not as important to the

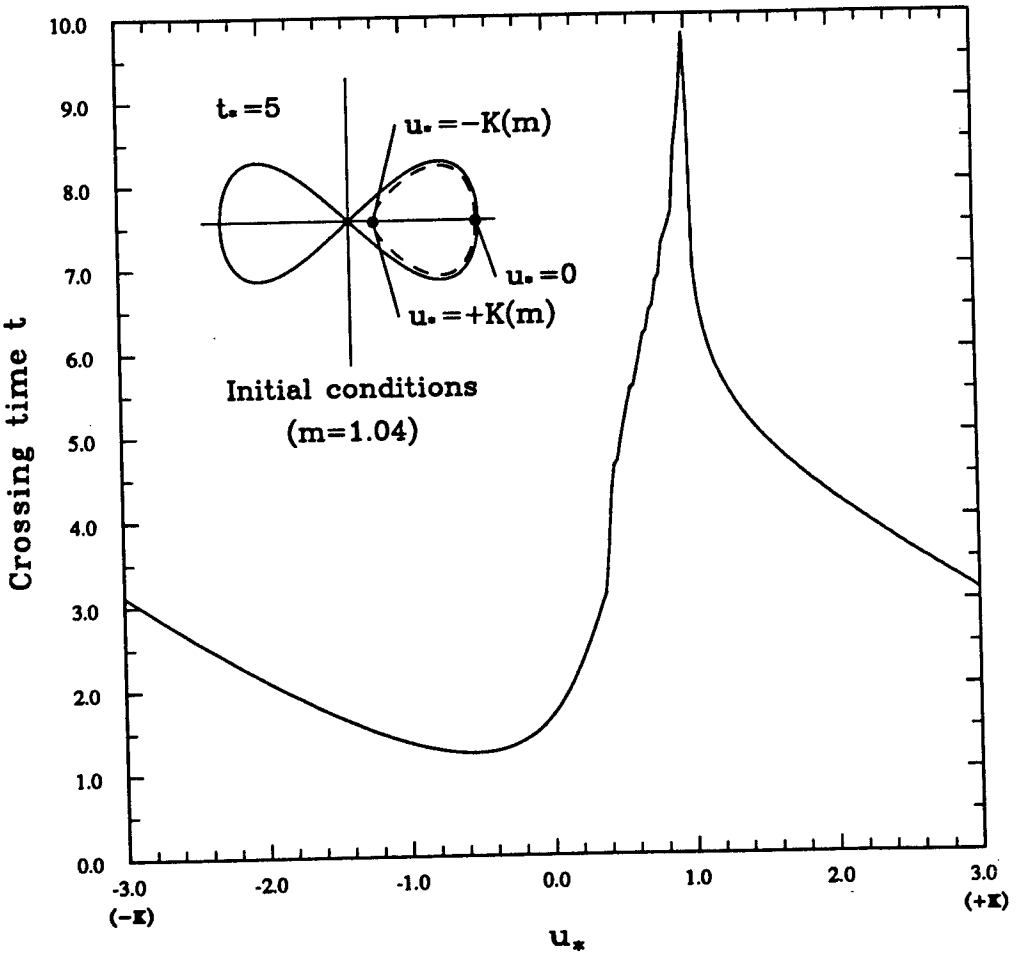

Fig.9.2 Separatrix crossing time, computed without the near-saddle approximation, for a set of points located inside the right separatrix loop defined by $\sigma_* = \sigma_{bl} = 0.4$, $t_* = 5.0$, and $\epsilon = 0.1$. This corresponds to m = 1.04 initially, see the initial condition inset. Points exit the b.l. when $\sigma = -\sigma_{bl}$. Points carried near the unstable manifold cross quickly (i.e., in small times); those carried near the stable manifold cross slowly (i.e., in large times).

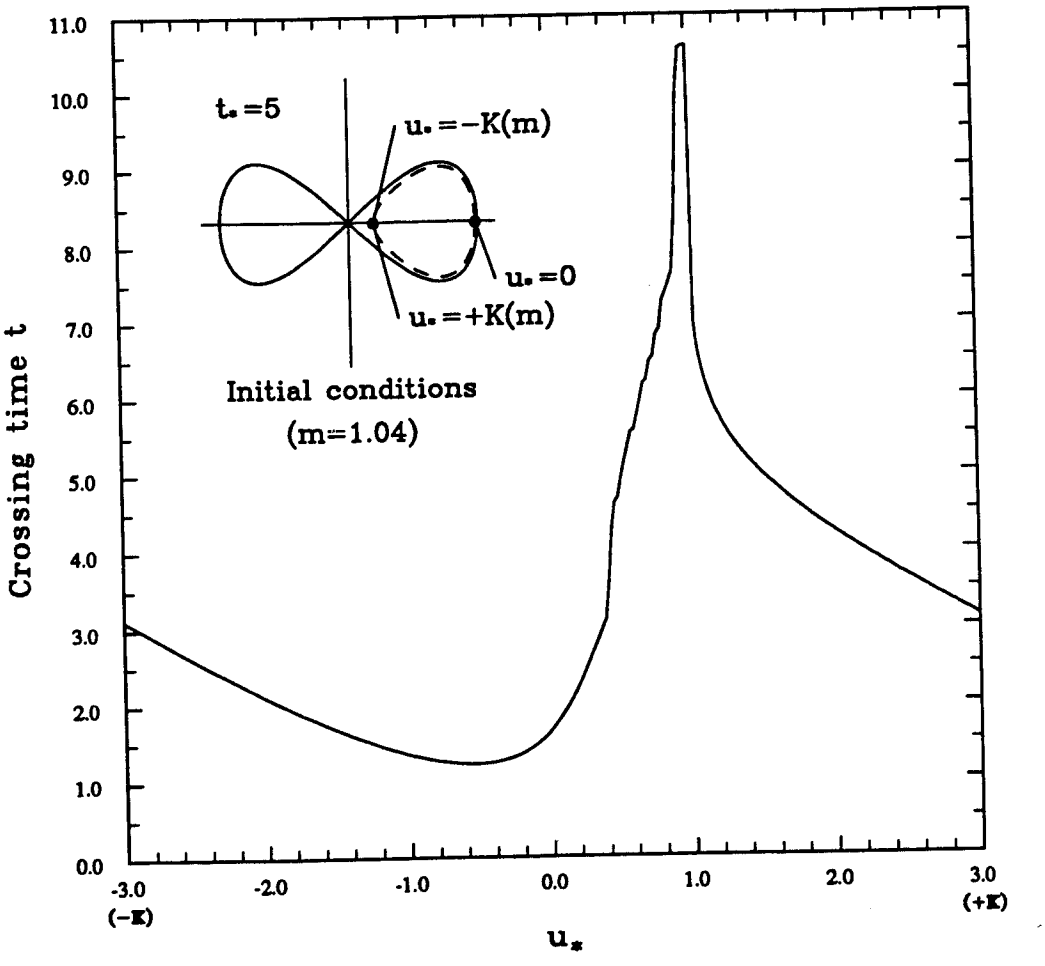

Fig.9.3 Separatrix crossing time, computed with the near-saddle approximation, for a set of points located inside the right separatrix loop defined by $\sigma_* = \sigma_{bl} = 0.4$, $t_* = 5.0$, and $\epsilon = 0.1$. This corresponds to m = 1.04 initially, see the initial condition inset. Points exit the b.l. when $\sigma = -\sigma_{bl}$. Points carried near the unstable manifold cross quickly (i.e., in small times); those carried near the stable manifold cross slowly (i.e., in large times). This figure is qualitatively the same as Fig.9.2.

qualitative behavior of the model as the approximation of crossing the separatrix away from the saddle.

For comparison of the model with the actual dynamics, we numerically integrated the same set of initial conditions. Using the energy h in eqs.(2.7) and (2.8), we computed a "fictitious" k^2 value which was used to monitor the system point. Using (9.13), we calculated σ and checked for exit of the boundary layer. The result is Fig.9.4, which is very similar to Figs.9.2 and 9.3. Fig.9.4 verifies the qualitative accuracy of the separatrix crossing model. Finally, we note that the averaging model predicts a single crossing time, t = 2.048, for each point u_*. This does not compare well with Fig.9.4, except for a small interval of u_*.

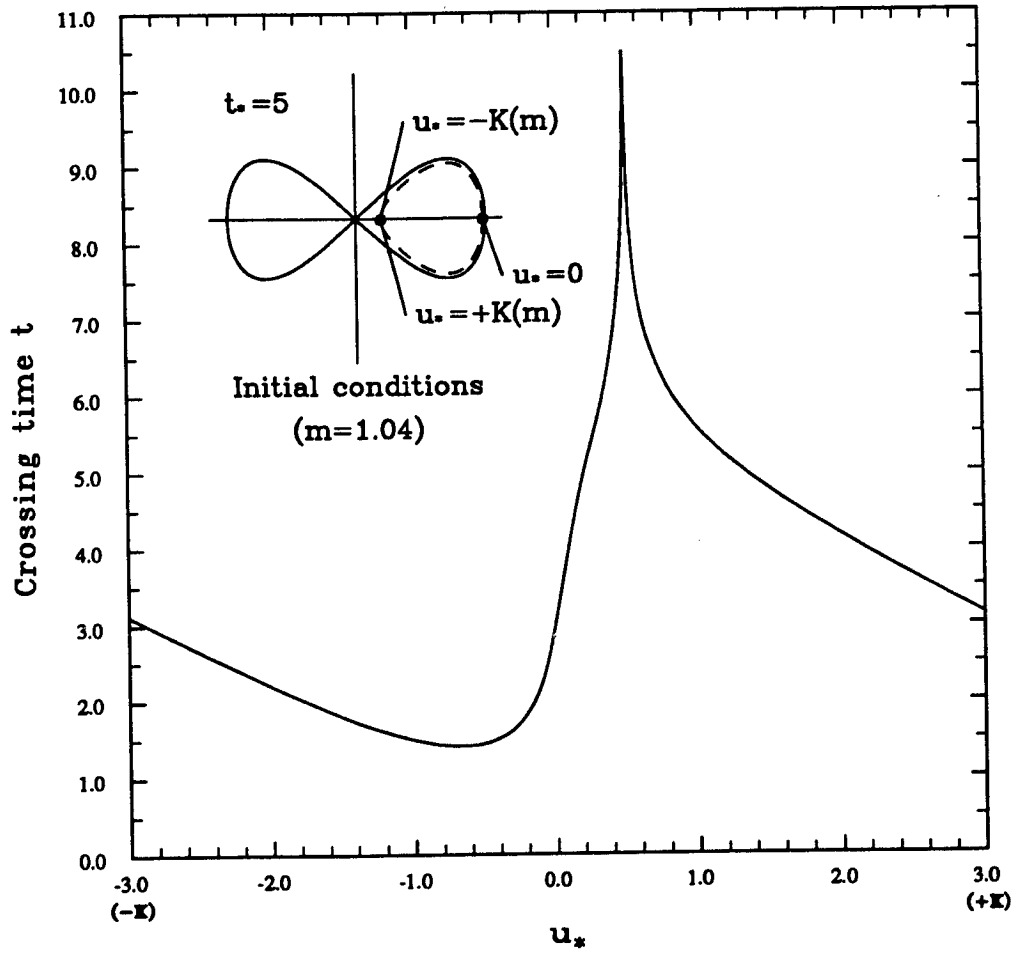

Fig.9.4 Separatrix crossing time, computed using numerical integration, for a set of points located inside the right separatrix loop defined by $\sigma_* = \sigma_{bl} = 0.4$, $t_* = 5.0$, and $\epsilon = 0.1$. This corresponds to m = 1.04 initially, see the initial condition inset. Points exit the b.l. when $\sigma = -\sigma_{bl}$. Points carried near the unstable manifold cross quickly (i.e., in small times); those carried near the stable manifold cross slowly (i.e., in large times). This figure compares well with Fig.9.2.

10. The forced Duffing equation

In chapters 3-9, we considered perturbations g which did not depend explicitly on the time t (but g could depend on $\tau = \epsilon t$, see chapter 3). Now, we shall consider the case in which g does exhibit explicit t dependence. The averaging method is again applied using a near-identity transformation; however, the method relies on Fourier series expansions which limits the usefulness of using cn(u,k) as the solution to the unperturbed system in each region of the α-β parameter plane (Fig.2.1). Furthermore, a computer program for this case was not attempted because it would need to be able to generate Fourier series expansions of products of cn^n, cn', and Z. Since the Fourier coefficients must be found using contour integration techniques in the complex plane (see the derivation of cn coefficients in section 1.6), such a computer program would be an enormous undertaking.

Still, the averaging method can be applied explicitly by hand, at least for simple problems. The best way to show its application is by example. Hence, we will consider the forced Duffing equation, i.e., small harmonic forcing of eq.(0.1) for fixed α and β.

First, we will determine resonance zones and compare resonances in the nonlinear system regions II and III with the linear system region I (of Fig.2.1). Then, we apply the method of averaging inside

and outside these resonance zones, and qualitatively predict the behavior of the original system. Next, we show the equivalence of the subharmonic Melnikov method approach [Guc86,Gre83,San85]. Finally, we qualitatively predict the dynamics of the forced Duffing equation with small damping.

10.1 Resonance Zones

We consider the forced Duffing equation given by:

$$x'' + \alpha x + \beta x^3 - \epsilon f \cos(\omega t) = 0 \tag{10.1}$$

We take α, β, f, and ω as parameters which do not depend on t in any way. From eq.(10.1), we see that the perturbation g depends explicitly on t. The phase space for (10.1) is $(x,x',t) \in \mathbb{R}^2 \times S^1$. We define projective phase space to be the projection from $\mathbb{R}^2 \times S^1$ onto $\mathbb{R}^2$. We shall restrict attention to the parameter range

$$\alpha \geq 0 \quad \text{and} \quad \beta \geq 0 \tag{10.2}$$

which corresponds to regions I, II, and III of Fig.2.1. This is done for convenience, since in these regions the unperturbed system (taking $\epsilon = 0$ in (10.1)) has cn(u,k) as its solution where

$$0 \leq k^2 \leq \frac{1}{2} \tag{10.3}$$

so that the Fourier series of cn(u,k) given by (1.42b) holds. For other regions of Fig.2.1, one must use the transformed variables (either (v,k_1) or (w,k_2), see section 1.2) because Fourier series do not transform to Fourier series under modulus transformations.

We note that the Fourier series of cn(u,k) given by (1.42b) contains expressions of the form $\frac{0}{0}$ when k = 0. This is because K'(0) = ∞ making the sech function zero and $\frac{1}{k}$ appears in (1.42b). Since cn(u,k) for k = 0 is simply cos(u), these indeterminate forms are fully known. For ease of writing the Fourier series expansion of cn(u,k), then, we use (10.4).

(10.4a) $$cn(u,k) = \sum_{n=1}^{\infty} c_n \cos(\gamma_n u)$$

(10.4b) $$\text{where } \gamma_n = \frac{(2n-1)\pi}{2K} \ , \ u = a\ t + u_0$$

and

(10.4c) $$c_n = \frac{\pi}{kK} \operatorname{sech}(\gamma_n K') \quad \text{for } k > 0$$

$$\text{where } K' = K(k') \ , \ k'^2 = 1 - k^2$$

$$c_1 = 1 \ , \ c_n = 0 \quad n > 1 \quad \text{for } k = 0$$

From (10.4), we find cn'(u,k):

(10.5) $$cn' = \frac{\partial cn}{\partial u} = - \sum_{n=1}^{\infty} \gamma_n c_n \sin(\gamma_n u)$$

Using the Fourier series expansion for cn', we are able to express the variational equation for r (eq.2.20a) as:

(10.6)
$$\begin{aligned} r' &= -\epsilon \frac{1}{a} g\, cn' = \epsilon \frac{1}{a} f\, cn' \cos(\omega t) \\ &= -\epsilon \frac{f}{a} \sum_{n=1}^{\infty} \gamma_n c_n \sin(\gamma_n u) \cos(\omega t) \\ &= -\frac{\epsilon}{2} \frac{f}{a} \sum_{n=1}^{\infty} \gamma_n c_n \left[\sin(\gamma_n u + \omega t) + \sin(\gamma_n u - \omega t)\right] \\ &= -\frac{\epsilon}{2} \frac{f}{a} \sum_{n=1}^{\infty} \gamma_n c_n \left[\sin(\psi_n^+) + \sin(\psi_n^-)\right] \\ &\equiv \epsilon F_1(r, \psi_n^{\pm}) \end{aligned}$$

where $\psi_n^{\pm} = \gamma_n u \pm \omega t$

F_1 depends on r via a, γ_n, c_n, k, K, and K'. From (10.6), we see that u and t reside on a two-torus. If the periods of cn' and cos are commensurate, then periodic motions of r exist (this defines a resonance); if they are incommensurate then r is quasi-periodic. The time derivative of each γ_n and $\psi_n^{\pm}$ is found to be:

(10.7)
$$\begin{aligned} \gamma_n' &= -(2n-1) \frac{\pi}{2} \frac{1}{K^2} \frac{dK}{dk} k' \\ &= -\gamma_n \frac{1}{K} \frac{dK}{dk} k' \end{aligned}$$

$$(10.8)\quad (\psi_n^{\pm})' = \gamma_n' u + \gamma_n u' \pm \omega$$
$$= \frac{1}{K}\frac{dK}{dk} k' (-\gamma_n u + \gamma_n u) + 4K\gamma_n \varphi' \pm \omega$$
$$= 4K\gamma_n \varphi' \pm \omega$$
$$= a\gamma_n \pm \omega + \epsilon F_2(r,\varphi,t)$$
$$\text{where } \varphi' = \frac{a}{4K} + \epsilon F_2(r,\varphi,t)$$

In (10.8), we have used (10.7), (2.22a), and (2.23). We note that both F_1 and F_2 are bounded in the regions specified by (10.2) and so (10.8) represents an asymptotic series in ϵ. We can then form the truncated system by ignoring the $O(\epsilon)$ terms if we assume either (1) $\omega = O(1)$ or (2) $a = O(1)$:

$$(10.9)\quad (\psi_n^{\pm})' = a\gamma_n \pm \omega$$
$$= \Omega_n^{\pm}$$

Since g is to depend on t and not ϵt, we must take $\omega = O(1)$, and (10.9) is asymptotically valid.

Taken together, eqs.(10.6) and (10.9) form an infinite dimensional system of differential equations of the variables $(r,\psi_n^{\pm})$. It is these equations which will determine the dynamics of (10.1). Note that the $(\psi_n^{\pm})'$ equations contain the O(1) piece of φ' equation so that the entire φ' equation only provides new information of $O(\epsilon)$. The variational equation for φ is not shown because writing this as a Fourier series involves knowing the Fourier series of Z cn' and cn^3

which have not been determined (but could be found, in principle, using contour integration, see section 1.6).

We define an exact resonance to be a value of $\Omega_n^{\pm} = 0$. This condition occurs for a $\tau_n \pm \omega = 0$. Without loss of generality, we take $\omega > 0$. Then resonances only occur for $\Omega_n^{-} = 0$ where:

$$\omega = a\,\tau_n = (2n-1)\,\frac{\pi}{2}\,\frac{a}{K} \tag{10.10}$$

We will now examine this resonance condition more closely in each of the regions I, II, and III.

In region I, $k = 0$, so that (10.10) becomes $\omega = (2n-1)\,\sqrt{\alpha}$ independent of the amplitude r. Thus, the entire projective phase space experiences resonance if (10.10) holds. For $n = 1$, this result agrees with the linear theory. However, linear theory does not predict a countably infinite number of resonant values ω, occurring at the subharmonic frequencies ($\sqrt{\alpha}$ is the natural frequency). If we investigate the Fourier coefficients c_n for this case (eq.(10.4)), we find that all the c_n are zero at each subharmonic ω. These are referred to in linear theory as higher order resonances because they appear as resonances only at higher orders of ϵ.

A graph of r vs. ω of the resonant condition (10.10) for region I is given in Fig.10.1a. Since the resonant condition is independent of r, the graph consists just of straight lines. Curves for the subharmonics are shown dashed.

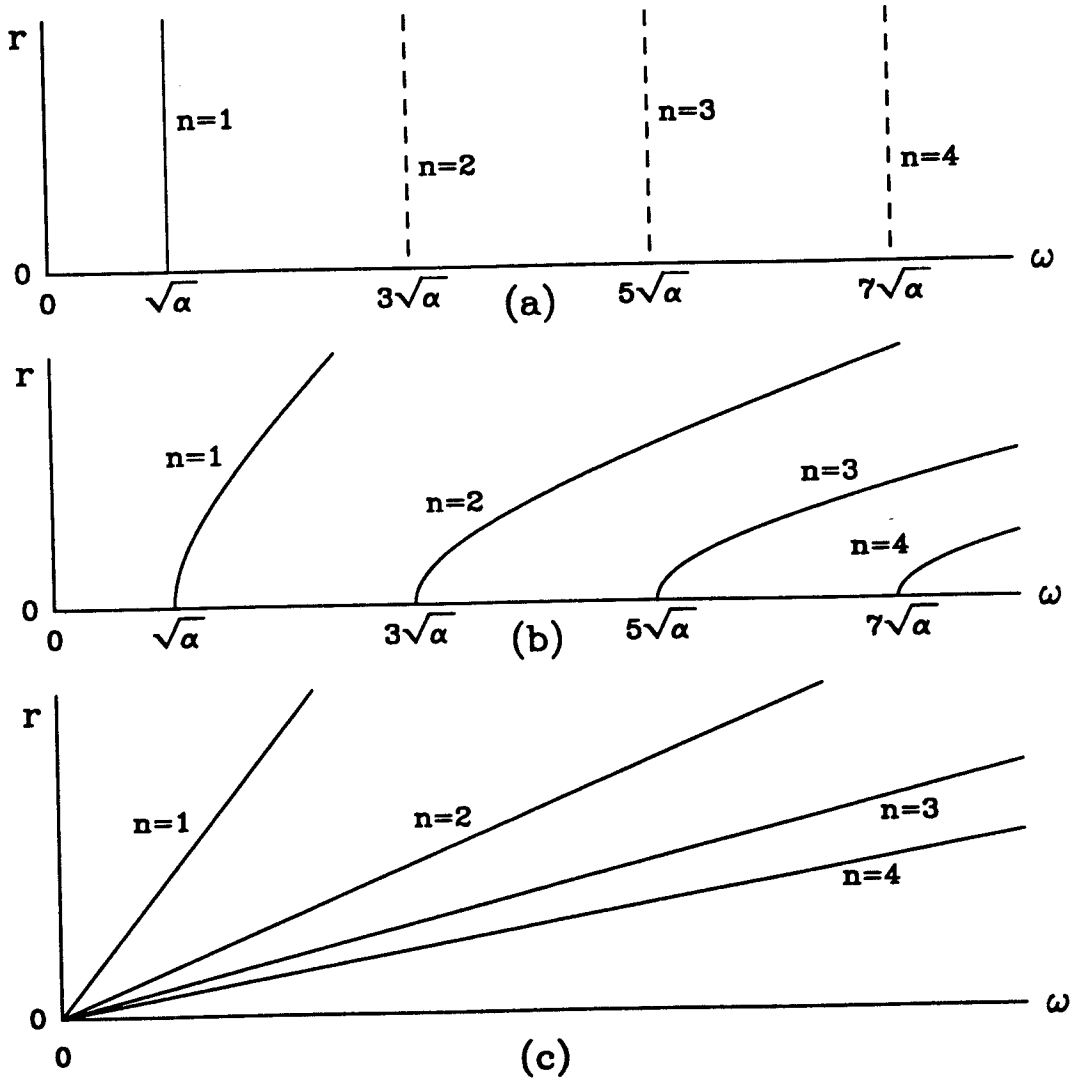

Fig.10.1 Resonant conditions for regions I (a), II (b) and III (c) defined by (10.10). In (a), the entire phase space experiences resonance or not, depending only on ω. The subharmonic resonances (i.e., $n \geq 2$) satisfy (10.10) but are not resonant to $O(\epsilon)$, see text. In (b), there are a finite number of resonant regions in the phase space, depending on ω. In (c), there is an infinite number of resonant regions for every ω.

For region II, resonances occur on specific orbits in projective phase space, since both a and K depend on the amplitude r in eq.(10.10). A graph of the resonant condition (10.10) for region II is given in Fig.10.1b. There is a resonance curve in (ω,r) given by (10.10) which emanates from each subharmonic. These curves are normal to the ω-axis at $r = 0$ and bend over depending on the size of β. Each curve is asymptotic to a line to infinity, with slopes decreasing as n increases. For a fixed ω value, there are a finite number N of resonant amplitudes in the phase space, where N is given by:

$$N = \text{integer of } \frac{1}{2}\left(\frac{\omega}{\sqrt{\alpha}} + 1\right) \tag{10.11}$$

As ω increases, N grows larger and resonant orbits begin to accumulate onto the origin in projective phase space.

For region III, eq.(10.10) becomes

$$\omega = (2n-1)\,\frac{\pi}{2}\,\frac{\sqrt{\beta}}{K}\,r \tag{10.12}$$

As in region II, there is a countably infinite number of resonant orbits. Each resonant curve, shown in Fig.10.1c, emanates from $(\omega,r) = (0,0)$ and is a straight line with slopes decreasing as $\frac{1}{2n-1}$. For each value of ω, there are an infinite number of resonant zones which accumulate onto the origin in projective phase space.

Then, in the progression from region I to II to III for fixed ω, the number of resonant orbits is built from 1 to N to infinity.

10.2 Averaging

We shall now average the r equation given in eq.(10.6) using a method from Sanders and Verhulst [San85]. A mixed variable near-identity transformation of the form

$$r = \bar{r} + \epsilon \sum_{n=1}^{\infty} \left[U_n^+(\bar{r}, \psi_n^+) + U_n^-(\bar{r}, \psi_n^-) \right] \tag{10.13}$$

is substituted into (10.6). Since $\bar{r}' = O(\epsilon)$, we find:

$$\bar{r}' = -\epsilon \sum_{n=1}^{\infty} \frac{f}{2a} \gamma_n c_n \left[\sin \psi_n^+ + \sin \psi_n^- \right] + \frac{\partial U_n^+}{\partial \psi_n^+} \Omega_n^+ + \frac{\partial U_n^-}{\partial \psi_n^-} \Omega_n^- + O(\epsilon^2) \tag{10.14}$$

where a, γ_n, c_n, and $\Omega_n^{\pm}$ are expressed in terms of $\bar{r}$

We now choose $U_n^{\pm}$ as follows:

$$\Omega_n^+ \frac{\partial U_n^+}{\partial \psi_n^+} = -\frac{f}{2a} \gamma_n c_n \sin \psi_n^+ \tag{10.15a}$$

$$U_n^+ = \frac{f}{2a} \frac{\gamma_n c_n}{\Omega_n^+} \cos \psi_n^+ \tag{10.15b}$$

(10.16a) $$\Omega_n^- \frac{\partial U_n^-}{\partial \psi_n^-} = -\frac{f}{2a}\gamma_n c_n \sin\psi_n^- \quad \text{if } \Omega_n^- \neq 0$$

(10.16b) $$U_n^- = \frac{f}{2a}\frac{\gamma_n c_n}{\Omega_n^-}\cos\psi_n^- \quad \text{if } \Omega_n^- \neq 0$$

$$= 0 \qquad \text{if } \Omega_n^- \approx 0$$

With this choice of generating functions $U_n^{\pm}$, almost every term ocurring in eq.(10.14) is zero. Then the averaged equations become:

(10.17a) Non-resonance: $$\bar{r}' = 0 + O(\epsilon^2)$$

$$(\psi_n^{\pm})' = \Omega_n^{\pm} \neq 0 \quad \forall n$$

(10.17b) Resonance: $$\bar{r}' = -\epsilon\frac{f}{2a}\gamma_n c_n \sin\psi_n^- + O(\epsilon^2)$$

$$(\psi_m^-)' = \Omega_m^- = \epsilon\sigma \approx 0$$

$$(\psi_m^+)' = \Omega_m^+ \neq 0$$

$$(\psi_n^{\pm})' = \Omega_n^{\pm} \neq 0 \quad \forall n \neq m$$

where σ is a detuning parameter

For regions of projective phase space away from resonant amplitudes, the non-resonance equations (10.17a) hold. They show that all motions are quasiperiodic and that $r = \bar{r} + O(\epsilon)$, where $\bar{r}$ is a constant (determined from initial conditions). Motions in the non-resonant regions of projective phase space remain ϵ-close to the unperturbed orbits of eq.(10.1).

For regions of projective phase space near resonant amplitudes, the resonant equations (10.17b) hold. Define σ by:

$$\epsilon\,\sigma = \bar{\Omega}_m = a\,\gamma_m - \omega \tag{10.18}$$

For region I, (10.18) defines σ in terms of ω independent of r. Therefore, one must detune in the forcing frequency ω. For regions II and III, (10.18) defines σ in terms of $\bar{r}$. One then can fix ω and detune from the resonant orbit by moving slightly in the phase space.

Results of the forced linear oscillator are well-known and will not be presented here. Results for the Duffing equation in which β is taken as $O(\epsilon)$ are also well-known. These results can be inferred from the region II discussion.

In regions II and III, we have defined $\sigma(\bar{r})$ by (10.18). We then can find σ' and form the phase space $(\sigma,\bar{\psi}_m)$, which is a cylinder. We see from eqs.(10.17b) that there exist two equilibrium points given by:

$$P_1:\ (\sigma,\bar{\psi}_m) = (0,0) \tag{10.19a}$$

$$P_2:\ (\sigma,\bar{\psi}_m) = (0,\pi) \tag{10.19b}$$

One equilibrium is exactly in-phase with the forcing; one equilibrium is exactly out-of-phase. A stability analysis shows that one equilibrium is elliptic and the other hyperbolic (as it must be).

This makes the $(\sigma,\bar{\psi}_m)$ phase space qualitatively identical with the simple pendulum, see Fig.10.2.

These equilibrium points correspond to periodic motions in (x,x',t), one stable (elliptic) and the other unstable (hyperbolic). This can be seen by finding the solution for x at these equilibria. First, let $\bar{r} = \bar{r}_*$ be the value of $\bar{r}$ satisfying $\sigma = 0$ in (10.18). Then to $O(\epsilon)$, $r = \bar{r}_*$ is the resonant amplitude at the equilibrium points and is constant. The value of u at the equilibrium points is found using $\bar{\psi}_m$:

$$u = \frac{1}{\gamma_m}(\bar{\psi}_m + \omega t) \tag{10.20}$$

$$u_1 = \frac{1}{\gamma_m}\omega t = a t \quad \text{corresponding to } P_1 \tag{10.21a}$$

$$u_2 = \frac{1}{\gamma_m}(\pi + \omega t) = \frac{\pi}{\gamma_m} + a t \quad \text{corresponding to } P_2 \tag{10.21b}$$

In (10.21), u_i is the value of u at P_i. Notice that u_i is not constant in time.

The solutions x_1 and x_2 corresponding to P_1 and P_2 are now easily determined:

$$x_1 = \bar{r}_* \, cn(u_1,k) \tag{10.22a}$$

$$x_2 = \bar{r}_* \, cn(u_2,k) \tag{10.22b}$$

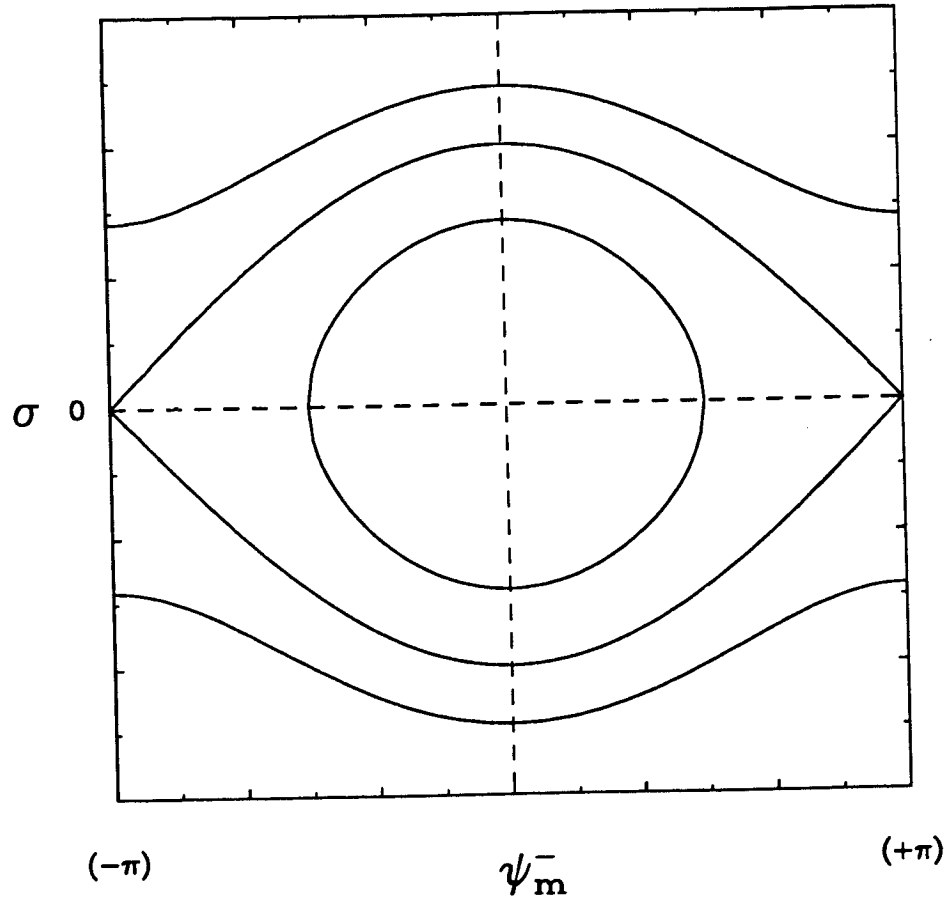

Fig.10.2 The (σ,ψ_m^-) cylindrical phase space for the forced Duffing equation is qualitatively a simple pendulum. σ (defined by 10.18) is a measure of the closeness to an exact resonance; ψ_m^- is the resonant phase angle. The center equilibrium at (0,0) corresponds to a periodic motion in-phase with the forcing. The saddle equilibrium at $(0,\pi) \equiv (0,-\pi)$ corresponds to a periodic motion out-of-phase with the forcing.

The period T in time of x_1 and x_2 are the same:

(10.23) $$\text{Period in } t = T = \frac{4K}{a}$$

But from eq.(10.18) at the equilibrium orbit:

(10.24) $$\frac{K}{a} = \frac{\pi}{2\omega}(2m-1)$$

Therefore, T becomes:

(10.25) $$T = (2m-1)\frac{2\pi}{\omega}$$

So, the period of the motions corresponding to P_1 and P_2 is a multiple of the forcing period. Therefore, P_1 and P_2 are (2m-1)-order subharmonic periodic orbits in (x,x',t). Moreover, a Poincare map defined on a cross-section Σ of the flow:

(10.26) $$\Sigma = \{(x,x',t) \mid t = 0 \bmod \frac{2\pi}{\omega}\}$$

will show (2m-1) centers and (2m-1) saddles corresponding to P_1 and P_2.

10.3 Melnikov's method for subharmonics

It is constructive to compare the averaging results of section 10.2 with the subharmonic Melnikov function [Guc86]. Specifically, we show that the Melnikov approach results in the same prediction of subharmonic orbits for systems of region II and III.

The subharmonic Melnikov function $M^{n/p}(t_0)$ for the system (10.1) is:

$$M^{n/p}(t_0) = \int_0^{2\pi m/\omega} cn'(u,k)\, f \cos(\omega t + \omega t_0)\, dt \tag{10.27}$$

$$\text{where } u = a\,(t - t_0) \text{ and } \frac{4Kp}{a} = \frac{2\pi m}{\omega}$$

where the exact resonance relation (10.10) holds. It is easily shown that $M^{n/p}(t_0) \equiv 0$ except when $p = 1$. For $p = 1$, (10.27) evaluates to:

$$M^{n/1}(t_0) = f \int_{-at_0}^{4K-at_0} cn'(u,k) \cos(\gamma_n u + \omega t_0)\, \frac{1}{a}\, du \tag{10.28}$$

$$= \frac{f}{a} \int_0^{4K} cn' \left[\cos(\gamma_n u) \cos(\omega t_0) - \sin(\gamma_n u) \sin(\omega t_0)\right] du$$

$$= -\frac{f}{a} \sin(\omega t_0) \int_0^{4K} cn'(u,k) \sin(\gamma_n u)\, du$$

$$= 4K \frac{f}{a} \gamma_n c_n \sin(\omega t_0) \qquad \text{for } n = 2m-1$$

In (10.28), we have used (10.5). For exact resonance, $\bar{\psi}_m = \gamma_m u_0 = -\gamma_m a t_0 = -\omega t_0$. So we can express (10.28) as

$$M^{(2m-1)/1}(\bar{\psi}_m) = -4K \frac{f}{a} \gamma_n c_n \sin \bar{\psi}_m \tag{10.29}$$

which shows that the subharmonic Melnikov function is simply a multiple of the averaged equation for r (eq.(10.17b)) in exact resonance.

Melnikov theory predicts the existence of subharmonic periodic orbits provided that (10.29) has simple zeroes and that the unperturbed system frequency a changes with amplitude r [Guc86]. This is satisfied for systems of regions II and III, but not I.

Obviously, if $M(\bar{\psi}_m)$ has simple zeroes then the $\bar{r}'$ equation has equilibrium points. The condition concerning the frequency is a statement about the detuning parameter σ. The condition requires that detuning occur in the phase space and not in the value of the forcing frequency.

Finally, we note that Holmes [Hol79] has used the Melnikov method to study the forced damped Duffing equation in which $\alpha = -1$. Such a system belongs to region IV of Fig.2.1. Using the Melnikov function on the separatrix, he shows that the system exhibits chaos. In addition, Greenspan and Holmes [Gre83] have studied a more complicated forced Duffing equation using the Melnikov method.

10.4 Combining averaging methods: Damped forced Duffing equation

We now wish to consider problems in which some of the perturbation terms in g depend explicitly on t while others do not. We shall take as an example the damped forced Duffing equation:

$$x'' + \alpha x + \beta x^3 + \epsilon \delta x' - \epsilon f \cos(\omega t) = 0 \tag{10.30}$$

Combining the averaging schemes of sections 3.1 and 10.2 to first order, we find the averaged equation for $\bar{r}$ as a sum of contributions from each perturbation term. We again take α and β as fixed on the range given by (10.2). Then the $\bar{r}$ equation becomes (using (3.31) and (10.17)):

$$\text{(10.31a) Non-resonance:} \quad \bar{r}' = \epsilon \delta \frac{1}{3\beta\bar{r}} \left[2\alpha \left(\frac{E}{K} - 1\right) - \beta \bar{r}^2\right] + O(\epsilon^2)$$

(10.31b) Resonance:

$$\bar{r}' = \epsilon \delta \frac{1}{3\beta\bar{r}} \left[2\alpha \left(\frac{E}{K} - 1\right) - \beta \bar{r}^2\right] - \epsilon \frac{f}{2a} \gamma_m c_m \sin \bar{\psi}_m + O(\epsilon^2)$$

$$= -\epsilon (\delta D + f F^m \sin \bar{\psi}_m)$$

where

$$D = -\frac{1}{3\beta\bar{r}} \left[2\alpha \left(\frac{E}{K} - 1\right) - \beta \bar{r}^2\right] \quad \text{and} \quad F^m = \frac{1}{2a} \gamma_m c_m$$

Note that both D and F^m are positive. We now present a short analysis of (10.31) for systems belonding regions II and III (i.e., we take β strictly positive). We take $\delta > 0$ and $f > 0$.

Outside the resonance regions, $\bar{r}$ decreases because of the damping. Once $\bar{r}$ reaches a resonant region, eq.(10.31b) holds. Fixed points of (10.31b) again correspond to periodic orbits. These can occur for:

$$\frac{\delta}{f} = -\frac{F^m}{D}\sin\bar{\psi}_m \tag{10.32}$$

provided that

$$-\pi < \bar{\psi}_m < 0 \quad \text{and} \quad 0 < \frac{\delta}{f} \leq \frac{F^m}{D} \equiv R^m(\omega) \tag{10.33}$$

Using (10.10), $R^m(\omega)$ is seen to be a function of ω. For $\frac{\delta}{f}$ outside the range specified in (10.33), $\bar{r}$ decreases through the resonant region. When equality holds in (10.33), a degenerate subharmonic orbit exists. The fixed point in the $(\sigma,\bar{\psi}_m)$ phase space is a saddle-node. For all other $\frac{\delta}{f}$ values in the range (10.33), two equilibria exist, one a saddle and the other a sink, see Fig.10.3. These correspond to periodic subharmonic orbits, one unstable and the other stable. The precise $(\sigma,\bar{\psi}_m)$ phase portrait, determined by particular parameter values, will determine the global basin of attraction for the sink. In Fig.10.3, all points approach the sink except the saddle. In this way, the initial conditions at entry in the resonant region (via $\bar{\psi}_m$) determine which steady state motion is attained [Nay79].

We plot a few of the equilibrium conditions, $R^m(\omega)$ vs. ω for systems of region II in Fig.10.4. Each curve quickly drops to zero indicating that for large ω the damping δ must be very small compared to the forcing f for subharmonic orbits to exist. The same type of plot for systems of region III is given in Fig.10.5. This figure is similar to Fig.10.4, except all curves possess a singularity at $\omega = 0$ since

$$R^m(\omega) \sim \frac{\sqrt{\beta}}{\omega^2} \tag{10.34}$$

Of course, in averaging the $\cos(\omega t)$ term using Fourier series, we had to take $\omega = O(1)$ so this region should really be ignored.

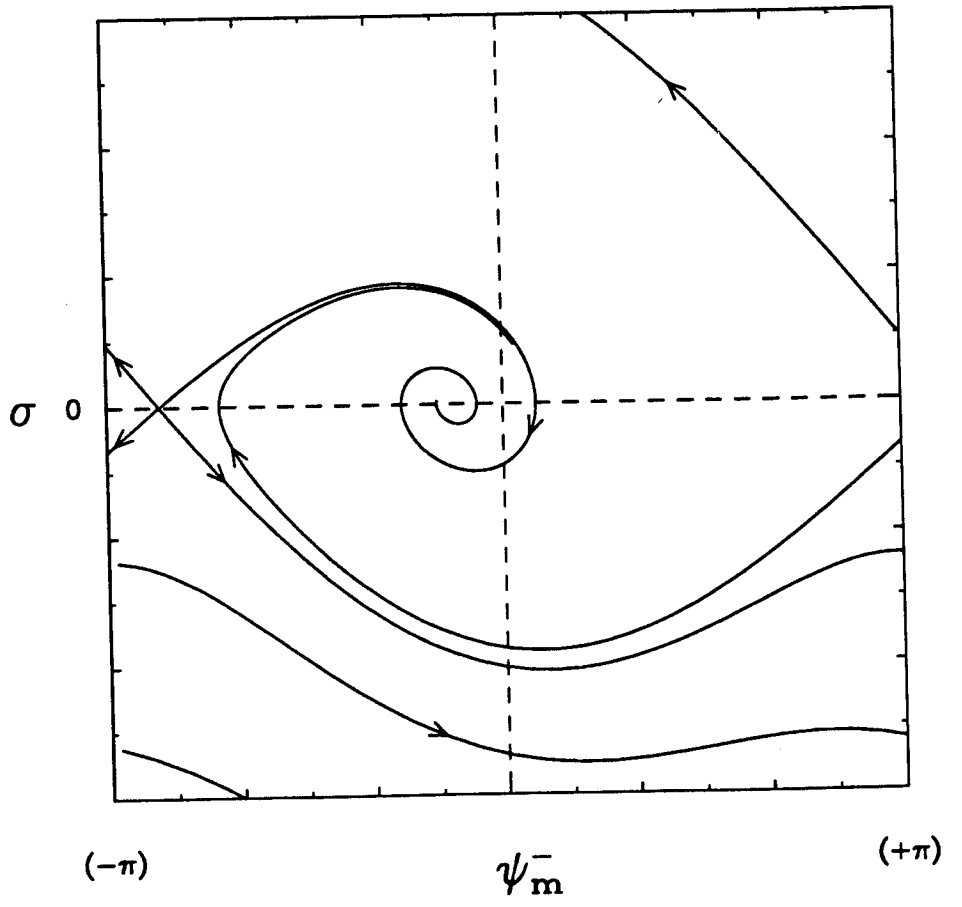

Fig.10.3 The $(\sigma,\bar{\psi}_m)$ cylindrical phase space for the forced damped Duffing equation is qualitatively a perturbed pendulum. σ (defined by 10.18) is a measure of the closeness to an exact resonance; $\bar{\psi}_m$ is the resonant phase angle. The sink corresponds to a periodic motion in-phase with the forcing. The saddle corresponds to a periodic motion out-of-phase with the forcing. The global basin of attraction for the sink (i.e., for the in-phase periodic motion) is determined by the particular parameter values α, β, δ, and f; in this figure, all points are attracted toward the sink except the saddle.

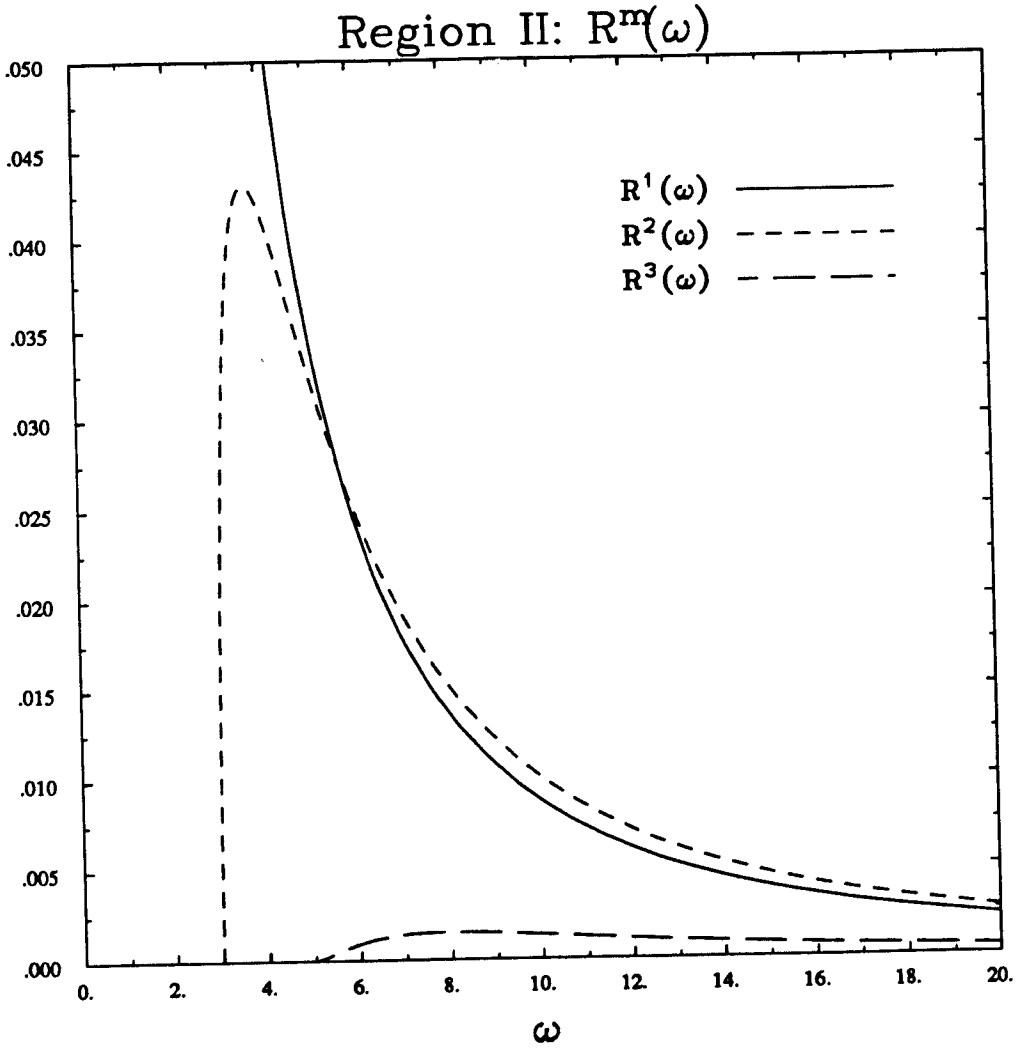

Fig.10.4 Equilibrium conditions for region II, plotting $R^m(\omega)$ vs. ω for m = 1, 2, and 3 where $R^m(\omega)$ is defined by (10.33) and (10.31b). For a given forcing frequency ω, the ratio of damping to forcing amplitude δ/f determines whether an attractive periodic orbit exists in the m^{th} subharmonic resonance zone. The value $R^m(\omega)$ is the maximum δ/f ratio for such an orbit to exist.

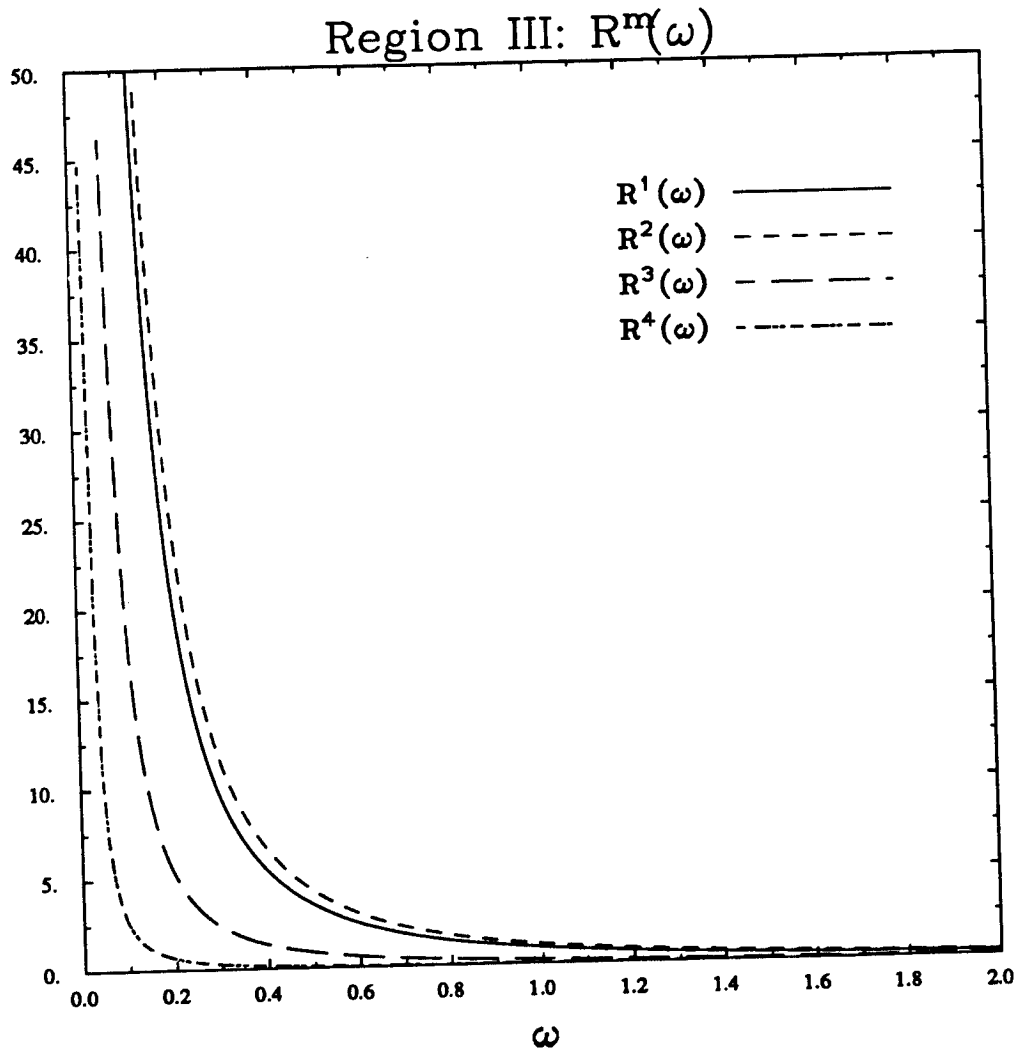

Fig.10.5 Equilibrium conditions for region III, plotting $R^m(\omega)$ vs. ω for m = 1, 2, and 3 where $R^m(\omega)$ is defined by (10.33) and (10.31b). For a given forcing frequency ω, the ratio of damping to forcing amplitude δ/f determines whether an attractive periodic orbit exists in the m^{th} subharmonic resonance zone. The value $R^m(\omega)$ is the maximum δ/f ratio for such an orbit to exist.

Appendix A The CNINT integration routine

The following program, written in the computer algebra system MACSYMA, computes the integral of cn^n using recursion. (An introduction to MACSYMA can be found in [Ran84]).

```
/* CN function integrator */

/* Routine finds the integral of g(xx) where g is polynomial in XX */
/* and XX stands for the cn function */

/* Symbols */

/* XX = cn function                                                  */
/* YY = cn' function (derivative of cn w.r.t. argument)              */
/* ZZ = Jacobian zeta function                                       */
/* SS = arcsin(k*sn(u,k)) = arcsin(k*sqrt(1-xx^2))                   */
/* UU = argument and hence 1st elliptic integral                     */
/* KC,EC = complete elliptic integrls of 1st, 2nd kinds              */
/* K  = modulus                                                      */

CNINT(V,K):=BLOCK([TEMP,HI,IC,VAL],

/* Find highest power of cn in V and kill integration function IC */

TEMP:EXPAND(V),
HI:HIPOW(TEMP,XX),
KILL(IC),

/* IC[II] = integration function array that defines */
/* the integral of xx^ii.  It is defined recursively */
/* If k=0, then cn=cos so set the IC to use cosine routine */

IF SCALARP(K) AND EV(K) = 0 THEN (
   IC[0]:UU,
   IC[1]:-YY,
   IC[II]:=RATSIMP((II-1)/II*IC[II-2]-1/II*XX^(II-1)*YY)
) ELSE (
   IC[0]:UU,
   IC[1]:SS/K,
   IC[2]:1/K^2*(ZZ+(EC/KC-(1-K^2))*UU),
```

```
    IC[3]:1/2/K^3*((2*K^2-1)*SS-K*YY),
    IC[II]:=RATSIMP((II-2)*(2*K^2-1)*IC[II-2]+(II-3)*(1-K^2)*IC[II-4]
                    -XX^(II-3)*YY)/K^2/(II-1)
),

/* Set VALue of the integral to zero */

VAL:0,

/* For each xx^ii expression found in V, substitute */
/* its integral IC[ii] */

FOR II:0 THRU HI DO VAL:VAL+RATCOEF(TEMP,XX,II)*IC[II],
VAL:EXPAND(VAL)
)$
```

Appendix B The GENINT integration routine

The following program, written in the computer algebra system MACSYMA, computes integrals of the functions appearing in (1.23).

```
/* F1,F2,W1,W2 integrator */

/* Routine to integrate integrands of the form : */
/*      (a) xx^m  (b) xx^m yy (c) zz xx^m  (d) zz xx^m yy */
/*      (e) ss xx^m  (f) ss xx^m yy  */

/* Symbols */

/* XX = cn function                                          */
/* YY = cn' function (derivative of cn w.r.t. argument)      */
/* ZZ = Jacobian zeta function                               */
/* SS = arcsin(k*sn(u,k)) = arcsin(k*sqrt(1-xx^2))           */
/* UU = argument and hence 1st elliptic integral             */
/* TH = ln(theta(u)/theta(0))                                */
/* S0 = integral of ss with respect to u                     */
/* S2 = integral of ss*xx^2 with respect to u                */
/* KC,EC = complete elliptic integrls of 1st,2nd kinds       */
/* K  = modulus                                              */

/* V contains the expression to be integrated.      */
/* Expressions are integrated w.r.t u.              */
/* For integrations w.r.t. phi, multiply by 1/4/kc */

GENINT(V,K):=BLOCK([TEMP,STERMS,XTERMS,ZTERMS,XYT,XT,SYT,ST,ZYT,ZT,
                    VALX,VALZ,VALS,VAL],
TEMP:EXPAND(V),

/* V is assumed to be linear in YY (Use (1.11b) if necessary) */

/* Separate V into categories:                  */
/*                                              */
/*   XT contains terms in V of the form (a) */
/*  XYT contains terms in V of the form (b) */
/*   ZT contains terms in V of the form (c) */
/*  ZYT contains terms in V of the form (d) */
/*   ST contains terms in V of the form (e) */
/*  SYT contains terms in V of the form (f) */
```

```
STERMS:EXPAND(DIFF(TEMP,SS)),
ZTERMS:EXPAND(DIFF(TEMP,ZZ)),
XTERMS:EXPAND(TEMP-SS*STERMS-ZZ*ZTERMS),
XYT:EXPAND(DIFF(XTERMS,YY)),
XT:EXPAND(XTERMS-YY*XYT),
SYT:EXPAND(DIFF(STERMS,YY)),
ST:EXPAND((STERMS-YY*SYT)),
ZYT:EXPAND(DIFF(ZTERMS,YY)),
ZT:EXPAND(ZTERMS-YY*ZYT),

/* Create XYINT function to integrate form (b) */

XYINT(VV):=BLOCK(VV:EXPAND(VV),EXPAND(INTEGRATE(VV,XX))),

/* Integrate forms (a) [using CNINT routine] and (b) */

VALX:CNINT(XT,K)+XYINT(XYT),

/* Integrate form (d) by integration by parts */

ARG:XYINT(ZYT),
VALZ:ZZ*ARG-CNINT(ARG*(1-K^2-EC/KC+K^2*XX^2),K),

/* Integrate form (f) by integration by parts */

ARG:XYINT(SYT),
VALS:SS*ARG-CNINT(ARG*K*XX,K),

/* Create a general Integration By Parts routine */
/* for forms (c) and (e) */

INTBYPARTS(VV,K,TYPE):=BLOCK([ARG,UUT,ZZT,SST,YYT,XXT,VALP],

   /* VV just contains the XX terms of forms (c) and (e) */
   /* TYPE indicates either form (c) or (e)              */
   /* Find DERIV, the derivative of TYPE w.r.t. u */

   IF TYPE = ZZ THEN DERIV:1-K^2-EC/KC+K^2*XX^2,
   IF TYPE = SS THEN DERIV:K*XX,

   /* Set ARG = integral of VV w.r.t. u [using CNINT routine] */

   ARG:CNINT(VV,K),
```

```
   /* Separate ARG into categories:                    */
   /*                                                  */
   /* UUT contains UU terms in ARG                     */
   /* ZZT contains ZZ terms in ARG                     */
   /* SST contains SS terms in ARG                     */
   /* YYT contains terms in ARG of the form (b)        */
   /* XXT contains terms in ARG of the form (a)        */

   UUT:DIFF(ARG,UU).
   ZZT:DIFF(ARG,ZZ).
   SST:DIFF(ARG,SS).
   YYT:DIFF(ARG,YY).
   XXT:EXPAND(ARG-UU*UUT-ZZ*ZZT-SS*SST-YY*YYT).

   /* Perform integration by parts */

   IF TYPE = ZZ THEN
      VALP:EXPAND(UUT*(UU*ZZ-TH)+ZZT*(ZZ^2/2)
           +EV(SST*SO*DERIV,XX=SQRT(S2/SO))
           +XYINT(YYT*DERIV)+CNINT(XXT*DERIV,K)).
   IF TYPE = SS THEN
      VALP:EXPAND(UUT*(UU*SS-SO)+ZZT*(ZZ*SS-K^2*S2-(1-K^2-EC/KC)*SO)
                  +SST*(SS^2/2)+XYINT(YYT*DERIV)+CNINT(XXT*DERIV,K)).
   VALP:EXPAND(TYPE*ARG-VALP)
).

/* Integrate forms (c) and (e) using INTBYPARTS */

VALZ:VALZ+INTBYPARTS(ZT,K,ZZ).
VALS:VALS+INTBYPARTS(ST,K,SS).

/* Add together */

VAL:EXPAND(VALX+VALZ+VALS)
)$
```

Appendix C Numerical routines for elliptic functions

This appendix lists numerical routines for the computation of many of the elliptic functions appearing in section 1.6. The routines are based on the formulas appearing in chapter 1, which are found in [Byr54]. The first set of routines is written in the computer algebra system MACSYMA; the second set is written in Fortran.

```
/* ELLIPTIC FUNCTIONS PACKAGE*/

/* by Vincent T. Coppola      25 Apr 1989     Cornell University */

/* Formulas>> Byrd & Friedman 'Handbook of Elliptic Integrals for */
/* Engineers and Scientists */

/* ALL ROUTINES REQUIRE 0 <= k^2 <= 1 EXCEPT FOR ELLK AND ELLE */

/* accuracy tolerance for all elliptic function evaluations */

define_variable(elltol,1.b-7,any)$
define_variable(ellnum,250,any)$

/* complete elliptic integral of first kind (KC) */

ellk(k):=block([temp,ksqr,kpsqr,km,bm,ln,val,float2bf],
     mode_declare([k,temp,ksqr,kpsqr,km,bm,ln,val,elltol],
                  any,float2bf,boolean),
     float2bf:true,
     val:0,
     k:bfloat(k),
     if k=1.b0 then (
        val:9.9b999,
        return(val)
     ),
```

```
    if k=0.b0 then (
       val:bfloat(%pi/2),
       return(val)
    ),
    ksqr:k^2,
    km:1.b0,
    if ksqr>1 then (ksqr:1/ksqr,km:bfloat(sqrt(ksqr))),
    if ksqr<0 then (ksqr:bfloat(-ksqr/(1.b0-ksqr)),
                    km:bfloat(sqrt(1.b0-ksqr))),
    /* ksqr now is between 0 and 1 */
    temp:1,
    if ksqr<.5b0 then (
       for n:0 while abs(temp)>elltol do (
           temp:bfloat(%pi/2/n!/n!*product(1/2+m,m,0,n-1)^2*ksqr^n),
           val:val+temp,
           if n>ellnum then temp:2*elltol
       )
    ) else (
       kpsqr:1.b0-ksqr,
       ln:bfloat(log(4/sqrt(kpsqr))),
       for n:0 while abs(temp)>elltol do (
           if n=0 then bm:0,
           if n>0 then bm:bm+1/n/(2*n-1),
           temp:bfloat(product(-1/2-m,m,0,n-1)^2/(n!)^2
                       *(ln-bm)*kpsqr^n),
           val:val+temp,
           if n>ellnum then temp:2*elltol
       )
    ),
    val:bfloat(km*val)
)$

/* complete elliptic integral of second kind (EC) */

elle(k):=block([temp,ksqr,kpsqr,km,bm,bm1,ln,val,float2bf],
     mode_declare([k,temp,ksqr,kpsqr,km,bm,bm1,ln,val,
                   elltol,function(ellk)],any,float2bf,boolean),
     float2bf:true,
     val:0,
     k:bfloat(k),
     ksqr:k^2,
     if ksqr=1.b0 then (
        val:1.b0,
        return(val)
     ),
     if ksqr=0.b0 then (
        val:bfloat(%pi/2),
        return(val)
     ),
     km:1.b0,
```

```
    if ksqr>1.b0 then (ksqr:1/ksqr,km:bfloat(sqrt(ksqr))),
    if ksqr<0.b0 then (ksqr:bfloat(-ksqr/(1.b0-ksqr)),
                       km:bfloat(sqrt(1.b0-ksqr))),
    /* ksqr now is between 0 and 1 */
    temp:1,
    if ksqr<.5b0 then (
       for n:0 while abs(temp)>elltol do (
           temp:bfloat(%pi/2/n!/n!*product(-1/2-m,m,0,n-1)^2
                       /(1-2*n)*ksqr^n),
           val:val+temp,
           if n>ellnum then temp:2*elltol
       )
    ) else (
       kpsqr:1.b0-ksqr,
       ln:bfloat(log(4/sqrt(kpsqr))),
       val:1.b0,
       bm:0,
       for n:0 while abs(temp)>elltol do (
           bm1:bm+1/(n+1)/(2*n+1),
           temp:bfloat(1/4*product(1/2+m,m,0,n-1)/n!
                       *product(3/2+m,m,0,n-1)/(n+1)!
                       *(2*ln-bm1-bm)*kpsqr^(n+1)),
           bm:bm1,
           val:val+temp,
           if n>ellnum then temp:2*elltol
       )
    ),
    if k^2<1.b0 then val:bfloat(1/km*val)
          else val:bfloat(1/km*(val-(1.b0-ksqr)*ellk(km))),
    val
)$

/* incomplete elliptic integrals as functions of angle theta */
/* (F(theta,k) and E(theta,k))*/

/* The following ei1 and ei2 functions were checked against */
/* exact values per formula 111.03, pg. 10, of Byrd & Friedman */

/* ei1 function (elliptic integral of first kind u in terms of */
/* angle theta) */

/* note:  this function calculates the principal part */
/* i.e. 0 <= angle <= pi/2 */

ei1(theta,k):=block([s,c,t,ln,kp2,val,rho2n,t2n,temp,float2bf,null],
     mode_declare([s,c,t,ln,kp2,val,rho2n,t2n,temp,theta,
                   k,elltol,null,function(ellk)],any,
                   float2bf,boolean),
     float2bf:true,
     val:0,
     k:bfloat(k),
```

```
    theta:bfloat(theta),
    if k=0.b0 then (
       val:theta,
       return(val)
    ),
    if cos(theta)=0.b0 then (
       val:ellk(k),
       return(val)
    ),
    if k=1.b0 then (
       val:bfloat(log(tan(theta)+sec(theta))),
       return(val)
    ),
    if k>1.b0 then return(null),
    s:bfloat(sin(theta)),
    c:bfloat(cos(theta)),
    t:s/c,
    ln:bfloat(log(t+1/c)),
    kp2:1-k^2,
    temp:1,
    if kp2*t^2<.5b0 then (
       for n:0 while abs(temp)>elltol do (
           if n=0 then rho2n:ln,
           if n=1 then rho2n:bfloat(1/2*(s/c^2-ln)),
           if n>1 then
                  rho2n:bfloat(1/2/n*(t^(2*n-1)/c+(1-2*n)*rho2n)),
           temp:bfloat(product(-1/2-m,m,0,n-1)/n!*kp2^n*rho2n),
           val:val+temp,
           if n>ellnum then temp:2*elltol
       )
    ) else (
       for n:0 while abs(temp)>elltol do (
           if n=0 then t2n:theta,
           if n=1 then t2n:bfloat(1/2*(theta-s*c)),
           if n>1 then
                  t2n:bfloat((2*n-1)/2/n*t2n-1/2/n*s^(2*n-1)*c),
           temp:bfloat(product(-1/2-m,m,0,n-1)/n!*(-k^2)^n*t2n),
           val:val+temp,
           if n>ellnum then temp:2*elltol
       )
    ),
    val
)$
```

```
/* ei2 function (elliptic integral of second kind u in terms */
/* of angle theta) */

/* note:  this function calculates the principal part */
/* i.e. 0 <= angle <= pi/2 */

ei2(theta,k):=block([s,c,t,ln,kp2,val,d2n,t2n,temp,null,float2bf],
     mode_declare([s,c,t,ln,kp2,val,d2n,t2n,temp,theta,k,
                   elltol,null,function(elle)],any,
                   float2bf,boolean),
     float2bf:true,
     val:0,
     k:bfloat(k),
     theta:bfloat(theta),
     if k=0.b0 then (
        val:theta,
        return(val)
     ),
     if cos(theta)=0.b0 then (
        val:elle(k),
        return(val)
     ),
     s:bfloat(sin(theta)),
     if k=1.b0 then (
        val:s,
        return(val)
     ),
     if k>1.b0 then return(null),
     c:bfloat(cos(theta)),
     t:s/c,
     ln:bfloat(log(t+1/c)),
     kp2:1-k^2,
     temp:1,
     if kp2*t^2<.5b0 then (
        for n:0 while abs(temp)>elltol do (
            if n=0 then d2n:s,
            if n=1 then d2n:bfloat(ln-s),
            if n>1 then
                   d2n:bfloat(1/2/(n-1)*(t^(2*n-1)*c+(1-2*n)*d2n)),
            temp:bfloat(product(1/2-m,m,0,n-1)/n!*kp2^n*d2n),
            val:val+temp,
            if n>ellnum then temp:2*elltol
        )
     ) else (
        for n:0 while abs(temp)>elltol do (
            if n=0 then t2n:theta,
            if n=1 then t2n:bfloat(1/2*(theta-s*c)),
            if n>1 then
                   t2n:bfloat((2*n-1)/2/n*t2n-1/2/n*s^(2*n-1)*c),
```

```
            temp:bfloat(product(1/2-m,m,0,n-1)/n!*(-k^2)^n*t2n),
            val:val+temp,
            if n>ellnum then temp:2*elltol
          )
      ),
      val
)$

/* elliptic funtions */

am(u,k):=block([kp,kcp,temp,kc,val,float2bf],
      mode_declare([u,k,kp,kcp,temp,kc,val,elltol,
                    function(ellk)],any,float2bf,boolean),
      float2bf:true,
      kc:ellk(k),
      kp:sqrt(1-k^2),
      kcp:ellk(kp),
      val:bfloat(%pi/2*u/kc),
      temp:1,
      for n:1 while abs(temp)>elltol do (
          temp:bfloat(1/n*sech(n*%pi*kcp/kc)*sin(n*%pi*u/kc)),
          val:val+temp,
          if n>ellnum then temp:2*elltol
      ),
      val
)$

sn(u,k):=block([float2bf],
      mode_declare([u,k,function(am)],any,float2bf,boolean),
      float2bf:true,
      bfloat(sin(am(u,k)))
)$

cn(u,k):=block([float2bf],
      mode_declare([u,k,function(am)],any,float2bf,boolean),
      float2bf:true,
      bfloat(cos(am(u,k)))
)$

dn(u,k):=block([float2bf],
      mode_declare([u,k,function(sn)],any,float2bf,boolean),
      float2bf:true,
      bfloat(sqrt(1-k^2*sn(u,k)^2))
)$

/* The inverse functions are defined on -1 <= y <= 1 */
/* for sninv and cninv and by sqrt(1-k^2) <= y <= 1 for dninv */
```

```
/* sninv returns values on -kc <= u <= kc */
/* (where kc = complete elliptic integral 1st kind) */

sninv(y,k):=block([theta,float2bf],
     mode_declare([y,k,theta,function(ei1)],any,float2bf,boolean),
     float2bf:true,
     theta:bfloat(asin(abs(y))),
     signum(y)*ei1(theta,k)
)$

/* cninv returns values on 0 <= u <= 2*kc */
/* (where kc = complete elliptic integral 1st kind) */

cninv(y,k):=block([theta,uu,float2bf],
     mode_declare([y,k,theta,uu,function(ei1,ellk)],any,
                  float2bf,boolean),
     float2bf:true,
     theta:bfloat(asin(sqrt(y^2/(1-k^2+k^2*y^2)))),
     uu:ei1(theta,k),
     ellk(k)-signum(y)*uu
)$

/* dninv returns values on 0 <= u <= kc */
/* (where kc = complete elliptic integral 1st kind) */

dninv(y,k):=block([theta,float2bf],
     mode_declare([y,k,theta,function(ei1)],any,float2bf,boolean),
     float2bf:true,
     theta:bfloat(asin(1/k*sqrt(1-y^2))),
     ei1(theta,k)
)$

/* zeta function */

zeta(u,k):=block([kp,kcp,kc,temp,k1,scl,val,float2bf],
     mode_declare([u,k,kp,kcp,kc,temp,k1,scl,val,elltol,
                   function(ellk)],any,float2bf,boolean),
     float2bf:true,
     val:0,
     k:bfloat(k),
     if k=1.b0 then (
        val:tanh(u),
        return(val)
     ),
     if k=0.b0 then return(val),
     if k<1.b0 then (
        kc:ellk(k),
        kp:sqrt(1-k^2),
        kcp:ellk(kp),
        scl:1
     ) else (
```

```
        k1:1/k,
        kp:sqrt(1-k1^2),
        kc:ellk(k1),
        kcp:ellk(kp),
        scl:k
      ),
      temp:1,
      for n:1 while abs(temp)>elltol do (
          temp:bfloat(%pi/kc/sinh(n*%pi*kcp/kc)
                      *sin(n*%pi*scl*u/kc)),
          val:val+temp,
          if n>ellnum then temp:2*elltol
      ),
      val:scl*val
)$
```

The following routines are written in Fortran.

```
c Elliptic Functions
c
c by Vincent T. Coppola     10 May 1989   Cornell University
c
c
c Formulas from Byrd & Friedman  "Handbook of Elliptic Integrals"
c
c
c Elliptic integral of first kind (for any k^2)
c
      function ellk(k2,elltol)
      real*8 ellk,k2,ksqr,kp2,bm,ln,val,km,temp,elltol,pi,coef
      pi=dacos(-1.d0)
      val=0.d0
      if (k2.eq.1.d0) then
           ellk=9.999999d99
           return
      endif
      ksqr=k2
      km=1.d0
      if (ksqr.gt.1.d0) then
           ksqr=1.d0/ksqr
           km=dsqrt(ksqr)
      endif
```

```
      if (ksqr.lt.0.d0) then
           ksqr=-ksqr/(1.d0-ksqr)
           km=dsqrt(1.d0-ksqr)
      endif
      temp=1.d0
      n=0
      if (ksqr.lt..5d0) then
10         if (dabs(temp).gt.elltol) then
               if (n.eq.0) coef=1.d0
               if (n.gt.0) coef=coef/dble(float(n))
     1                           *(.5d0+dble(float(n-1)))
               temp=pi/2.d0*coef**2*ksqr**n
               val=val+temp
               n=n+1
               if (n.gt.200) then
                  val=10.d0*val
                  goto 30
               endif
               goto 10
           endif
       else
           kp2=1.d0-ksqr
           ln=dlog(4.d0/dsqrt(kp2))
20         if (dabs(temp).gt.elltol) then
               if (n.eq.0) then
                    bm=0.d0
                    coef=1
               endif
               if (n.gt.0) then
                    bm=bm+1.d0/dble(float(n))/dble(float(2*n-1))
                    coef=coef/dble(float(n))
                         *(-.5d0-dble(float(n-1)))
               endif
               temp=coef**2*(ln-bm)*kp2**n
               val=val+temp
               n=n+1
               if (n.gt.200) then
                  val=10.d0*val
                  goto 30
               endif
               goto 20
            endif
      endif
30    ellk=val*km
      return
      end
```

```
c
c Elliptic integral of second kind (for any k^2)
c
      function elle(k2,elltol)
      real*8 elle,ellk,k2,ksqr,kp2,bm,bm1,ln,val,km,temp,
      real*8 elltol,pi,coef
      pi=dacos(-1.d0)
      val=0.d0
      if (k2.eq.1.d0) then
           elle=1.d0
           return
      endif
      ksqr=k2
      km=1.d0
      if (ksqr.gt.1.d0) then
           ksqr=1.d0/ksqr
           km=dsqrt(ksqr)
      endif
      if (ksqr.lt.0.d0) then
           ksqr=-ksqr/(1.d0-ksqr)
           km=dsqrt(1.d0-ksqr)
      endif
      temp=1.d0
      n=0
      if (ksqr.lt..5d0) then
   10      if (dabs(temp).gt.elltol) then
                if (n.eq.0) coef=1.d0
                if (n.gt.0) coef=coef/dble(float(n))
     1                           *(-.5d0-dble(float(n-1)))
                temp=pi/2.d0*coef**2/dble(float(1-2*n))*ksqr**n
                val=val+temp
                n=n+1
                if (n.gt.200) goto 30
                goto 10
           endif
       else
           kp2=1.d0-ksqr
           ln=dlog(4.d0/dsqrt(kp2))
           val=1.d0
           bm=0.d0
   20      if (dabs(temp).gt.elltol) then
                if (n.eq.0) coef=1
                if (n.gt.0) coef=coef/dble(float(n*(n+1)))
     1               *(.5d0+dble(float(n-1)))
     2               *(1.5d0+dble(float(n-1)))
                bm1=bm+1.d0/dble(float((n+1)*(2*n+1)))
                temp=.25d0*coef*(2.d0*ln-bm1-bm)*kp2**(n+1)
                val=val+temp
                bm=bm1
                n=n+1
```

```
                if (n.gt.200) goto 30
                goto 20
             endif
          endif
       30 if (k2.lt.1.d0) elle=1.d0/km*val
          if (k2.gt.1.d0) elle=1.d0/km*(val-(1.d0-ksqr)
                                *ellk(ksqr,elltol))
          return
          end

c
c Incomplete Elliptic Integrals
c
c
c Incomplete elliptic integral of first kind for k^2 < 1
c

          function ei1(theta,k2,elltol)
          real*8 ei1,theta,k2,elltol,val,temp,ellk,s,c,ln,t,kp2
          real*8 rho2n,t2n,dfn,coef
          val=0.d0
          if (k2.eq.0.d0) then
             ei1=theta
             return
          endif
          if (dcos(theta).eq.0.d0) then
             ei1=ellk(k2,elltol)
             return
          endif
          s=dsin(theta)
          c=dcos(theta)
          t=dtan(theta)
          ln=dlog(t+1.d0/c)
          kp2=1.d0-k2
          temp=1.d0
          n=0
          if (k2.eq.1.d0) then
             ei1=ln
             return
          endif
          if (kp2*t**2.lt..5d0) then
       10    if (dabs(temp).gt.elltol) then
                dfn=dble(float(n))
                if (n.eq.0) then
                   rho2n=ln
                   coef=1.d0
                endif
                if (n.eq.1) then
                   rho2n=.5d0*(s/c**2-ln)
                   coef=-.5d0
                endif
```

```
            if (n.gt.1) then
               rho2n=.5d0/dfn*(t**(2*n-1)/c+dble(float(1-2*n))*rho2n)
               coef=coef/dfn*(-.5d0-dble(float(n-1)))
            endif
            temp=coef*kp2**n*rho2n
            val=val+temp
            n=n+1
            if (n.gt.200) goto 30
            goto 10
         endif
      else
   20    if (dabs(temp).gt.elltol) then
            dfn=dble(float(n))
            if (n.eq.0) then
               t2n=theta
               coef=1.d0
            endif
            if (n.eq.1) then
               t2n=.5d0*(theta-s*c)
               coef=-.5d0
            endif
            if (n.gt.1) then
               t2n=dble(float(2*n-1))/2.d0/dfn*t2n
     1             -.5d0/dfn*s**(2*n-1)*c
               coef=coef/dfn*(-.5d0-dble(float(n-1)))
            endif
            temp=coef*(-k2)**n*t2n
            val=val+temp
            n=n+1
            if (n.gt.200) goto 30
            goto 20
         endif
      endif
   30 ei1=val
      return
      end

c
c Incomplete elliptic integral of second kind for k^2 < 1
c
      function ei2(theta,k2,elltol)
      real*8 ei2,theta,k2,elltol,val,temp,elle,s,c,t,ln,kp2
      real*8 dfn,d2n,t2n,coef
      val=0.d0
      if (k.eq.0.d0) then
         ei2=theta
         return
      endif
```

```
      if (dcos(theta).eq.0.d0) then
         ei2=elle(k2,elltol)
         return
      endif
      s=dsin(theta)
      c=dcos(theta)
      t=dtan(theta)
      ln=dlog(t+1.d0/c)
      kp2=1.d0-k2
      temp=1.d0
      n=0
      if (k2.eq.1.d0) then
         ei2=s
         return
      endif
      if (kp2*t**2.lt..5d0) then
10       if (dabs(temp).gt.elltol) then
            dfn=dble(float(n))
            if (n.eq.0) then
               d2n=s
               coef=1.d0
            endif
            if (n.eq.1) then
               d2n=ln-s
               coef=.5d0
            endif
            if (n.gt.1) then
               d2n=.5d0/dble(float(n-1))*(t**(2*n-1)*c
     1              +dble(float(1-2*n))*d2n)
               coef=coef/dfn*(.5d0-dble(float(n-1)))
            endif
            temp=coef*kp2**n*d2n
            val=val+temp
            n=n+1
            if (n.gt.200) goto 30
            goto 10
         endif
      else
20       if (dabs(temp).gt.elltol) then
            dfn=dble(float(n))
            if (n.eq.0) then
               t2n=theta
               coef=1.d0
            endif
            if (n.eq.1) then
               t2n=.5d0*(theta-s*c)
               coef=.5d0
            endif
```

```
            if (n.gt.1) then
               t2n=dble(float(2*n-1))/2.d0/dfn*t2n
     1             -.5d0/dfn*s**(2*n-1)*c
               coef=coef/dfn*(.5d0-dble(float(n-1)))
            endif
            temp=coef*(-k2)**n*t2n
            val=val+temp
            n=n+1
            if (n.gt.200) goto 30
            goto 20
         endif
      endif
   30 ei2=val
      return
      end

c
c Elliptic functions for 0 < k < 1
c
      function am(u,k2,elltol)
      real*8 am,u,k2,elltol,kc,kp2,kcp,val,temp,pi,ellk,dfn
      pi=dacos(-1.d0)
      kc=ellk(k2,elltol)
      kp2=(1.d0-k2)
      kcp=ellk(kp2,elltol)
      val=pi/2.d0*u/kc
      temp=1.d0
      n=1
    10 if (dabs(temp).gt.elltol) then
            dfn=dble(float(n))
            temp=1/dfn/dcosh(dfn*pi*kcp/kc)*dsin(dfn*pi*u/kc)
            val=val+temp
            n=n+1
            if (n.gt.200) goto 20
            goto 10
      endif
    20 am=val
      return
      end
 c
      function sn(u,k2,elltol)
      real*8 sn,u,k2,elltol,am
      sn=dsin(am(u,k2,elltol))
      return
      end
 c
      function cn(u,k2,elltol)
      real*8 cn,u,k2,elltol,am
      cn=dcos(am(u,k2,elltol))
      return
      end
```

```
c
      function dn(u,k2,elltol)
      real*8 dn,u,k2,elltol,sn
      dn=dsqrt(1.d0-k2*sn(u,k2,elltol)**2)
      return
      end
c
c Inverse Elliptic functions
c
c
c sninv returns values on -kc <= u <= kc (kc=ellk(k))
c
      function sninv(yval,k2,elltol)
      real*8 sninv,yval,k2,elltol,ei1,theta
      theta=dasin(dabs(yval))
      sninv=dsign(1.d0,yval)*ei1(theta,k2,elltol)
      return
      end
c
c cninv returns values on 0 <= u <= 2*kc (kc=ellk(k))
c
      function cninv(yval,k2,elltol)
      real*8 cninv,yval,k2,elltol,theta,uu,ellk,ei1
      theta=dasin(dsqrt(yval**2/(1.d0-k2+k2*yval**2)))
      uu=ei1(theta,k2,elltol)
      cninv=ellk(k2,elltol)-dsign(1.d0,yval)*uu
      return
      end
c
c dninv returns values on 0 <= u <= kc (kc=ellk(k))
c
      function dninv(yval,k2,elltol)
      real*8 dninv,yval,k2,elltol,theta,ei1
      theta=dasin(1.d0/dsqrt(k2)*dsqrt(1.d0-yval**2))
      dninv=ei1(theta,k2,elltol)
      return
      end
c
c Zeta function
c
      function zeta(u,k2,elltol)
      real*8 zeta,u,k2,elltol,val,kc,kcp,kp2,temp
      real*8 pi,pikc,pikcp,dfn
      val=0.d0
      if (k2.eq.1.d0) then
         zeta=dtanh(u)
         return
      endif
```

```
      if (k2.eq.0.d0) then
         zeta=val
         return
      endif
      kc=ellk(k2,elltol)
      kp2=1.d0-k2
      kcp=ellk(kp2,elltol)
      pi=dacos(-1.d0)
      pikc=pi/kc
      pikcp=pikc*kcp
      temp=1.d0
      n=0
   10 if (dabs(temp).gt.elltol) then
         n=n+1
         dfn=dble(float(n))
         temp=pikc/dsinh(dfn*pikcp)*dsin(dfn*pikc*u)
         val=val+temp
         if (n.lt.201) goto 10
      endif
      zeta=val
      return
      end
```

Appendix D Derivation of the variational equations for (r,u) using MACSYMA

This appendix shows the derivation of the variational equations for (r,u) in a MACSYMA session. Readers unfamiliar with MACSYMA should consult [Ran84].

```
/* Derivation of the variational equations for (r,u) */

/* Set dependencies for derivatives */
/* Set kval to the value of k */

(C3) (REMOVE(U,DEPENDENCY),
     DEPENDS(K,[AL,BE,RR],[RR,X,Y,TAU,U],T,[AL,BE],TAU,CNF,[U,K]))$

(C4) KVAL:RR*SQRT(BE/2/(AL+BE*RR^2))$

/* Derivative simplification rules */

(C5) SIMPS:[DIFF(TAU,T)=EPS,DIFF(K,BE)=DIFF(KVAL,BE),
            DIFF(K,AL)=DIFF(KVAL,AL),DIFF(K,RR)=DIFF(KVAL,RR),
            DIFF(RR,T)=RDOT,DIFF(U,T)=UDOT]$

(C6) SIMPS:MAP(RADCAN,SIMPS);
```

(D6)

$$[\frac{dTAU}{dT} = EPS,\ \frac{dK}{dBE} = \frac{AL\ RR\ SQRT(BE\ RR^{2} + AL)}{2\ SQRT(2)\ BE^{5/2}\ RR^{4} + 4\ SQRT(2)\ AL\ BE^{3/2}\ RR^{2} + 2\ SQRT(2)\ AL^{2}\ SQRT(BE)},$$

$$\frac{dK}{dAL} = - \frac{SQRT(BE)\ RR\ SQRT(BE\ RR^{2} + AL)}{2\ SQRT(2)\ BE^{2}\ RR^{4} + 4\ SQRT(2)\ AL\ BE\ RR^{2} + 2\ SQRT(2)\ AL^{2}},$$

$$\frac{dK}{dRR} = \frac{SQRT(2)\ AL\ SQRT(BE)\ SQRT(BE\ RR^2 + AL)}{2\ BE^2\ RR^4 + 4\ AL\ BE\ RR^2 + 2\ AL^2}, \quad \frac{dRR}{dT} = RDOT, \quad \frac{dU}{dT} = UDOT]$$

```
(C7) CNSMPS1:[DIFF(CNF,U,2)=CNF*(2*KVAL^2-1-2*KVAL^2*CNF^2),
        DIFF(CNF,U)^2=1-KVAL^2+(2*KVAL^2-1)*CNF^2-KVAL^2*CNF^4,
        DIFF(CNF,U)^3=DIFF(CNF,U)*(1-KVAL^2+
                      (2*KVAL^2-1)*CNF^2-KVAL^2*CNF^4)]$

(C8) CNSMPS1:MAP(RADCAN,CNSMPS1)$

(C9) CNSMPS2:RADCAN(DIFF(CNF,U,1,K,1)=1/DIFF(CNF,U)
             *(-KVAL*(1-CNF^2)^2+DIFF(CNF,U,2)*DIFF(CNF,K)))$

/* Compute x and its derivative */

(C10) X:RR*CNF$

(C11) XDOT:DIFF(%,T);
```

$$(D11)\quad RR\left(\frac{dCNF}{dU}\frac{dU}{dT} + \frac{dCNF}{dK}\left(\frac{dBE}{dTAU}\frac{dK}{dBE}\frac{dTAU}{dT} + \frac{dAL}{dTAU}\frac{dK}{dAL}\frac{dTAU}{dT} + \frac{dK}{dRR}\frac{dRR}{dT}\right)\right) + CNF\,\frac{dRR}{dT}$$

```
(C12) XDOT:EV(XDOT,SIMPS)$

/* Compute y and its derivative */

(C13) Y:RR*SQRT(AL+BE*RR^2)*DIFF(CNF,U)$

(C14) DIFF(%,T);
```

$$(D14)\quad RR\,SQRT(BE\,RR^2 + AL)\left(\frac{d^2CNF}{dU^2}\frac{dU}{dT} + \frac{d^2CNF}{dK\,dU}\left(\frac{dBE}{dTAU}\frac{dK}{dBE}\frac{dTAU}{dT} + \frac{dAL}{dTAU}\frac{dK}{dAL}\frac{dTAU}{dT} + \frac{dK}{dRR}\frac{dRR}{dT}\right)\right) + \frac{dCNF}{dU}SQRT(BE\,RR^2 + AL)\frac{dRR}{dT}$$

$$+\frac{\frac{dCNF}{dU}\,RR\left(\frac{dBE}{dTAU}\,RR\,\frac{2\,dTAU}{dT}+\frac{dAL}{dTAU}\,\frac{dTAU}{dT}+2\,BE\,RR\,\frac{dRR}{dT}\right)}{2\,SQRT(BE\,RR^2+AL)}$$

```
(C15) YDOT:EV(%,SIMPS)$

/* Create the matrix equation [W] [DOT] = [B] which */
/* arises from setting xdot = y and ydot = diff(x,t,2) in eq.(*) */

(C16) W:MATRIX([RATCOEF(XDOT,RDOT),RATCOEF(XDOT,UDOT)],
               [RATCOEF(YDOT,RDOT),RATCOEF(YDOT,UDOT)])$

(C17) DETW:EXPAND(DETERMINANT(W))$

(C18) DETW:EV(DETW,CNSMPS2)$

(C19) DETW:EV(DETW,CNSMPS1)$

(C20) DETW:FACTOR(DETW);
                                                    2
(D20)                                  - RR SQRT(BE RR  + AL)

(C21) B:MATRIX([RATSIMP(Y-EV(XDOT,RDOT=0,UDOT=0))],
               [RATSIMP(-EV(YDOT,RDOT=0,UDOT=0)-AL*X-BE*X^3-EPS*G)])$

/* Compute the solution for [rdot,udot] by inversion */
/* and store as ANSwer */

(C22) ANS:INVERT(W).B$

/* Simplify solution */

(C23) ANS:EV(ANS,CNSMPS2)$

(C24) ANS:EV(ANS,CNSMPS1,RATSIMP)$

(C25) ANS:EV(ANS,CNSMPS1,RATSIMP)$

/* Show the equation for rdot in simplified form */

(C26) REQN:FACTOR(RATCOEF(ANS[1],G))*G
          +FACTOR(RATCOEF(ANS[1],DIFF(AL,TAU)))*DIFF(AL,TAU)
          +FACTOR(RATCOEF(ANS[1],DIFF(BE,TAU)))*DIFF(BE,TAU);
```

$$(D26)\ \left[-\frac{\frac{dCNF}{dU}\,EPS\,G}{SQRT(BE\,RR^2+AL)}+\frac{\frac{dAL}{dTAU}\,(CNF-1)\,(CNF+1)\,EPS\,RR}{2\,SQRT(BE\,RR^2+AL)}\right.$$

$$\left.+\frac{\frac{dBE}{dTAU}\,(CNF-1)\,(CNF+1)\,(CNF^2+1)\,EPS\,RR^3}{4\,(BE\,RR^2+AL)}\right]$$

```
/* Simplify the equation for udot */

(C27) REMOVE(U,DEPENDENCY)$

(C28) UO:EV(ANS[2],DIFF(CNF,K)=-DIFF(CNF,U)*DUDK)$

(C29) UO:EV(UO,RADCAN)$

(C30) UO:PART(UO,1)$

(C31) UO:EXPAND(UO)$

(C32) U1:MAP(FACTOR,UO)$

(C33) U1:SUBST(2*AA^2*DNF^2,BE*CNF^2*RR^2+BE*RR^2+2*AL,U1)$

(C34) U1:SUBST(AA^2,BE*RR^2+AL,U1)$

(C35) U2:MAP(FACTOR,U1)$

(C36) U2:SUBST(AA,ABS(AA),U2)$

(C37) U2:MAP(FACTOR,U2)$

/* Parse U2, the simplified solution for udot */
/* into four pieces and simplifiy further */

(C38) U2G:MAP(FACTOR,EXPAND(RATCOEF(U2,G)*G))$

(C39) U2G:SUBST(AA^2,BE*RR^2+AL,U2G)$

(C40) U2A:MAP(FACTOR,EXPAND(RATCOEF(U2,DIFF(AL,TAU))*DIFF(AL,TAU)))$

(C41) U2A:FACTOR(RATCOEF(U2A,DUDK))*DUDK+FACTOR(EV(U2A,DUDK = 0))$

(C42) U2B:MAP(FACTOR,EXPAND(RATCOEF(U2B,DIFF(BE,TAU))*DIFF(BE,TAU)))$
```

```
(C43) U2B:FACTOR(RATCOEF(U2B,DUDK))*DUDK+FACTOR(EV(U2B,DUDK = 0))$

(C44) U2E:FACTOR(EXPAND(EV(U2,EPS=0)))$

(C45) U2E:SUBST(AA^2,BE*RR^2+AL,U2E)$

/* Show equation for udot */

(C46) UEQN:U2E+U2G+U2A+U2B;
```

$$
\begin{aligned}
(D46)\quad AA - \frac{\mathrm{SQRT}(2)\ AL\ \mathrm{SQRT}(BE)\ \frac{dCNF}{dU}\ DUDK\ EPS\ G}{2\ AA^{4}}
\end{aligned}
$$

$$
+ \frac{BE\ CNF\ EPS\ G\ RR}{AA^{3}} + \frac{AL\ CNF\ EPS\ G}{AA^{3}\ RR} + \frac{\frac{dAL}{dTAU}\ CNF\ \frac{dCNF}{dU}\ EPS}{2\ AA^{2}\ DNF^{2}}
$$

$$
- \frac{\mathrm{SQRT}(2)\ \frac{dAL}{dTAU}\ \mathrm{SQRT}(BE)\ DUDK\ EPS\ RR}{2\ AA^{5}} (BE\ RR^{2} - AL\ CNF^{2} + 2\ AL)
$$

$$
+ \frac{\mathrm{SQRT}(2)\ AL\ \frac{dBE}{dTAU}\ DUDK\ EPS\ RR}{4\ AA^{5}\ \mathrm{SQRT}(BE)} (BE\ CNF^{4}\ RR^{2} + BE\ RR^{2} + 2\ AL)
$$

$$
+ \frac{\frac{dBE}{dTAU}\ CNF\ (CNF^{2} + 1)\ \frac{dCNF}{dU}\ EPS\ RR^{2}}{4\ AA^{2}\ DNF^{2}}
$$

```
/* The above form of udot can be simplified further by hand */

Symbolics 3670 time = 2 hrs
```

Appendix E The AVERAGE program listing

This appendix lists the AVERAGE program which applies the method of averaging to eq.(0.1) using elliptic functions. The program calls the CNINT and GENINT routines of appendices A and B.

```
/* Elliptic averaging of: */
/*   x'' + alpha(tau) x + beta(tau) x^3 + e g(x,x',tau) = 0  */
/* where tau = eps t and g is polynomial in x and x' */

/* Second order version where the phi eqn is averaged to 1st order */
/* but r is to 2nd order */

/* This is incomplete for k^2>1 (within the double homoclinic */
/* loops) where some expressions cannot be averaged analytically. */
/* These do not always occur for k^2>1, but when they do they are */
/* identified as, for example, by: mean_of_zsqrcn^3 */

/* Variable names and their meanings */
/*                                   */
/* X = variable in differential equation */
/* Y = dx/dt */
/* T = time */
/* TAU = eps*t */
/* G = g(x,x',tau) = g(x,y,tau) is a perturbation */
/* AL = alpha(tau) */
/* BE = beta(tau) */
/* RR = amplitude */
/* AA = instantaneous time frequency */
/* BB = phase angle constant */
/* K = modulus of the elliptic functions */
/* U = argument of elliptic functions */
/* CN(U,K) = a jacobi elliptic function */
/* CN'(U,K) = - sn(u,k) dn(u,k) = derivative of cn(u,k) w.r.t. */
/*                the argument u */
/* ZZ = jacobi zeta function */
/* KC = complete elliptic integral of the first kind */
/* EC = complete elliptic integral of the second kind */
/* PHI = angle variable [where u = 4 kc phi] */
/* MU = +1 or -1 depending on the sign of the x-initial condition */
/*      when alpha < 0 */
```

```
/* KSQR_GT_1 = 1 when k^2 > 1 otherwise 0.  This is a flag for an */
/*             orbit being within the double homoclinic loop      */
/*             separatrix.  This equals H(k^2-1), where H is the  */
/*             Heaviside step function                            */

/* The 2nd order differential equation is written as */
/* 2 first order equations: */
/*                                                   */
/* x' = y                                            */
/* y' = - eps g(x,y,tau) - alpha(tau) x - beta(tau) x^3 */

/* For alpha and beta fixed */
/* [and proper interpretation of elliptic variables */
/* for k between minf and inf], the differential equation is */
/* solved exactly by: */
/*                                                                */
/*   x = mu rr cn(u,k)   y = mu rr aa cn'(u,k)   u = aa t + bb    */
/*          aa^2 = al + be rr^2   k^2 = be rr^2/2/aa^2            */
/*                                                                */

/* where initial conditions determine the values of rr and bb */

/* But, it is more convenient to find slow flow equation */
/* for phi [using uu] rather than bb */

/* The Variational equations to be averaged are: */
/*                                               */
/*  diff(rr,t) = eps F[1]                        */
/* diff(phi,t) = aa/4/kc + eps F[2]              */


/* Averaging uses a near-identity transformation as follows: */
/*                                                           */
/*  rr=  rbar+eps*W1(rbar,phi)+eps^2*V1(rbar,phi)            */
/* phi=phibar+eps*W2(rbar,phi)+eps^2*V2(rbar,phi)            */

/* Symbols used in the computation */

/* XX = cn function                                          */
/* YY = cn' function                                         */
/* ZZ = zeta function                                        */
/* SS = arcsin(k*sn(u,k)) = arcsin(k*sqrt(1-xx^2))           */
/* UU = argument                                             */
/* SD = sn/dn                                                */
/* TH = LN(THETA(U)/THETA(0))                                */
/* S0 = integral of SS with respect to u                     */
/* S2 = integral of SS*XX^2 with respect to u                */
```

```
/* Symbols used on output */

/* CNF = cn elliptic function          */
/* CNP = cn' elliptic function         */
/* SNF = sn elliptic function          */
/* ZETA = Jacobi zeta function         */
/* THETA = an elliptic theta function */
/* SO = see above                      */
/* S2 = see above                      */

AVERAGE():=BLOCK([X,Y,XX,YY,H,V,K,AL,BE,RR,ZZ,SS,SO,S2,
                  UU,TH,TAU,KC,EC,EPS,RBAR,KBAR,PHIBAR,
                  CNF,SNF,CNP,THETA,ZETA,ARCSIN],

/* Input problem */

        PRINT("AVERAGING OF X'' + ALPHA(TAU) X + BETA(TAU) X^3",
              "+ EPS G(X,X',TAU) = 0"),
        PRINT("   WHERE TAU = EPS T AND G IS POLYNOMIAL IN",
              "X AND X'"),
        PRINT(" "),ALVAL:READ("ENTER ALPHA(TAU):"),
        PRINT(" "),BEVAL:READ("ENTER BETA(TAU): "),
        PRINT(" "),PRINT("ENTER G(X,X',TAU) USING Y=X':"),
        G:READ(),
        PRINT(" "),
        PRINT("UNPERTURBED SOLUTION IS:  X = RR CN(U,K)",
              "AND X' = Y = RR AA CN'(U,K)"),
        PRINT("WHERE  RR = AMPLITUDE AND U = 4 KC PHI = PHASE"),

/* Kill variables used by routine */
/* and check for AL and BE dependency on tau */

        KILL(K,AL,BE,RR,XX,YY,ZZ,SS,SO,S2,UU,SD,TAU,KC,EC,EPS,
             RBAR,KBAR,PHIBAR,CNF,SNF,CNP,THETA,ZETA,ARCSIN,
             KSQR_GT_1,FF,CNMEAN),
        DEPENDS([AL,BE],TAU),
        IF ALVAL = 0 THEN K:SQRT(1/2),
        IF BEVAL = 0 THEN K:0,
        IF SCALARP(ALVAL) AND ALVAL>=0 THEN KSQR_GT_1:0,
        IF SCALARP(K) THEN SCALARPK:TRUE ELSE SCALARPK:FALSE,
        IF NOT SCALARPK
           AND (DIFF(ALVAL,TAU)#0 OR DIFF(BEVAL,TAU)#0) THEN
           TAUFLAG:TRUE ELSE TAUFLAG:FALSE,

/* Input whether to do phi eqn and the averaging order (1 or 2) */

        PRINT(" "),DOPHI:READ("DO PHI EQN (Y/N)? "),
        IF DOPHI # Y THEN DOPHI:FALSE ELSE DOPHI:TRUE,
        PRINT(" "),
```

```
        IF SCALARPK AND DOPHI THEN DOSEC:READ("DO SECOND ORDER IN R",
                                              "AND PHI (Y/N)?")
                              ELSE DOSEC:READ("DO SECOND ORDER IN R",
                                              "(Y/N)?"),
        IF DOSEC # Y THEN DOSEC:FALSE ELSE DOSEC:TRUE,

        PRINT(" "),PRINT("AVERAGING WILL USE A NEAR-IDENTITY",
                         "TRANSFORMATION FROM"),
        PRINT("(RR,PHI) TO (RBAR,PHIBAR) AS FOLLOWS:"),
        PRINT(" "),
        IF DOSEC THEN PRINT("RR  = RBAR   + EPS*W1(RBAR,PHI)",
                            "+ EPS^2*V1(RBAR,PHI)")
                 ELSE PRINT("RR  = RBAR   + EPS*W1(RBAR,PHI)"),
        IF DOPHI THEN (
           IF DOSEC AND SCALARPK THEN
              PRINT("PHI = PHIBAR + EPS*W2(RBAR,PHI)",
                    "+ EPS^2*V2(RBAR,PHI)")
           ELSE
              PRINT("PHI = PHIBAR + EPS*W2(RBAR,PHI)")
        ),
        PRINT(" "),

/* Create REDUC routine that reduces an expression involving */
/* YY (cn') into its even and odd components and apply the */
/* identity (cn')^2 = (1-cn^2)*(1-k^2+k^2*cn^2) */

        REDUC(EXPR):=BLOCK([EVEN,ODD,VAL],
           EVEN:EXPAND((EXPR+EV(EXPR,YY=-YY))/2),
           ODD:EXPAND((EXPR-EVEN)/YY),
           ODD:YY*EXPAND(EV(ODD,YY=SQRT((1-XX^2)*(1-K^2+K^2*XX^2)))),
           EVEN:EXPAND(EV(EVEN,YY=SQRT((1-XX^2)*(1-K^2+K^2*XX^2)))),
           VAL:EVEN+ODD
        ),

/* Substitute x = r cn and y = r a cn' into g */

        G:EV(G,X=RR*XX,Y=RR*SQRT(AL+BE*RR^2)*YY),

/* Compute F[1] and F[2] */

        F[1]:-REDUC(YY*G)/SQRT(BE*RR^2+AL),
        IF DIFF(ALVAL,TAU)#0 THEN
          F[1]:F[1]+DIFF(AL,TAU,1)*RR*(XX-1)*(XX+1)/(2*(BE*RR^2+AL)),
        IF DIFF(BEVAL,TAU)#0 THEN
          F[1]:F[1]+DIFF(BE,TAU,1)*RR^3*(XX-1)*(XX+1)*(XX^2+1)
                                              /(4*(BE*RR^2+AL)),

        F[2]:-REDUC(G*(2*AL*BE*RR^2*YY*ZZ+2*AL^2*YY*ZZ
                       -AL*BE*RR^2*XX^3-BE^2*RR^4*XX-2*AL*BE*RR^2*XX
                       -2*AL^2*XX))
                        /(4*RR*(BE*RR^2+AL)^(3/2)*(BE*RR^2+2*AL)*KC),
```

```
        IF DIFF(ALVAL,TAU)#0 THEN
          F[2]:F[2]+DIFF(AL,TAU,1)*(AL*XX^2*ZZ-BE*RR^2*ZZ-2*AL*ZZ
                   +AL*XX*YY)/(4*(BE*RR^2+AL)*(BE*RR^2+2*AL)*KC),
        IF DIFF(BEVAL,TAU)#0 THEN
          F[2]:F[2]+DIFF(BE,TAU,1)*(AL*BE*RR^2*XX^4*ZZ+AL*BE*RR^2*ZZ
                   +2*AL^2*ZZ+AL*BE*RR^2*XX^3*YY+BE^2*RR^4*XX*YY
                   +2*AL*BE*RR^2*XX*YY)
                   /(8*BE*(BE*RR^2+AL)*(BE*RR^2+2*AL)*KC),

/* If k=0 or k^2=1/2 then simpify above */

        IF K = 0 THEN (
           F[1]:EV(F[1],BE=0),
           F[2]:EV(F[2],ZZ=0,BE=0)
        ),

        IF K = SQRT(1/2) THEN (
           F[1]:EV(F[1],AL=0),
           F[2]:EV(F[2],AL=0)
        ),

/* Integrate F[1], find mean of F[1], F1BAR */

        FI1:GENINT(F[1],K),
        FF1:EV(FI1,XX=0,YY=0,ZZ=0),
        F1BAR:RATCOEF(FF1,UU)+KSQR_GT_1*RATCOEF(FF1,SS)*%PI/2/KC,

/* Find W1 */

        KILL(W1,W1MEAN,W1INT,W1r,W2),
        W1:1/SQRT(AL+BE*RR^2)*( EV(FI1,UU=0)
           -KSQR_GT_1*RATCOEF(FF1,SS)*%PI/2/KC*UU ),
        W1INT:GENINT(W1,K),
        /* when ksqr_gt_1 then ss-%pi/2/kc*uu has zero mean */
        W1MEAN:RATCOEF(W1INT,UU,1)
               +KSQR_GT_1*RATCOEF(W1INT,SS)*%PI/2/KC,
        W1:W1-W1MEAN,
        PRINT("DONE WITH FIRST ORDER RR EQN"),

/* Find W2 */

        IF DOPHI THEN (
           W1R:SQRT(BE*RR^2+AL)*(BE*RR^2*KC+2*AL*KC-2*AL*EC)
               /(4*RR*(BE*RR^2+2*AL)*KC^2),
           IF ALVAL=0 THEN (W1R:EV(W1R,AL=0),W1R:EV(W1R,ABS(RR)=RR)),
           IF BEVAL=0 THEN W1R:0,
           FI2:GENINT(F[2],K),
           FF2:EV(FI2,XX=0,YY=0,ZZ=0,TH=0),
           F2BAR:RATCOEF(FF2,UU)+KSQR_GT_1*RATCOEF(FF2,SS)*%PI/2/KC,
```

```
        W2:1/SQRT(AL+BE*RR^2)*( EV(FI2,UU=0)
              -KSQR_GT_1*RATCOEF(FF2,SS)*%PI/2/KC*UU
              -W1R*(W1INT-W1MEAN*UU) ),
        DW2PHI:4*KC/SQRT(AL+BE*RR^2)*(F[2]-F2BAR+W1R*W1),
        PRINT("DONE WITH FIRST ORDER PHI EQN")
      ),

/* Goto end if first order */

    IF NOT DOSEC THEN GO(JUMPEND),

/* Reduce expression swell by parsing F[1] and W1, i.e., by */
/* replacing the very large coefficients of function forms */
/* appearing in F[1] and W1 by dummy expressions */

      PRINT("PARSING F[1] AND W1"),
      F[1]:EXPAND(F[1]),W1:EXPAND(W1),
      F1PARSE:0,W1PARSE:0,
      KILL(F1XXCOEF,F1YYCOEF,W1XXCOEF,W1YYCOEF,W1SSCOEF,
           W1ZZCOEF,W1UUCOEF,F1BARCOEF),

      HI:MAX(HIPOW(F[1],XX),HIPOW(W1,XX)),
      COEFVALS:[],
      FOR II:0 THRU HI DO (
          TEMP:RATCOEF(F[1],XX,II),
          TEMPNOY:EV(TEMP,YY=0),
          TEMPY:DIFF(TEMP,YY),

          /* Find xx^ii coefficients in F[1] */
          IF TEMPNOY # 0 THEN (
             COEFVALS:APPEND(COEFVALS,
                             [F1XXCOEF[II]=FACTOR(TEMPNOY)]),
             F1PARSE:F1PARSE+F1XXCOEF[II]*XX^II
          ),

          /* Find xx^ii*yy coefficients in F[1] */
          IF TEMPY # 0 THEN (
             COEFVALS:APPEND(COEFVALS,
                             [F1YYCOEF[II]=FACTOR(TEMPY)]),
             F1PARSE:F1PARSE+F1YYCOEF[II]*YY*XX^II
          ),
          TEMP:RATCOEF(W1,XX,II),
          IF II = 0 THEN (

             /* Find zz coefficients in W1 */
             TEMPZ:DIFF(TEMP,ZZ),
             IF TEMPZ # 0 THEN (
                COEFVALS:APPEND(COEFVALS,[W1ZZCOEF=FACTOR(TEMPZ)]),
                W1PARSE:W1PARSE+W1ZZCOEF*ZZ
             ),
```

```
            /* Find ss coefficients in W1 */
            TEMPS:DIFF(TEMP,SS),
            IF TEMPS # 0 THEN (
               COEFVALS:APPEND(COEFVALS,[W1SSCOEF=FACTOR(TEMPS)]),
               W1PARSE:W1PARSE+W1SSCOEF*SS
            ),

            /* Find uu coefficients in W1 */
            TEMPU:DIFF(TEMP,UU),
            IF TEMPU # 0 THEN (
               COEFVALS:APPEND(COEFVALS,[W1UUCOEF=FACTOR(TEMPU)]),
               W1PARSE:W1PARSE+W1UUCOEF*UU
            ),
            TEMP:EV(TEMP,ZZ=0,SS=0,UU=0)
         ),
         TEMPNOY:EV(TEMP,YY=0),
         TEMPY:DIFF(TEMP,YY),

         /* Find xx^ii coefficients in W1 */
         IF TEMPNOY # 0 THEN (
            COEFVALS:APPEND(COEFVALS,
                            [W1XXCOEF[II]=FACTOR(TEMPNOY)]),
            W1PARSE:W1PARSE+W1XXCOEF[II]*XX^II
         ),

         /* Find xx^ii*yy coefficients in W1 */
         IF TEMPY # 0 THEN (
            COEFVALS:APPEND(COEFVALS,
                            [W1YYCOEF[II]=FACTOR(TEMPY)]),
            W1PARSE:W1PARSE+W1YYCOEF[II]*YY*XX^II
         )
      ),

/* Store real coefficient values in a list called COEFVALS */

      COEFVALS:APPEND(COEFVALS,[F1BARCOEF=FACTOR(F1BAR)]),

/* Give dummy coefficients proper dependencies */

      DEPENDS([F1XXCOEF,F1YYCOEF,W1XXCOEF,W1YYCOEF,W1ZZCOEF,
               W1SSCOEF,W1UUCOEF],RR),
   IF TAUFLAG THEN DEPENDS([W1XXCOEF],TAU),
   /* need not consider others */

/* Set dependencies of elliptic functions */

      DEPENDS([XX,YY,ZZ,SS,UU],RR),
      IF NOT SCALARPK THEN DEPENDS([KC,EC],K,K,RR),
   IF TAUFLAG THEN DEPENDS([XX,YY,K],TAU),
   /* need not consider z,ss,uu */
```

```
/* Define elliptic derivatives */

        IF K # 0 THEN
           DIFVALS:[DIFF(UU,RR)=U/KC/K/(1-K^2)*DIFF(K,RR)
                               *(EC-(1-K^2)*KC),
                    DIFF(XX,RR)=-1/K/(1-K^2)*DIFF(K,RR)
                               *(ZZ*YY+K^2*XX*(1-XX^2)),
                    DIFF(YY,RR)=-1/K/(1-K^2)*DIFF(K,RR)
                               *(ZZ*XX*(2*K^2-1)-2*K^2*XX^3*ZZ
                               +K^2*YY*(1-2*XX^2)),
                    DIFF(ZZ,RR)=-K/(1-K^2)*DIFF(K,RR)
                               *(ZZ*XX^2+XX*YY),
                    DIFF(SS,RR)=DIFF(K,RR)*(SD-1/(1-K^2)
                               *(ZZ*XX-K^2*SD*XX^2))]
        ELSE
           DIFVALS:[DIFF(UU,RR)=0,
                    DIFF(XX,RR)=0,
                    DIFF(YY,RR)=0],

        IF TAUFLAG THEN
           DIFVALS:APPEND(DIFVALS,
                          [DIFF(XX,TAU)=DIFF(K,TAU)/DIFF(K,RR)
                                       *EV(DIFF(XX,RR),DIFVALS),
                           DIFF(YY,TAU)=DIFF(K,TAU)/DIFF(K,RR)
                                       *EV(DIFF(YY,RR),DIFVALS)]
                    ),

/* Find diff(W1,phi) */

        DW1PHI:4*KC/SQRT(AL+BE*RR^2)*(F1PARSE-F1BARCOEF),

/* Find diff(F[1],rr) */

        PRINT("FINDING DIFF(F1,RR)"),
        DF1R:DIFF(F1PARSE,RR),
        DF1R:EV(DF1R,DIFVALS),

/* Find diff(W1,rr) */

        PRINT("FINDING DIFF(W1,RR)"),
        WW:EV(W1PARSE,ZZ=0,SS=0,UU=0),
        /* zz,ss,uu contribute zero mean in diff(w1,rr) */
        DW1R:DIFF(WW,RR),
        DW1R:EV(DW1R,DIFVALS),
```

```
/* Find diff(W1,tau) */

        DW1TAU:0,
        IF TAUFLAG THEN (
           PRINT("FINDING DIFF(W1,TAU)"),
           DW1TAU:DIFF(WW,TAU),
           DW1TAU:EV(DW1TAU,DIFVALS)
        ),

/* Find H2 */

        IF DOPHI AND SCALARPK THEN (
           DF2R:DIFF(F[2],RR),
           DF2R:EV(DF2R,DIFVALS),
           H2:EXPAND(DF2R*W1PARSE-DW2PHI*(F[2]+W1R*W1PARSE)),
           H2:REDUC(H2)
        ),

/* Remove elliptic function dependencies */

        REMOVE([XX,YY,ZZ,SS,UU],DEPENDENCY),

/* Find H1 */

        PRINT("FINDING H1"),
        H1:EXPAND(-F1BARCOEF*DW1R-F[2]*DW1PHI-DW1TAU+DF1R*W1PARSE),

/* Find length of H1 and parse into two pieces: */
/* H1Y contains yy; H1NOY does not */

        LEN:LENGTH(H1),
        PRINT("DIVIDING UP H1  (",LEN," TERMS)"),
        H1Y:0,H1NOY:0,
        FOR II:1 THRU LEN DO (
            TEMP:PART(H1,II),
            EVEN:EXPAND(1/2*(TEMP+EV(TEMP,YY=-YY))),
            ODD:EXPAND(1/2/YY*(TEMP-EV(TEMP,YY=-YY))),
            H1NOY:H1NOY+EXPAND(EV(EVEN,
                                  YY=SQRT((1-XX^2)*(1-K^2+K^2*XX^2)))),
            H1Y:H1Y+EXPAND(EV(ODD,
                                  YY=SQRT((1-XX^2)*(1-K^2+K^2*XX^2))))
        ),
        KILL(H1),

/* Parse H1Y into pieces */

        PRINT("PARSING H1Y"),
        TEMP:DIFF(H1Y,UU),
        H1YZAPU:EV(TEMP,ZZ=0),   /* Functions: uu*xx^ii*yy */
        TEMP:DIFF(H1Y,SS),
        H1YZAPS:EV(TEMP,ZZ=0),   /* Functions: ss*xx^ii*yy */
```

```
        TEMP:DIFF(H1Y,ZZ),
        H1YZAPZ:EV(TEMP,SS=0,UU=0,ZZ=0), /* Functions: zz*xx^ii*yy */
        KILL(H1Y),

/* Find means of functions indicated above using formulas */
/* where cnmean[ii] = mean of cn^ii = mean of xx^ii       */

        PRINT("FINDING H1Y MEANS"),

        HI:HIPOW(H1YZAPZ,XX),H1YZAPZBAR:0,
        FOR II:0 THRU HI DO
            H1YZAPZBAR:H1YZAPZBAR-RATCOEF(H1YZAPZ,XX,II)/(II+1)
                                 *( (1-K^2-EC/KC)*CNMEAN[II+1]
                                    +K^2*CNMEAN[II+3] ),
        HI:HIPOW(H1YZAPS,XX),H1YZAPSBAR:0,
        FOR II:0 THRU HI DO
            H1YZAPSBAR:H1YZAPSBAR-RATCOEF(H1YZAPS,XX,II)
                                 *K/(II+1)*CNMEAN[II+2],
        HI:HIPOW(H1YZAPU,XX),H1YZAPUBAR:0,
        FOR II:0 THRU HI DO
            H1YZAPUBAR:H1YZAPUBAR-RATCOEF(H1YZAPU,XX,II)
                                 *K/(II+1)*CNMEAN[II+1],
        KILL(H1YZAPZ,H1YZAPU,H1YZAPS),

/* Parse H1NOY into pieces */

        PRINT("PARSING H1NOY"),
        /* Functions: xx^ii */
        H1NOYZAPX:EV(H1NOY,ZZ=0,SS=0,UU=0,SD=0),
        H1NOYZ2:1/2*DIFF(H1NOY,ZZ,2),   /* Functions: zz^2*xx^ii */
        H1NOYZS:DIFF(H1NOY,SS,1,ZZ,1),  /* Functions: zz*ss*xx^ii */
        H1NOYZU:DIFF(H1NOY,UU,1,ZZ,1),  /* Functions: zz*uu*xx^ii */
        KILL(H1NOY),

/* Find means of functions indicated above */

        PRINT("FINDING MEANS"),

        /* Find mean of xx^ii */
        HI:HIPOW(H1NOYZAPX,XX),H1NOYZAPXBAR:0,
        FOR II:0 THRU HI DO H1NOYZAPXBAR:H1NOYZAPXBAR
                                 +RATCOEF(H1NOYZAPX,XX,II)*CNMEAN[II],

        /* If k=0 then rest of the means are zero: skip to end */
        IF K=0 THEN (
           H1NOYZUBAR:0,
           H1NOYZ2BAR:0,
           H1NOYZSBAR:0,
           GO(JUMP1)
        ),
```

```
HI2:HIPOW(H1NOYZ2,XX),HIS:HIPOW(H1NOYZS,XX),
HIU:HIPOW(H1NOYZU,XX),

/* Separate H1NOYZU, H1NOYZS, and H1NOYZ2 into even */
/* and odd pieces in xx */

/* Use flags for means of functions which cannot */
/* be explicitly computed */
HI:MAX(HI2,HIS,HIU),H1NOYZ2BARODD:0,
H1NOYZUBAR:0,H1NOYZSODD:0,
FOR II:1 THRU HI STEP 2 DO (
    H1NOYZUBAR:H1NOYZUBAR+RATCOEF(H1NOYZU,XX,II)
                          /4/KC*INT_OVER_4KC_OF_ZUCN^II,
    H1NOYZ2BARODD:H1NOYZ2BARODD+RATCOEF(H1NOYZ2,XX,II)
                                *KSQR_GT_1*MEAN_OF_ZSQRCN^II,
    H1NOYZSODD:H1NOYZSODD+RATCOEF(H1NOYZS,XX,II)*XX^II
),
HI:MAX(HI2,HIS,2),
H1NOYZSBAREVEN:RATCOEF(H1NOYZS,XX,0)*KSQR_GT_1*MEAN_OF_ZSU,
H1NOYZ2EVEN:RATCOEF(H1NOYZ2,XX,0),
FOR II:2 THRU HI STEP 2 DO (
    H1NOYZSBAREVEN:H1NOYZSBAREVEN+RATCOEF(H1NOYZS,XX,II)
                                    *KSQR_GT_1*MEAN_OF_ZSUCN^II,
    H1NOYZ2EVEN:H1NOYZ2EVEN+RATCOEF(H1NOYZ2,XX,II)*XX^II
),

/* Find mean of H1NOYZS (for xx odd) by procedures B,C */

TEMP1:GENINT(SS*H1NOYZSODD,K),
TEMP2:1/2*DIFF(TEMP1,SS,2),
TEMP1:EV(TEMP1,SS=0,YY=0),
TEMP1:EXPAND(-TEMP1*(1-K^2-EC/KC+K^2*XX^2)),
HI:HIPOW(TEMP1,XX),TEMP1BAR:0,
FOR II:0 THRU HI DO TEMP1BAR:TEMP1BAR+RATCOEF(TEMP1,XX,II)
                                        *CNMEAN[II],
TEMP2BAR:-TEMP2*(1-K^2-EC/KC)*MEAN_OF_SS^2
         -TEMP2*K^2*MEAN_OF_SS_SQR_CN^2,
H1NOYZSBARODD:TEMP1BAR+TEMP2BAR,

/* Find mean of H1NOYZ2 (for xx even) by procedure A */

TEMP1:GENINT(H1NOYZ2EVEN,K),
TEMP1:EXPAND(-TEMP1*2*(1-K^2-EC/KC+K^2*XX^2)),
TEMP2:DIFF(TEMP1,YY),
HI:HIPOW(TEMP2,XX),TEMP2BAR:0,
FOR II:0 THRU HI DO
    TEMP2BAR:TEMP2BAR-RATCOEF(TEMP2,XX,II)/(II+1)
                     *( (1-K^2-EC/KC)*CNMEAN[II+1]
                        +K^2*CNMEAN[II+3] ),
```

```
        TEMP3:DIFF(TEMP1,UU),
        TEMP3BAR:-RATCOEF(TEMP3,XX,0)*MEAN_OF_TH
                 -RATCOEF(TEMP3,XX,2)/K^2/2*(
                          MEAN_OF_Z^2+2*(EC/KC+K^2-1)*MEAN_OF_TH ),
        TEMP1:DIFF(TEMP1,ZZ),
        TEMP1BAR:RATCOEF(TEMP1,XX,0)*MEAN_OF_Z^2
                 +RATCOEF(TEMP1,XX,2)/3
                      *(-2/K^2*(1-K^2-EC/KC)^2*MEAN_OF_TH
                 +1/K^2*(EC/KC+K^2-1)
                      *(MEAN_OF_Z^2+2*(EC/KC+K^2-1)*MEAN_OF_TH)
                 -2/K^2*(1-K^2-EC/KC)*MEAN_OF_Z^2),
        H1NOYZ2BAREVEN:RATSIMP(TEMP1BAR)+TEMP2BAR+TEMP3BAR,

/* Add together the even and odd components to the mean */
/* of H1NOYZS and H1NOYZ2 */

        H1NOYZ2BAR:H1NOYZ2BAREVEN+H1NOYZ2BARODD,
        H1NOYZSBAR:H1NOYZSBAREVEN+H1NOYZSBARODD,

        JUMP1,  /* jump for k=0 */

/* Find H1BAR */

        H1BAR:H1YZAPZBAR+H1YZAPSBAR+H1YZAPUBAR+H1NOYZAPXBAR
              +H1NOYZ2BAR+H1NOYZSBAR+H1NOYZUBAR,

/* Find H2BAR if able */

        IF DOPHI AND SCALARPK THEN (
           H2X:EV(H2,YY=0,ZZ=0,SS=0),
           H2Y:DIFF(H2,YY),
           H2YZ:DIFF(H2Y,ZZ),
           H2YS:DIFF(H2Y,SS),
           H2Z2:DIFF(H2,ZZ,2)/2,
           H2S2:DIFF(H2,SS,2)/2,
           H2BAR:H2Z2*MEAN_OF_Z^2+H2S2*MEAN_OF_SS^2,
           HI:MAX(HIPOW(H2X,XX),HIPOW(H2YZ,XX),HIPOW(H2YS,XX)),
           FOR II:0 THRU HI DO
               H2BAR:H2BAR
                     +RATCOEF(H2X,XX,II)*CNMEAN[II]
                     -RATCOEF(H2YZ,XX,II)/(II+1)*((1-K^2+EC/KC)
                          *CNMEAN[II+1]+K^2*CNMEAN[II+3])
                     -RATCOEF(H2YS,XX,II)/(II+1)*K*CNMEAN[II+2]
        ),
```

```
/* Find cnmean[ii] */

        IF K=SQRT(1/2) THEN KBAR:SQRT(1/2),
        IF K=0 THEN (
           CNMEAN[0]:1,CNMEAN[1]:0,CNMEAN[2]:1/2,CNMEAN[3]:0,
           CNMEAN[II]:=RATSIMP((II-1)/II*CNMEAN[II-2])
        ) ELSE (
           CNMEAN[0]:1,
           CNMEAN[1]:KSQR_GT_1*%PI/2/KC/KBAR,
           CNMEAN[2]:1/KBAR^2*(EC/KC-1+KBAR^2),
           CNMEAN[3]:KSQR_GT_1/2/KBAR^3*(2*KBAR^2-1)*%PI/2/KC,
           CNMEAN[II]:=RATSIMP(1/(II-1)/KBAR^2*(
                        (II-2)*(2*KBAR^2-1)*CNMEAN[II-2]
                       +(II-3)*(1-KBAR^2)*CNMEAN[II-4]))
        ),

/* Simplify H1BAR */

        H1BARSIMP:RATSIMP(EV(H1BAR)),
        PRINT("EVALUATING H1BAR IN TERMS OF COEF VALS"),
        H1BARSIMP:EV(H1BARSIMP,COEFVALS,DIFF),
        H1BARSIMP:EV(H1BARSIMP,DIFF(K,RR)=AL*SQRT(BE/2)
                                          /(BE*RR^2+AL)^(3/2)),
        H1BARSIMP:EV(H1BARSIMP,
                     DIFF(K,TAU)=RR^2/4/KBAR/(AL+BE*RR^2)^2
                                 *(AL*DIFF(BEVAL,TAU)-
                                   BE*DIFF(ALVAL,TAU))),

/* Simplify H2BAR */

        IF DOPHI AND SCALARPK THEN (
           H2BARSIMP:RATSIMP(EV(H2BAR)),
           H2BARSIMP:EV(H2BARSIMP,COEFVALS)
        ),

     JUMPEND,  /* jump for first order r only */

/* Create a list of substitution rules for output */

        IF SCALARPK AND K = 0 THEN
           PF:[XX=COS(2*%PI*PHI),YY=-SIN(2*%PI*PHI),
               UU=2*%PI*PHI,ABS(RR)=RBAR,
               RR=RBAR,KC=%PI/2,EC=%PI/2,AL=ALVAL,BE=BEVAL]
        ELSE
           PF:[XX=CNF(4*KC*PHI),YY=CNP(4*KC*PHI),ZZ=ZETA(4*KC*PHI),
               TH=LOG(THETA(4*KC*PHI)/THETA(0)),
               SS=ARCSIN(KBAR*SNF(4*KC*PHI)),
               UU=4*KC*PHI,ABS(RR)=RBAR,RR=RBAR,AL=ALVAL,BE=BEVAL],
```

```
        IF NOT SCALARPK THEN
           PFK:[   K=RBAR*SQRT(BEVAL/2/(BEVAL*RBAR^2+ALVAL)),
                KBAR=RBAR*SQRT(BEVAL/2/(BEVAL*RBAR^2+ALVAL))]
        ELSE PFK:[],

/* Change results to output form */

        F1BAR:RATSIMP(EV(F1BAR,PF,PFK,DIFF)),
        IF DOPHI THEN F2BAR:RATSIMP(EV(F2BAR,PF,PFK,DIFF)),
        IF DOSEC THEN H1BARSIMP:RATSIMP(EV(H1BARSIMP,PF,PFK,DIFF)),
        IF DOSEC AND DOPHI AND SCALARPK THEN (
           H2BARSIMP:RATSIMP(EV(H2BARSIMP,PF,PFK)),
           H2BARSIMP:EV(H2BARSIMP,ABS(RBAR)=RBAR)
        ),

/* Save averaged system into Rflow and Pflow */

        RFLOW:EPS*FACTOR(F1BAR),
        IF DOSEC THEN RFLOW:RFLOW+EPS^2*FACTOR(H1BARSIMP),
        IF DOPHI THEN (
           PFLOW:EV(1/4/KC*SQRT(AL+BE*RR^2),PF)+EPS*FACTOR(F2BAR),
           IF DOSEC AND SCALARPK THEN
              PFLOW:PFLOW+EPS^2*FACTOR(H2BARSIMP)
        ),
        RFLOW:FACTOR(EV(RFLOW,ABS(RBAR)=RBAR)),
        PFLOW:EV(PFLOW,ABS(RBAR)=RBAR),

/* Print averaged system, k^2, kc and ec */
/* (VAL contains this list of output) */

        DERIVABBREV:TRUE,
        VAL:[DIFF(RBAR(T),T)=RFLOW],
        IF DOPHI THEN VAL:APPEND(VAL,[DIFF(PHIBAR(T),T)=PFLOW]),
        VAL:APPEND(VAL,['KBAR^2=FACTOR(BEVAL*RBAR^2/2
                                       /(ALVAL+BEVAL*RBAR^2))]),
        IF K=0 THEN VALCOMP:[KC=%PI/2,EC=%PI/2]
        ELSE VALCOMP:[KC=KC(KBAR),EC=EC(KBAR)],
        VAL:APPEND(VAL,VALCOMP),

        PRINT("THE AVERAGED EQUATIONS ARE"),
        PRINT(" "),PRINT(VAL),PRINT(" "),

/* Simplify transformation */

        PRINT("SIMPLIFYING TRANSFORMATION"),
        W1:EXPAND(EV(W1,PF,PFK,DIFF)),W1:EV(W1,ABS(RBAR)=RBAR),
        IF DOPHI THEN (
           W2:EXPAND(EV(W2,PF,PFK,DIFF)),
           W2:EV(W2,ABS(RBAR)=RBAR)
        ),
        RTRANS:RR=RBAR+EPS*MAP(FACTOR,W1)+EPS^2*V1NOTCOMPUTED,
```

```
        IF DOPHI THEN (
           PTRANS:PHI=PHIBAR+EPS*MAP(FACTOR,W2),
           IF DOSEC AND SCALARPK THEN
              PTRANS:PHI=PHIBAR+EPS*MAP(FACTOR,W2)
                         +EPS^2*V2NOTCOMPUTED,
           TRANSF:[RTRANS,PTRANS]
        ) ELSE TRANSF:RTRANS,

        /* Print transformation on request */
        Q2:READ("DO YOU WISH TO SEE THE TRANSFORMATION? (Y/N)"),
        IF Q2#N THEN (
           PRINT("THE TRANSFORMATION IS :"),
           PRINT(" "),PRINT(TRANSF)
        )
)$
```

References

[Abr72] Abramowitz, M. and Stegun, I. Handbook of Mathemetical Functions, New York: Dover, 1972.

[And71] Andronov, A. et al. Theory of Bifurcations of Dynamic Systems on a Plane, Jerusalem: Israel Program for Scientific Translations, 1971.

[Arn84] Arnold, V. Mathematical Methods of Classical Mechanics, Graduate Texts in Mathematics vol. 60, New York: Springer-Verlag, 1984.

[Ben78] Bender, C. and Orzag, S. Advanced Mathematical Methods for Scientists and Engineers, New York: McGraw-Hill, 1978.

[Bog61] Bogoliubov, N. and Mitropolsky, Y. Asymptotic methods in the theory of oscillations, New York: Gordon and Breach, 1961.

[Bou88] Bourland, F. and Haberman, R. "The Modulated Phase Shift for Strongly Nonlinear, Slowly Varying, and Weakly Damped Oscillators", *SIAM J. Appl. Math.* 48(4), 737-748 (1988).

[Byr54] Byrd, P. and Friedman, M. Handbook of Elliptic Integrals for Engineers and Physicists, Berlin: Springer-Verlag, 1954.

[Cap73] Cap, F. "Averaging method for the solution of non-linear differential equations with perioidc non-harmonic solutions", *Int. J. Nonlinear Mech.* 9, 441-450 (1973).

[Car81] Carr, J. Applications of Center Manifold Theory, New York: Springer-Verlag, 1981.

[Car86] Cary, J., Escande, D., and Tennyson, J. "Adiabatic-invariant change due to separatrix crossing", *Phys. Rev.* A 34(5), 4256-4275 (1986).

[Chi79] Chirikov, B. "A Universal Instability of Many Dimensional Oscillator Systems", *Phys. Reports* 52, 263-379 (1979).

[Cop89a] Coppola, V. and Rand, R. "Averaging Using Elliptic Functions: Approximation of Limit Cycles", to appear in *Acta Mechanica*, 1989.

[Cop89b] Coppola, V. and Rand, R. "MACSYMA Program to Implement Averaging Using Elliptic Functions", to appear in the proceedings of the conference on Computer Assisted Proofs in Analysis, 1989.

[Cop89c] Coppola, V. and Rand, R. "Symbolic Computation and Perturbation Methods Using Elliptic Functions", Transactions of the Sixth Army Conference on Mathematics and Computing, 639-676 (1989).

[Dav62] Davis, H. Introduction to Nonlinear Differential and Integral Equations, New York: Dover, 1962.

[Dev87] Devaney, R. An Introduction to Chaotic Dynamical Systems, New York: Addison-Wesley, 1987.

[Gar87] Garcia-Margallo, J. and Bejarano, J. "A Generalization of the Method of Harmonic Balance", *J. Sound Vib.* 116(3), 591-595 (1987).

[Gar] Garcia-Margallo, J. and Bejarano, J. "Stability of Limit Cycles and Bifurcations of Generalized van der Pol Oscillators", preprint.

[Gol80] Goldstein, H. Classical Mechanics, 2nd ed., Reading, Mass: Addison-Wesley, 1980.

[Gre78] Greenberg, M. Foundations of Applied Mathematics, Englewood Cliffs, NJ: Prentice Hall, 1978.

[Gre83] Greenspan, B. and Holmes, P. "Repeated Resonance and Homoclinic Bifurcation in a Periodically Forced Family of Oscillators", *SIAM J. Math. Anal.* 15(1), 69-97 (1983).

[Gre65] Greenwood, D. Principles of Dynamics, Englewood Cliffs, N.J.: Prentice-Hall, 1965.

[Guc86] Guckenheimer, J. and Holmes, P. Nonlinear Oscillations, Dynamical Systems, and Bifurcations of Vector Fields, Applied Mathematical Sciences vol. 42, New York: Springer-Verlag, 1986.

[Hag82] Hagedorn, P. Non-Linear Oscillations, New York: Oxford University Press, 1982.

[Hal63] Hale, J. Oscillations in Nonlinear Systems, New York: McGraw-Hill, 1963.

[Han10] Hancock, H. Theory of Elliptic Functions, Vol. I, 1st ed., New York: John Wiley and Sons, 1910.

[Hen82] Henrard, J. "Capture into Resonance: An Extension of the Use of Adiabatic Invariants", *Celest. Mech.* 27, 3-22 (1982).

[Hen] Henrard, J. "The Adiabatic Invariant in Classical Mechanics", preprint.

[Hir74] Hirsch, M. and Smale, S. Differential Equations, Dynamical Systems, and Linear Algebra, Pure and Applied Mathematics vol.60, Orlando, Florida: Academic Press, 1974.

[Hol79] Holmes, P. "A Nonlinear Oscillator with a Strange Attractor", *Phil. Trans. Roy. Soc.* 292(1394), 419-448 (1979).

[Kea75] Keane, M. "Interval Exchange Transformations", *Math. Z.* 141, 25-31 (1975).

[Kev81] Kevokian, J. and Cole, J. Perturbation Methods in Applied Mathematics, Applied Mathematical Sciences vol. 34, New York: Springer-Verlag, 1981.

[Kry37] Krylov, N. and Bogoliubov, N. Introduction to nonlinear Mechanics (in Russian), Patent No. 1, Kiev, 1937.

[Kuz59] Kuzmak, G. "Asymptotic Soltuions of Nonlinear Second Order Differential equations with Variable Coefficients", *P.M.M.* (English translation), 23(3), 515-526 (1959).

[Mic86] Mickens, R. "A Generalization of the Method of Harmonic Balance", *J. Sound Vib.* 111(3), 515-518 (1986).

[Mic84] Mickens, R. "Comments on the Method of Harmonic Balance", *J. Sound Vib.* 94(3), 456-460 (1984).

[Min62] Minorsky, N. Nonlinear Oscillations, New York: Van Nostrand, 1962.

[Mit65] Mitropolsky, Y. Problems of the Asymptotic Theory of Nonstationary Vibrations, Jerusalem: Israel Program for Scientific Translations, 1965.

[Nay73] Nayfeh, A. Perturbation Methods, New York: Wiley-Interscience, 1973.

[Nay79] Nayfeh, A. and Mook, D. Nonlinear Oscillations, New York: John Wiley and Sons, 1979.

[Nev71] Neville, E. Elliptic Functions: A Primer, New York: Pergamon Press, 1971.

[Poc81] Pocobelli, G. "Electron Motion in a Slowly Varying Wave", *Phys. Fluids* 24(12), 2173-2176 (1981).

[Poi57] Poincare, H. Les Methodes Nouvelle de la Mecanique Celeste, New York: Dover, 1957.

[Ran84] Rand, R. Computer Algebra in Applied Mathematics: An Introduction to MACSYMA, Research Notes in Mathematics vol. 94, Boston, Pitman Publishing, 1984.

[Ran87] Rand, R. and Armbruster, D. Perturbation Methods, Bifurcation Theory, and Computer Algebra, Applied Mathematical Sciences vol. 65, New York: Springer-Verlag, 1987.

[San85] Sanders, J. and Verhulst, F. Averaging Methods in Nonlinear Dynamical Systems, Applied Mathematical Sciences vol. 59, New York: Springer-Verlag, 1985.

[Set67] Sethna, P. "An Extension of the Method of Averaging", *Quarterly of Appl. Math.* 25(2), 205-211 (1967).

[Sim86] Simmonds, J. and Mann, J. A First Look at Perturbation Theory, Malabar, FL: Robert E. Krieger Publishing, 1986.

[Sto50] Stoker, J. Nonlinear Vibrations, New York: Wiley, 1950.

[Tak74] Takens, F. "Forced oscillations and bifurcations", *Comm. Math. Inst.*, Rijkuniversiteit Utrecht 3, 1-59 (1974).

[Yus86] Yuste, S. and Bejarano, J. "Construction of Approximate Analytical Solutions to a New Class Of Non-Linear Oscillator Equations", *J. Sound Vib.* 110(2), 347-350 (1986).